MICROCOPY RESOLUTION TEST CHART
NATIONAL BUREAU OF STANDARDS-1963-A

AFOSR-TR. 86-0638

HYDROPHONE INVESTIGATIONS
OF EARTHQUAKE AND EXPLOSION GENERATED
HIGH-FREQUENCY SEISMIC PHASES
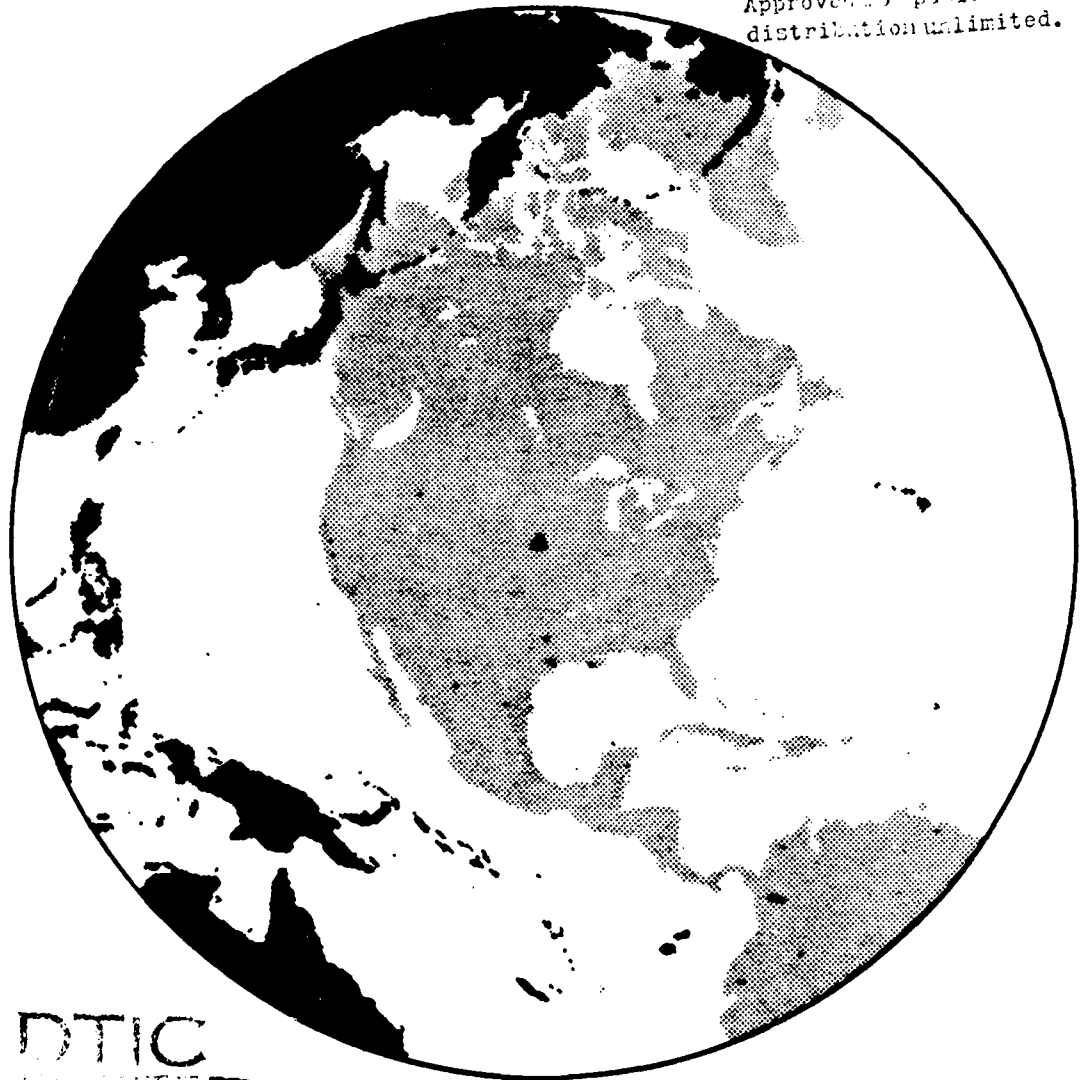
AD-A172 543

ŪTIU FILE COPY
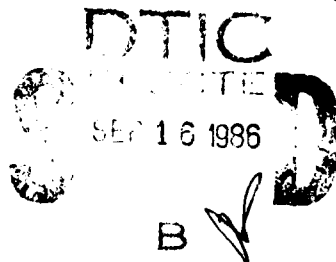
Technical Report
to the
Air Force Office of Scientific Research

30 April 1986

DISCLAIMER NOTICE

THIS DOCUMENT IS BEST QUALITY
PRACTICABLE. THE COPY FURNISHED
TO DTIC CONTAINED A SIGNIFICANT
NUMBER OF PAGES WHICH DO NOT
REPRODUCE LEGIBLY.

REPORT DOCUMENTATION PAGE

1a. REPORT SECURITY CLASSIFICATION	1b. RESTRICTIVE MARKINGS
UNCLASSIFIED	N/A

2a. SECURITY CLASSIFICATION AUTHORITY	3. DISTRIBUTION/AVAILABILITY OF REPORT
N/A	UNCLASSIFIED/UNLIMITED
2b. DECLASSIFICATION DOWNGRADING SCHEDULE	
N/A	

4. PERFORMING ORGANIZATION REPORT NUMBER(S)	5. MONITORING ORGANIZATION REPORT NUMBER(S)
N/A	N/A AFOSR·TR· 86-0638

6a. NAME OF PERFORMING ORGANIZATION	6b. OFFICE SYMBOL (If applicable)	7a. NAME OF MONITORING ORGANIZATION
HAWAII INST. OF GEOPHYSICS		AIR FORCE OFFICE OF SCIENTIFIC RESEARCH

6c. ADDRESS (City, State and ZIP Code)	7b. ADDRESS (City, State and ZIP Code)
UNIVERSITY OF HAWAII HONOLULU, HAWAII 96822	BOLLING AFB, WASHINGTON, D.C. 20332 AFOSR/NP Bld 410

8a. NAME OF FUNDING/SPONSORING ORGANIZATION	8b. OFFICE SYMBOL (If applicable)	9. PROCUREMENT INSTRUMENT IDENTIFICATION NUMBER
AFOSR	NP	F49620-84-C-0003

8c. ADDRESS (City, State and ZIP Code)	10. SOURCE OF FUNDING NOS.			
AIR FORCE OF SCIENTIFIC RESEARCH BOLLING AFB, WASHINGTON D.C. 20332	PROGRAM ELEMENT NO.	PROJECT NO.	TASK NO.	WORK UNIT NO

11. TITLE (Include Security Classification)				
Hydrophone Investigations of . . .	61102F	2309	A3 .4	

12. PERSONAL AUTHOR(S)
DANIEL A. WALKER

13a. TYPE OF REPORT	13b. TIME COVERED 1985	14. DATE OF REPORT (Yr., Mo., Day)	15. PAGE COUNT
FINAL	FROM Oct. 1983 To Sept.	1986, April 30	11 with appendices

16. SUPPLEMENTARY NOTATION

17.	COSATI CODES		18. SUBJECT TERMS (Continue on reverse if necessary and identify by block number)
FIELD	GROUP	SUB. GR.	Underground Nuclear Explosions; Body-Waves; Spectral Analysis; Hydrophone Recordings; Discrimination; Noise Levels; . . .

19. ABSTRACT (Continue on reverse if necessary and identify by block number)

See Attached Sheet.

AIR FORCE OFFICE OF SCIENTIFIC RESEARCH (AFSC)
NOTICE OF TRANSMITTAL TO DTIC
This technical report has been reviewed and is
approved for public release IAW AFR 190-12.
Distribution is unlimited.
MATTHEW J. KERPER
Chief, Technical Information Division

20. DISTRIBUTION/AVAILABILITY OF ABSTRACT	21. ABSTRACT SECURITY CLASSIFICATION
UNCLASSIFIED/UNLIMITED ☒ SAME AS RPT ☒ DTIC USERS ☐	UNCLASSIFIED

22a. NAME OF RESPONSIBLE INDIVIDUAL	22b. TELEPHONE NUMBER (Include Area Code)	22c. OFFICE SYMBOL
	202-767-4908	

DD FORM 1473, 83 APR   EDITION OF 1 JAN 73 IS OBSOLETE.

REPORT DOCUMENTATION PAGE (cont'd)

11. Earthquake and Explosion Generated High Frequency Seismic Phases

18. Marine Seismology; Guided Phases; Po/So Phases; T-Phases

A-1

86   9   15   12
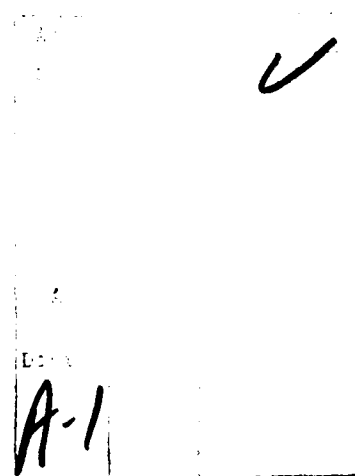
<u>Technical Report</u>

to the

Air Force Office of Scientific Research

from

Daniel A. Walker

Hawaii Institute of Geophysics

University of Hawaii

Honolulu, Hawaii 96822

Title of Work: Hydrophone Investigations of Earthquake and Explosion

Generated High-Frequency Seismic Phases

ABSTRACT

Data from the Wake Island Hydrophone Array has been used in a number of studies related to the detection and discrimination of underground nuclear explosions. These include: (1) comparative studies of explosion P phases from sites at comparable epicentral distances in the highly efficient propagational distance range of 60° to 90°; (2) some preliminary estimates of detection level thresholds; (3) estimates of deep ocean noise levels and comparisons to quiet continental sites; (4) determinations of the stability of yield estimates; and, (5) the location of significant earthquakes unreported by both the NEIS and ISC, but well-recorded at great distances by elements of the Wake array, in the interior and along the subducting margins of the Western Pacific Basin. The unreported earthquakes in the southwest Pacific have led, in part, to the discovery of a new subduction zone – the Micronesian Trench. Unreported earthquakes in the interior of the basin and along its subducting margins may also have associated gravitational effects of Air Force relevance. Finally, data from the Wake array has been useful in a partial resolution of the reported "mystery cloud" of 9 April 1984 and in the analysis of T-phases from underground explosions in the Tuamotus.

TABLE OF CONTENTS

I.   Wake Island Hydrophone Array: Recordings of Worldwide Underground
     Nuclear Explosions from September 1982 through December 1984, by
     Daniel A. Walker, Firmin J. Oliveira, and Charles S. McCreery, Data
     Report to the Air Force Office of Scientific Research and the U.S.
     Arms Control and Disarmament Agency, 201 pp., April 1986.

II. "Spectral comparisons between explosion P signals from the Tuamotu
     Islands, Nevada, and eastern Kazakh", by C.S. McCreery and D.A.
     Walker, Geophys. Res. Lett., 12, 353-356, 1985.

III. "Ambient infrasonic ocean noise and wind", by C.S. McCreery, in
     internal review at HIG, to be submitted to the Bulletin of the
     Seismological Society of America.

IV. "Deep ocean seismology", by D.A. Walker, Eos, 65, 2-3, 1984.

V.   "Significant unreported earthquakes in "aseismic" regions of the Western Pacific", by D.A. Walker and C.S. McCreery, <u>Geophys. Res. Lett.</u>, <u>12</u>, 433-436, 1985.

VI.   "Significant unreported earthquakes along the subducting margins of the Western Pacific basin, within its interior, and along the recently postulated Micronesian trench", by D. Walker, C. McCreery, and M. Iwatake, <u>Trans. Amer. Geophys. Union,</u> <u>66</u>, 1071, 1985.

VII. "Evidence for the formation of a new trench in the Western Pacific", by L. Kroenke and D. Walker, <u>Eos</u>, <u>67</u>, 145-146, 1986.

VIII. "T-Phases from test explosions in the Tuamotu Islands recorded by the Wake hydrophone array", by C.S. McCreery and D.A. Walker, <u>Technical Report to AFOSR</u>, Appendix 5, December 1984.

IX.   "Kaitoku Seamount and the mystery cloud of 9 April 1984, by D.A. Walker, C.S. McCreery, and F.J. Oliveira, <u>Science,</u> <u>227</u>, 607-611, 1985.

X.   "The Mystery Cloud", letter to the Editor, <u>Science</u>, submitted 1986.

XI.   "Stability of yield estimates based on P and P coda recorded by ocean hydrophones", by C. S. McCreery, in preparation.

XII. "Earthquakes in the 'aseismic' regions of the Western Pacific," by K. Muirhead and R. Adams, <u>Geophys. Res. Lett.</u>, 13, 169-172, 1986.

INTRODUCTION

Among the world's seismic stations, the Wake array is a unique facility. Not only is it one of the world's largest arrays with a maximum aperture of about 300 km, but it is also, to our knowledge, the world's deepest array with an average depth below sea level in excess cf 3 km. Relative to this array, most of the world's nuclear test sites are located within the highly efficient propagational distances range of 60° and 90° where mantle refracted paths are nearly vertical through highly attenuating regions of the upper mantle. Many of the test sites are at similar distances to Wake, thus providing unique opportunities for comparative studies. Also, total attenuation in the thin oceanic crust under the Northwestern Pacific Basin may be substantially lower than in the much thicker (and, perhaps, more complex) crust under conventional land-based seismic stations.

Furthermore, we contend that basins of the world's oceans have great potential as quiet sites for the detection of weak short-period seismic signals and that technological advancements will eventually permit the emplacement of economical worldwide arrays of deep ocean sensors. We also know that the existing networks of conventional stations are incapable of detecting some significant earthquakes within the interior of the Northwesten Pacific Basin and along its presumably well-monitored subducting margins.

These findings have far-reaching implications in terms of basic and applied research. One example in terms of basic research is the recently postulated Micronesian Trench characterized in part by earthquakes

unreported by the conventional worldwide array of seismic stations. Examples of implications for applied research are: (a) deep ocean basins may be the best sites for comprehensive and reliable comparative studies of underground nuclear explosions; and, (b) just as the existing worldwide array of conventional seismic stations is incapable of detecting some significant earthquakes in the interior of the Northwesten Pacific Basin and along its subducting margins, underground explosions in the interior of oceanic plates and along their subducting margins may also be similarly undetected by conventional land-based seismic stations.

In this final technical report, we summarize the accomplishments made possible by investigations of the Wake Island hydrophone data with the support provided by the Air Force Office of Scientific Research.

OVERVIEW

When work began on the current contract in October of 1983, our perceived tasks related entirely to the detection and discrimination of worldwide underground nuclear explosions. Specific areas of investigation included: (1) comparative studies of mantle-refracted P phases from explosions at existing test sites; (2) studies of ocean bottom noise levels; (3) array processing to determine threshold levels; and, (4) time permitting, some basic research on Po/So phases in recognition of possible future clandestine explosions in subducting margins and/or under the oceans. At the completion of the contract, comparative studies of explosion P phases and studies of ocean bottom noise levels were made. Comprehensive array processing appeared as an increasingly elusive, difficult, and time-consuming task - requiring. at the very least, more comprehensive long-term

studies of noise levels on the differing hydrophones; and, perhaps, ultimately requiring special calibration experiments. Nonetheless, some preliminary conservative estimates of detection thresholds for the differing test sites were made from an analysis of spectrums and noise-reduced spectograms for explosion P phases recorded on the two best hydrophones.

The major unexpected development during the course of the contract grew out of what was intended to be a minor investigation of Po/So phases which were well recorded at Wake, but not reported by the National Earthquake Information Service (NEIS) or the International Seismological Center (ISC). This minor degression led to the discovery of significant unreported earthquakes in the interior of the Western Pacific Basin, along the recently postulated Micronesian Trench, and along subducting margins of the Western Pacific Basin.

Finally, throughout the course of the contract period, copies of data tapes were sent to DARPA's Center for Seismic Studies for use by interested colleagues.

<center>SUMMARY OF ACCOMPLISHMENTS</center>

Explosion P Studies

Wake Island Hydrophone Array: Recordings of Worldwide Underground Nuclear Explosions from September 1982 through December 1984, by Daniel A. Walker, Firmin J. Oliveira, and Charles S. McCreery, Data Report to the Air Force Office of Scientific Research and the U.S. Arms Control and Disarmament Agency, 201 pp., April 1986.

Synopsis. This is a comprehensive and unprecedented presentation of all explosion P phases recorded by the Wake array from September 1982 through December 1984, with comparisons of signal strengths and frequencies using time series plots, spectrums, and spectrograms for the two hydrophones generally having the greatest signal-to-noise ratios.

Major Conclusions. Twenty-nine explosion P's were recorded from ten of the thirteen test sites reported for this time period. Signals from the differing sites are systematically characterized by very different spectral shapes and signal strengths. In general, signals for mb's in the high 4's from European and Asian sites may be observable under low-noise conditions. Higher thresholds are apparent for Tuamotu and Nevada explosions. These threshold estimates do not take into account any improvements possible from array processing, siting instruments in quieter ocean-floor locations, or the filtering out of noise incident at angles other than would be expected for explosion P phases. Thirteen events were recorded from E. Kazakh and possibly four from Nevada. Since the remaining twelve explosions were recorded from eight test sites, additional data is needed to verify some of the suggestions in this study.

"Spectral comparisons between explosion P signals from the Tuamotu Islands, Nevada, and eastern Kazakh", by C.S. McCreery and D.A. Walker, Geophys. Res. Lett., 12, 353-356, 1985.

Synopsis. In this study, the spectral content of P phases from underground nuclear explosions at three different test sites is examined. The Wake array is ideally suited for such a study because of low noise in the deep-oceans at high frequencies, the presence of high-frequency energy in P phases from underground explosions at great distances, and the general

equivalence of epicentral distances to Wake from each of the test sites (73° from E. Kazakh, 68° from Nevada, and 68° from the Tuamotus).

Major conclusions. For explosions of comparable magnitudes, the Tuamotu event appears to be the richest at frequencies below 1 Hz and the E. Kazakh event is the most energetic at frequencies above 2 Hz. Assuming that differences between the spectral character of these signals are due mostly to attenuation differences near the source, the data indicate increasing source attenuation from E. Kazakh to NTS to the Tuamotus, in that order. Additional data would also be needed to confirm these preliminary conclusions.

Ocean Bottom Noise

"Ambient infrasonic ocean noise and wind", by C.S. McCreery, in internal review at HIG, to be submitted to the Bulletin of the Seismological Society of America.

Synopsis. A comprehensive, long-term investigation of ocean bottom noise, based on random samples taken every six hours on four hydrophones for an entire year.

Major conclusions. For frequencies of 1/2 to 30 Hz the ambient ocean bottom noise level is strongly correlated with surface wind speeds. Worldwide values of average surface wind speeds indicate that many ocean bottom sites could be quieter than Wake, where noise levels are already generally comparable to quiet continental sites for frequencies greater than 3 Hz.

postulated Micronesian trench", by D. Walker, C. McCreery, and M. Iwatake, Trans. Amer. Geophys. Union, 66, 1071, 1985.

Synopsis. This is a comprehensive analysis of all unreported earthquakes recorded at Wake from September 1982 through December 1983.

Major Conclusions. Significant unreported earthquakes are not only found in the interior of the Western Pacific Basin and along the recently postulated Micronesian Trench, but also in the Marianas subduction zone. Similarly, comparable underground explosions, were they to occur in similar locations, might also be undetected by the existing conventional network of worldwide seismic stations.

"Evidence for the formation of a new trench in the Western Pacific", by L. Kroenke and D. Walker, Eos, 67, 145-146, 1986.

Synopsis. The tectonic history of the Southwest Pacific is summarized, and recent unreported earthquakes in the area are plotted.

Major Conclusions. A new subduction zone, the Micronesian Trench, is forming in the Southwest Pacific.

Other Investigations

"T-Phases from test explosions in the Tuamotu Islands recorded by the Wake hydrophone array", by C.S. McCreery and D.A. Walker, Technical Report to AFOSR, Appendix 5, December 1984.

Synopsis. In this report, T-phases from underground nuclear explosions in the Tuamotus on bottom and SOFAR hydrophones of the Wake array are analyzed and compared to similarly recorded T-phases from earthquakes at roughly comparable distances.

Major Conclusions. The explosion T-phases are relatively weaker than earthquake T-phases at frequencies above 10 Hz. Since it is uncertain whether this difference is primarily a source or path effect, further investigations would be needed to evaluate the utility of these observations for discrimination purposes. Regarding detection, it is probable that on the basis of SOFAR recorded T-phases, explosions with magnitudes as small as 3.3 mb could be detected.

"Kaitoku Seamount and the mystery cloud of 9 April 1984, by D.A. Walker, C.S. McCreery, and F.J. Oliveira, Science, 227, 607-611, 1985.

Synopsis. In this research article, data from the Wake hydrophone array is used to investigate the sightings, by the crews of three commercial aircraft, of an unusual cloud off the coast of Japan. The cloud was estimated to be 200 miles in diameter rising from a height of about 14,000 ft to 60,000 ft in approximately two minutes. These sightings were reported in differing news media, including Newsweek (p. 25, 30 April 1984). Although no unusual levels of radioactivity were found on any of the aircraft, speculation about the source of the cloud included the explosion of a nuclear submarine. Responsibility for the cloud was not acknowledged by any government.

Major Conclusions. In our investigations, initiated by inquiries for assistance from Teledyne Geotech, no T-phases were found on the SOFAR recordings at times which could be related to an underwater explosion at the site of the cloud. Since it is very unlikely that an underwater explosion which produced a 200-mile diameter cloud ascending from 14,000 ft to 60,000 ft in two minutes could go undetected on the SOFAR hydrophones, one conclusion is that the source of the cloud was not an underwater explosion.

Many other hypotheses were tested, with the final conclusion being that the mystery cloud was produced by either an as yet unknown natural phenomenon or a man-made atmospheric explosion.

"The Mystery Cloud", letter to the Editor, Science, submitted 1986.

Synopsis. The presumed location of the mystery cloud was reexamined with new testimony provided by the pilots of two aircraft.

Major Conclusions. The cloud was larger than estimated and further to the northwest, probably over the Kuril Islands or the Sea of Okhotsk, increasing the likelihood that it was associated with a Soviet test.

Software Development

Implicit in the foregoing studies are expenditures of effort for the development of software. One general program which has been developed is for plotting multiplexed digital data, such as the Wake digital hydrophone data, in a variety of ways. This program has proven to be extremely helpful, since a visual display of time series data is usually the starting point for more sophisticated analysis. The program is easy to set up and use, and it generates a raster file for direct output to a plotter. The program was used extensively in most of the recent studies discussed in this report. Many other investigators at HIG are now using this software for their own studies.

Other software developments necessary for our research included: (1) modifications of our spectrum and spectrogram generating programs to accept any length FFT, (2) creation of an epicenter location program using Po, So, and T arrival times, (3) creation of a suite of programs to strip off and

analyze data used for the long-term noise study, and (4) creation of a map-making program for plotting Wake data in more useful projections.

Related Studies

"Stability of yield estimates based on P and P coda recorded by ocean hydrophones", by C. S. McCreery, in preparation.

Synopsis. The stability of yield estimates determined from spectral amplitudes of teleseismic P and P coda recorded by ocean hydrophones is being evaluated using data from the Wake Island Array.

Major Conclusions. Based upon results of I. N. Gupta et al. ("Use of P Coda for Determination of Yield of Nuclear Explosions"; DARPA Technical Report) showing more precise yield estimates computed from spectral amplitudes of P coda relative to those from P, we expect to find similar improvements in the stability of yield estimates computed from P coda recorded by the Wake Island Array relative to those computed from P which were previously reported as having a standard deviation of around 0.03 mb for E. Kazakh events.

"Earthquakes in the °aseismic' regions of the Western Pacific," by K. Muirhead and R. Adams, Geophys. Res. Lett., 13, 169-172, 1986.

Synopsis. ISC data was reexamined for evidence of the previously unreported earthquakes discussed by Walker and McCreery in an earlier report in this journal.

Major Conclusions. Only the largest of the unreported events discussed by Walker and McCreery could be located upon reexamination of the ISC data.

The Wake array is a particularly sensitive installation for detecting earthquakes in this area of the Pacific.

CONCLUDING REMARKS

We are grateful to AFOSR for the support which made these exciting discoveries possible. We are convinced of their importance to basic and applied research, and we hope that our performance will serve to encourage AFOSR in continuing its advocacy of university supported research.

WAKE ISLAND HYDROPHONE ARRAY:

RECORDINGS OF WORLDWIDE UNDERGROUND NUCLEAR

EXPLOSIONS FROM SEPTEMBER 1982 THROUGH DECEMBER 1984

by

Daniel A. Walker

Charles S. McCreery

Firmin J. Oliveira

April 1986

Data Report

for the

Air Force Office of Scientific Research and

the U.S. Arms Control and Disarmament Agency

PREFACE

Among the world's seismic stations, the Wake array is a unique facility. Not only is it one of the world's largest arrays with a maximum aperture of about 300 km, but also is, to our knowledge, the world's deepest array with an average depth below sea level in excess of 3 km. Relative to this array, most of the world's nuclear test sites are located within the highly efficient propagational distance range of 60° to 90° where mantle refracted paths are nearly vertical through highly attenuating regions of the upper mantle. Also, total attenuation in the thin oceanic crust under the Northwestern Pacific Basin may be substantially lower than in the much thicker (and, perhaps, more complex) crust under conventional land-based seismic stations.

Furthermore, we contend that basins of the world's oceans have great potential as quiet sites for the detection of weak short-period seismic signals [D. Walker, "Deep ocean seismology", Eos, 65, 2-3, 1984.] and that technological advancements will eventually permit the emplacement of economical worldwide arrays of deep ocean sensors. We also know that the existing networks of conventional stations are incapable of detecting significant earthquakes within the interior of the Northwestern Pacific Basin and along its presumably well-monitored subducting margins [D. Walker and C. McCreery, "Significant unreported earthquakes in `aseismic' regions of the western Pacific", Geophys. Res. Lett., 12, 433-436, 1985; and D. Walker, C. McCreery, and M. Iwatake, "Significant unreported earthquakes along the subducting margins of the Western Pacific Basin, within its interior, and along the recently postulated Micronesian Trench", Eos, 66, 1071, 1985.]

These findings have far-reaching implications in terms of basic and applied research. One example in terms of basic research is the recently postulated Micronesian Trench characterized in part by earthquakes unreported by the conventional worldwide array of seismic stations [L. Kroenke and D. Walker, "Evidence for the formation of a new trench in the western Pacific", Eos, 67, 145-146, 1986.] Examples of implications for applied research are: (a) deep ocean basins may be the best sites for comprehensive and reliable comparative studies of underground nuclear explosions; and, (b) just as the existing worldwide array of conventional seismic stations is incapable of detecting significant earthquakes in the interior of the Northwestern Pacific Basin and along its subducting margins, underground explosion in the interior of ocean plates and along their subducting margins may also be similarly undetected by conventional land-based seismic stations.

In the data report which follows, our attention is directed specifically towards a preliminary qualitative comparison of all the mantle-refracted P phases from underground tests recorded on the Wake array from September 1982 through December 1984. The data examined includes time series plots, spectrums, and noise reduced spectrograms. Recordings on three of the best hydrophones of the eleven element array are used. It is suggested that apparent differences in responses to signals from differing sites are due to: (a) effects near the test sites; and, (b) small variations in azimuths and the emergence angles of signals combined with structural irregularities along the mantle-refracted P path near the receivers. The largest data set from a single test site consists of thirteen observations. The smallest data set of one observation was found for six sites, each only having one reported explosion. Other sites

contained four, two, and, possibly, four observations. Thus, additional data is needed to verify some of the preliminary observations found in this report. Data from the Wake Island hydrophone array is sent to the Center for Seismic Studies for use by interested colleagues.

TABLE OF CONTENTS

Errata:

    - The analysis of Siberian explosions does not begin on page 100
      as indicated in the "Table of Contents". It begins, instead,
      on page 110.

    - The time series plots for event numbers 2223 through 2927 are
      mislabeled for two of the channels. Channel 1 is, in fact, a
      repetition of channel 73, while channel 4 is a repetition of
      channel 74.

INTRODUCTION

In September of 1982, the Hawaii Institute of Geophysics installed a computer-controlled, digital tape-recording system on Wake Island to monitor signals from a 300-km aperture, eleven element array of hydrophones located on the deep-ocean floor and in the SOFAR channel near Wake. Support for this installation and for subsequent investigations was provided by the Air Force Office of Scientific Research and the U.S. Arms Control and Disarmament Agency. Areas of interest included mantle-refracted P phases from the world's major underground nuclear test sites, as well as Po/So and T-phases from the Western Pacific. Although research reports have been published concerning explosion P phases, a data report was needed for comprehensive comparisons of all explosion P phases recorded on all the different hydrophones.

Figure 1 shows the relative distribution of elements in the Wake array. An estimated response curve for the hydrophone and recording system is given in Figure 2. Figure 3 shows the locations of tests from September 1982 through December 1984 as taken from "Preliminary Determination of Epicenters" (PDE) lists provided by the U.S. National Earthquake Information Service (NEIS). Table 1 contains NEIS data for explosions at these sites from September 1982 through December 1984. Estimates of noise levels on hydrophones 74, 76, and 2, which generally have the highest signal-to-noise ratios for explosion P phases, are given in Figures 4, 5, and 6. A comparison between the mean noise levels of these three hydrophones is given in Figure 7.
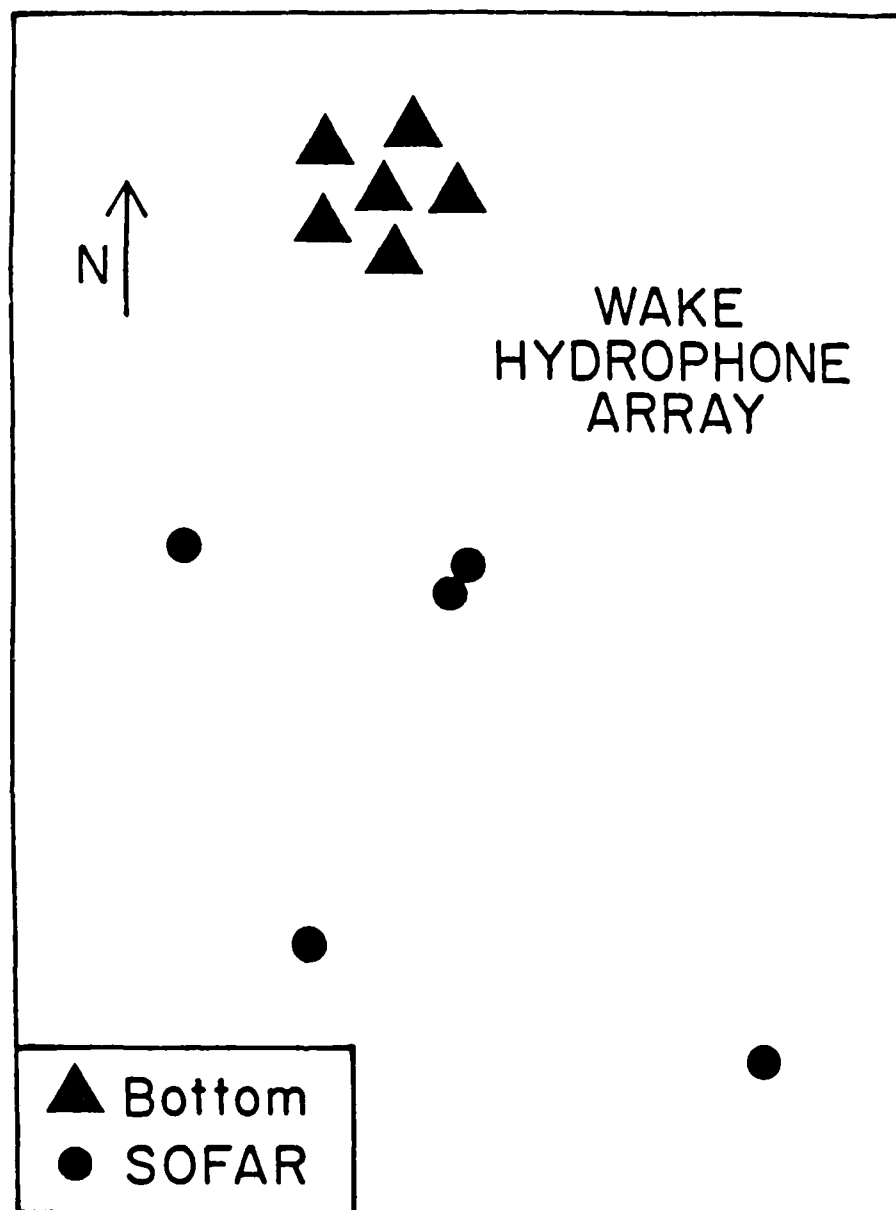
Figure 1. Relative locations of bottom and SOFAR hydrophones of the Wake array.
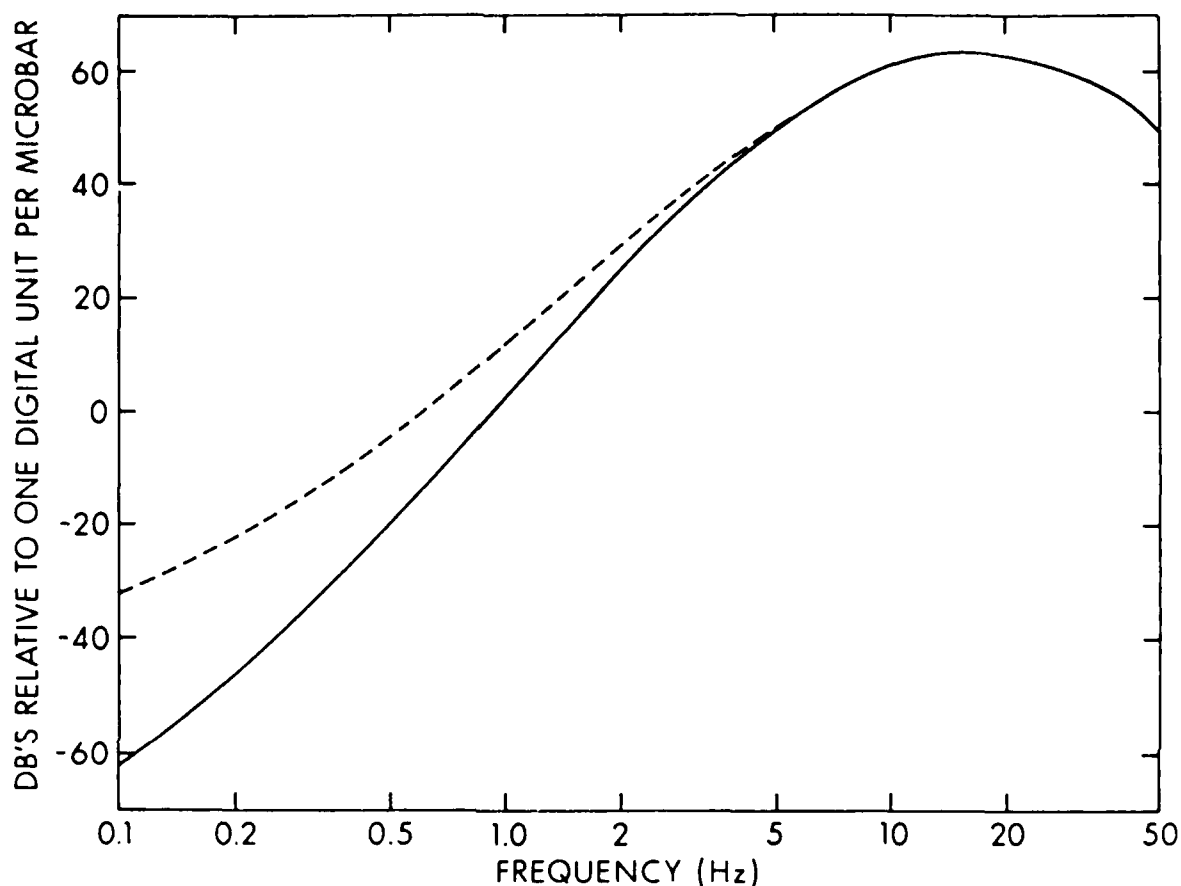
Figure 2. Amplitude response of the Wake array hydrophones and digital
recording system. The solid curve represents a combination of
the hydrophone response, taken from a Columbia University
technical report ("OBS Calibration Manual" by S. N. Thanos; 15
April 1966), and the response of the amplifiers and filters of
the recording system at Wake, measured in situ. The Columbia OBS
used a hydrophone identical to those of the Wake array. The
response values reported in their manual were not measured, but
simply extrapolated from higher frequency response data and
considerations of the actual hydrophone design. One of those

considerations was a small pressure compensation hole in the instrument case, resulting in an additional falloff of 6 dB per octave below 3.5 Hz. Since the hydrophones have been in place for over 20 years, it may be that this hole is now filled. The dashed curve shows the system response without the pressure compensation hole (i.e. without the 3.5 Hz corner). This curve is shown for reference only, since the spectra in this report which show absolute pressure levels were computed using the solid curve. A factor not considered in this curve is the response of the cables connecting the hydrophones to Wake. This factor, different for each hydrophone, is unknown but could reduce the response at higher frequencies (>10 Hz) by 10 dB or more.
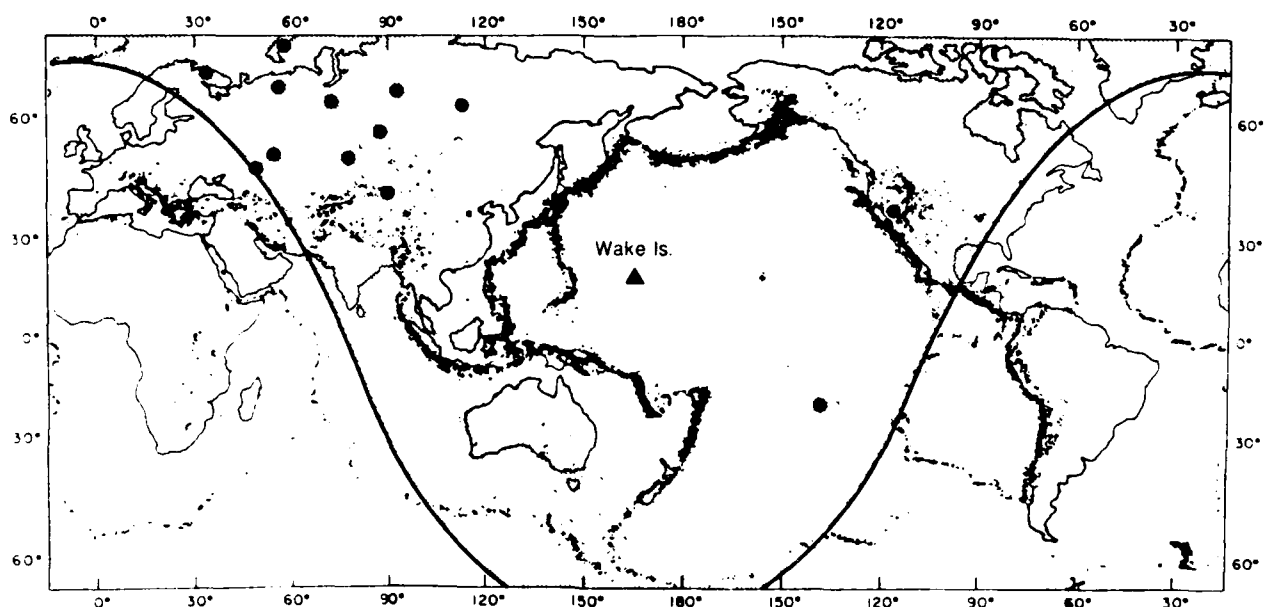
Figure 3. Map showing the location of Wake Island relative to the world's major nuclear test sites (solid circles). The shaded region approximates distances to Wake from 60° to 90°. At distances greater than about 60°, only a small portion of the P travel path is in the highly attenuating asthenosphere. At distances beyond 90°, no P energy is observed because of refraction into the core. Earthquake epicenters (small dots) show the world's active seismic zones.

TABLE 1.

```
EVNT ******ORIGIN TIME****** **COORDINATES*** *********LOCATION*********    ****
*NO* YR*MO*DA*JUL*HR*MN*SECS  **LAT*****LON*** ********DESCRIPTION*******    *MB*

0074 82 09 21 264 02:57:01.1 49.909N  78.229E EASTERN KAZAKH SSR             5.2
0082 82 09 23 266 16:00:00.0 37.212N 116.207W SOUTHERN NEVADA               4.9
0083 82 09 23 266 17:00:00.0 37.175N 116.088W SOUTHERN NEVADA               4.9
0094 82 09 25 268 17:59:57.0 64.311N  91.859E CENTRAL SIBERIA               5.1
0110 82 09 29 272 13:30:00.1 37.091N 116.045W SOUTHERN NEVADA               0.0
0154 82 10 10 283 04:59:56.8 61.555N 112.833E SIBERIA                       5.3
0158 82 10 11 284 07:14:58.1 73.368N  54.532E NOVAYA ZEMLYA                 5.6
0170 82 10 16 289 05:59:57.2 46.727N  48.162E SOUTHWESTERN USSR             5.2
0171 82 10 16 289 06:04:57.1 46.723N  48.222E SOUTHWESTERN USSR             5.3
0172 82 10 16 289 06:09:57.1 46.748N  48.258E SOUTHWESTERN USSR             5.2
0173 82 10 16 289 06:14:57.1 46.707N  48.230E SOUTHWESTERN USSR             5.4
0268 82 11 12 316 19:17:00.1 37.024N 116.032W SOUTHERN NEVADA               4.4
0345 82 12 05 339 03:37:12.6 49.907N  78.843E EASTERN KAZAKH SSR            6.1
0363 82 12 10 344 15:20:00.0 37.030N 116.072W SOUTHERN NEVADA               4.8
0438 82 12 26 360 03:35:14.3 50.070N  79.009E EASTERN KAZAKH SSR            5.7
0649 83 02 11 042 16:00:00.1 37.051N 116.045W SOUTHERN NEVADA               0.0
0674 83 02 17 048 17:00:00.0 37.163N 116.063W SOUTHERN NEVADA               4.0
0836 83 03 26 085 20:20:00.0 37.301N 116.460W SOUTHERN NEVADA               5.1
0898 83 04 12 102 03:41:05.2 49.815N  78.222E EASTERN KAZAKH SSR            4.9
0912 83 04 14 104 19:05:00.1 37.073N 116.046W SOUTHERN NEVADA               5.7
0939 83 04 19 109 18:52:58.4 21.864S 138.941W TUAMOTU ARCHIPELAGO REGION    5.6
0951 83 04 22 112 13:53:00.0 37.112N 116.022W SOUTHERN NEVADA               4.0
1010 83 05 05 125 15:20:00.0 37.012N 116.089W SOUTHERN NEVADA               4.5
1075 83 05 25 145 17:30:58.2 21.912S 138.936W TUAMOTU ARCHIPELAGO REGION    5.9
1084 83 05 26 146 15:00:00.0 37.103N 116.006W SOUTHERN NEVADA               4.3
1111 83 05 30 150 03:33:44.6 49.740N  78.210E EASTERN KAZAKH SSR            5.4
1157 83 06 09 160 17:10:00.0 37.158N 116.089W SOUTHERN NEVADA               4.6
1170 83 06 12 163 02:36:43.5 49.894N  78.964E EASTERN KAZAKH SSR            6.1
1252 83 06 28 179 17:45:58.2 21.815S 138.950W TUAMOTU ARCHIPELAGO REGION    5.4
1312 83 07 10 191 03:59:57.0 51.327N  53.286E EUROPEAN USSR                 5.3
1313 83 07 10 191 04:04:57.0 51.336N  53.290E EUROPEAN USSR                 5.4
1314 83 07 10 191 04:09:57.1 51.357N  53.301E EUROPEAN USSR                 5.2
1434 83 08 03 215 13:33:00.0 37.119N 116.089W SOUTHERN NEVADA               4.2
1487 83 08 18 230 16:09:58.6 73.373N  54.839E NOVAYA ZEMLYA                 5.9
1541 83 09 01 244 14:00:00.0 37.273N 116.355W SOUTHERN NEVADA               5.4
1567 83 09 11 254 06:33:10.1 49.801N  78.244E EASTERN KAZAKH SSR            5.1
1607 83 09 21 264 15:00:00.0 37.210N 116.210W SOUTHERN NEVADA               0.0
1610 83 09 22 265 15:00:00.0 37.106N 116.049W SOUTHERN NEVADA               0.0
1623 83 09 24 267 04:59:56.9 46.773N  48.300E SOUTHWESTERN USSR             5.1
1624 83 09 24 267 05:04:56.8 46.763N  48.281E SOUTHWESTERN USSR             5.0
1625 83 09 24 267 05:09:57.7 46.872N  48.214E SOUTHWESTERN USSR             4.9
1626 83 09 24 267 05:14:56.9 46.748N  48.299E SOUTHWESTERN USSR             5.1
1627 83 09 24 267 05:19:57.0 46.772N  48.267E SOUTHWESTERN USSR             5.2
1628 83 09 24 267 05:24:56.8 46.758N  48.257E SOUTHWESTERN USSR             5.2
1636 83 09 25 268 13:09:57.7 73.341N  54.501E NOVAYA ZEMLYA                 5.8
```

TABLE 1.   (cont'd)

| EVNT | | | |ORIGIN TIME| | | | |COORDINATES| | |LOCATION DESCRIPTION| |MB |
|---|---|---|---|---|---|---|---|---|---|---|---|---|---|
| *NO* | YR | MO | DA | JUL | HR | MN | SECS | *LAT* | *LON* | | | | *MB* |
| 1674 | 83 | 10 | 06 | 279 | 01 | 47 | 06.6 | 49.933N | 78.833E | EASTERN KAZAKH SSR | | | 6.0 |
| 1727 | 83 | 10 | 26 | 299 | 01 | 55 | 04.8 | 49.883N | 78.856E | EASTERN KAZAKH SSR | | | 6.1 |
| 1816 | 83 | 11 | 20 | 324 | 03 | 27 | 04.4 | 50.069N | 79.033E | EASTERN KAZAKH SSR | | | 5.4 |
| 1844 | 83 | 11 | 29 | 333 | 02 | 19 | 06.5 | 49.795N | 78.191E | EASTERN KAZAKH SSR | | | 5.4 |
| 1913 | 83 | 12 | 16 | 350 | 18 | 30 | 00.0 | 37.140N | 116.072W | SOUTHERN NEVADA | | | 5.1 |
| 1952 | 83 | 12 | 26 | 360 | 04 | 29 | 06.8 | 49.829N | 78.215E | EASTERN KAZAKH SSR | | | 5.5 |
| 2157 | 84 | 02 | 15 | 046 | 17 | 00 | 00.1 | 37.221N | 116.181W | SOUTHERN NEVADA | | | 5.0 |
| 2177 | 84 | 02 | 19 | 050 | 03 | 57 | 03.3 | 49.888N | 78.788E | EASTERN KAZAKH SSR | | | 5.9 |
| 2223 | 84 | 03 | 01 | 061 | 17 | 45 | 00.0 | 37.066N | 116.046W | SOUTHERN NEVADA | | | 5.9 |
| 2247 | 94 | 03 | 07 | 067 | 02 | 39 | 06.3 | 50.022N | 78.978E | EASTERN KAZAKH SSR | | | 5.6 |
| 2352 | 84 | 03 | 29 | 089 | 05 | 19 | 08.1 | 49.934N | 79.013E | EASTERN KAZAKH SSR | | | 5.9 |
| 2372 | 84 | 03 | 31 | 091 | 14 | 30 | 00.0 | 37.146N | 116.084W | SOUTHERN NEVADA | | | 4.3 |
| 2459 | 84 | 04 | 15 | 106 | 03 | 17 | 05.2 | 49.766N | 78.185E | EASTERN KAZAKH SSR | | | 5.7 |
| 2498 | 84 | 04 | 25 | 116 | 01 | 09 | 03.5 | 49.934N | 78.915E | EASTERN KAZAKH SSR | | | 6.0 |
| 2523 | 84 | 05 | 01 | 122 | 19 | 05 | 00.0 | 37.106N | 116.022W | SOUTHERN NEVADA | | | 5.3 |
| 2554 | 64 | 05 | 12 | 133 | 17 | 30 | 58.2 | 21.808S | 139.013W | TUAMOTU ARCHIPELAGO REGION | | | 5.7 |
| 2608 | 84 | 05 | 26 | 147 | 03 | 13 | 12.3 | 49.949N | 79.060E | EASTERN KAZAKH SSR | | | 6.1 |
| 2629 | 64 | 05 | 31 | 152 | 01 | 04 | 00.1 | 37.103N | 116.048W | SOUTHERN NEVADA | | | 5.7 |
| 2695 | 84 | 06 | 16 | 168 | 17 | 43 | 57.7 | 21.932S | 139.020W | TUAMOTU ARCHIPELAGO REGION | | | 5.4 |
| 2709 | 84 | 06 | 20 | 172 | 15 | 15 | 00.0 | 37.000N | 116.043W | SOUTHERN NEVADA | | | 4.8 |
| 2812 | 84 | 07 | 14 | 196 | 01 | 09 | 10.4 | 49.902N | 78.988E | EASTERN KAZAKH SSR | | | 6.1 |
| 2848 | 84 | 07 | 21 | 203 | 02 | 59 | 57.1 | 51.366N | 53.253E | EUROPEAN USSR | | | 5.3 |
| 2849 | 84 | 07 | 21 | 203 | 03 | 04 | 57.0 | 51.384N | 53.271E | EUROPEAN USSR | | | 5.2 |
| 2850 | 84 | 07 | 21 | 203 | 03 | 09 | 57.1 | 51.366N | 53.276E | EUROPEAN USSR | | | 5.3 |
| 2876 | 84 | 07 | 25 | 207 | 15 | 30 | 00.0 | 37.268N | 116.411W | SOUTHERN NEVADA | | | 5.4 |
| 2898 | 84 | 08 | 02 | 215 | 15 | 00 | 00.0 | 37.017N | 116.008W | SOUTHERN NEVADA | | | 4.8 |
| 2927 | 84 | 08 | 11 | 224 | 18 | 59 | 57.4 | 65.079N | 55.287E | URAL MOUNTAINS REGION | | | 5.2 |
| 2992 | 84 | 08 | 25 | 238 | 18 | 59 | 58.5 | 61.889N | 72.149E | WESTERN SIBERIA | | | 5.3 |
| 2997 | 84 | 08 | 27 | 240 | 05 | 59 | 57.5 | 67.831N | 33.450E | EUROPEAN USSR AREA 2 | | | 4.4 |
| 3011 | 84 | 08 | 30 | 243 | 14 | 45 | 00.1 | 37.090N | 115.998W | SOUTHERN NEVADA | | | 4.4 |
| 3040 | 84 | 09 | 09 | 253 | 02 | 59 | 06.3 | 49.873N | 78.208E | EASTERN KAZAKH SSR | | | 5.0 |
| 3047 | 84 | 09 | 13 | 257 | 14 | 00 | 00.0 | 37.087N | 116.071W | SOUTHERN NEVADA | | | 5.0 |
| 3052 | 84 | 09 | 17 | 261 | 02 | 59 | 57.4 | 55.835N | 87.408E | CENTRAL USSR | | | 4.9 |
| 3090 | 94 | 10 | 03 | 277 | 05 | 59 | 57.7 | 41.633N | 88.781E | SOUTHERN XINJIANG, CHINA | | | 5.3 |
| 3110 | 84 | 10 | 18 | 292 | 04 | 57 | 05.4 | 49.787N | 78.004E | EASTERN KAZAKH SSR | | | 4.6 |
| 3123 | 84 | 10 | 25 | 299 | 06 | 29 | 57.6 | 73.365N | 54.979E | NOVAYA ZEMLYA | | | 5.8 |
| 3126 | 84 | 10 | 27 | 301 | 01 | 50 | 10.6 | 49.950N | 78.842E | EASTERN KAZAKH SSR | | | 6.2 |
| 3127 | 84 | 10 | 27 | 301 | 05 | 59 | 58.6 | 47.044N | 47.919E | SOUTHWESTRN USSR | | | 4.8 |
| 3143 | 84 | 11 | 02 | 307 | 20 | 44 | 58.3 | 21.904S | 139.003W | TUAMOTU ARCHIPELAGO REGION | | | 5.7 |
| 3202 | 84 | 12 | 02 | 337 | 03 | 19 | 06.2 | 49.989N | 79.091E | EASTERN KAZAKH SSR | | | 5.8 |
| 3217 | 84 | 12 | 06 | 341 | 17 | 28 | 58.3 | 21.890S | 138.954W | TUAMOTU ARCHIPELAGO REGION | | | 5.7 |
| 3222 | 84 | 12 | 09 | 344 | 19 | 40 | 00.0 | 37.270N | 116.498W | SOUTHERN NEVADA | | | 5.5 |
| 3229 | 84 | 12 | 15 | 350 | 14 | 45 | 00.0 | 37.281N | 116.305W | SOUTHERN NEVADA | | | 5.4 |
| 3230 | 84 | 12 | 16 | 351 | 03 | 55 | 02.7 | 49.968N | 78.893E | EASTERN KAZAKH SSR | | | 6.1 |
| 3249 | 84 | 12 | 28 | 363 | 03 | 50 | 10.5 | 49.863N | 78.785E | EASTERN KAZAKH SSR | | | 6.0 |
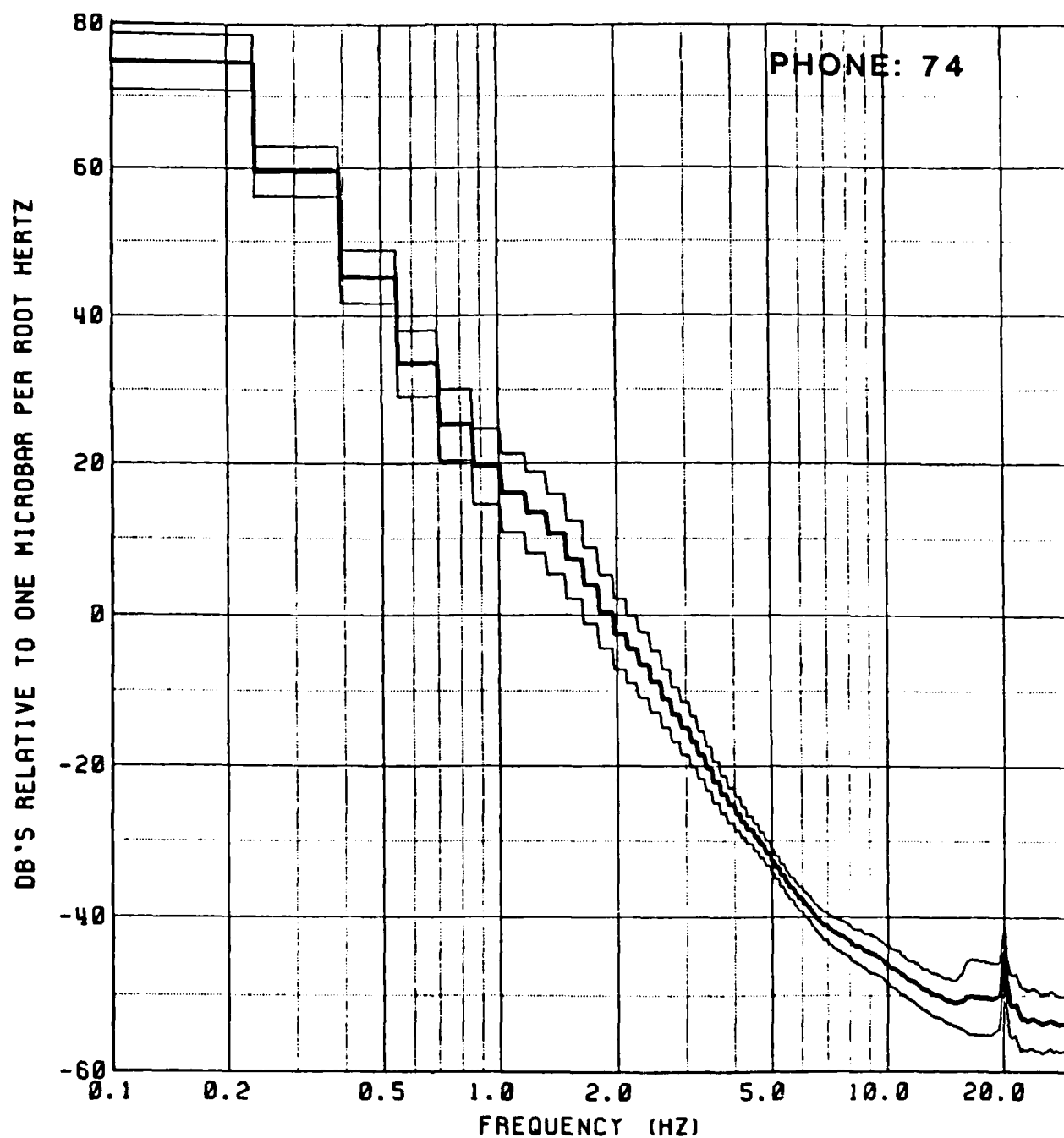
Figure 4. One-year average ambient noise level, plus and minus one
standard deviation, from hydrophone 74, based on 1460 three-
minute noise samples taken approximately every six hours between
8 September 1982 and 8 September 1983. The standard deviations
shown may be somewhat misleading, however, since the actual
distribution of levels at each frequency is generally not
Gaussian. The spike at 20 Hz is due to aliasing from a large 60
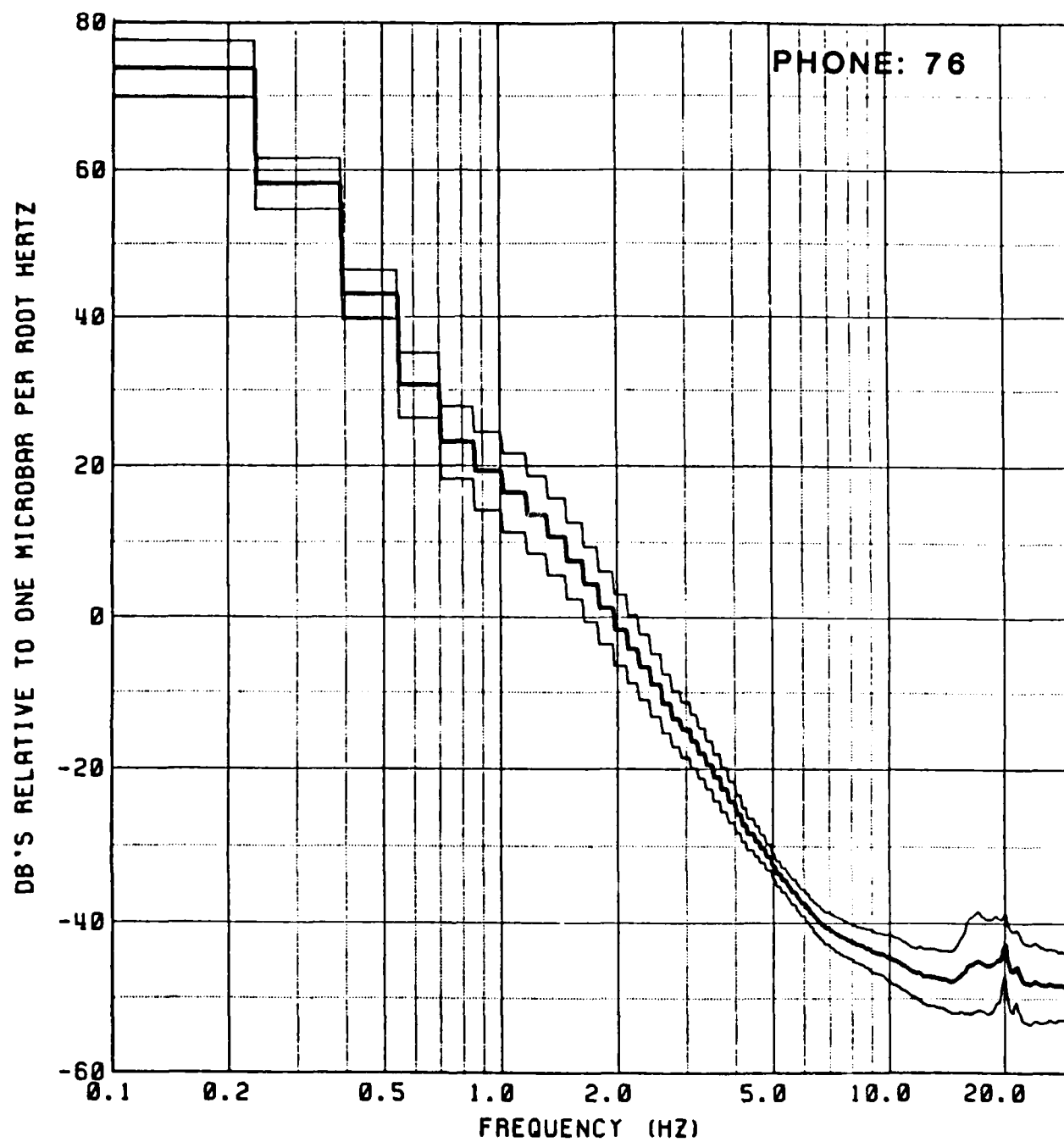Hz spike in the original data.

9

Figure 5. One year average ambient noise levels on phone 76.
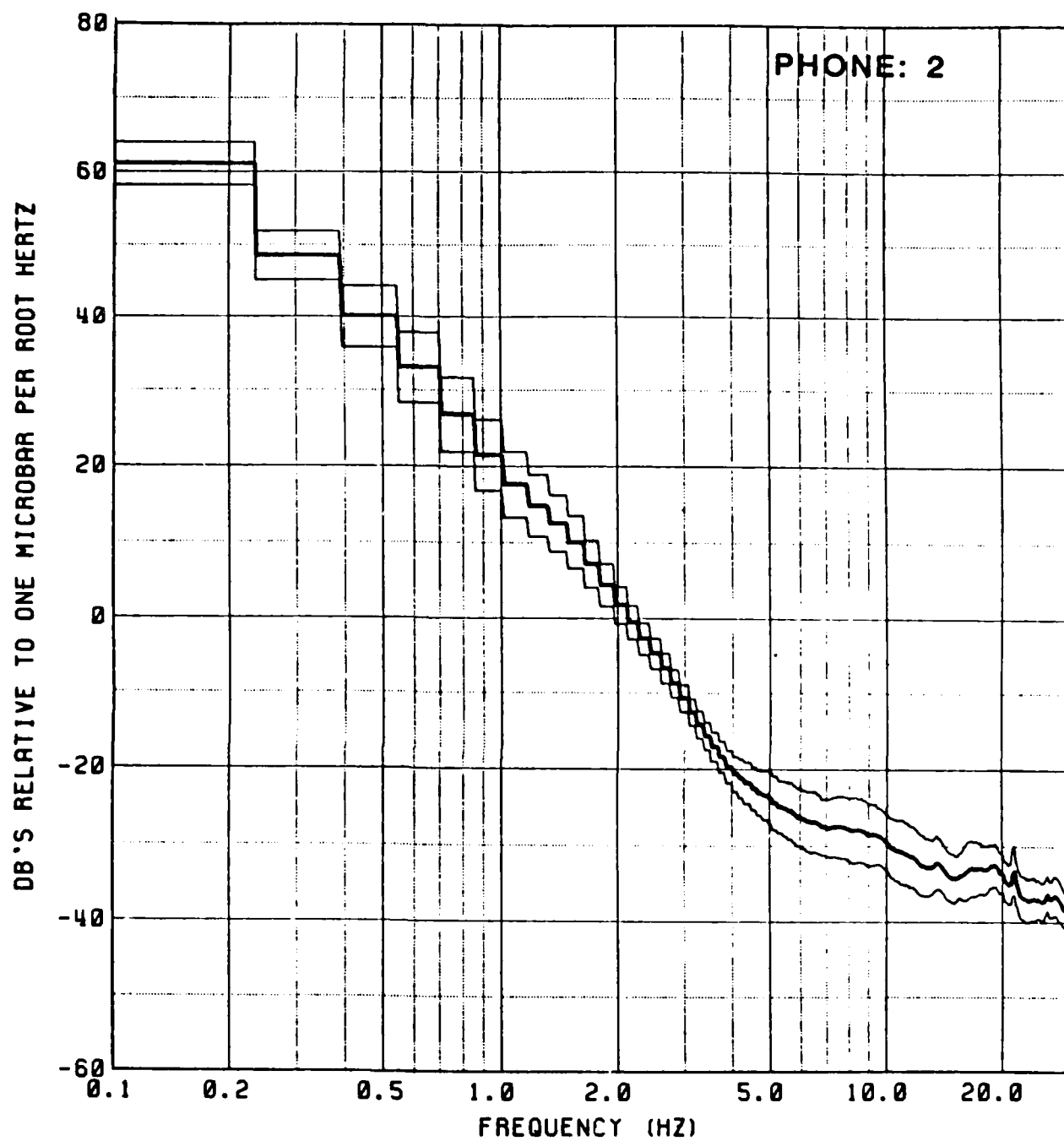
Figure 6. One year average ambient noise levels on phone 2.
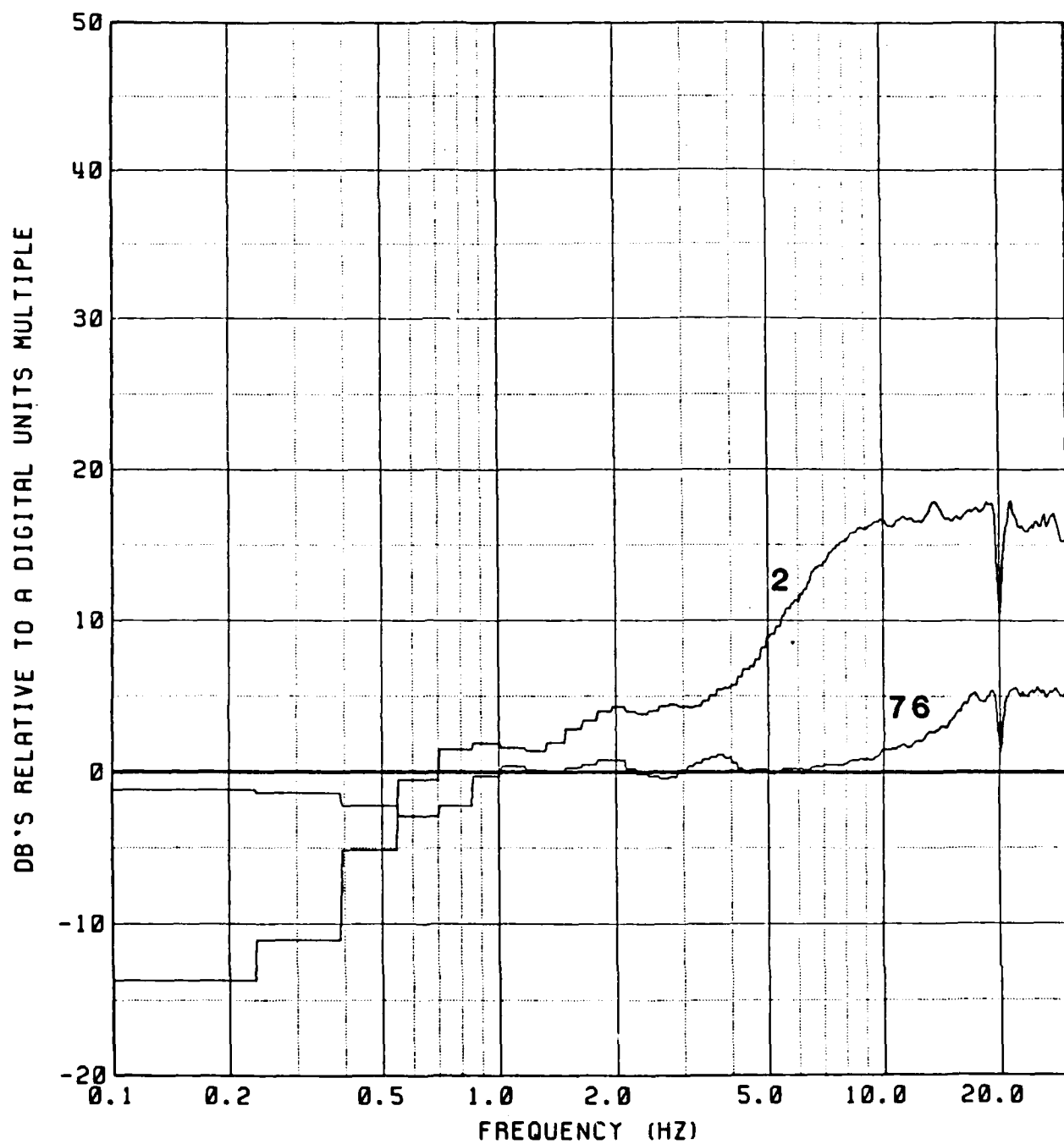
Figure 7. Yearly mean noise levels of phones 76 and 2 measured with
respect to the yearly mean noise level of phone 74. Differences
between 76 and 74 are fairly small except at the higher
frequencies (>10 Hz) where differences may be due to the

differing cable lengths of hydrophones 74 and 76. Differences
between 2 and 74 are much larger and are probably due to a
combination of the much noisier high-frequency environment at
phone 2's location in the SOFAR channel and the decreased
amplitudes of the lower frequency noise due to phone 2's closer
proximity to the ocean's free surface. Cable lengths of 2 and
74 are nearly identical.

DESCRIPTION OF DATA PRESENTED

Explosion generated P phases recorded by elements of the Wake array are presented in a variety of formats. These include time series plots, spectrums, and spectrograms. Time series plots are shown for five of the bottom hydrophones and three of the SOFAR hydrophones; spectrums are presented only for hydrophones 74, 76, and 2; and noise-reduced spectrograms are presented for hydrophone 74. Also, for each test site, a table is presented which summarizes the NEIS data given in Table 1. For those explosions which have, or appear to have, some signature on one or more of the hydrophones, an additional table includes the epicentral distances to phones 74, 76, and 2, as well as the signal and noise levels estimated to the nearest 0.5 dB at 2 Hz on each of these hydrophones as taken from their respective spectrums. Time series plots, spectrums, and spectrograms are only shown for those explosions which have, or appear to have, some signature on one or more of the hydrophones. Presentations for each test site conclude with a brief discussion of the data. Examples and detailed descriptions of the different plots follow.

Time Series Plots

These plots (e.g., Fig. 8) show the time series of the P arrival on the different hydrophones indicated at the left of each plot. The time series were bandpass filtered between 1.5 and 5 Hz with a 4-pole Butterworth filter. The absolute scale for each time series is the same for all channels and all events. For each event vertical lines represent the same time on all traces, so P arrivals are offset from one another by an amount
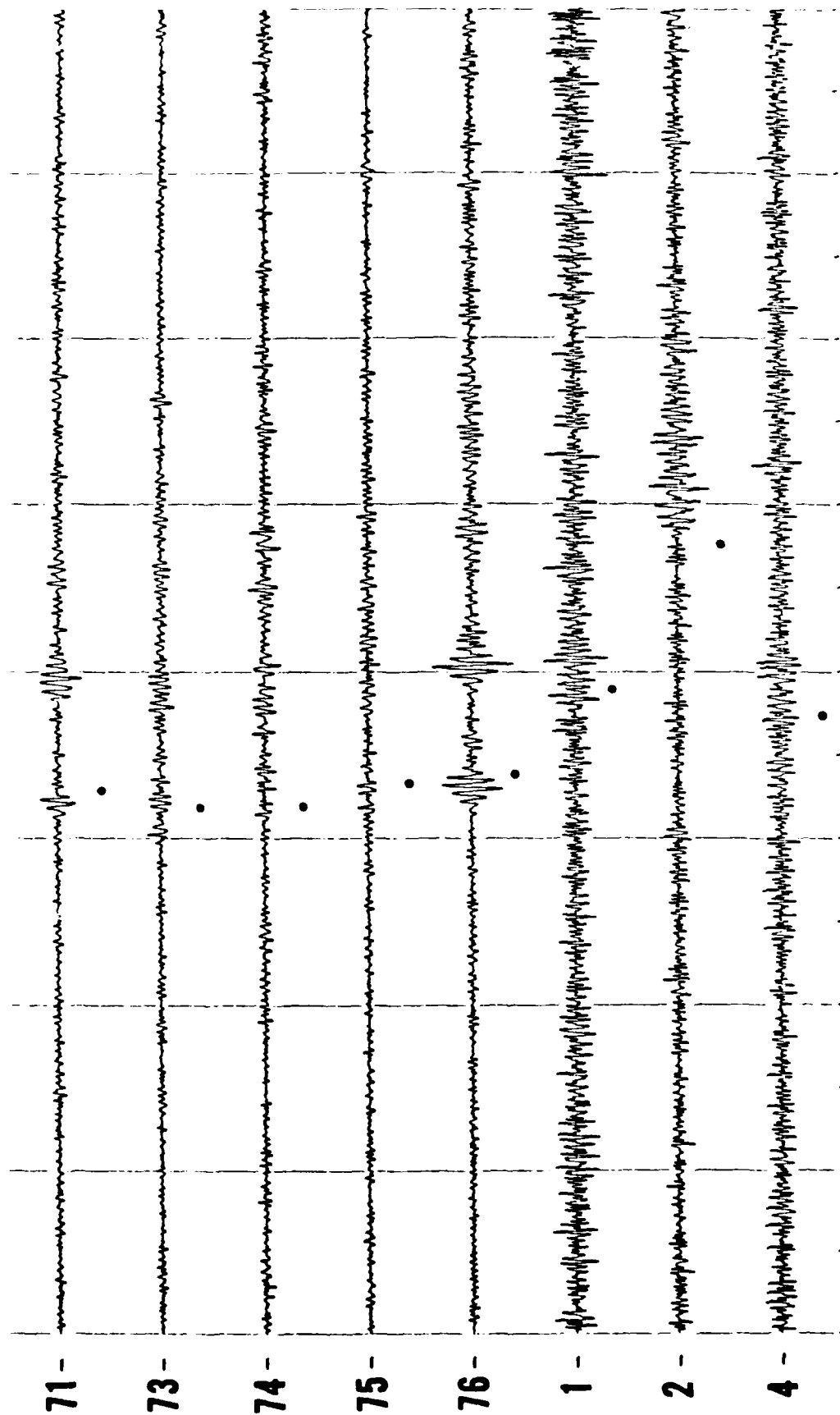
Figure 8. Example of a time series plot. See text for explanation.

appropriate to differences in their travel paths. On the bottom phones, the initial P pulse, which is not always clear, is followed by a series of water column multiples, each with a 180° phase shift, at approximately seven-second intervals corresponding to the round-trip water-column travel-time at 5.5-km depth. The first of these multiples is often larger than the initial pulse because it is the combination of both downward and upward propagating energy at the ocean-sediment interface. Water column multiples with smaller offsets are also present on the SOFAR hydrophones but are less obvious. Solid circles indicate the expected arrival times for the initial pulse. Open circles were used if there was uncertainty in identifying apparent pulses on all of the hydrophone channels shown in the time series plot.

Spectra

Spectra (e.g., Fig. 9) were computed by averaging the power spectral estimates from 512-point FFT's applied to the section of the time series of interest digitized at 80 samples/sec. The top of the shaded region in each figure represents 115.2 seconds (35 FFT's) of noise immediately prior to the P arrival. The heavy, sometimes broken, curve represents 22.4 seconds (6 FFT's) at the time of the P onset where the power level was at least 1 dB above the noise. FFT's for the P and its noise were taken with a 50% overlap to avoid losing important parts of signal near FFT boundaries which might have been tapered out by the window. The thin curve represents an average of 1460, 3-minute noise samples (28 FFT's per 3-minute sample) from the appropriate hydrophone spaced approximately every six hours over an entire year (9/8/82 - 9/8/83). FFT's taken on each of these 3-minute samples did not overlap.
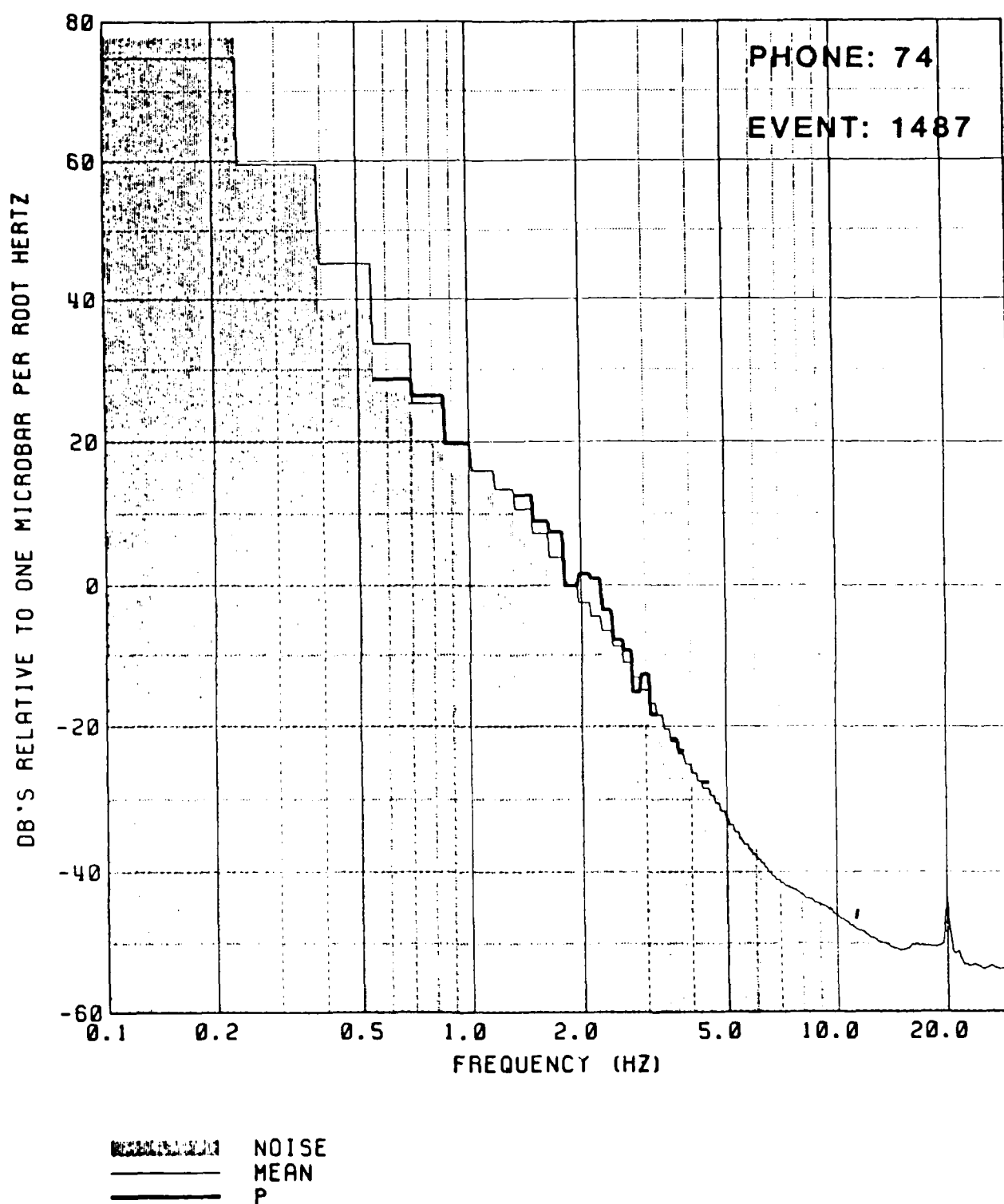
Figure 9. Example of a spectrum. See text for explanation.

Noise Reduced Spectrograms

Spectrograms (e.g., Fig. 10) were made by dividing the time series into
50% overlapping, 512-point segments, Lanczos-squared windowing the segments,
and performing a fast Fourier transform (FFT) on each segment. In the
horizontal direction, the width of each shaded block (i.e., the interval
between the marks along the axis) corresponds to one of the 512-point
segments in the time series. In the vertical direction, each block is the
average of 0.80 adjacent power spectral estimates out of the FFT. Only
frequencies from 0 to 10 Hz are shown, although the Nyquist frequency was 40
Hz. For noise reduction, mean spectral values and standard deviations
(S.D.'s) were determined for each frequency block using a 3-minute sample of
noise just prior to the onset of the P phase. Then in the noise reduced
spectrograms shown, only those levels that were at least 1.25 S.D.'s above
the mean noise value at each frequency were plotted as a gray block. Actual
signal levels, uncorrected for system response, are indicated by the gray
shades, with 10 dB between shades.

18

PHONE: 74

EVENT: 1487
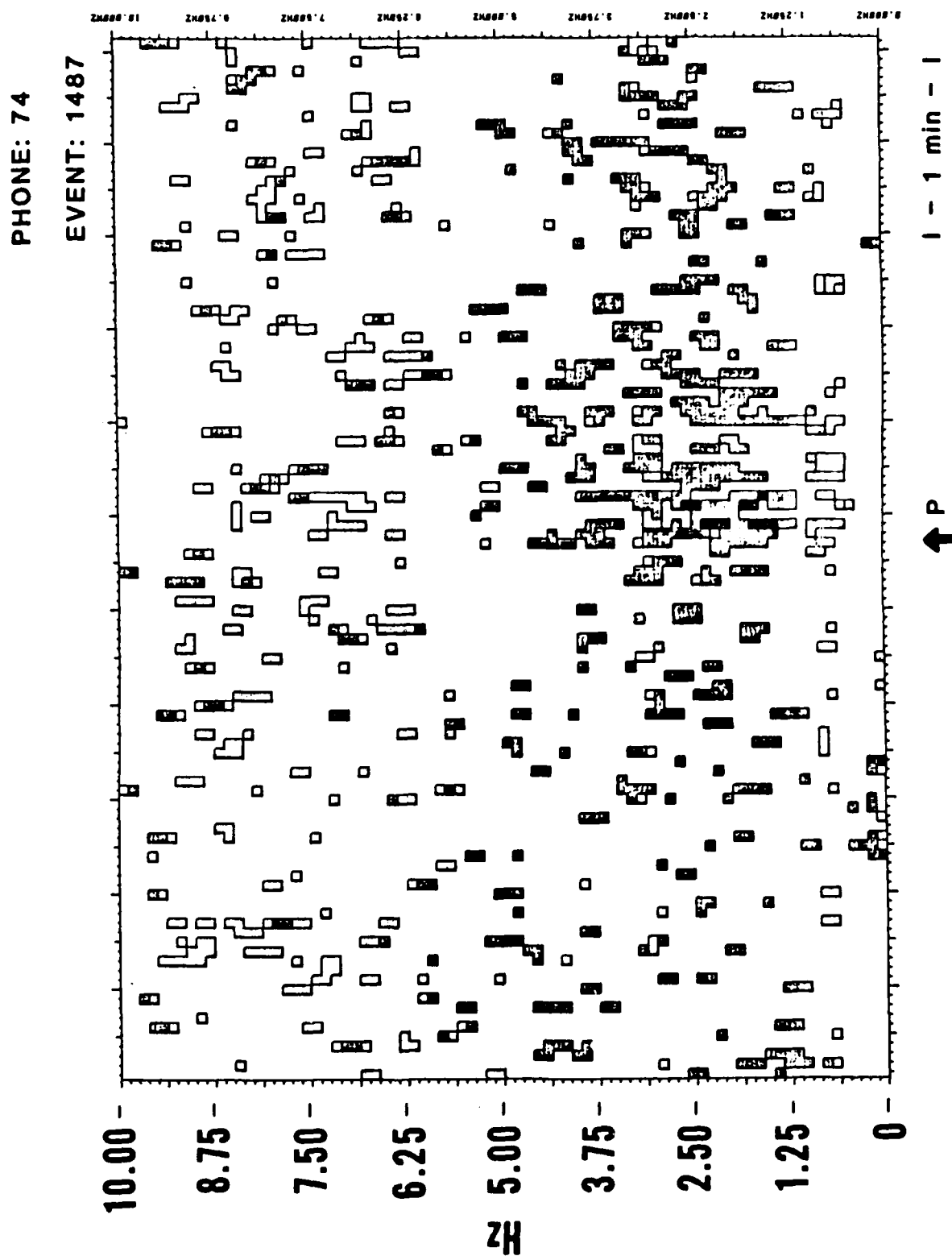
Figure 10. Example of a noise reduced spectrogram. See text for explanation.

```
EVNT ******ORIGIN TIME****** **COORDINATES***   ****
*NO* YR*MO*DA*JUL*HR*MN*SECS **LAT*****LON***    *MB*

NOVAYA ZEMLYA

0158 82 10 11 284 07:14:58.1 73.368N   54.532E   5.6
1487 83 08 18 230 16:09:58 6 73.373N   54.839E   5.9
1635 93 09 25 268 13:09:57.7 73.341N   54.501E   5.8
3123 84 10 25 299 06:29 57.6 73.365N   54.979E   5.8
```

NOVAYA ZEMLYA

	ORIGIN TIME				COORDINATES		DISTANCE (DEG)			SIGNAL LEVELS			NOISE LEVELS			
NO	YR/MD/DAY	HR	MIN	SEC	N	E	74	76	2	74	76	2	74	76	2	MB
158	82/10/11	7	14	58 1	73.37	54.53	76.47	76.81	79.28	*****	7.5	9.5	1.0	2.0	3.0	5.6
1487	83/ 8/18	16	9	58 6	73.37	54.84	76.39	76.73	79.20	2.0	10.5	6.0	-7.0	-7.0	-2.5	5.9
1636	83/ 9/25	13	9	57 7	73.34	54.50	76.49	76.83	79.30	****	9.5	*****	0.5	2.0	3.0	5.8
3123	84/10/25	6	29	57 6	73.36	54.98	76.35	76.70	79.17	1.0	9.0	3.0	-7.5	-5.0	-4.0	5.8
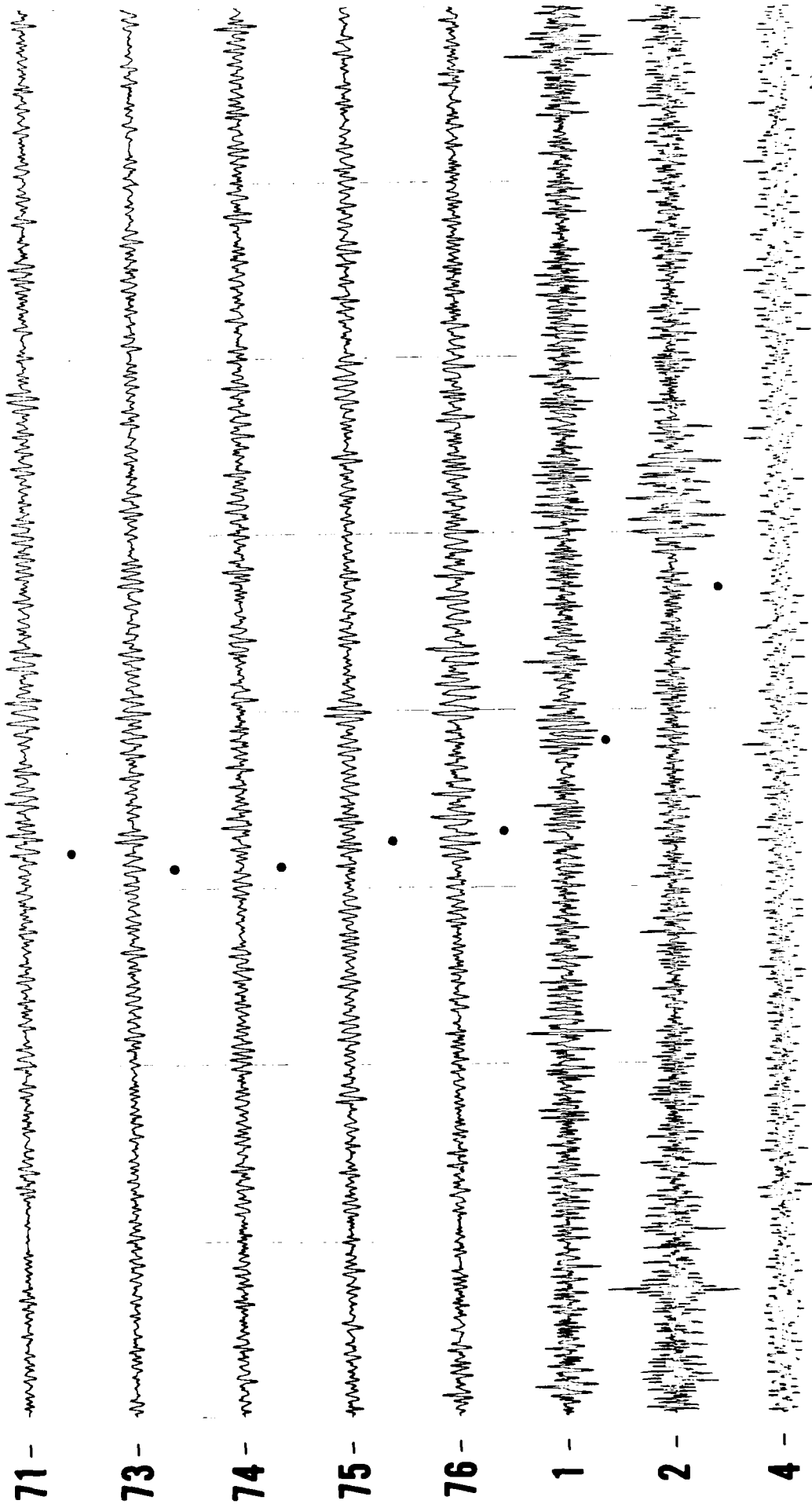
EVENT: 158

71 -
73 -
74 -
75 -
76 -
1 -
2 -
4 -

21

EVENT: 1487

71 -
73 -
74 -
75 -
76 -
1 -
2 -
4 -

22
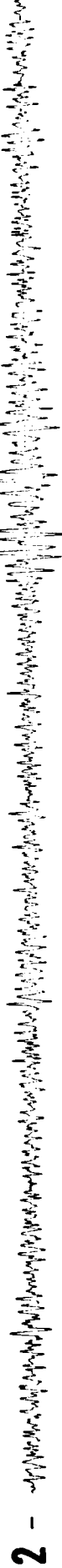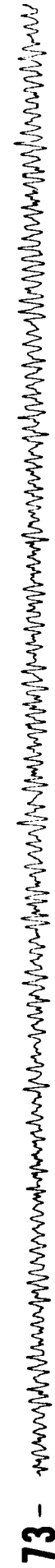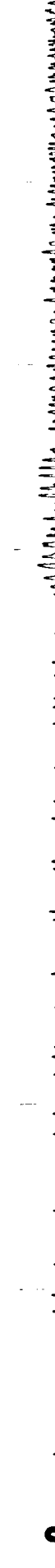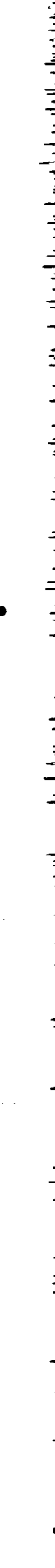
EVENT: 1636

71 -
73 -
74 -
75 -
76 -
1 -
2 -
4 -

23.

EVENT: 3123

71 -
73 -
74 -
75 -
76 -
1 -
2 -
4 -

24

PHONE: 74

EVENT: 158

FREQUENCY (HZ)

D3'S RELATIVE TO ONE MICROBAR PER ROOT HERTZ

NOISE
MEAN
P

PHONE: 76   EVENT: 158

Y-axis: DB'S RELATIVE TO ONE MICROBAR PER ROOT HERTZ

X-axis: FREQUENCY (HZ)
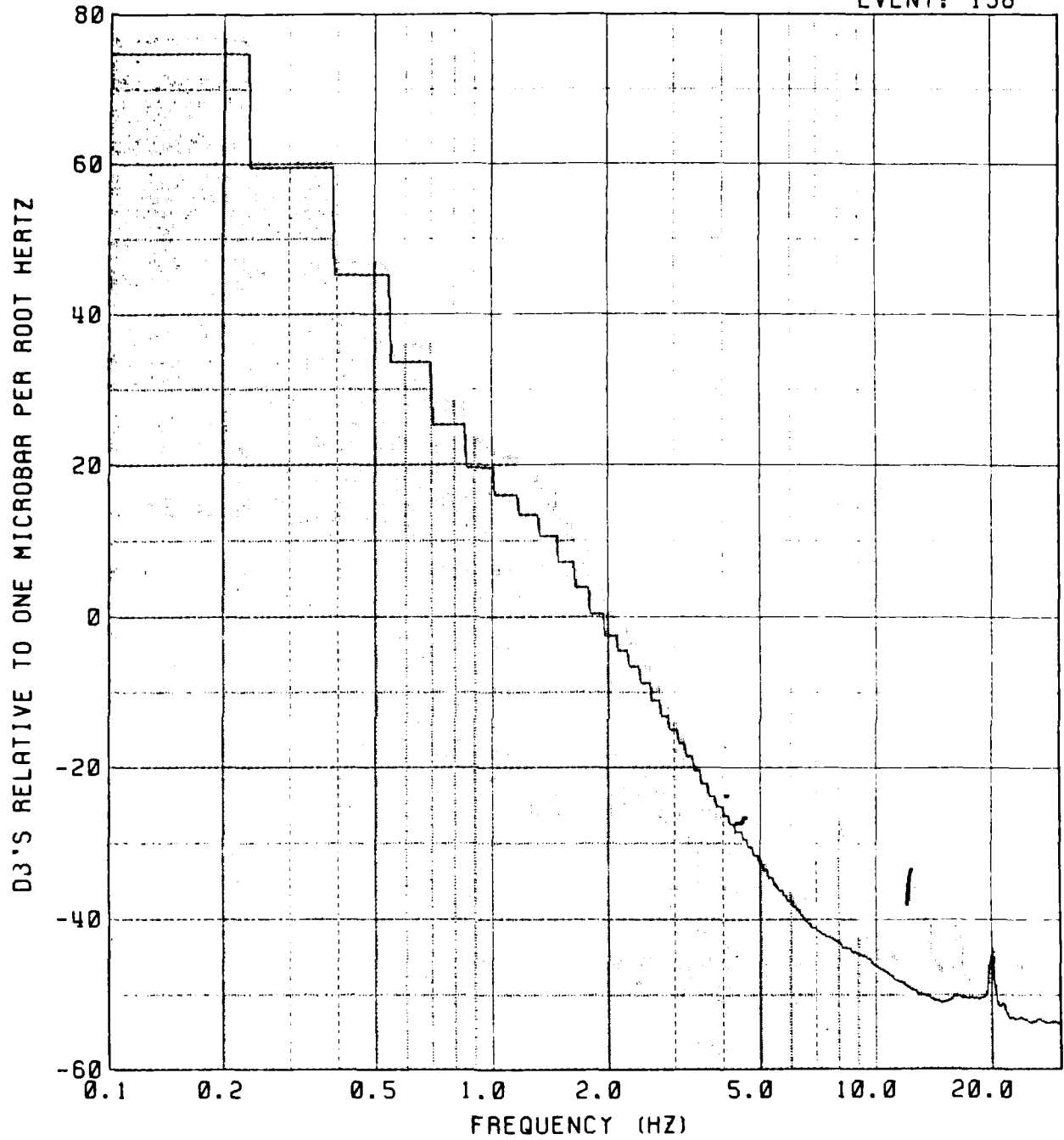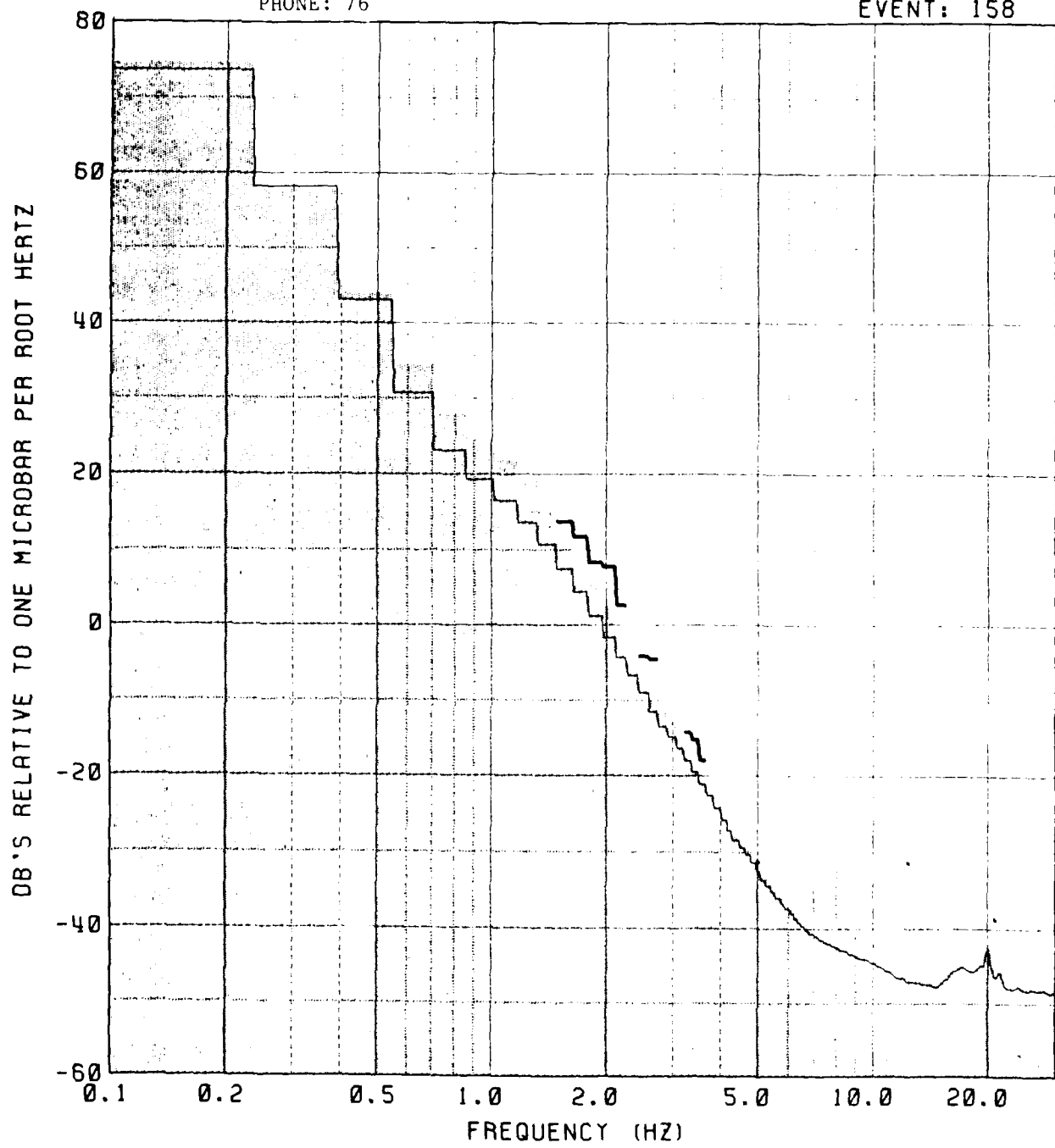
Legend:
- NOISE
- MEAN
- P

PHONE: 2   EVENT: 158

PHONE: 74

DB'S RELATIVE TO ONE MICROBAR PER ROOT HERTZ

FREQUENCY (HZ)
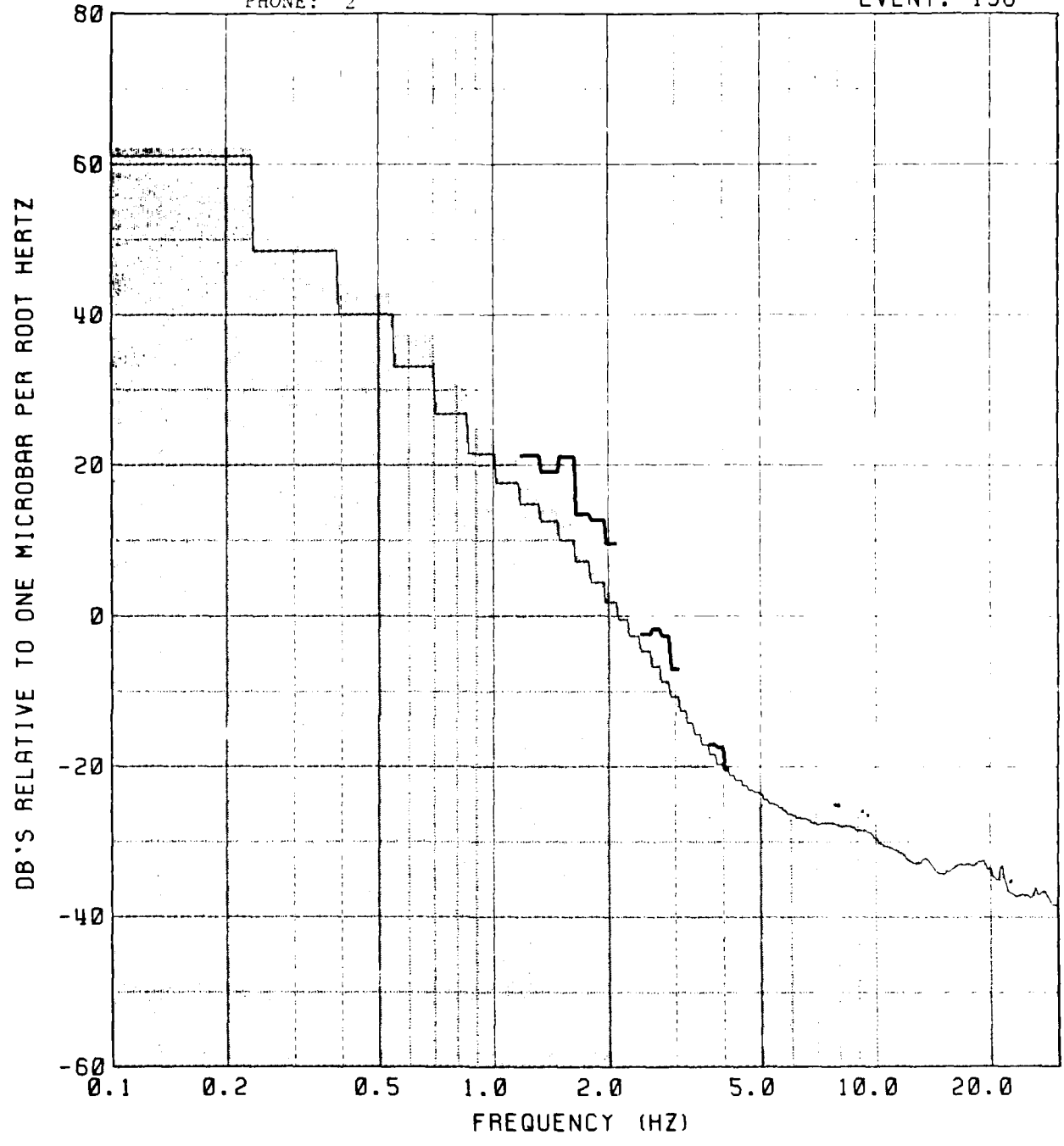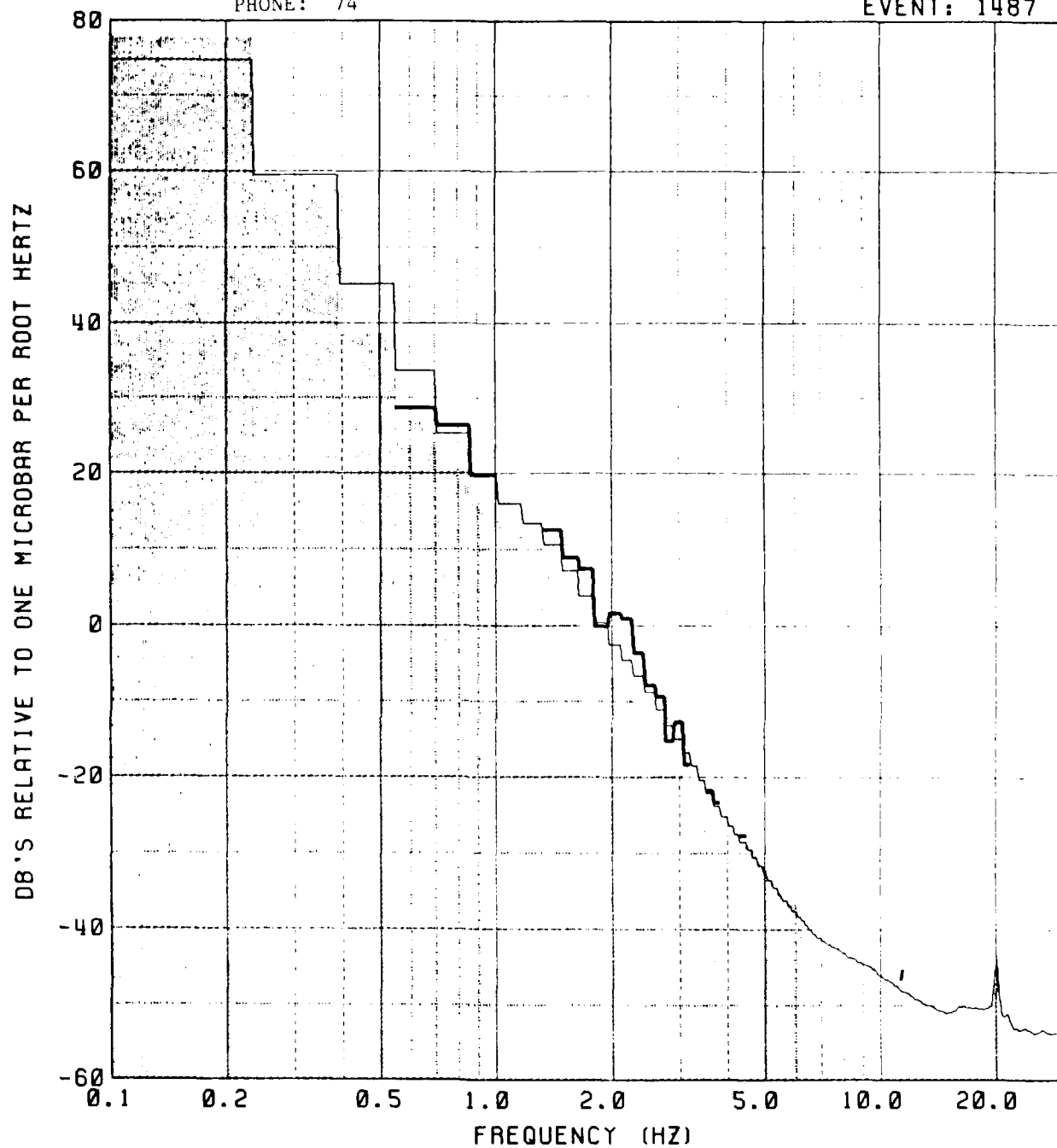
NOISE
MEAN
P

PHONE: 2
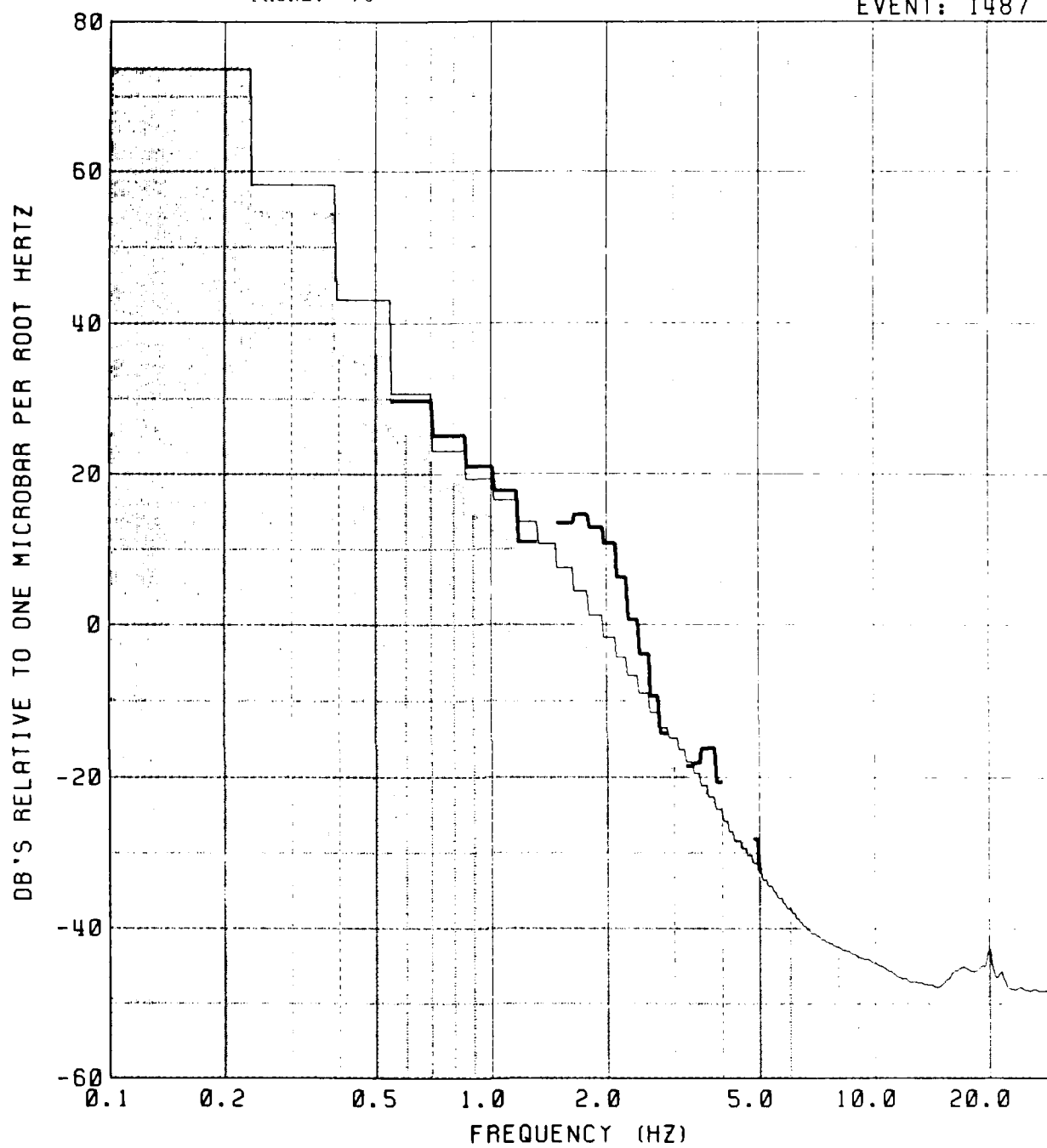
NOISE
MEAN
P
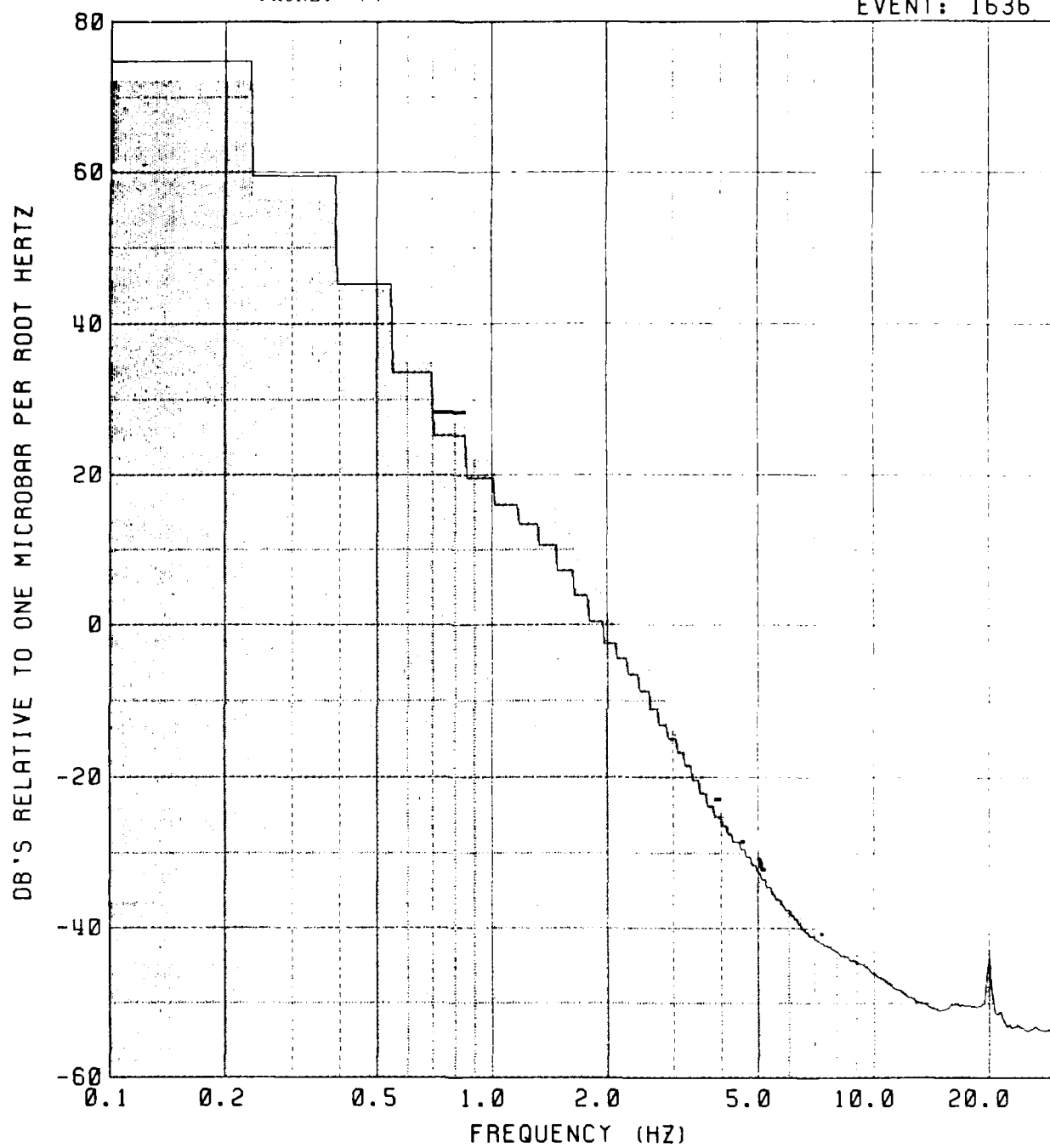
PHONE: 74

NOISE
MEAN
P

PHONE: 76   EVENT: 1636

NOISE
MEAN
P

PHONE: 2

33
EVENT: 1636

FREQUENCY (HZ)

DB'S RELATIVE TO ONE MICROBAR PER ROOT HERTZ

NOISE
MEAN
P

PHONE: 74

34

EVENT: 3123

FREQUENCY (HZ)

DB'S RELATIVE TO ONE MICROBAR PER ROOT HERTZ

NOISE
MEAN
P

PHONE: 76   EVENT: 3123

FREQUENCY (HZ)

DB'S RELATIVE TO ONE MICROBAR PER ROOT HERTZ
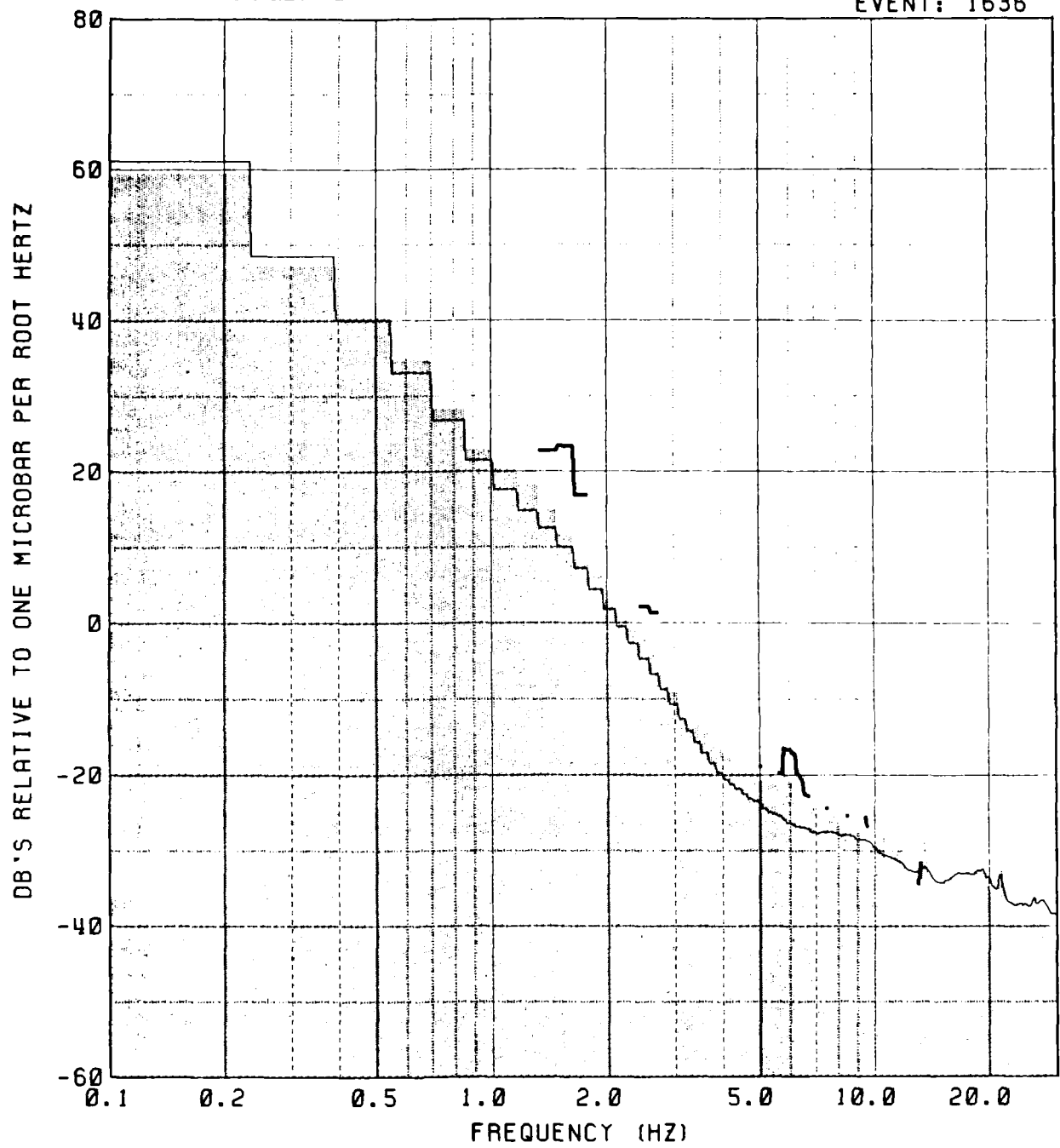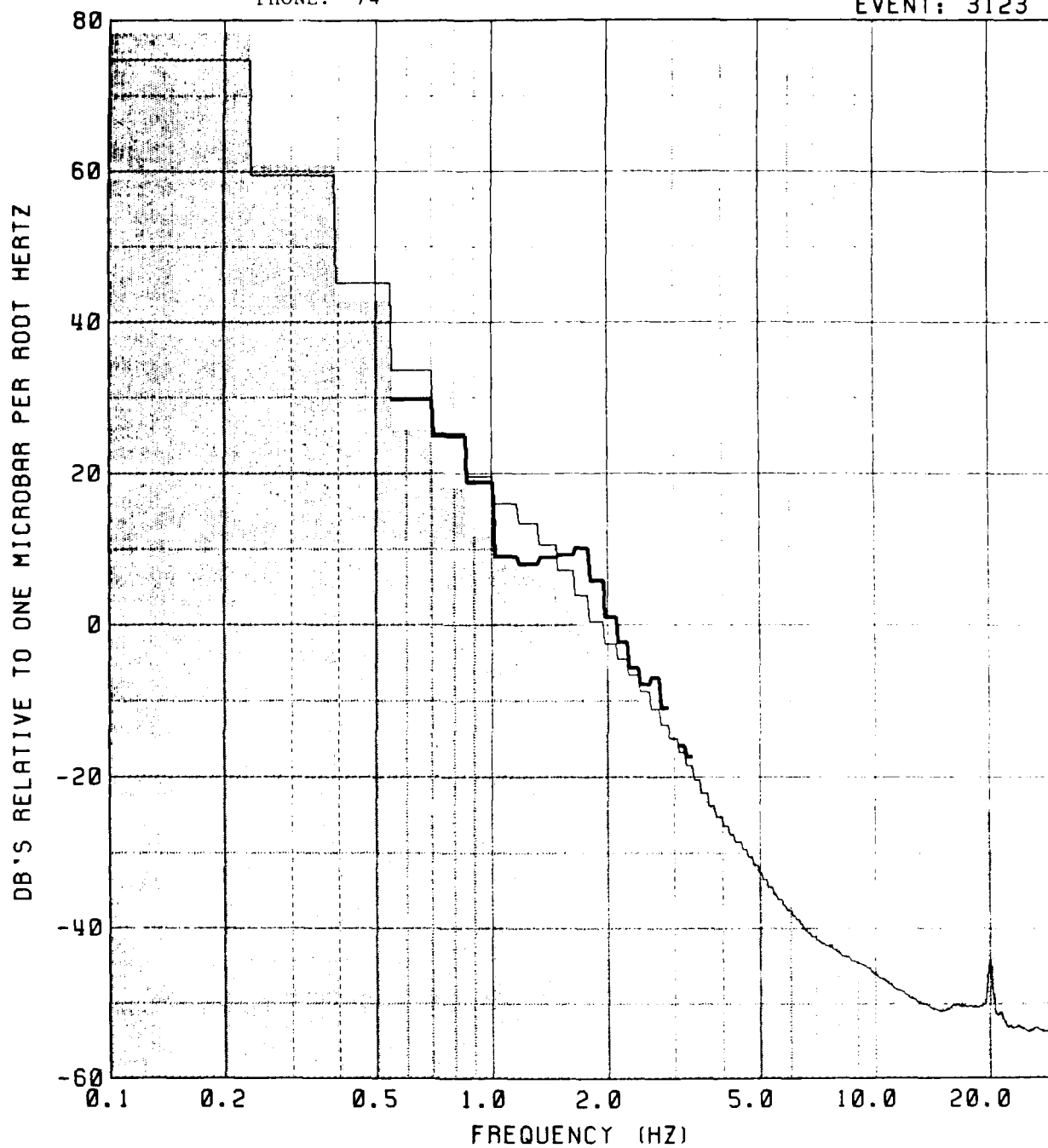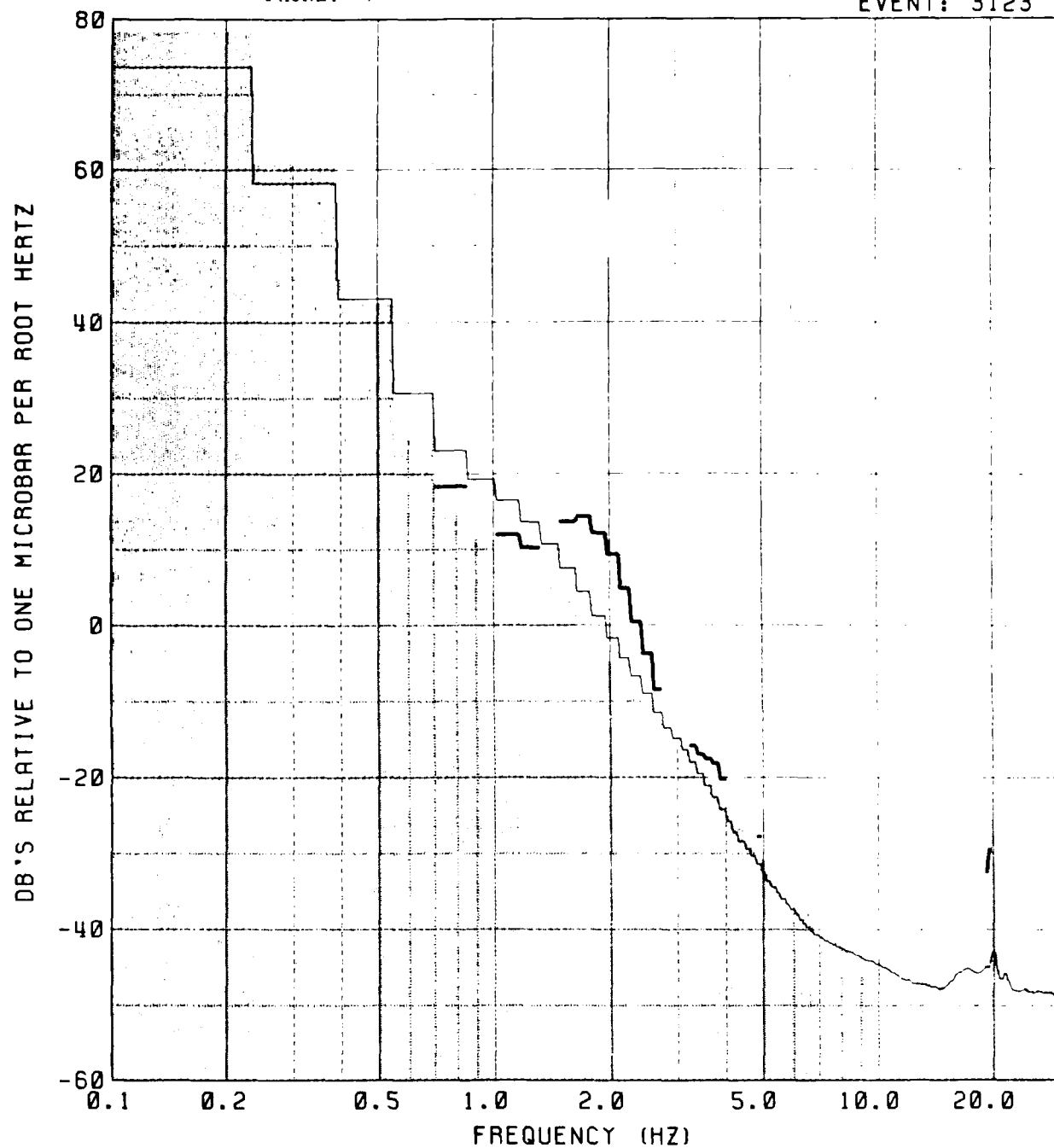
NOISE
MEAN
P

PHONE: 2

EVENT: 3123

NOISE
MEAN
P

10.000HZ 8.750HZ 7.500HZ 6.250HZ 5.000HZ 3.750HZ 2.500HZ 1.250HZ 0.000HZ

10.00
8.75
7.50
6.25
5.00
3.75
2.50
1.25
0

HZ

EVENT: 158

38

HZ

10.00
8.75
7.50
6.25
5.00
3.75
2.50
1.25
0

10.000HZ 8.750HZ 7.500HZ 6.250HZ 5.000HZ 3.750HZ 2.500HZ 1.250HZ 0.000HZ

EVENT: 1487

10.000HZ 8.750HZ 7.500HZ 6.250HZ 5.000HZ 3.750HZ 2.500HZ 1.250HZ 0.000HZ

10.00 — 8.75 — 7.50 — 6.25 — 5.00 — 3.75 — 2.50 — 1.25 — 0

HZ

EVENT: 1636
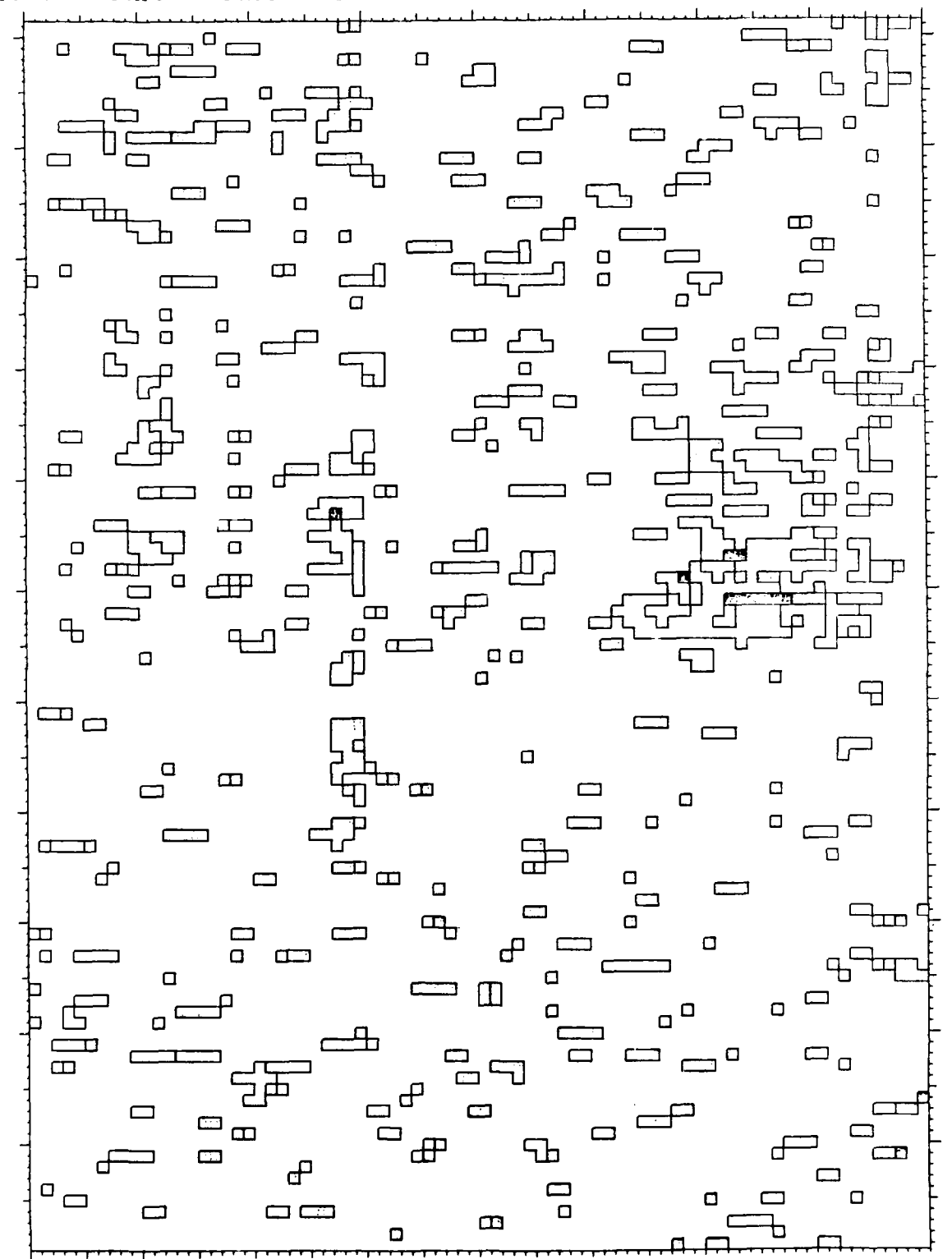
EVENT: 3123

HZ

Novaya Zemlya - Discussion

A total of four events from this site were recorded. The strongest signals were on phones 2 and 76, with phone 2 having the highest S/N ratios - at frequencies of around 1.5 Hz. Phone 76 appears to have somewhat relatively richer signals than phone 2 at higher frequencies. Signals on phone 74 are weak compared to those found on phones 2 and 76. Noise reduced spectrograms for phone 74 significantly enhance otherwise marginal indications of signals on this channel in its time series plots and spectrums. Of the four events, the smallest recorded was a 5.6 mb. Considering signal levels and body wave magnitudes of the recorded Novaya Zemlya explosions, it appears possible that events substantially lower than 5.6 could be recorded under low noise conditions.

```
EVNT ******ORIGIN TIME****** **COORDINATES***   ****
*NO* YR*MO*DA*JUL*HR*MN*SECS **LAT****<*LON***   *MB*
```

EASTERN KAZAKH SER
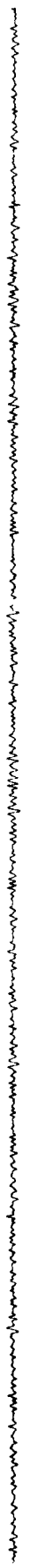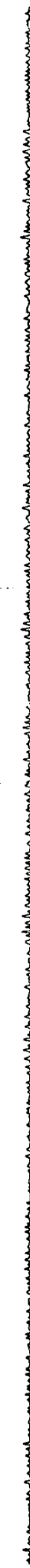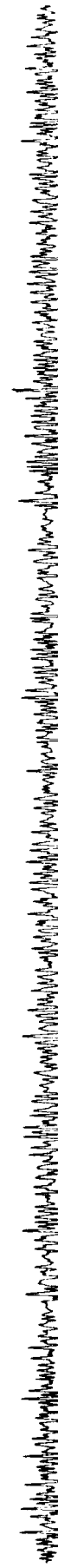
EVNT NO	YR	MO	DA	JUL	HR	MN	SECS	LAT	LON	MB
0074	82	09	21	264	02	57	01.1	49.909N	78.229E	5.2
0345	82	12	05	339	03	37	12.6	49.907N	78.843E	6.1
0438	82	12	26	360	03	35	14.3	50.070N	79.009E	5.7
0898	83	04	12	102	03	41	05.2	49.815N	78.222E	4.9
1111	83	05	30	150	03	33	44.6	49.740N	78.210E	5.4
1170	83	06	12	163	02	36	43.5	49.874N	78.964E	6.1
1567	83	09	11	254	06	33	10.1	49.801N	78.244E	5.1
1674	83	10	06	279	01	47	06.6	49.933N	78.833E	6.0
1727	83	10	26	299	01	55	04.8	49.883N	78.856E	6.1
1816	83	11	20	324	03	27	04.4	50.069N	79.033E	5.4
1844	83	11	29	333	02	19	06.5	49.775N	78.191E	5.4
1952	83	12	26	360	04	29	06.8	49.829N	78.215E	5.5
2177	84	02	19	050	03	57	03.3	49.886N	78.788E	5.9
2247	84	03	07	067	02	39	06.3	50.022N	78.978E	5.6
2352	84	03	29	089	05	19	08.1	49.934N	79.013E	5.9
2459	84	04	15	106	03	17	09.2	49.766N	78.185E	5.7
2479	84	04	25	116	01	09	03.5	49.934N	78.915E	6.0
2608	84	05	26	147	03	13	12.3	49.949N	79.060E	6.1
2812	84	07	14	196	01	09	10.4	49.902N	78.988E	6.1
3040	84	09	09	253	02	59	06.3	49.873N	78.208E	5.0
3110	84	10	18	292	04	57	05.4	49.787N	78.004E	4.6
3126	84	10	27	301	01	50	10.6	49.950N	78.842E	6.2
3202	84	12	02	337	03	19	06.2	49.989N	79.091E	5.8
3230	84	12	16	351	03	55	02.7	49.968N	78.893E	6.1
3249	84	12	28	363	03	50	10.5	49.863N	78.785E	6.0

EASTERN KAZAKH SSR

43

	ORIGIN TIME				COORDINATES		DISTANCE (DEG)			SIGNAL LEVELS			NOISE LEVELS			
NO	YR/MO/DAY	HR	MIN	SEC	N	E	74	76	2	74	76	2	74	76	2	MB
74	82/09/21	02	57	1.1	49.91	78.23	73.44	73.69	76.04	*****	*****	11.0	-6.5	-9.0	2.5	5.2
345	82/12/05	03	37	12.6	49.91	78.84	73.05	73.30	75.65	12.0	12.5	11.0	-1.5	-1.0	3.0	4.6
438	82/12/26	03	35	14.3	50.07	79.01	72.91	73.16	75.52	14.5	15.0	15.0	-12.5	-6.0	2.0	5.7
1170	83/06/12	02	36	43.5	49.89	78.96	72.98	73.23	75.58	10.0	4.0	*****	-1.0	0.0	4.0	4.1
1727	83/10/26	01	55	4.8	49.88	78.86	73.05	73.30	75.65	11.5	10.0	8.5	1.5	2.0	3.5	4.6
2177	84/02/19	03	57	3.3	49.89	78.79	73.09	73.34	75.69	10.5	9.5	8.0	1.5	2.0	4.0	5.9
2352	84/03/29	05	19	8.1	49.93	79.01	72.94	75.19	75.54	11.0	7.0	*****	0.0	-1.5	3.5	5.9
2459	84/04/15	03	17	9.2	49.77	78.18	73.50	73.75	76.10	2.0	6.0	*****	0.0	-1.0	2.5	5.7
2498	84/04/25	01	09	3.5	49.93	78.91	73.00	73.25	75.60	10.0	*****	*****	1.5	-1.0	2.5	5.0
2608	84/05/26	03	13	12.3	49.95	79.06	72.90	73.15	75.51	22.0	20.0	15.0	-1.0	-1.0	3.0	4.6
2812	84/07/14	01	09	10.4	49.90	78.99	72.96	73.21	75.56	10.0	-1.0	5.0	-7.0	-6.5	0.0	4.1
3230	84/12/16	03	55	2.7	49.97	78.89	73.01	73.26	75.61	18.0	16.0	9.0	-0.5	-2.0	-1.0	4.6
3249	84/12/28	03	50	10.5	49.86	78.78	73.10	73.35	75.70	18.0	14.0	17.0	-9.0	-6.0	2.0	4.0

EVENT: 74

71 –
73 –
74 –
75 –
76 –
1 –
2 –
4 –

44

EVENT: 345

45

71 -

73 -

74 -

75 -

76 -

1 -

2 -

4 -

EVENT: 438

71 -
73 -
74 -
75 -
76 -
1 -
2 -
4 -

46

EVENT: 1170

71 -
73 -
74 -
75 -
76 -
1 -
2 -
4 -

47

EVENT: 1727

71-

73-

74-

75-

76-

1-

2-

4-

48

49

71 –

73 –

74 –

75 –

76 –

1 –

2 –

4 –

50

71 —

73 —

74 —

75 —

76 —

1 —

2 —

4 —

EVENT: 2459

51

71-

73-

74-

75-

76-

1-

2-

4-

EVENT: 2498

52

71 -
73 -
74 -
75 -
76 -
1 -
2 -
4 -

EVENT: 2608

53

71-
73-
74-
75-
76-
1-
2-
4-

EVENT: 2312

71-
73-
74-
75-
76-
1-
2-
4-

54

EVENT: 3230

55

71 -
73 -
74 -
75 -
76 -
1 -
2 -
4 -

EVENT : 3249

56

PHONE: 74   EVENT: 74

NOISE
———————   MEAN
━━━━━━   P

PHONE: 76

EVENT: 74

FREQUENCY (HZ)

DB'S RELATIVE TO ONE MICROBAR PER ROOT HERTZ
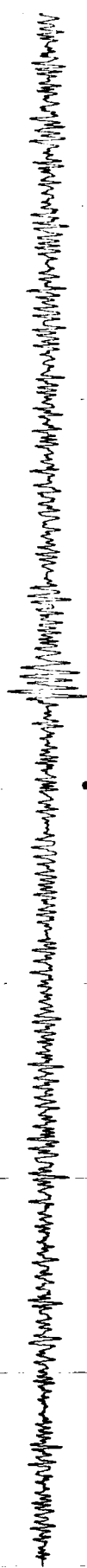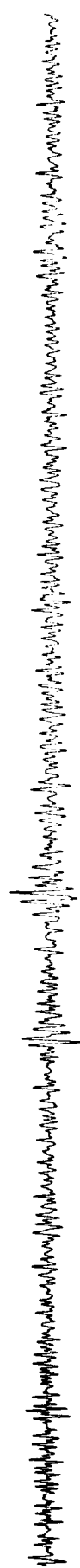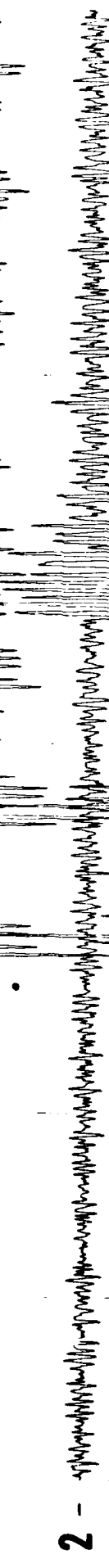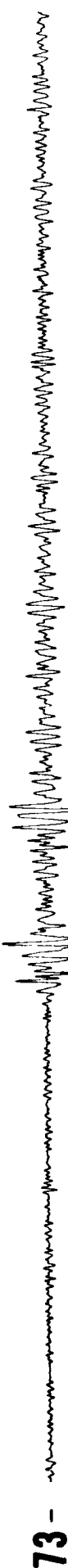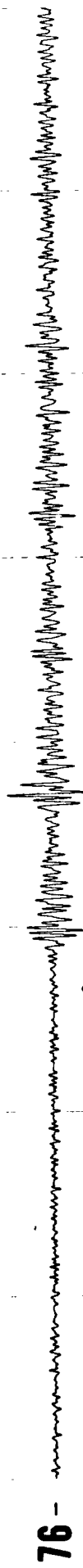
NOISE
MEAN
P

PHONE: 2   EVENT: 74

NOISE
——————— MEAN
—————— P

PHONE: 76

61

EVENT: 345

NOISE
MEAN
P

Legend:

- .... NOISE
- ------- MEAN
- ——— P

X-axis: FREQUENCY (HZ)

Y-axis: DB'S RELATIVE TO ONE MICROBAR PER ROOT HERTZ

PHONE: 74

NOISE

MEAN

P

PHONE: 76

64
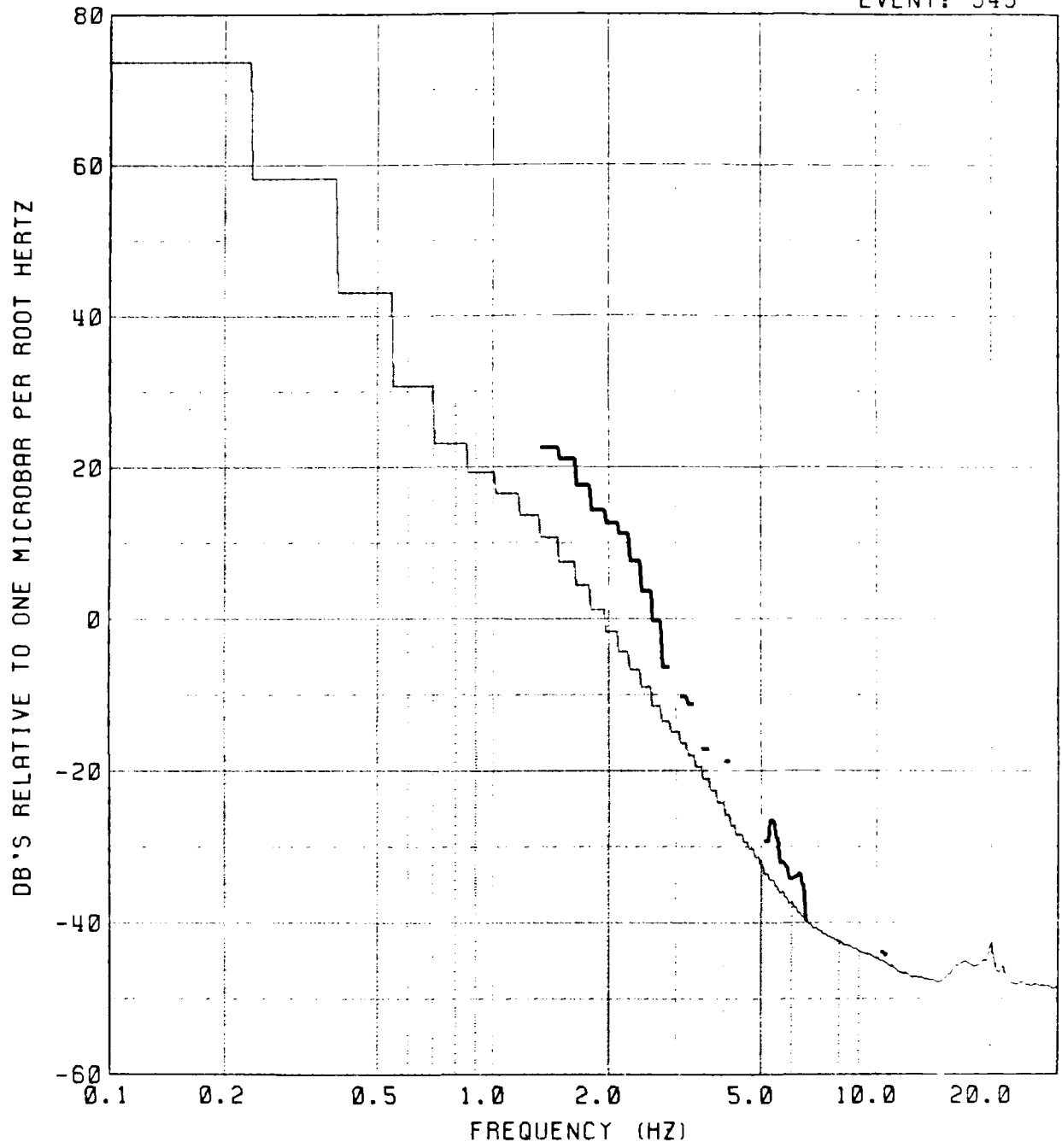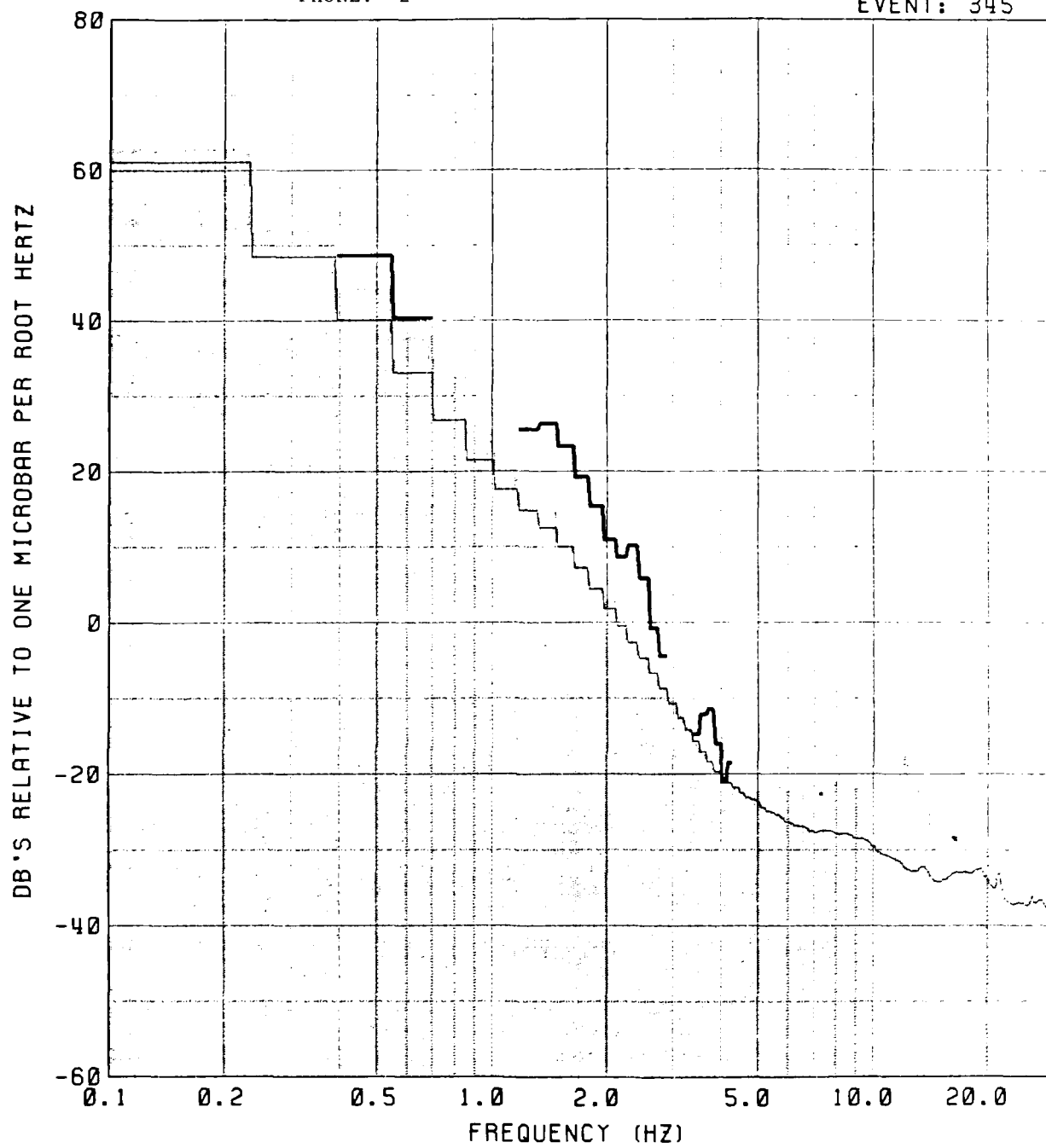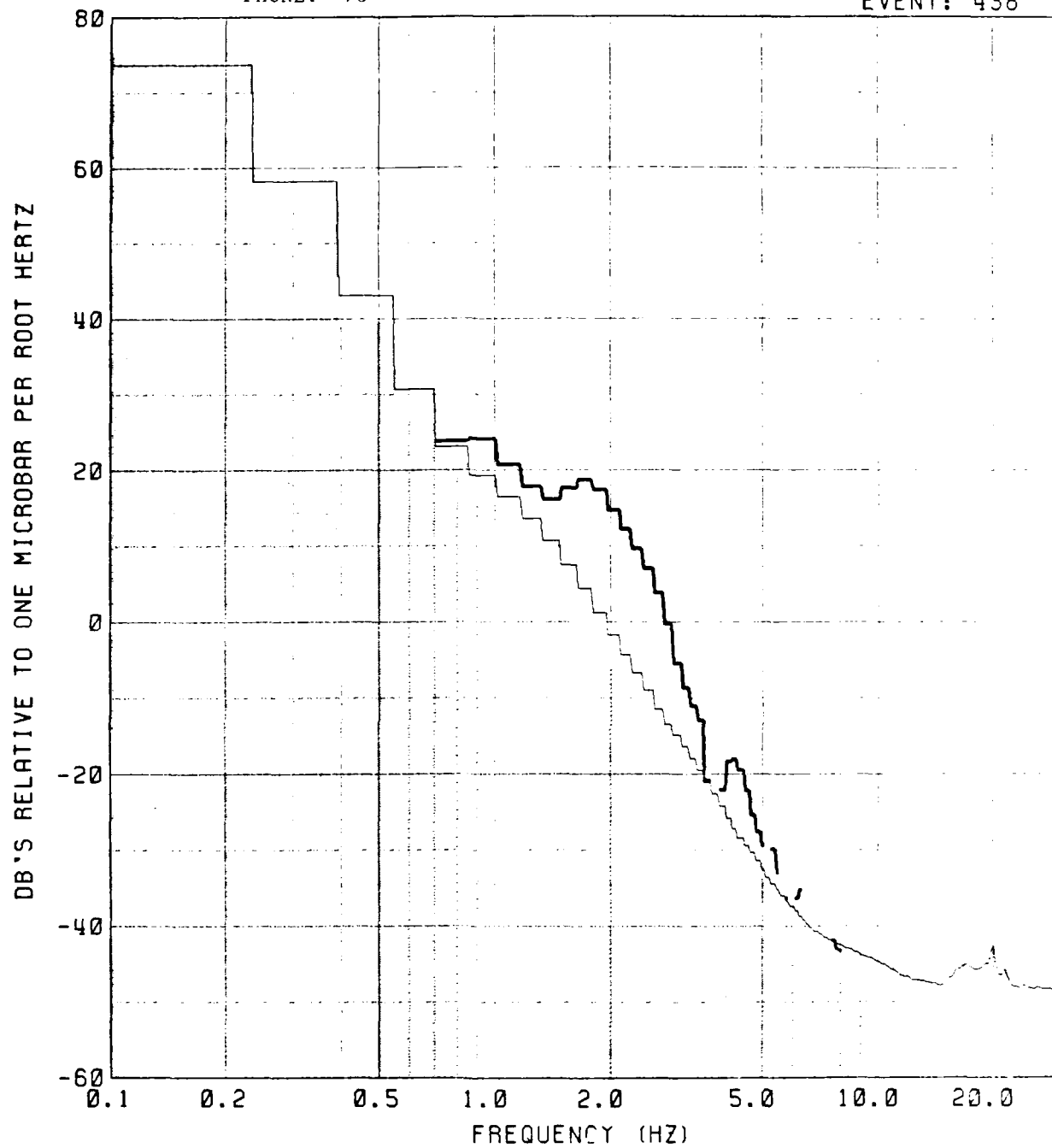
EVENT: 438
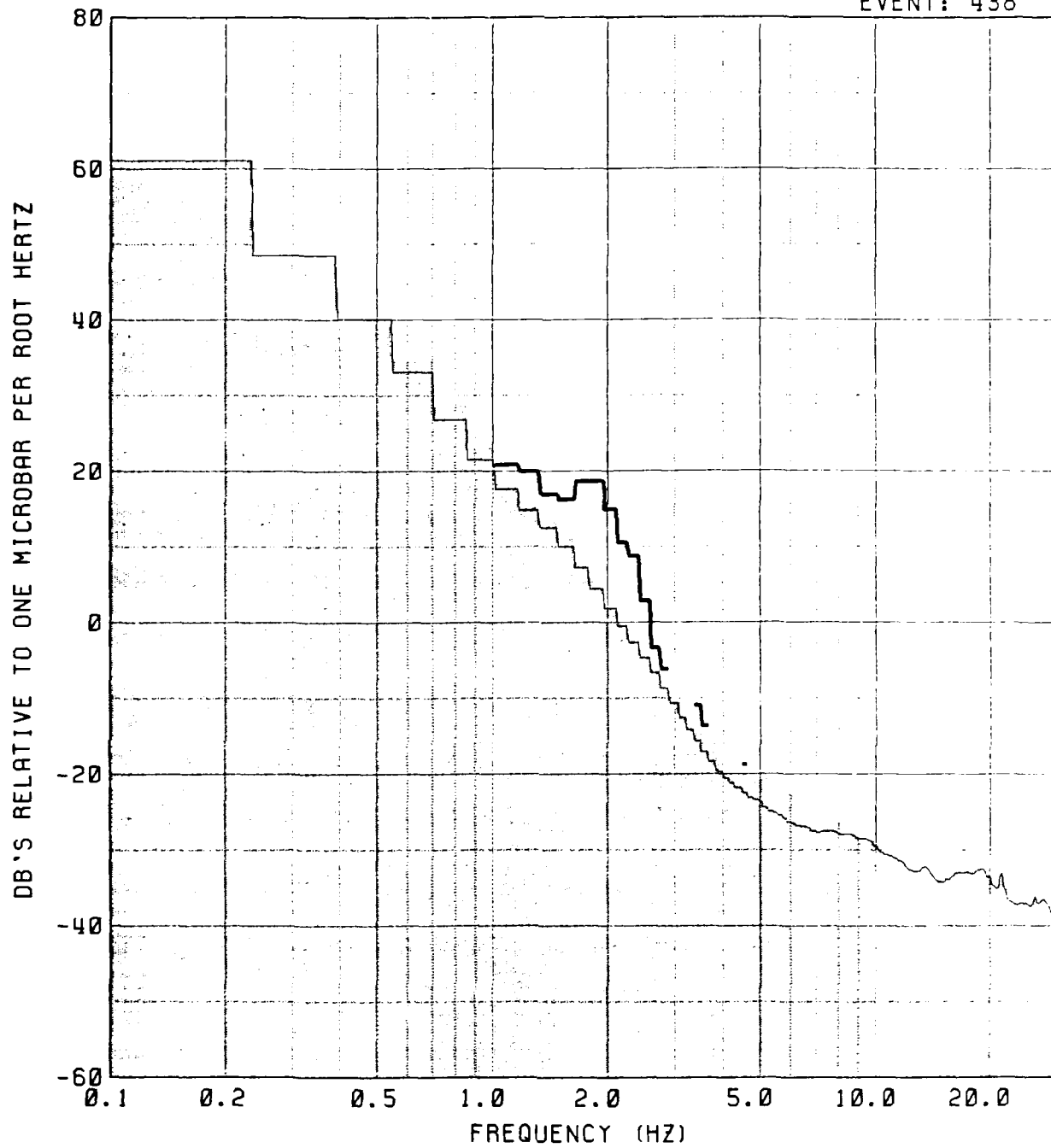
NOISE
MEAN
P

PHONE: 2   EVENT: 438
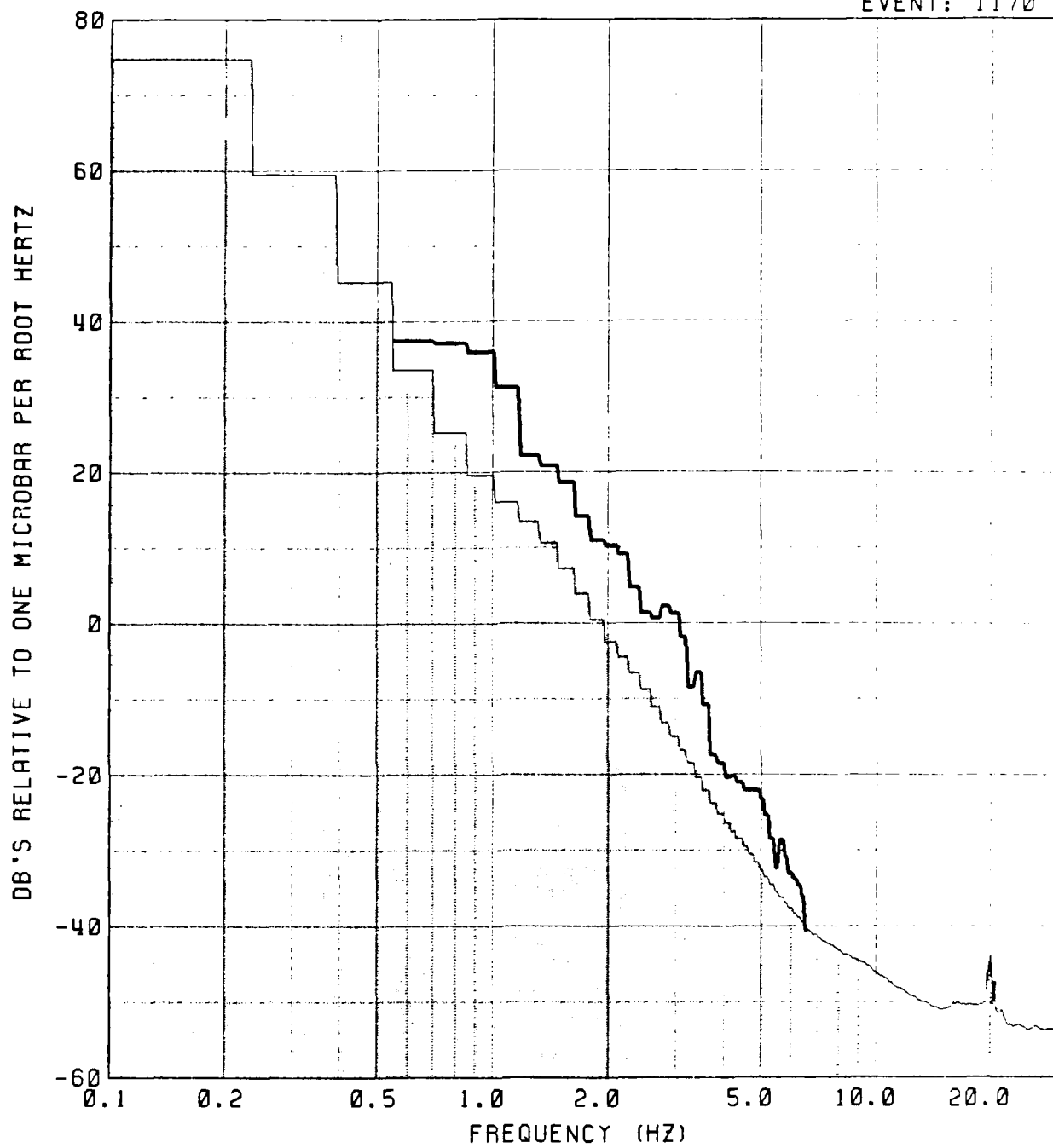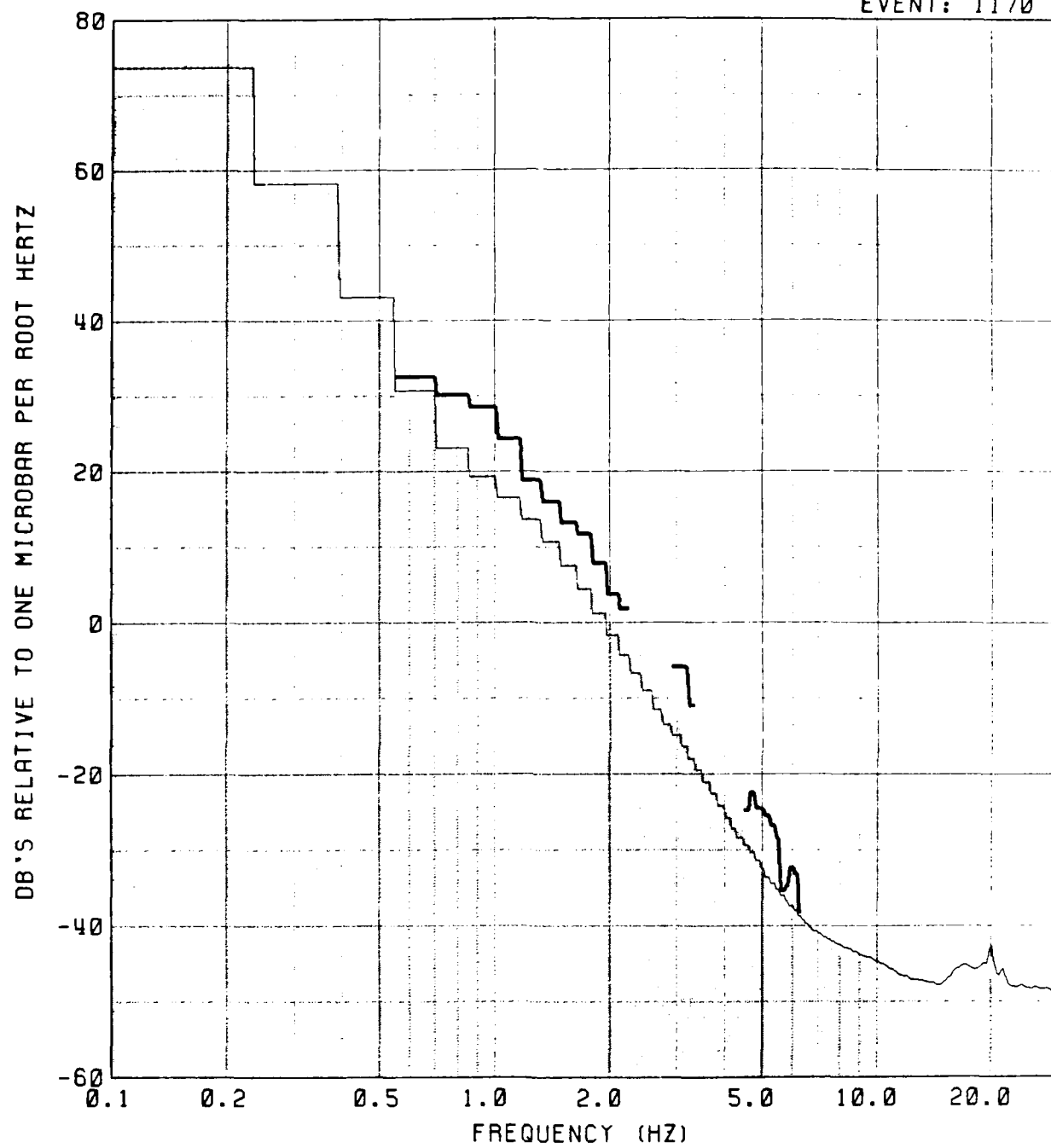
FREQUENCY (HZ)

DB'S RELATIVE TO ONE MICROBAR PER ROOT HERTZ

· · · · · ·   NOISE
————————   MEAN
——————— · —   P

PHONE: 74

NOISE
MEAN
P

PHONE: 76

FREQUENCY (HZ)

DB'S RELATIVE TO ONE MICROBAR PER ROOT HERTZ

NOISE
MEAN
P

PHONE: 2

NOISE
MEAN
P

PHONE: 76   EVENT: 1727

DB'S RELATIVE TO ONE MICROBAR PER ROOT HERTZ

FREQUENCY (HZ)
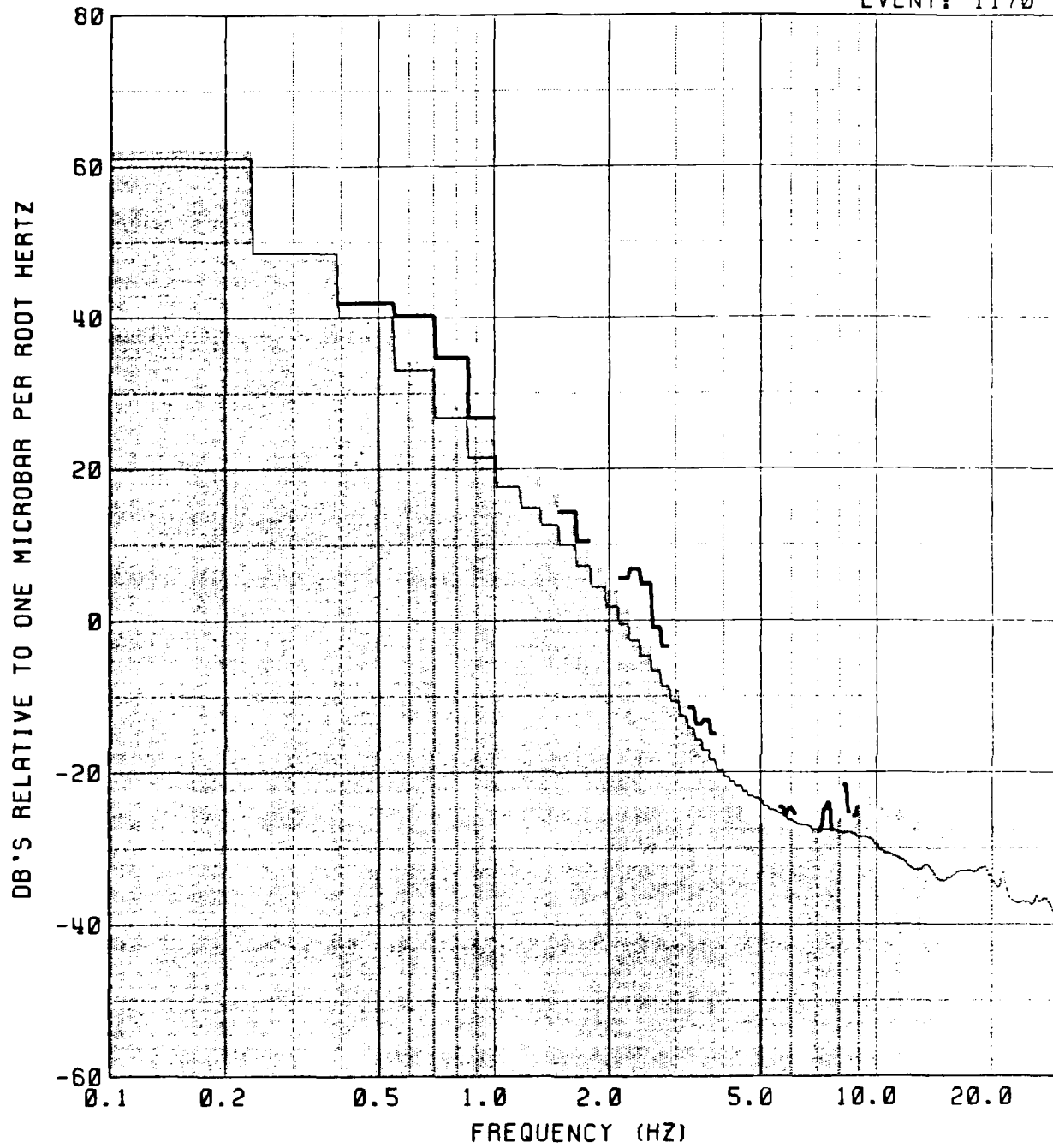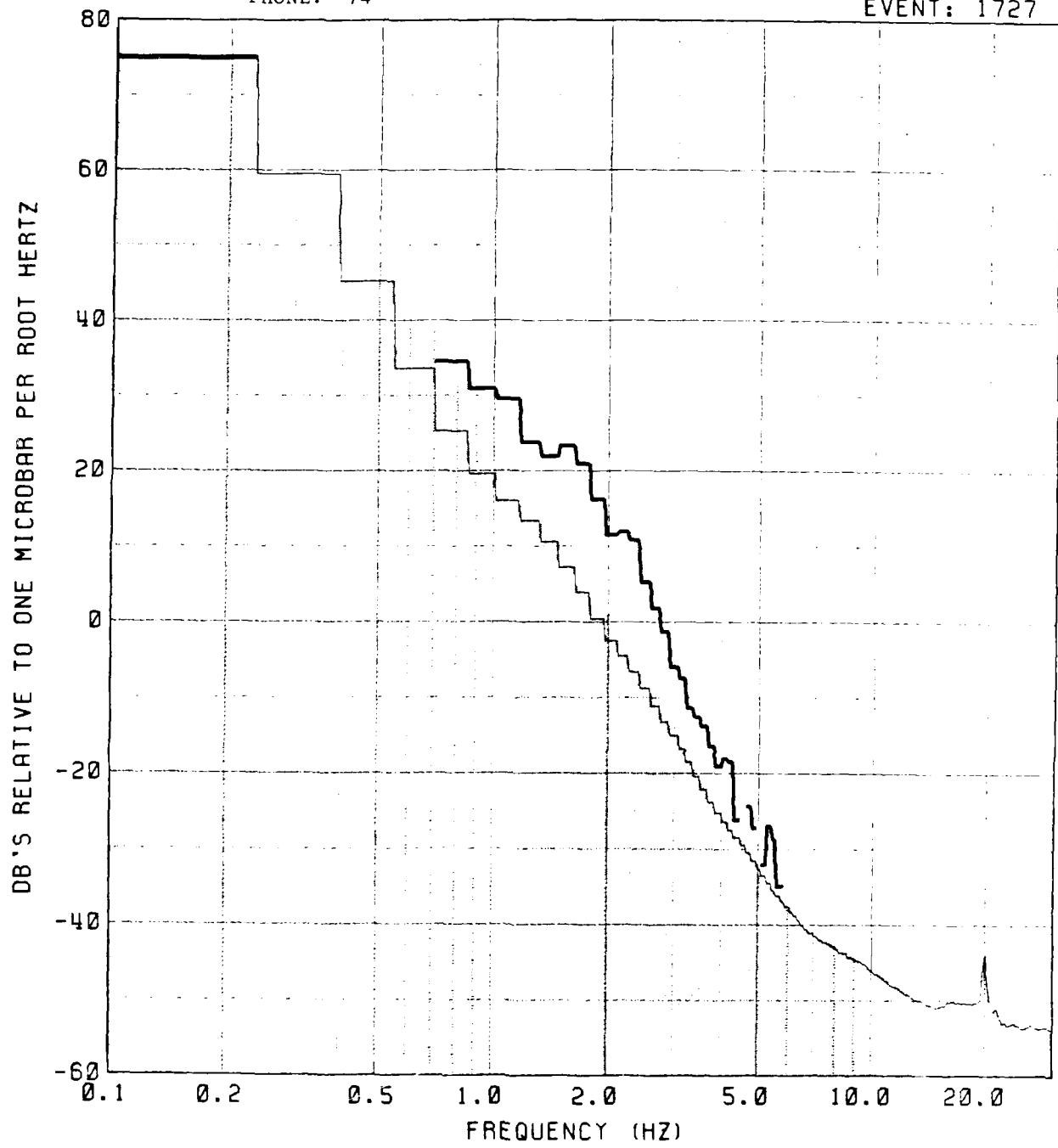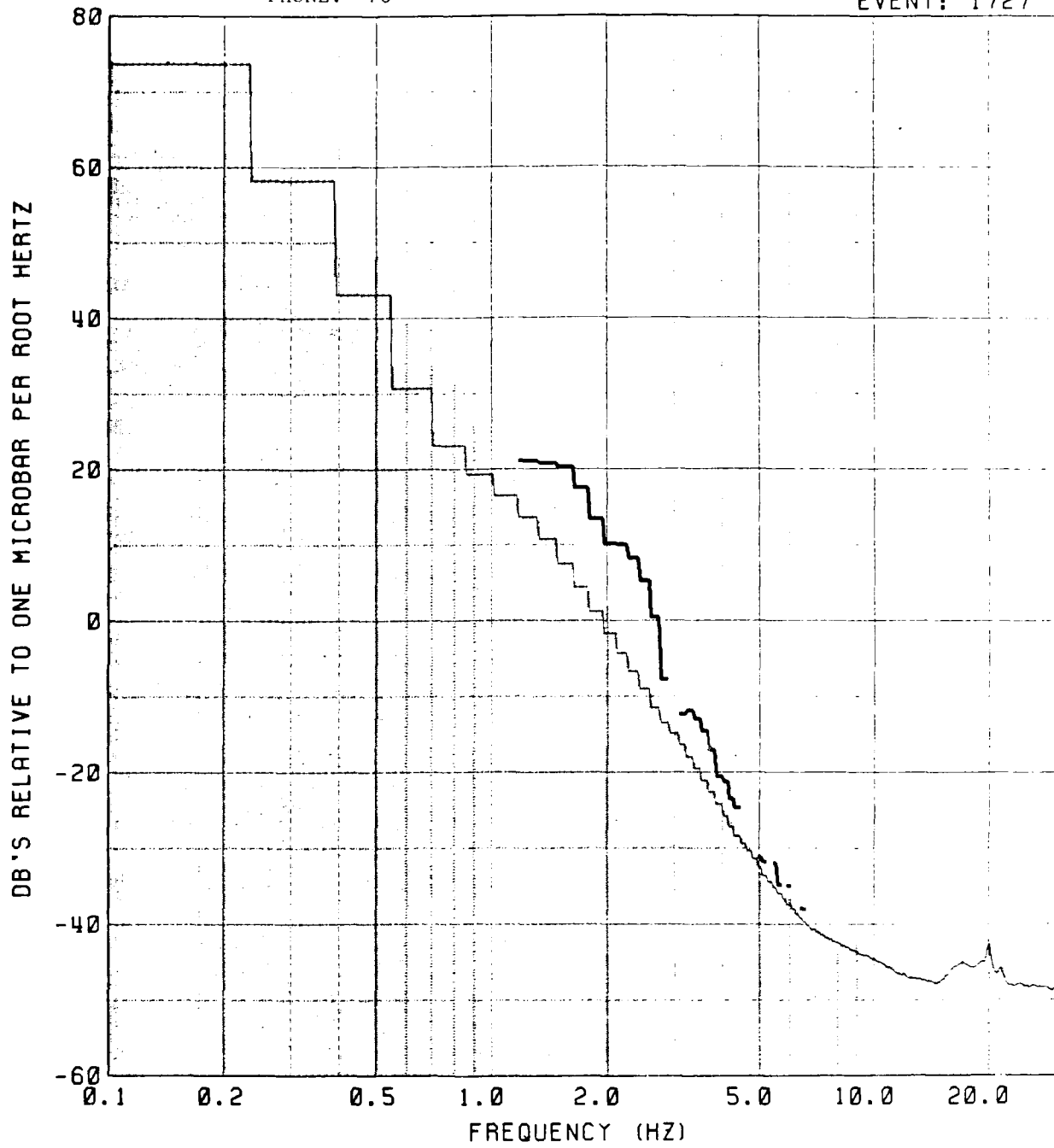
NOISE
MEAN
P

PHONE: 2　　　　　　　　　　　　　　　EVENT: 1727

PHONE: 74

72
EVENT: 2177
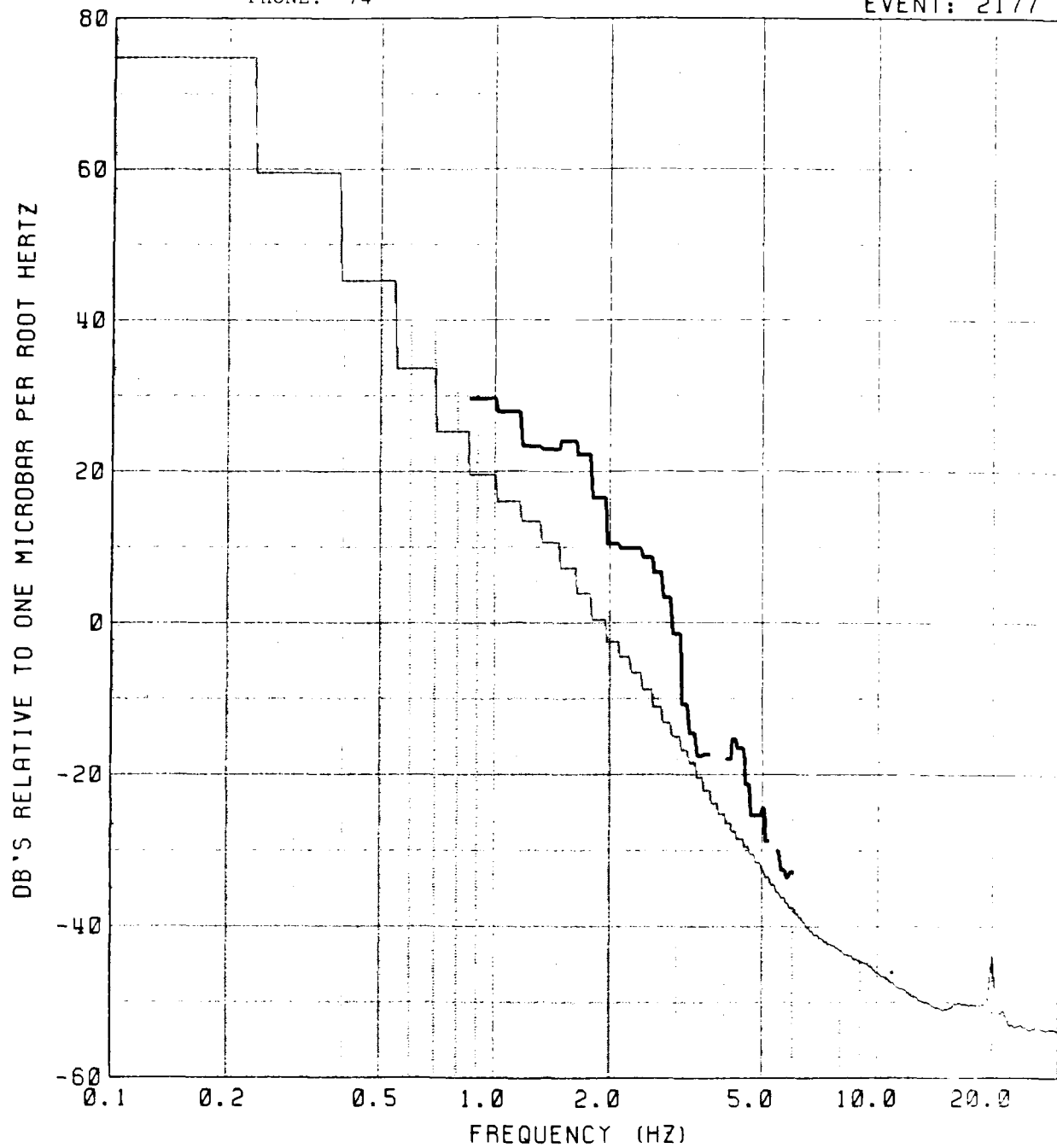
FREQUENCY (HZ)

DB'S RELATIVE TO ONE MICROBAR PER ROOT HERTZ

NOISE
MEAN
P

1.0	2.8	2.5
	3.2	2.2
	3.6	
	4.0	2.0
1.1		1.8
1.25	1.4	1.6

MICROCOPY RESOLUTION TEST CHART
NATIONAL BUREAU OF STANDARDS 1963 A

PHONE: 2

FREQUENCY (HZ)

DB'S RELATIVE TO ONE MICROBAR PER ROOT HERTZ

NOISE
MEAN
P

PHONE: 76   EVENT: 2352

PHONE: 2

NOISE
MEAN
P

PHONE: 74

DB'S RELATIVE TO ONE MICROBAR PER ROOT HERTZ

FREQUENCY (HZ)

NOISE
MEAN
P

PHONE: 76

NOISE
MEAN
P

PHONE: 74

DB'S RELATIVE TO ONE MICROBAR PER ROOT HERTZ

FREQUENCY (HZ)

NOISE
MEAN
P

PHONE: 76

82

EVENT: 2498

FREQUENCY (HZ)

DB'S RELATIVE TO ONE MICROBAR PER ROOT HERTZ
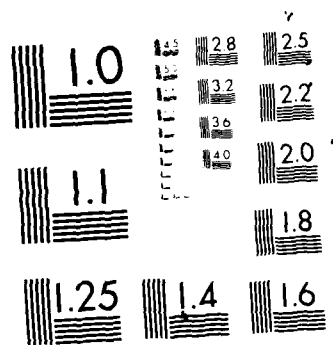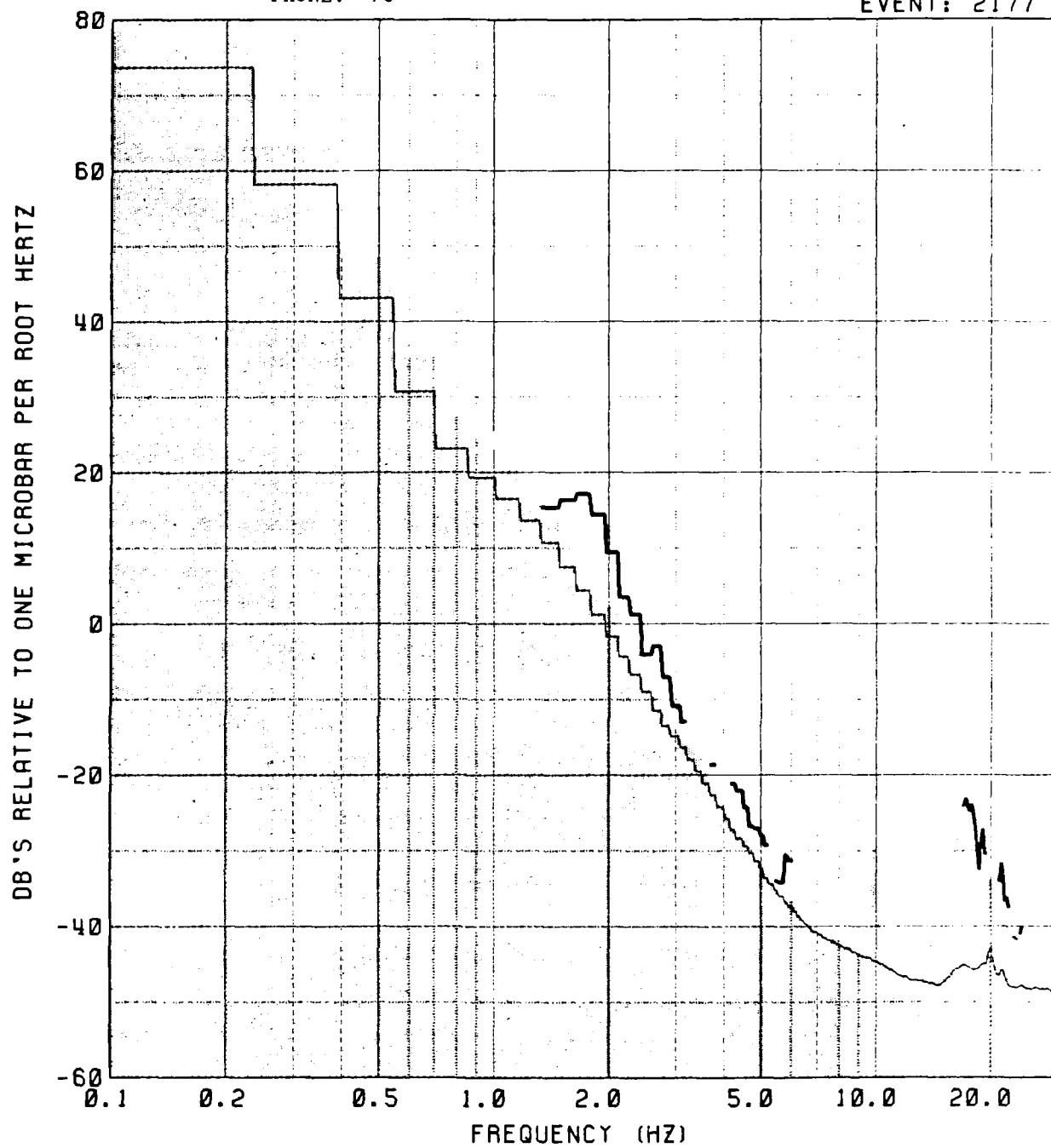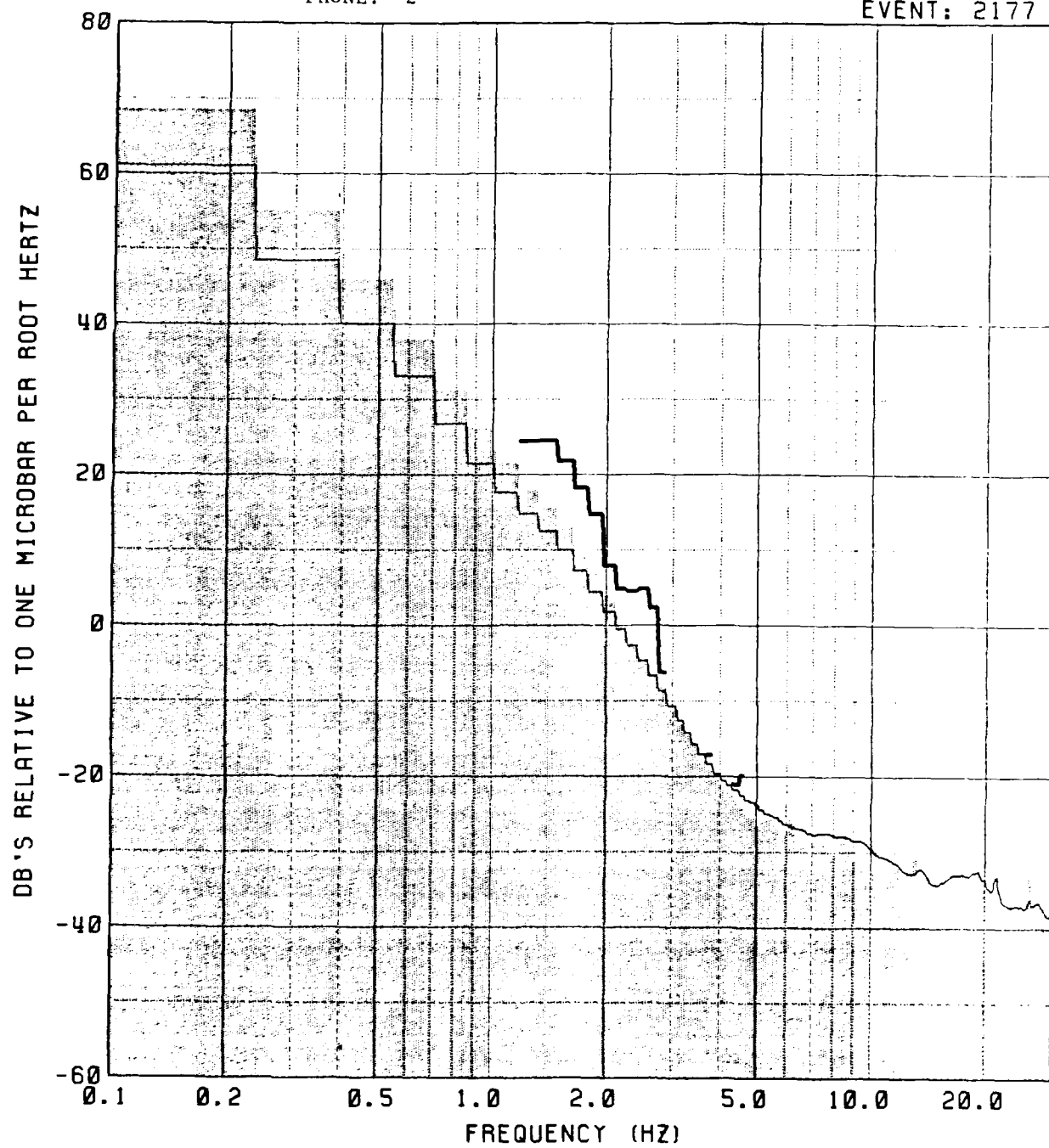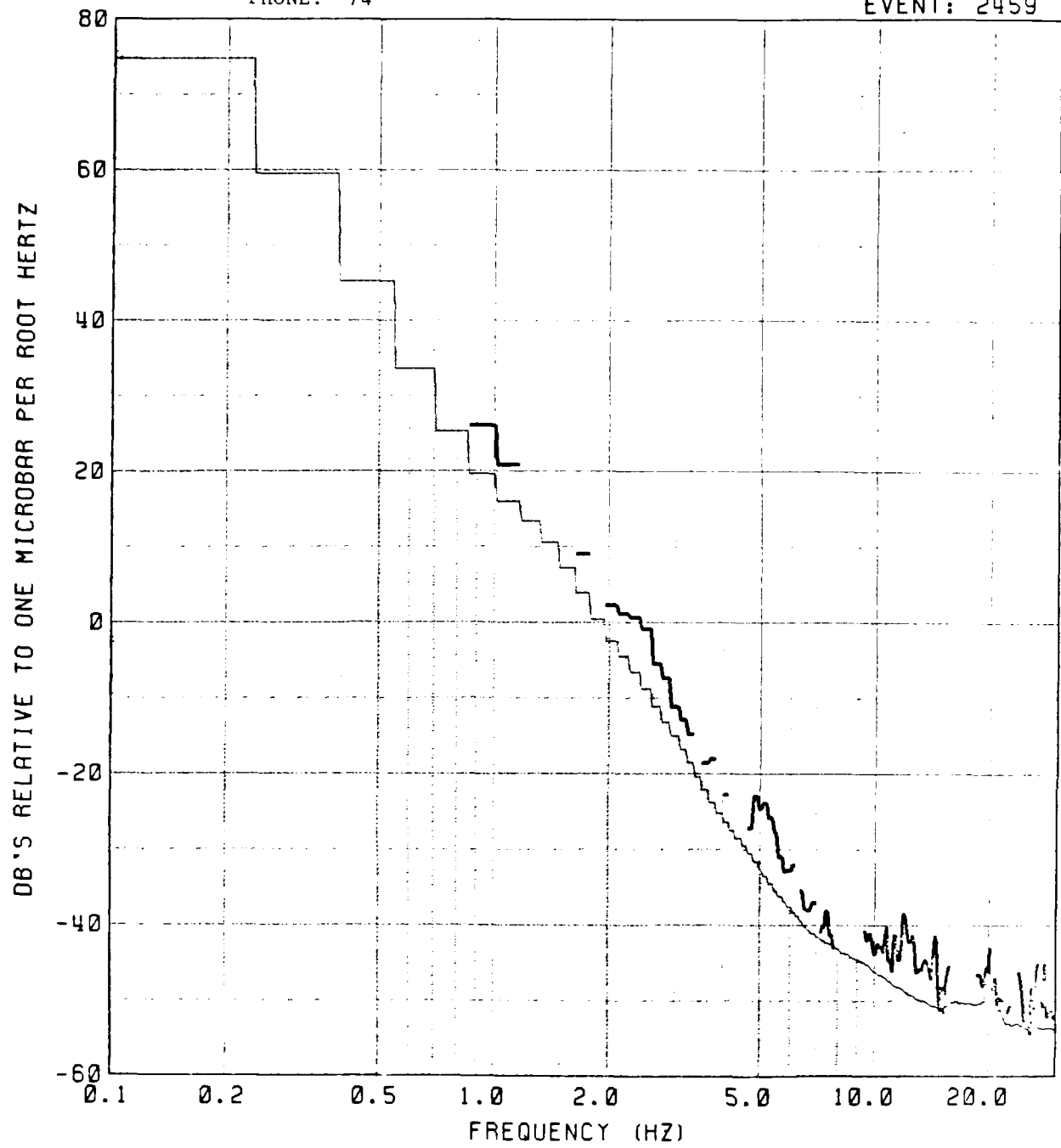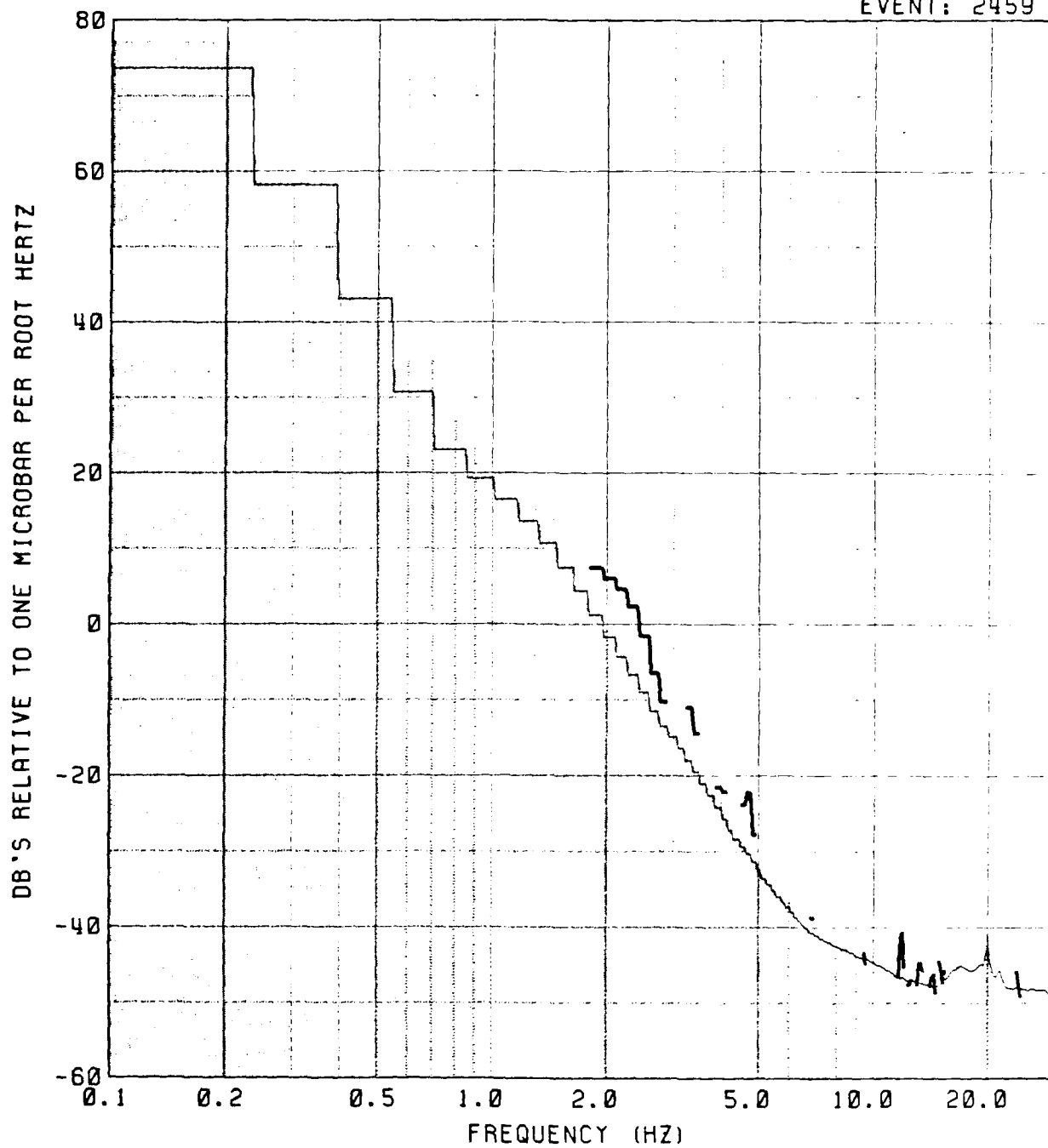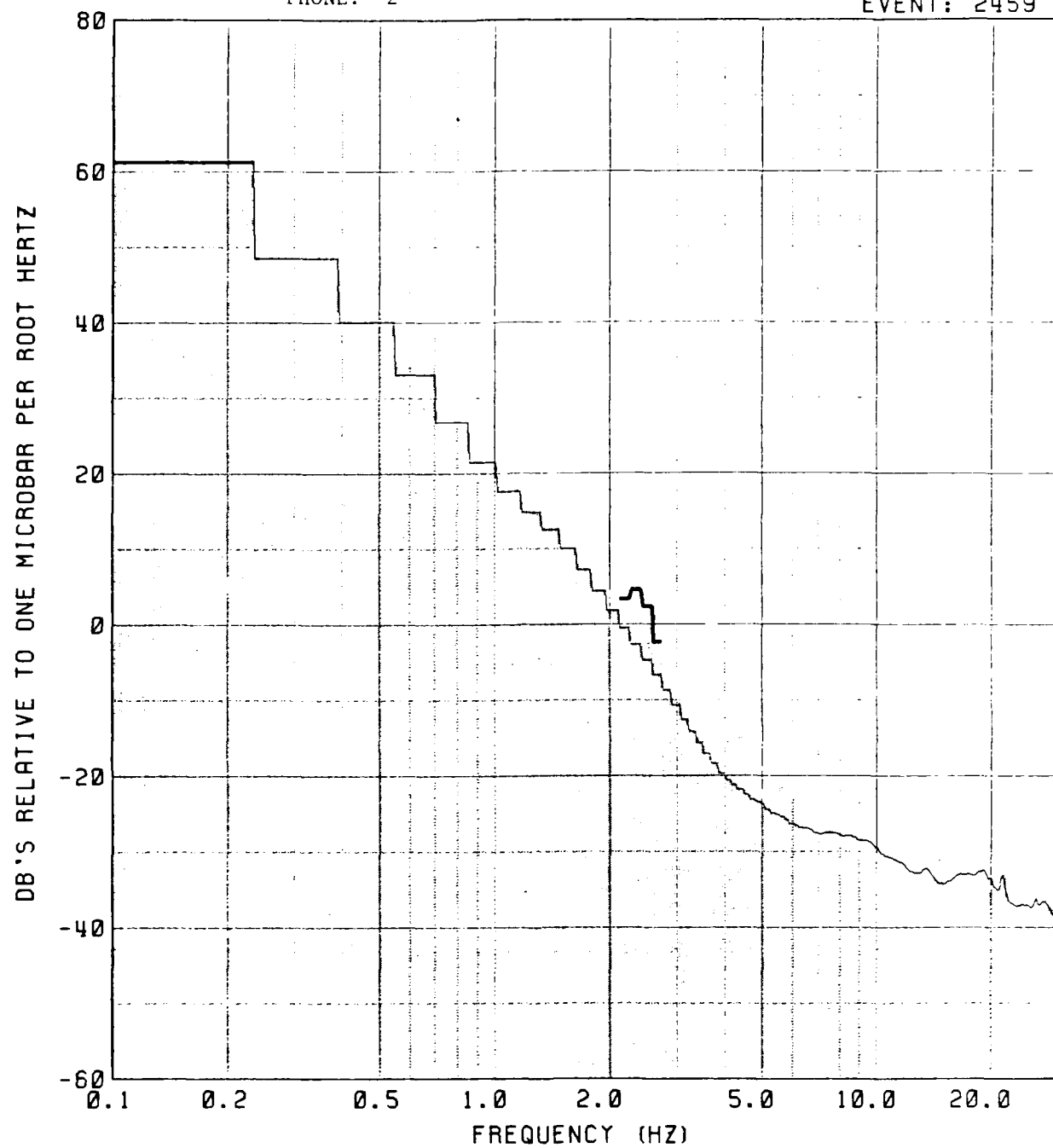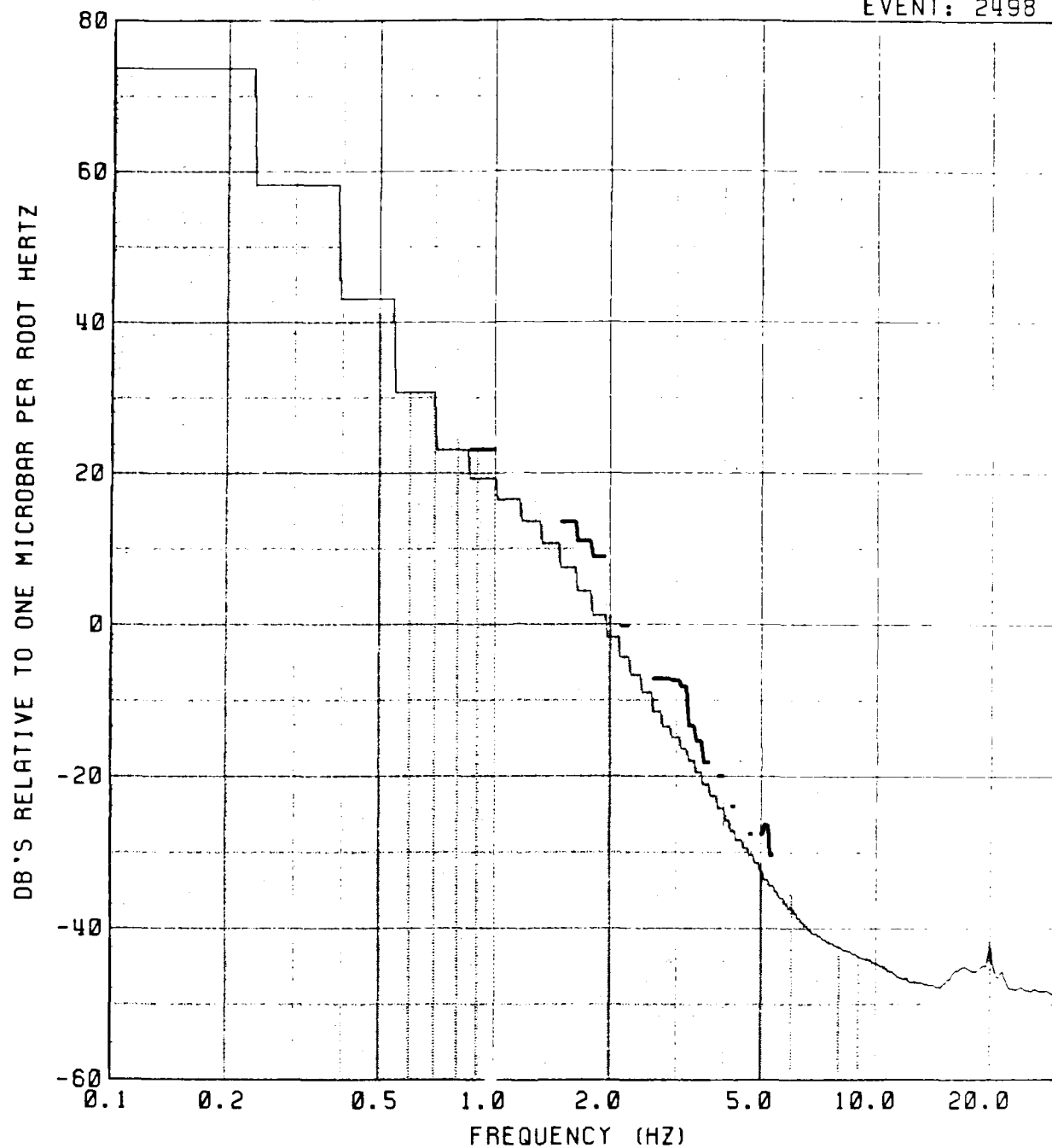
NOISE
MEAN
P

PHONE: 2

EVENT: 2498

NOISE
MEAN
P

PHONE: 74
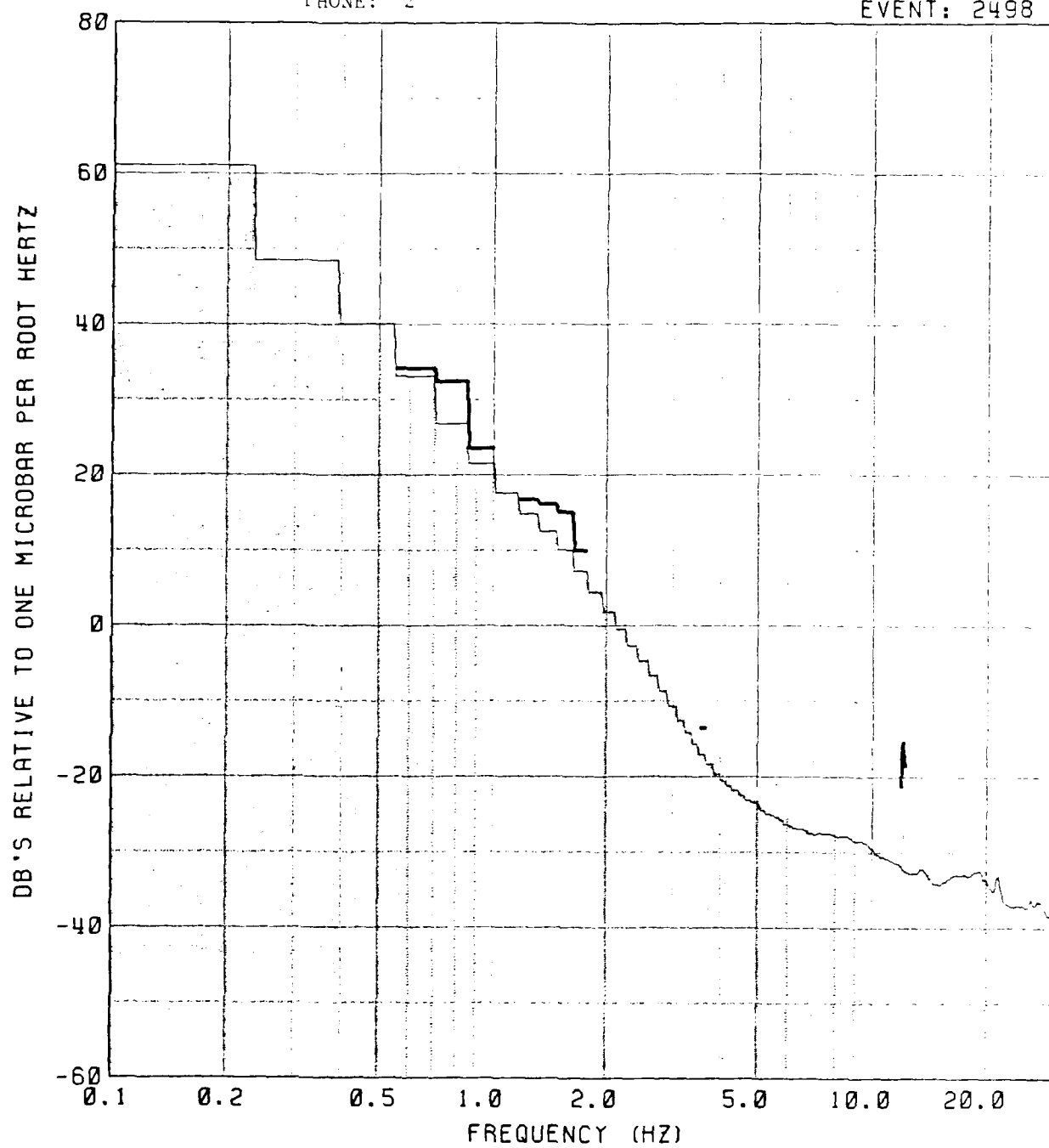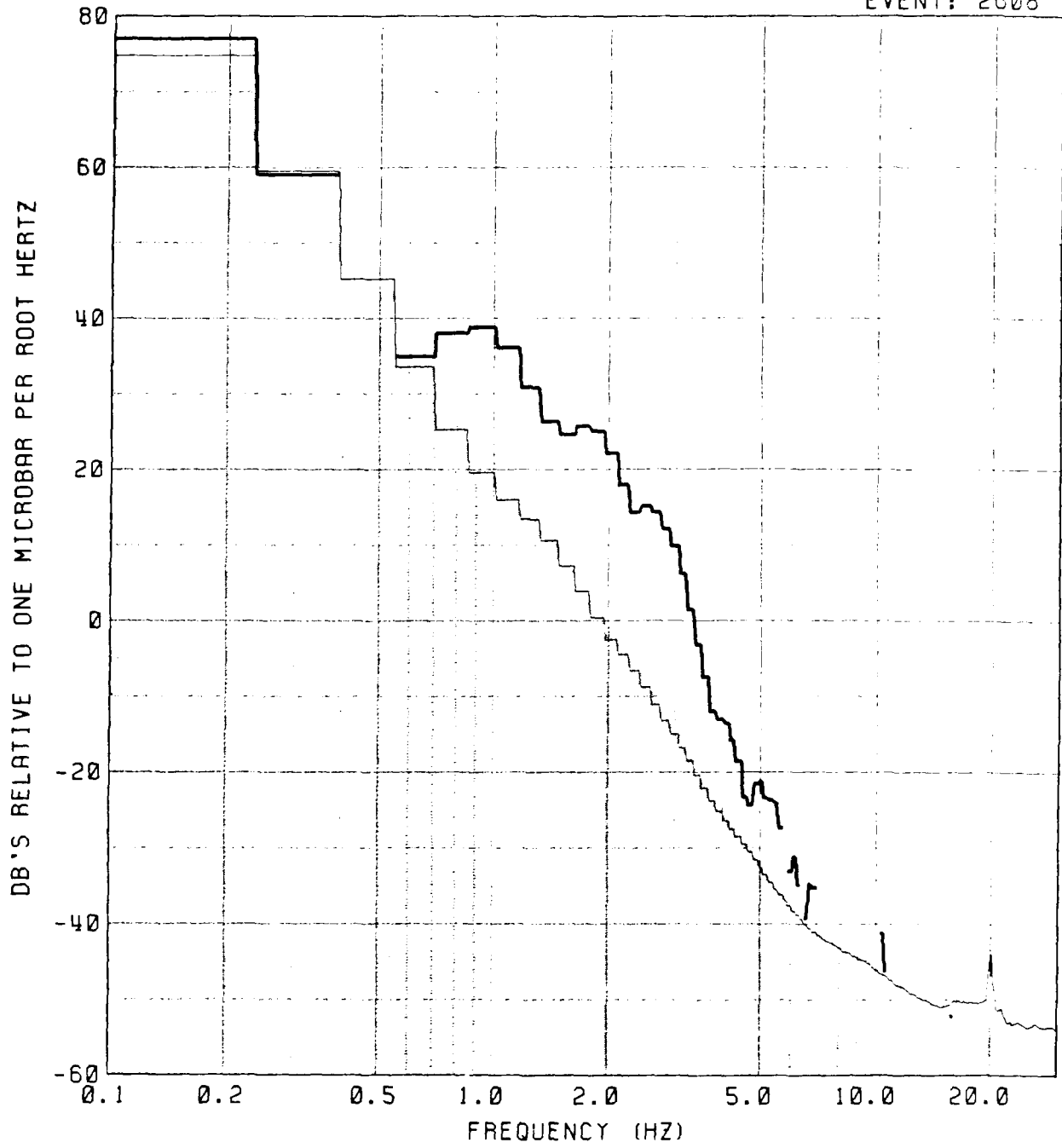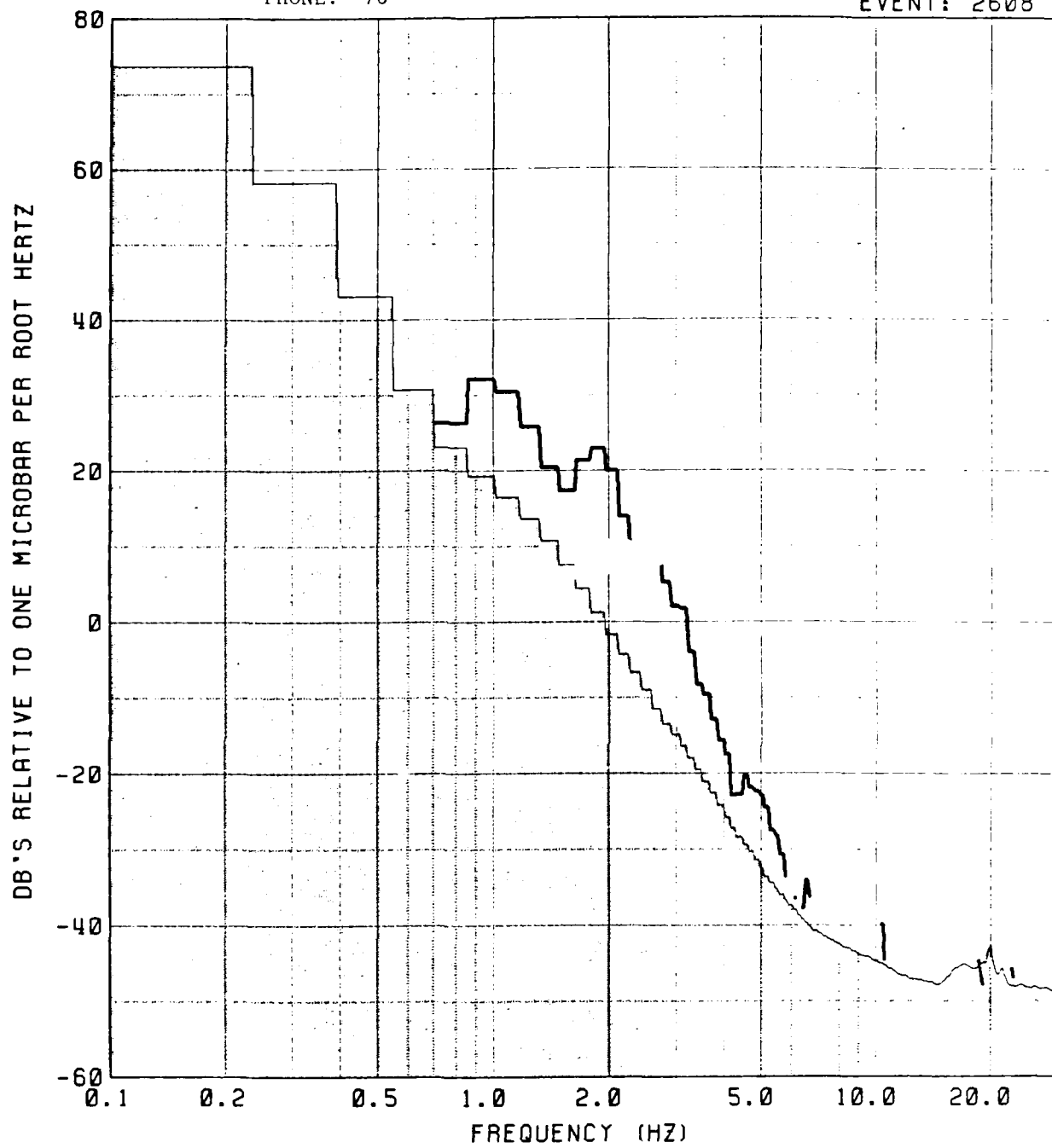
FREQUENCY (HZ)

DB'S RELATIVE TO ONE MICROBAR PER ROOT HERTZ

NOISE
MEAN
P

PHONE: 74   EVENT: 3230

FREQUENCY (HZ)

DB'S RELATIVE TO ONE MICROBAR PER ROOT HERTZ

NOISE
MEAN
P

PHONE: 76

NOISE
MEAN
P

PHONE: 2   EVENT: 3230

NOISE
MEAN
P

DB'S RELATIVE TO ONE MICROBAR PER ROOT HERTZ

FREQUENCY (HZ)

NOISE
MEAN
P

PHONE: 76

NOISE
MEAN
P

EVENT: 74

Hz

10.00
8.75
7.50
6.25
5.00
3.75
2.50
1.25
0

10.000HZ 8.750HZ 7.500HZ 6.250HZ 5.000HZ 3.750HZ 2.500HZ 1.250HZ 0.000HZ

10.000HZ 8.750HZ 7.500HZ 6.250HZ 5.000HZ 3.750HZ 2.500HZ 1.250HZ 0.000HZ

10.00 8.75 7.50 6.25 5.00 3.75 2.50 1.25 0

HZ

EVENT: 345

EVENT: 438

EVENT: 1170

Hz

EVENT: 1727

EVENT: 2177

EVENT: 2352

102

EVENT: 2459

10.00 — 8.75 — 7.50 — 6.25 — 5.00 — 3.75 — 2.50 — 1.25 — 0

HZ

EVENT: 2498

104

EVENT: 2608

EVENT: 2812

EVENT: 3230

10.00 —
8.75 —
7.50 —
6.25 —
5.00 —
3.75 —
2.50 —
1.25 —
0 —

Hz

EVENT: 3249

10.000HZ
8.750HZ
7.500HZ
6.250HZ
5.000HZ
3.750HZ
2.500HZ
1.250HZ
0.000HZ
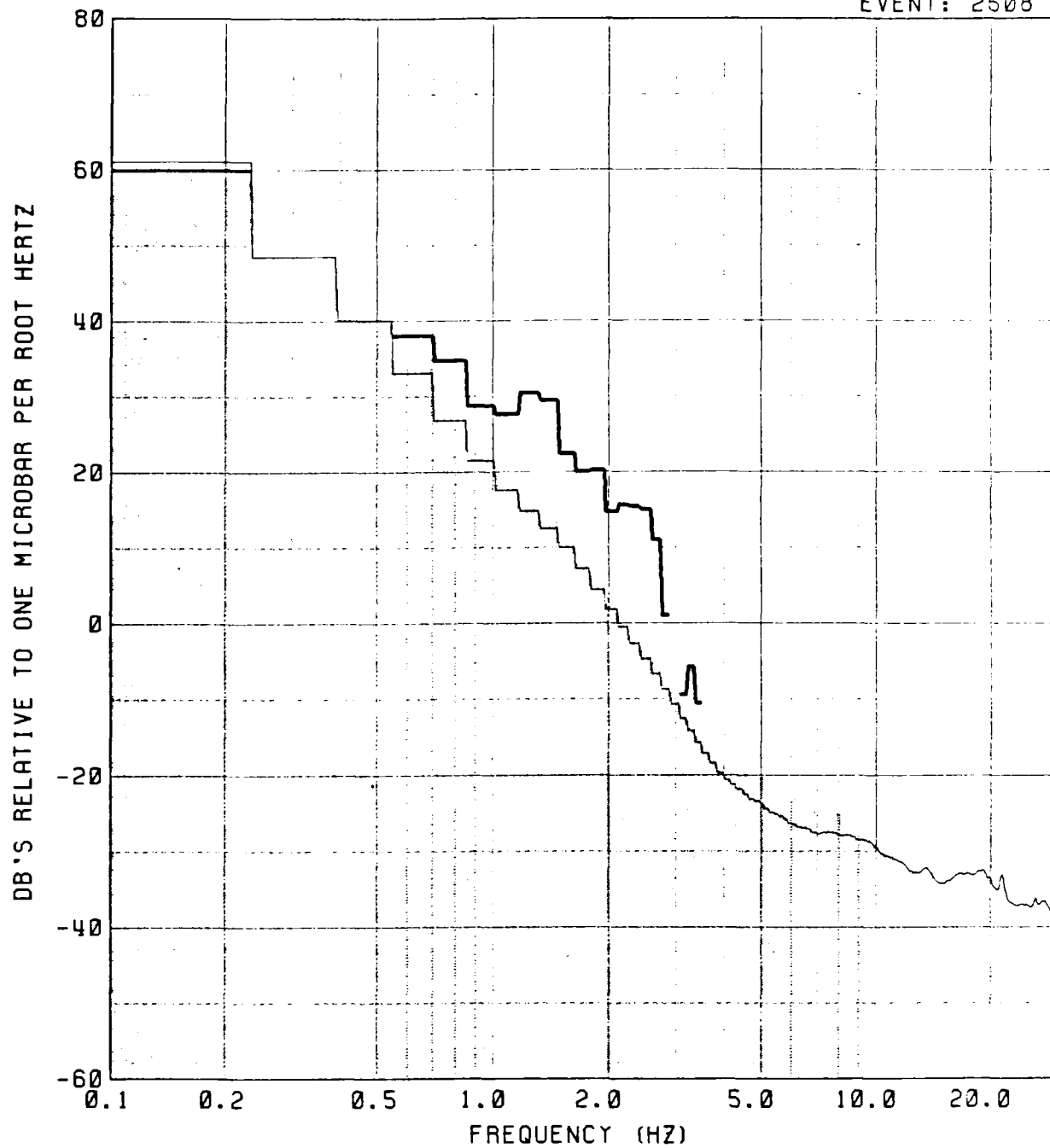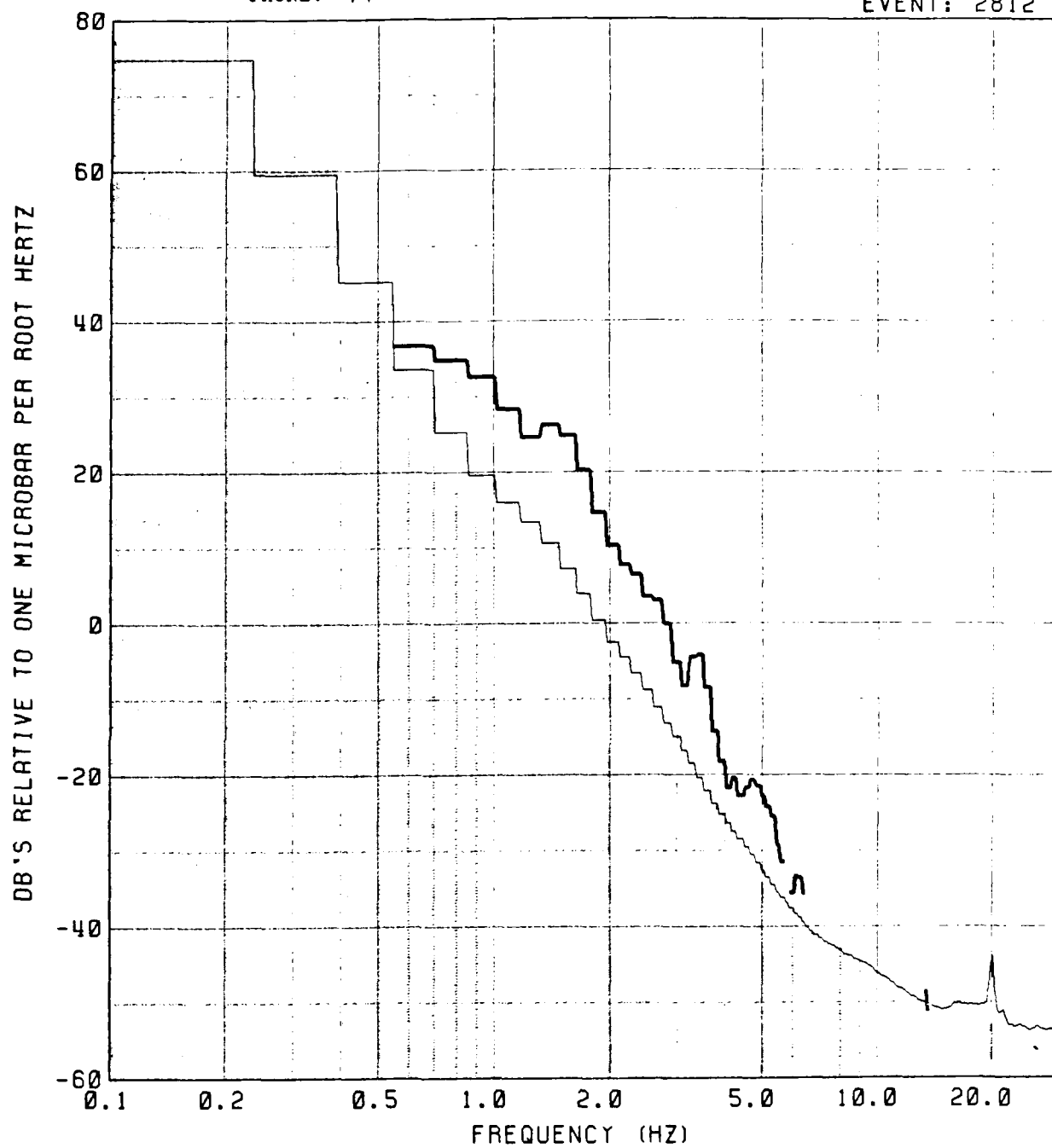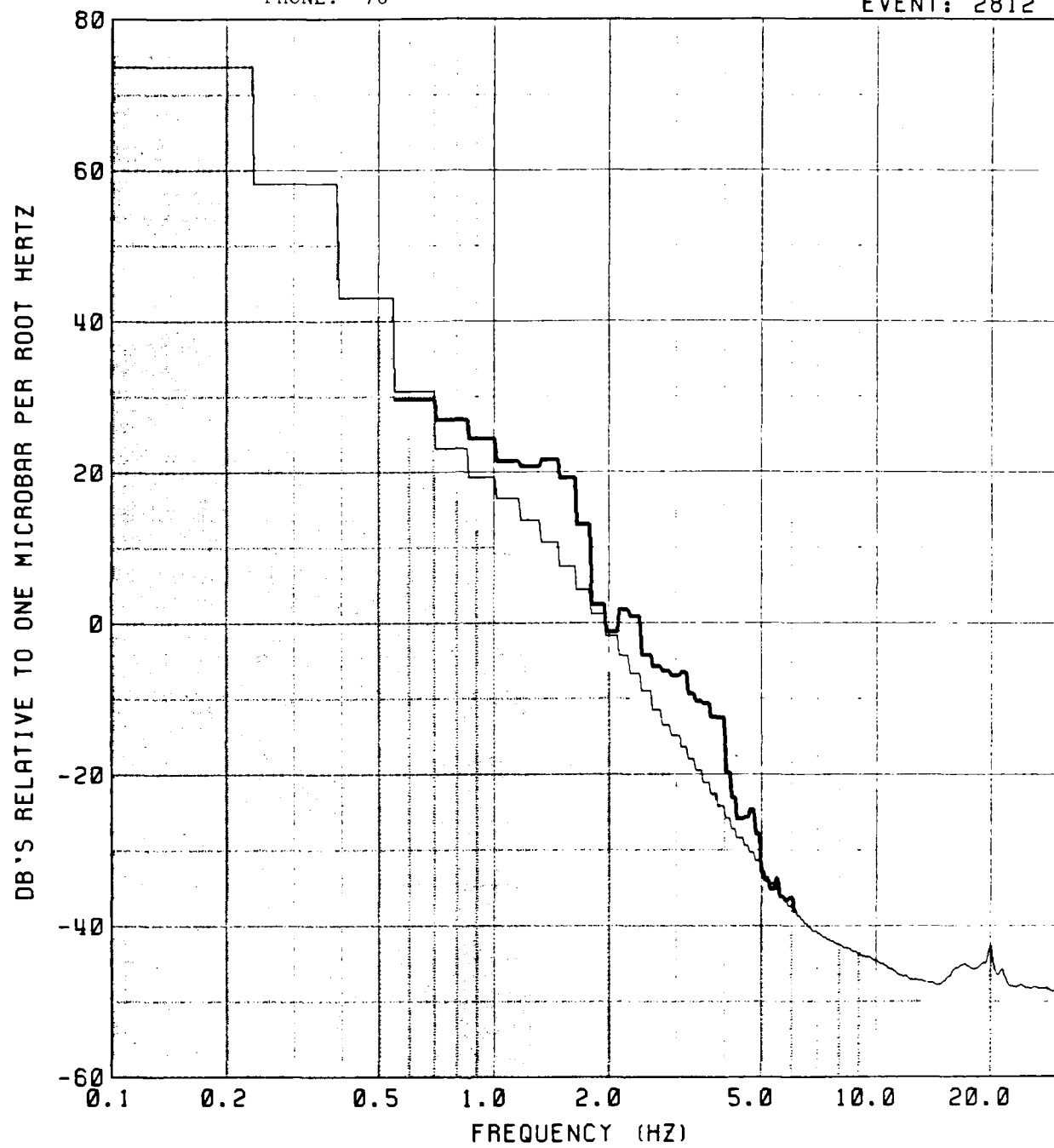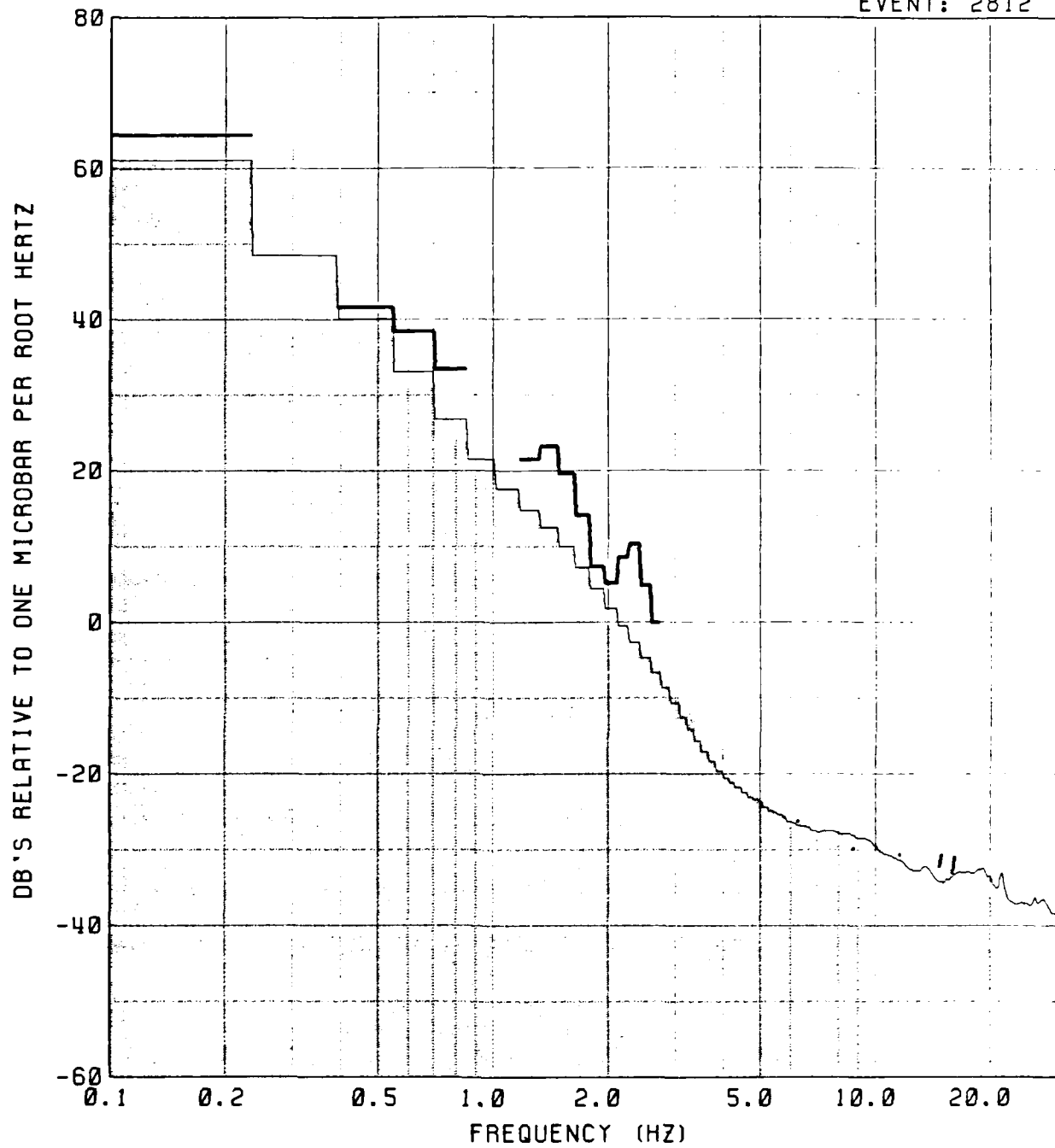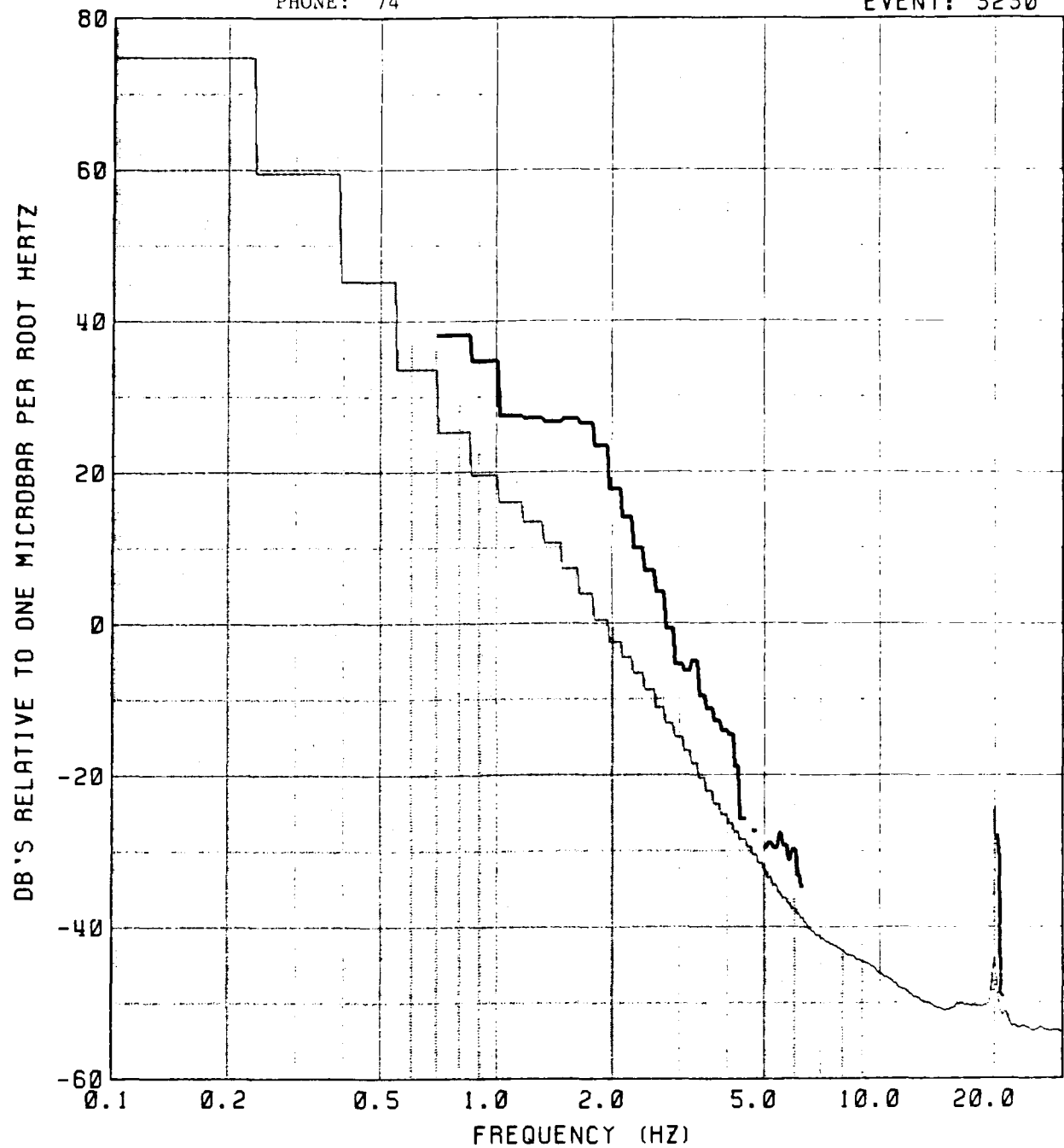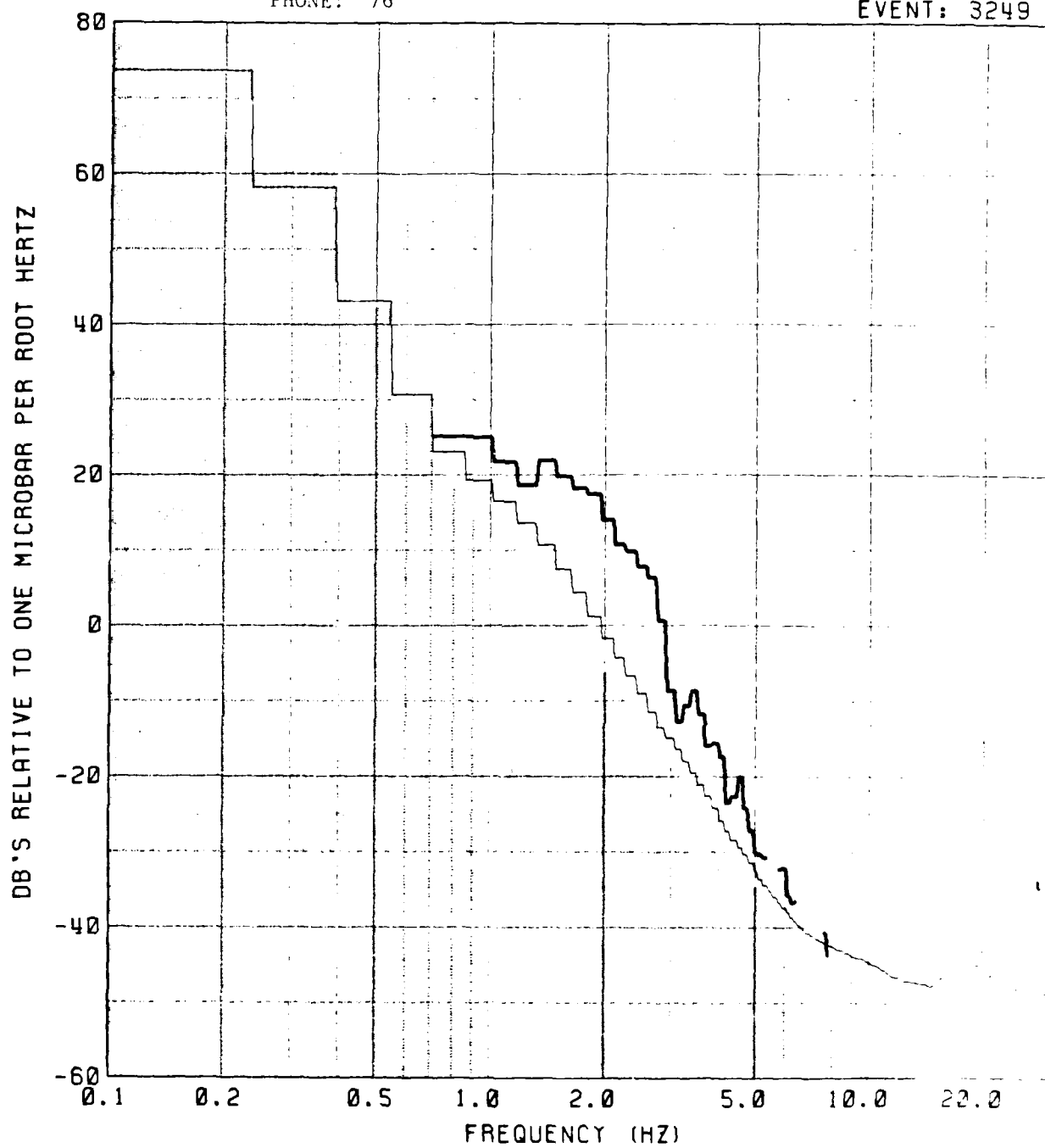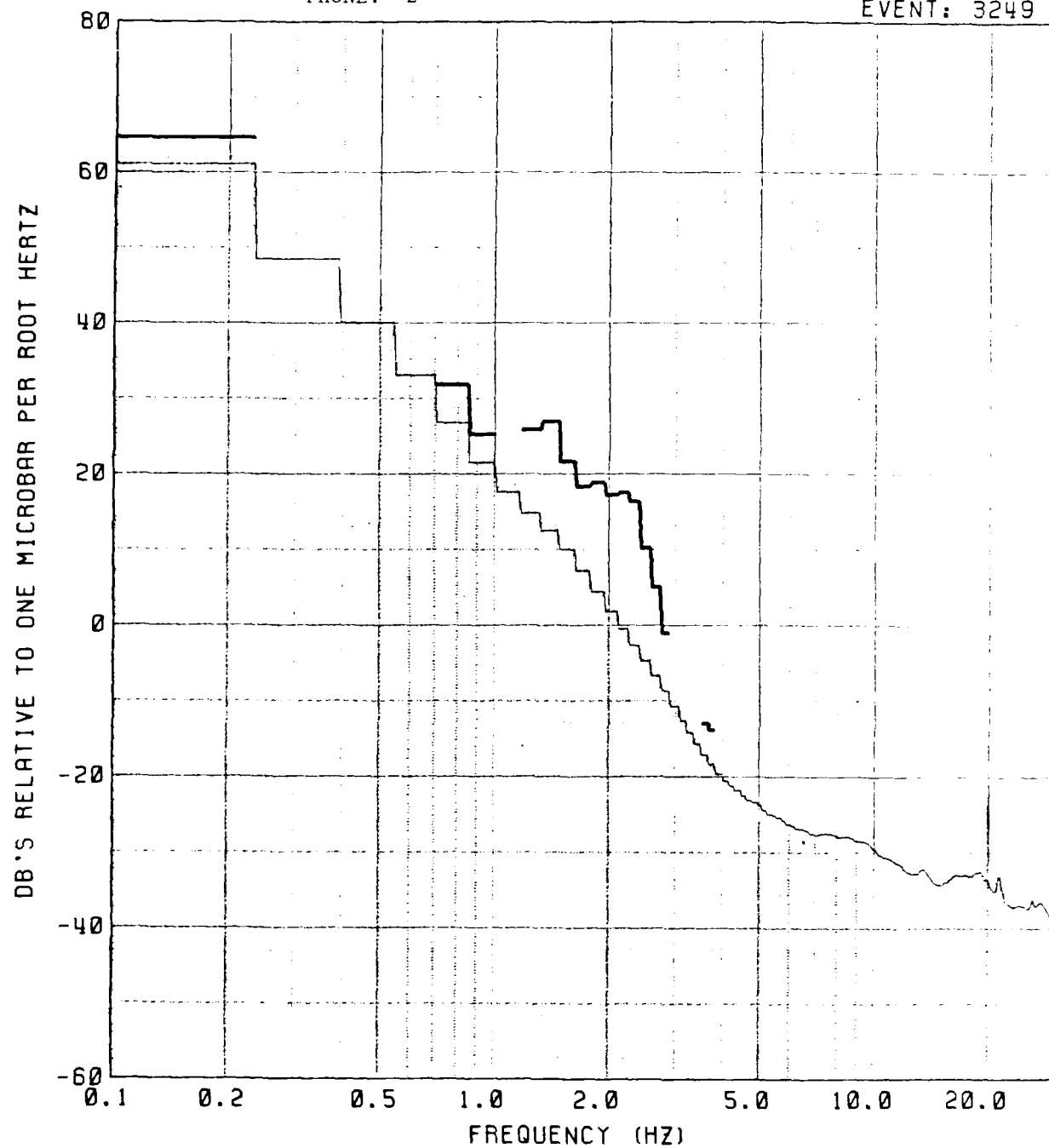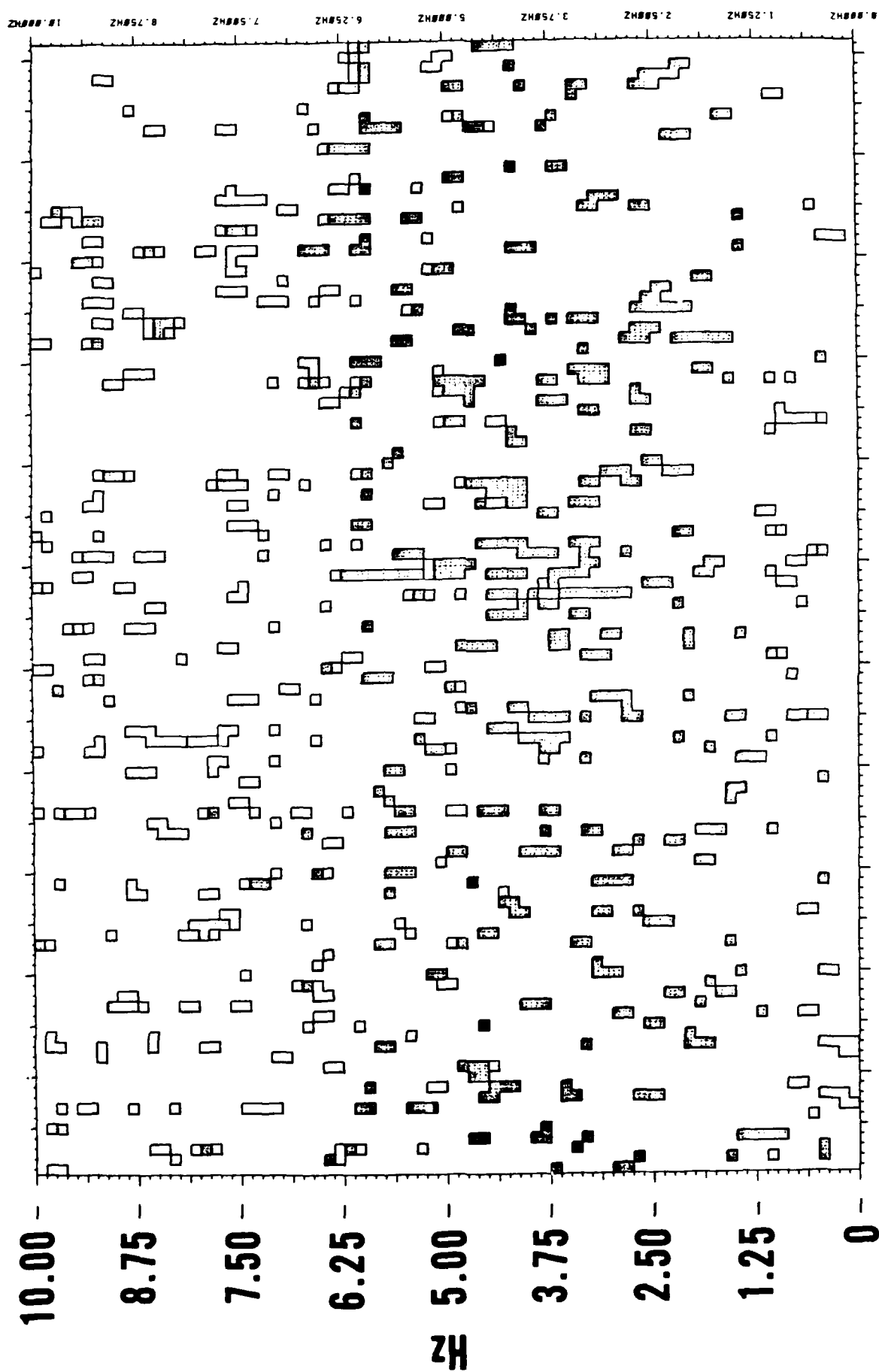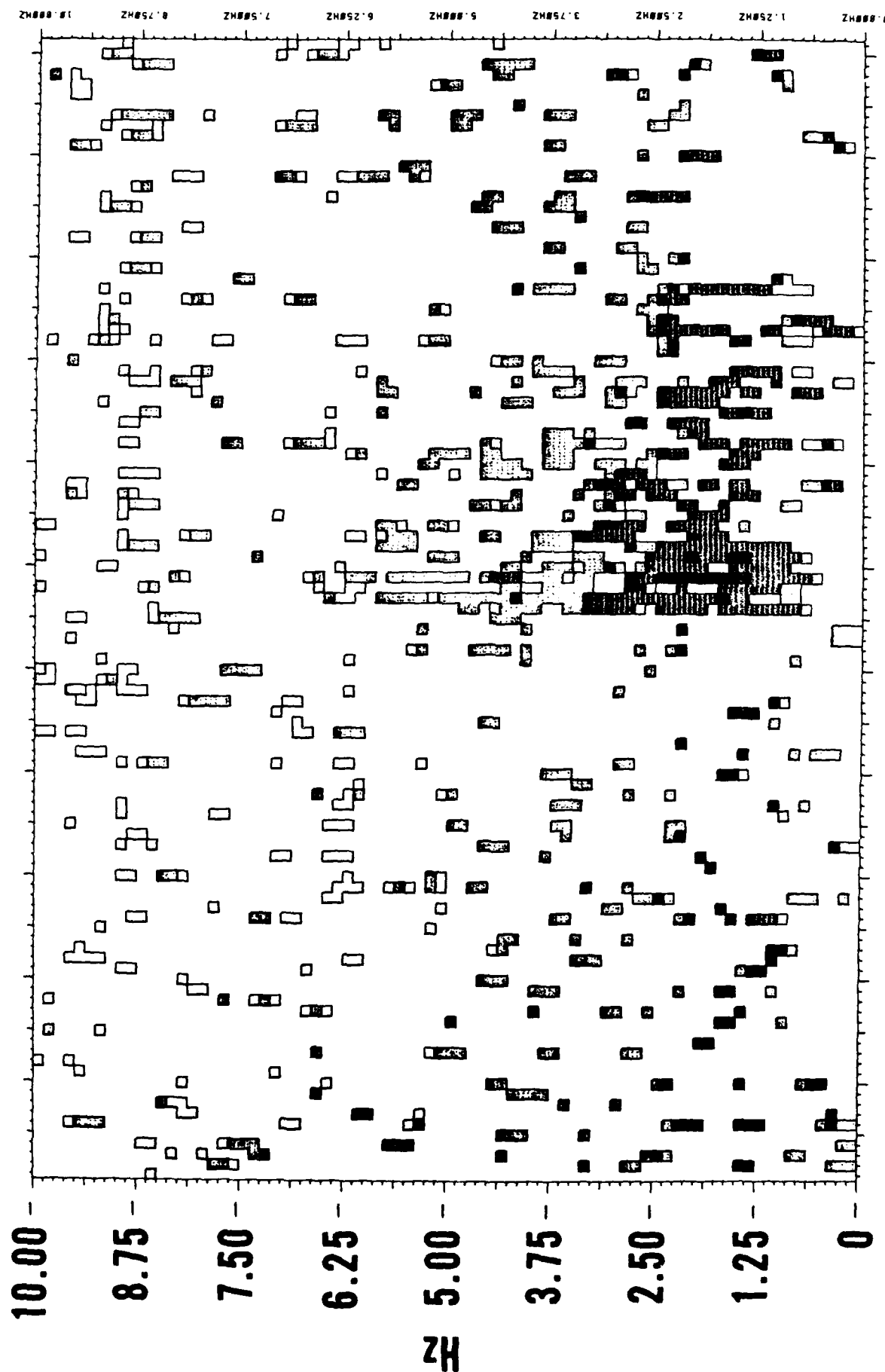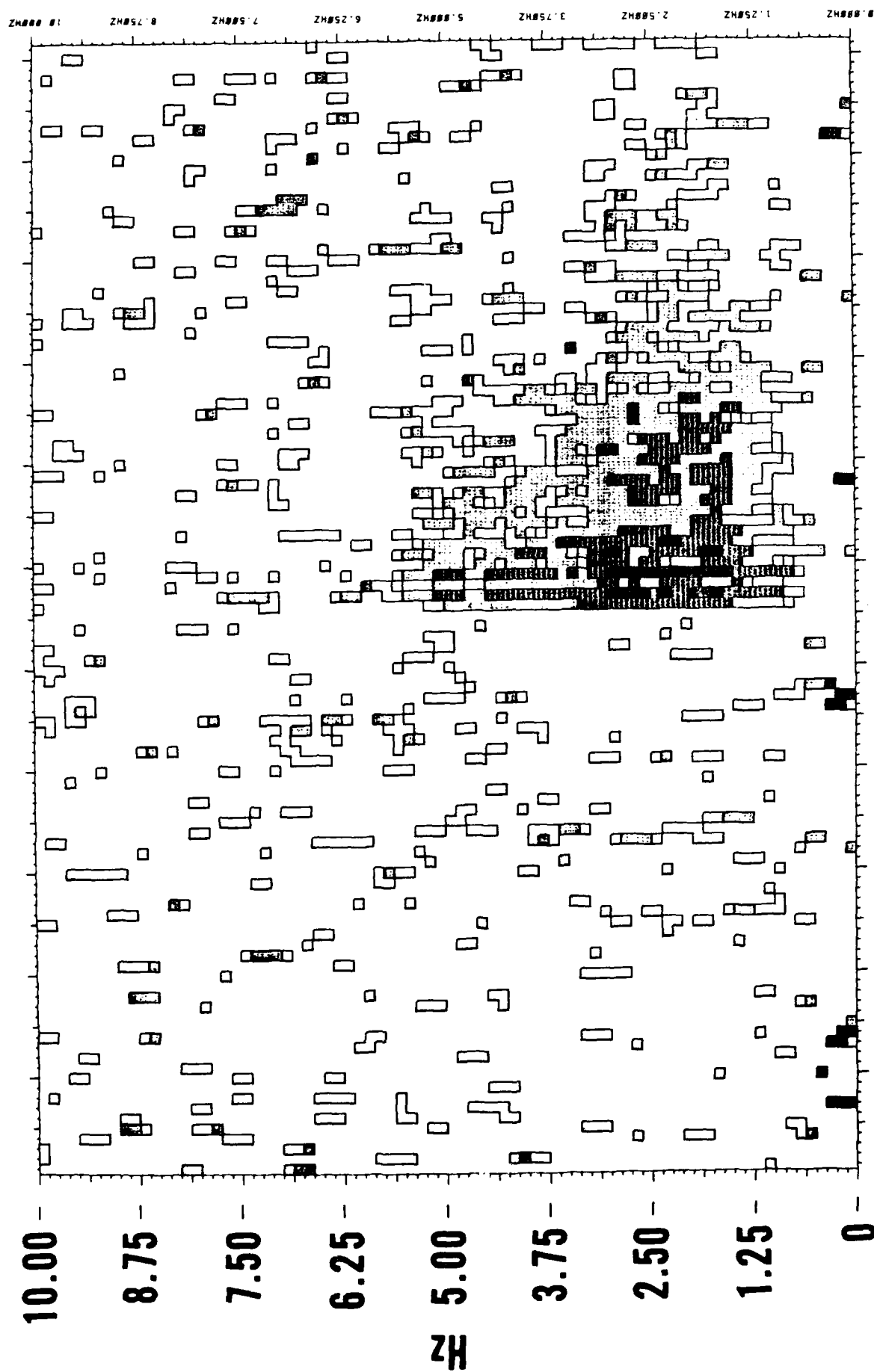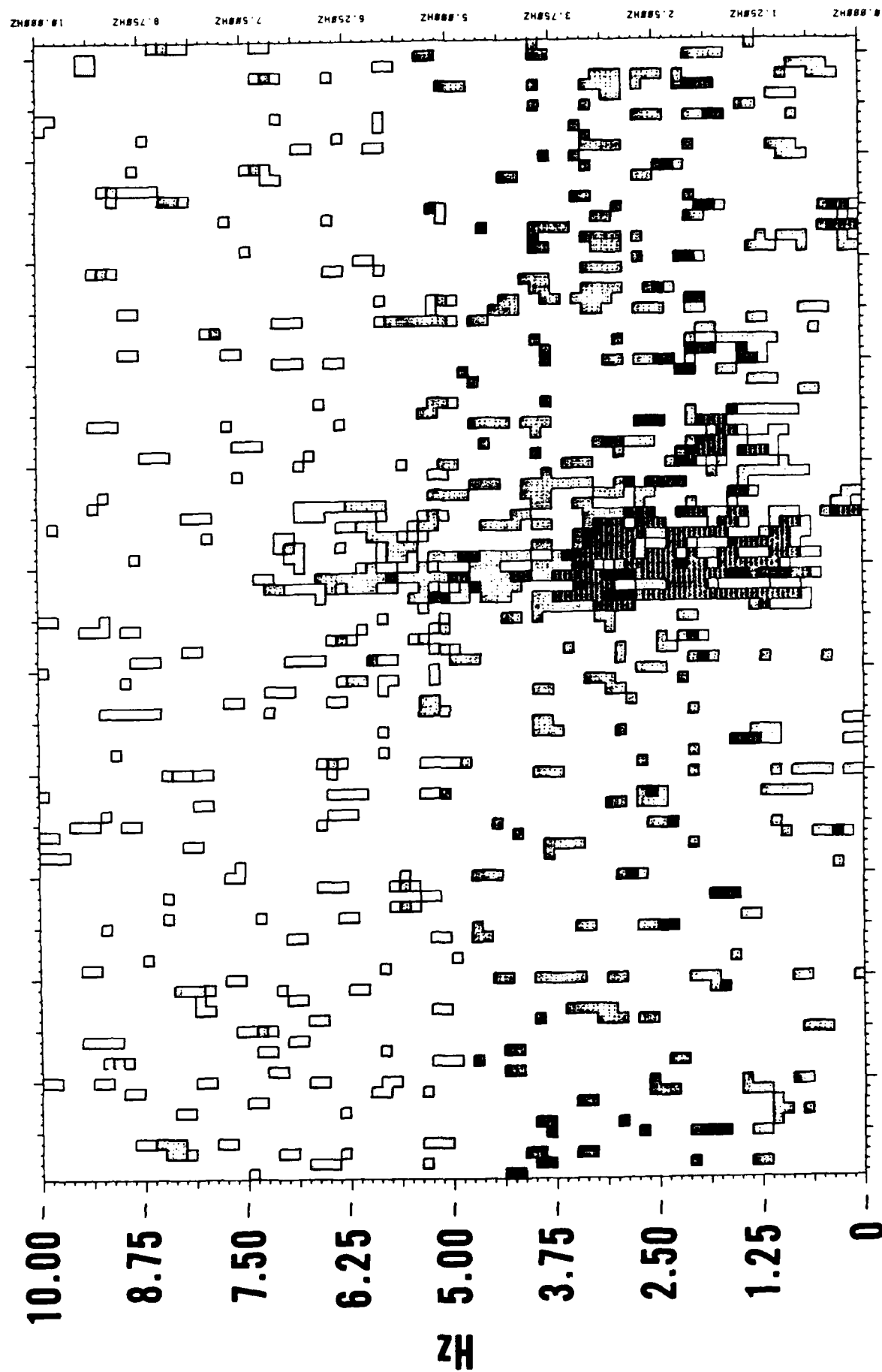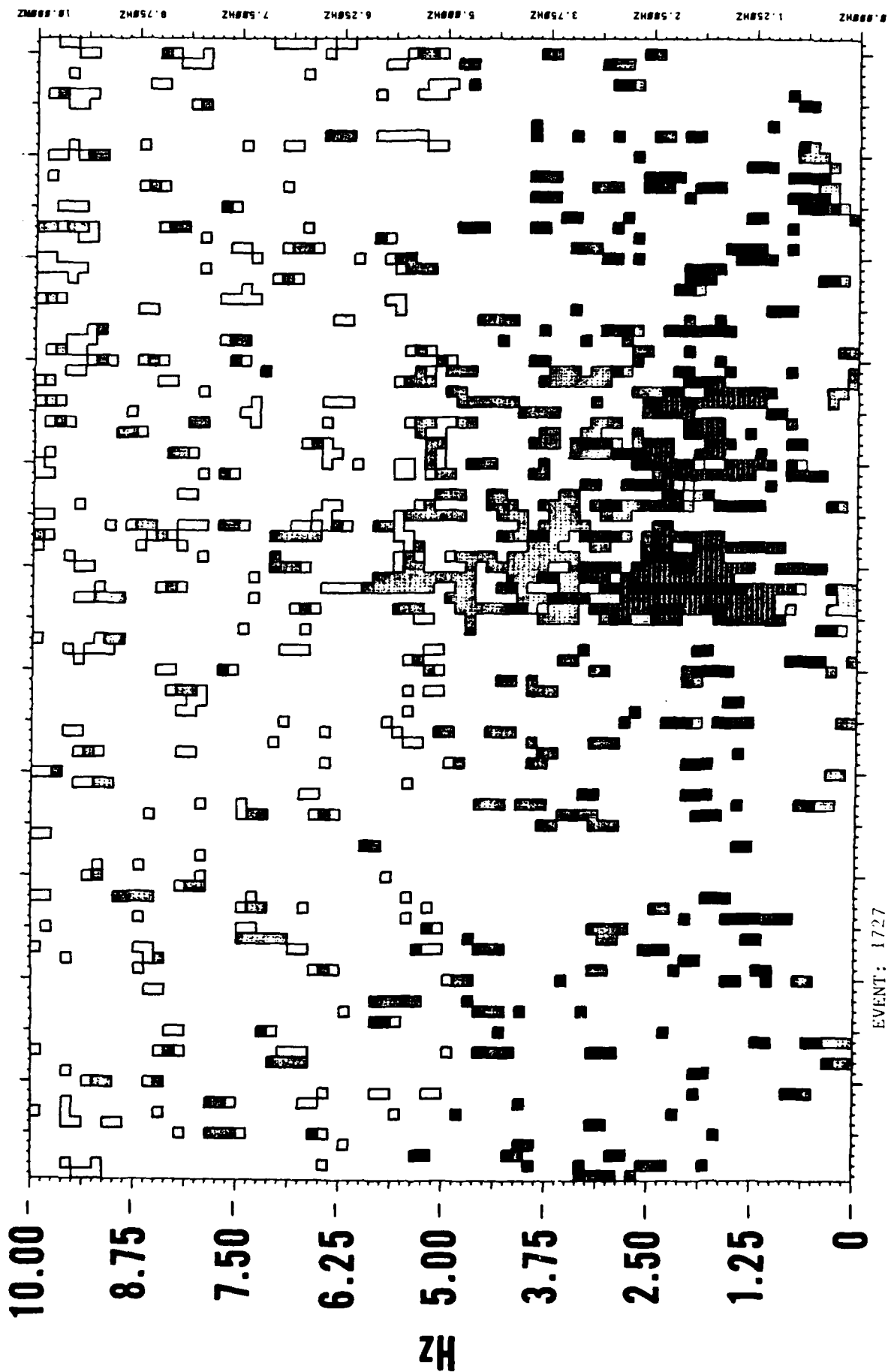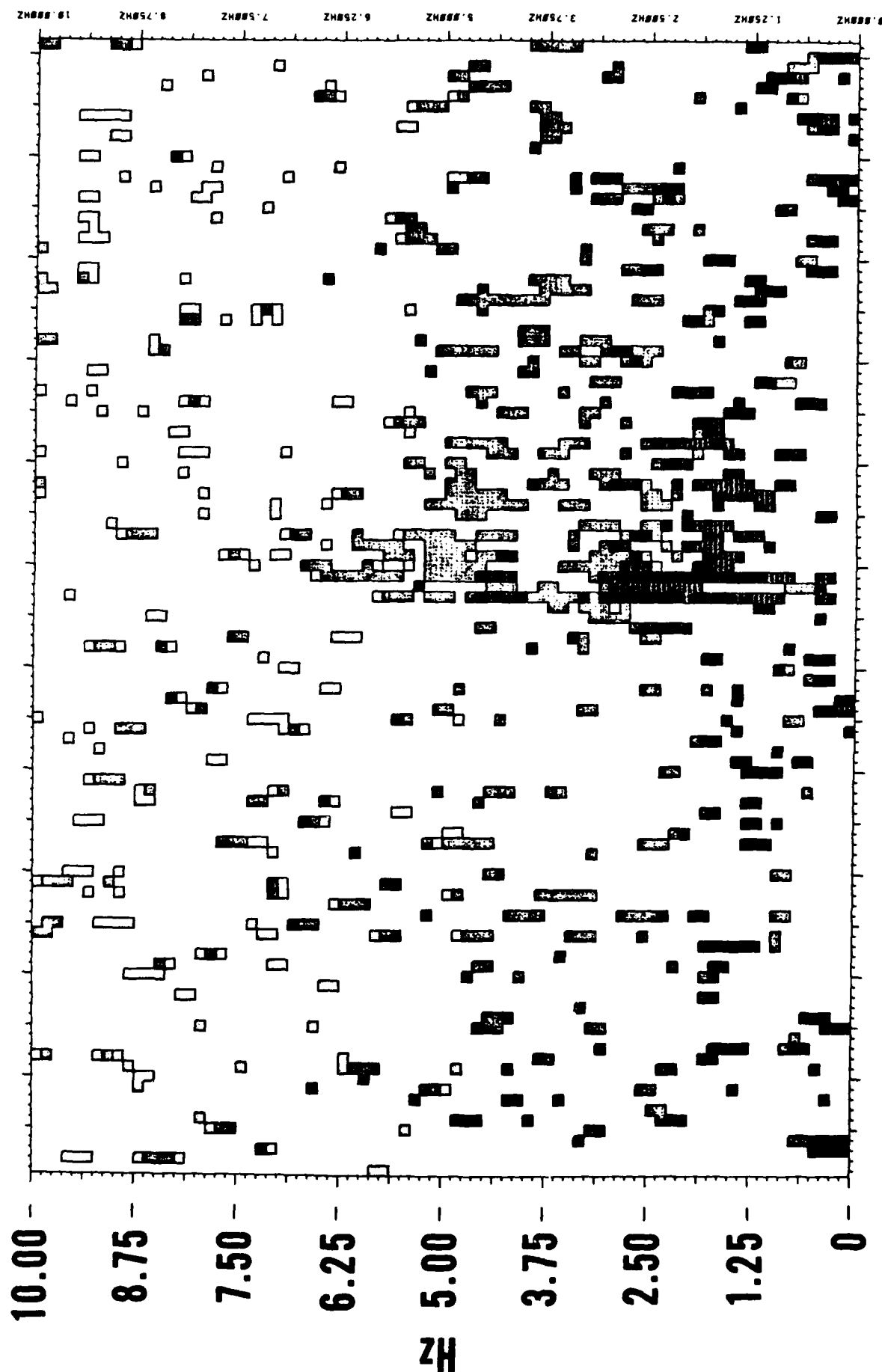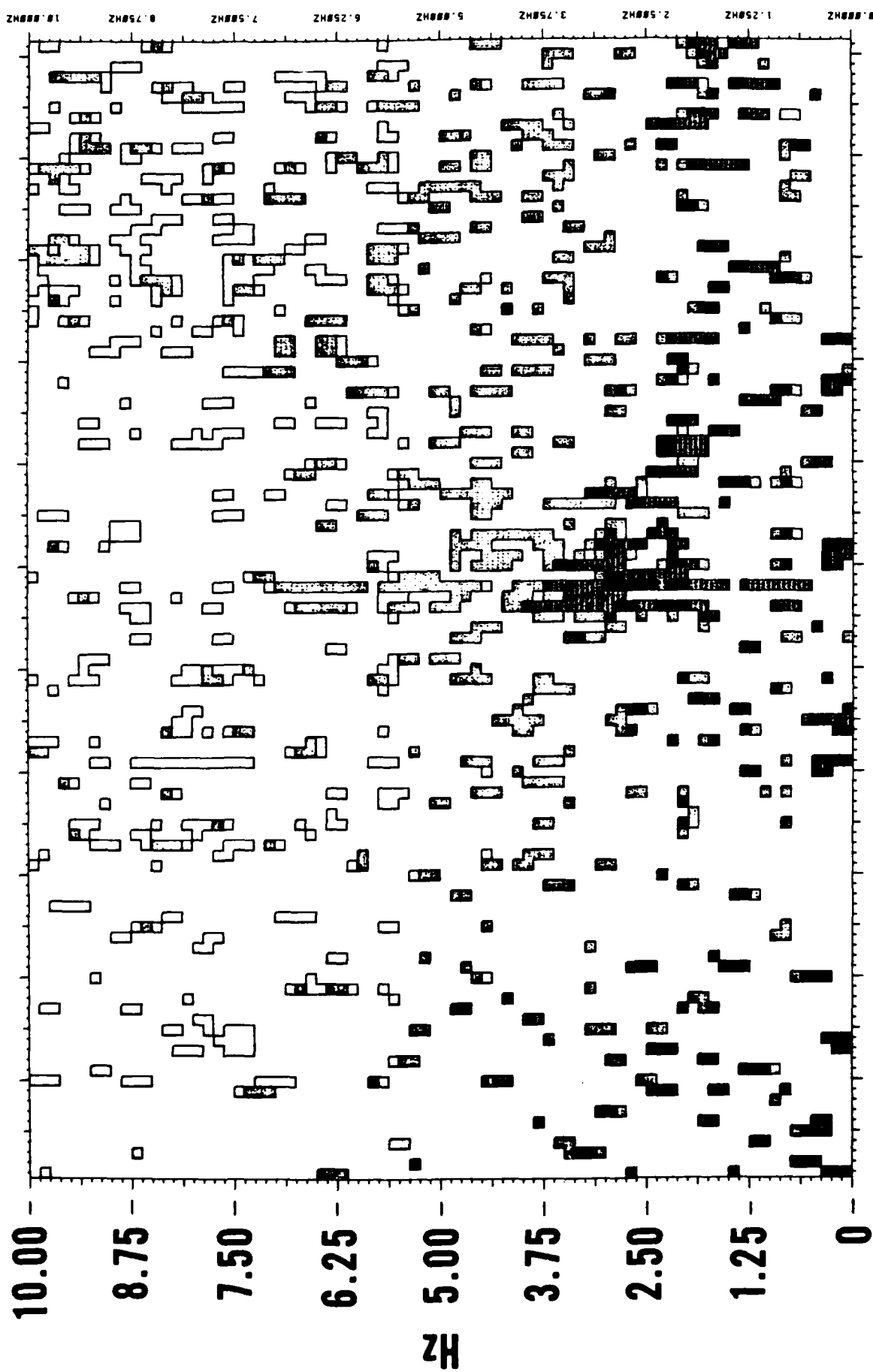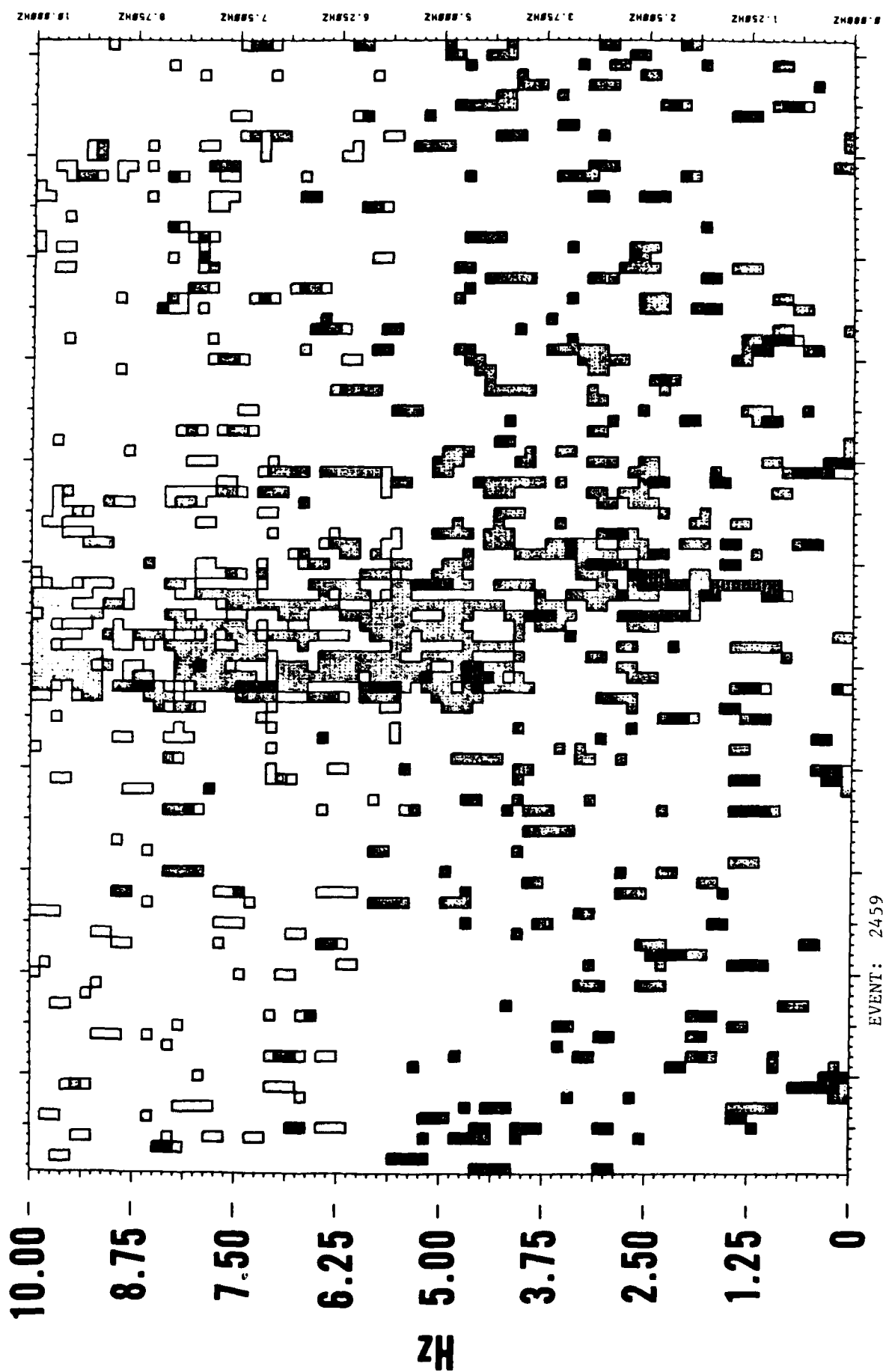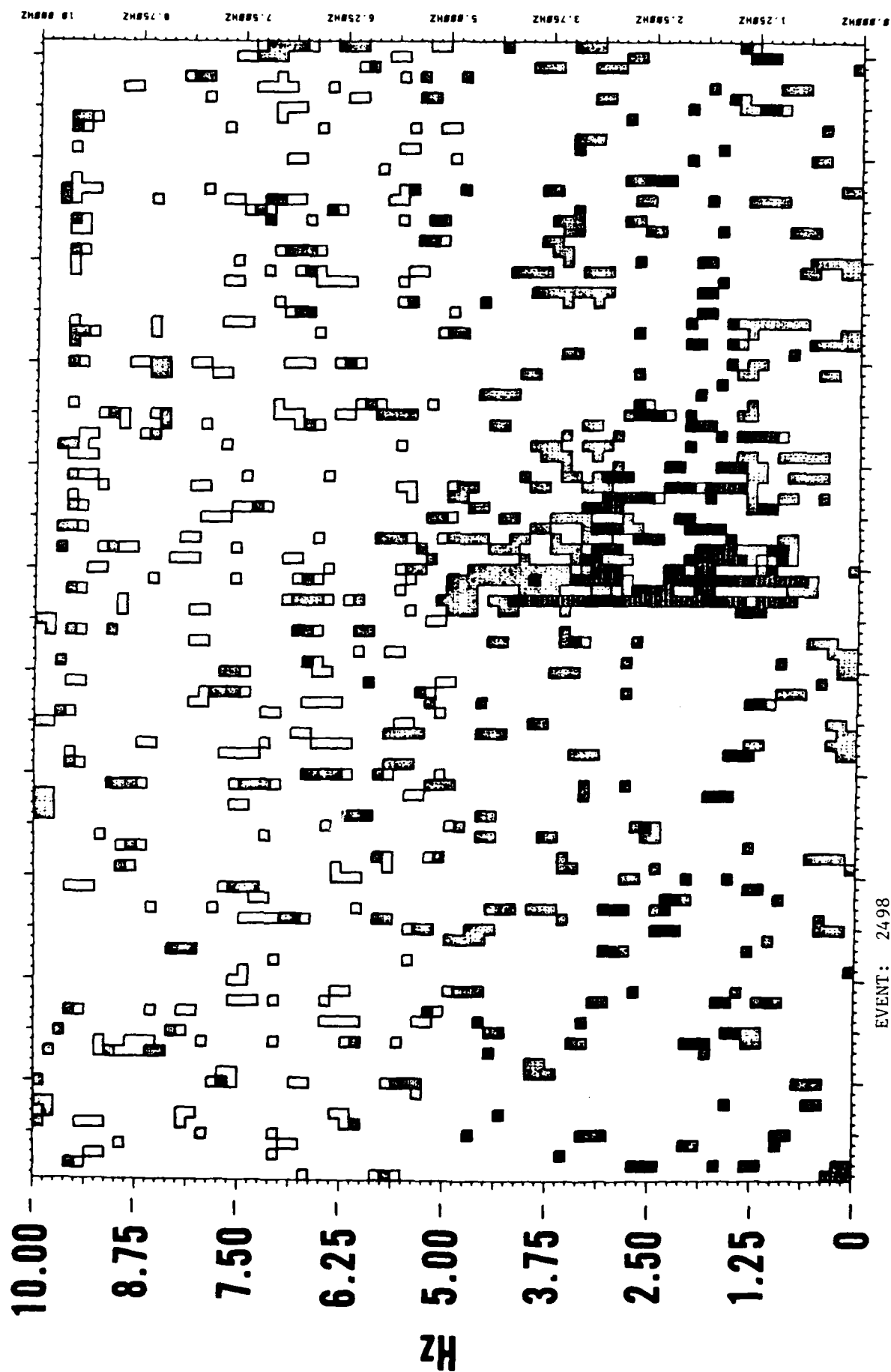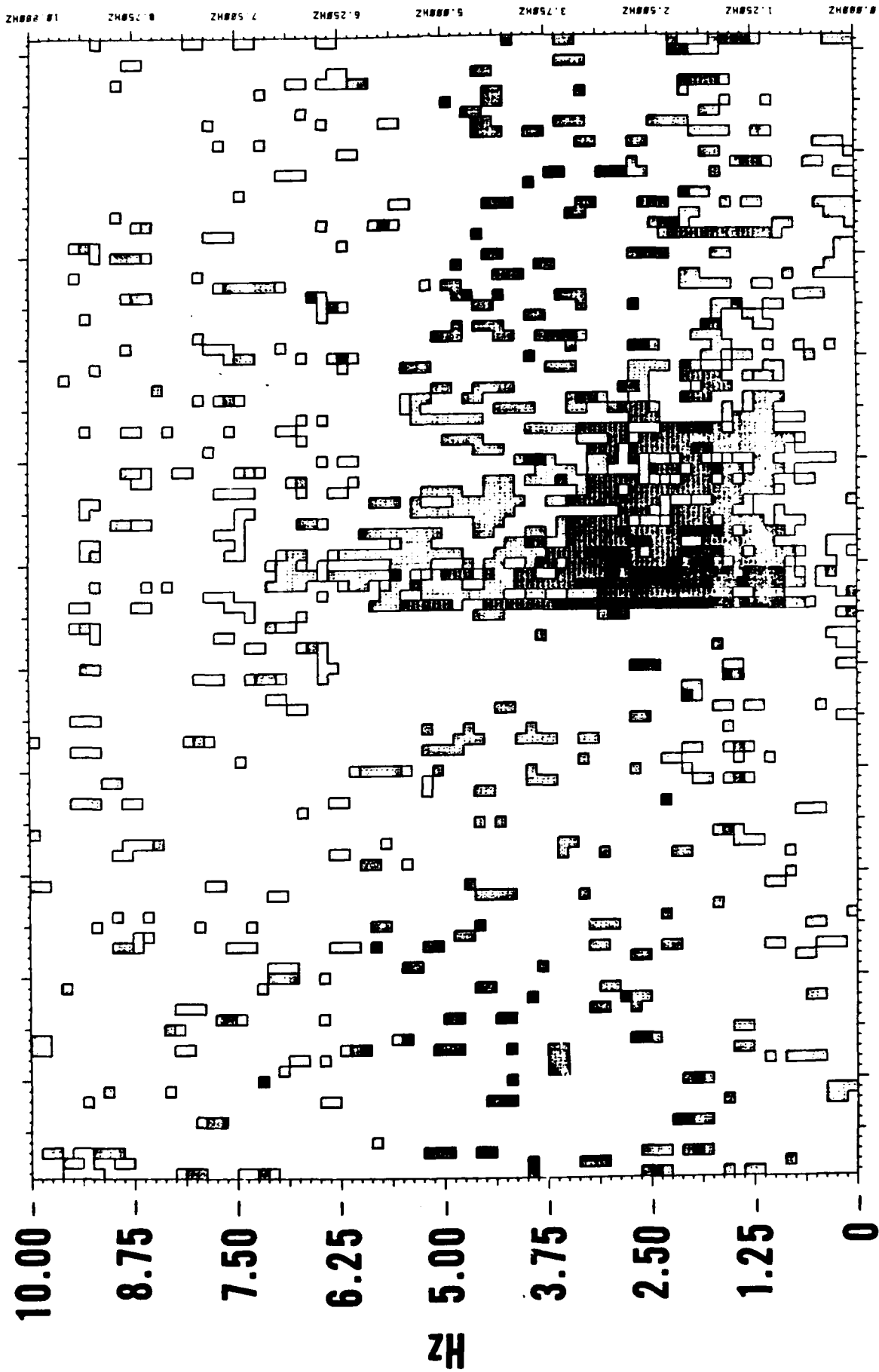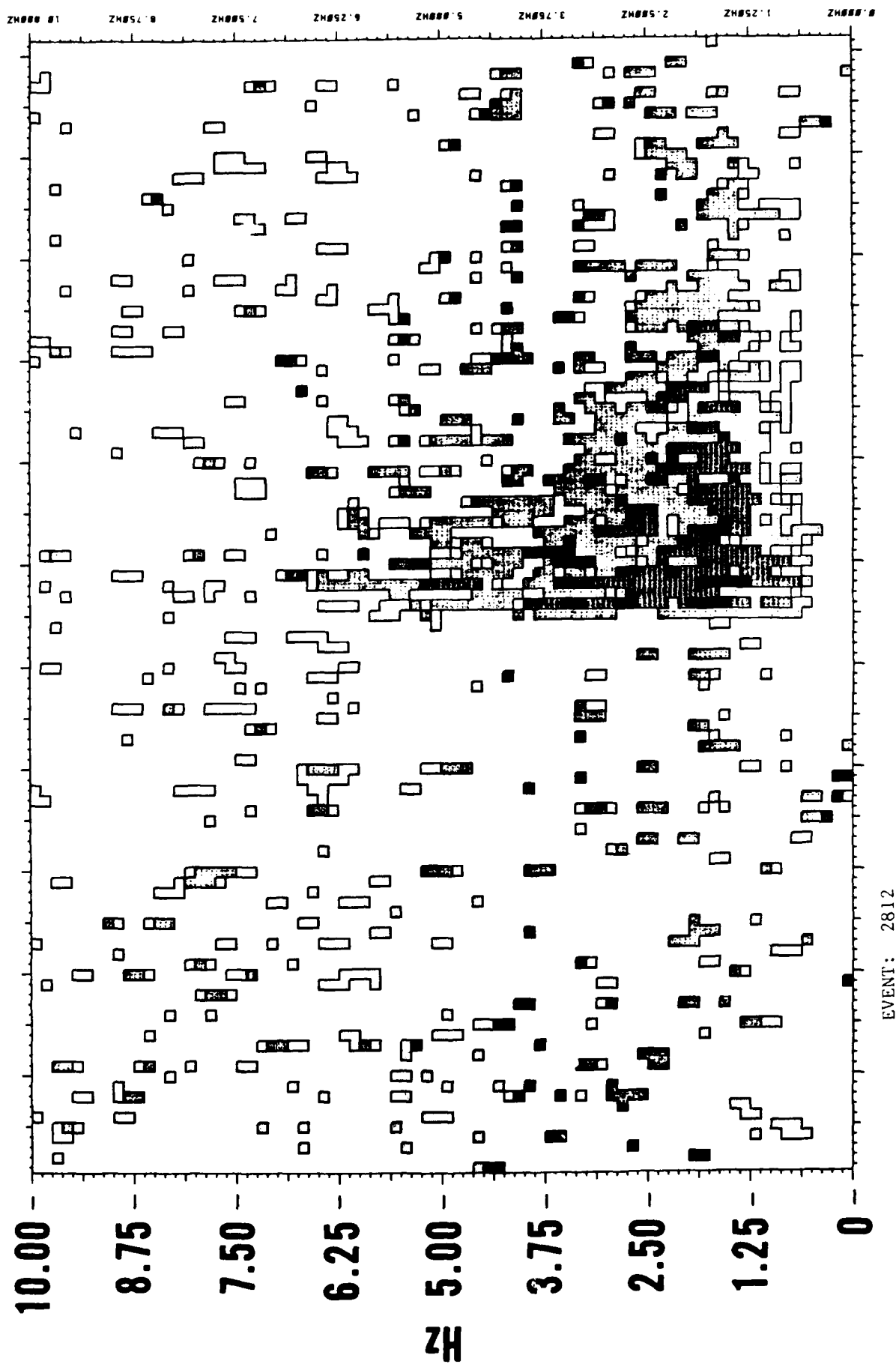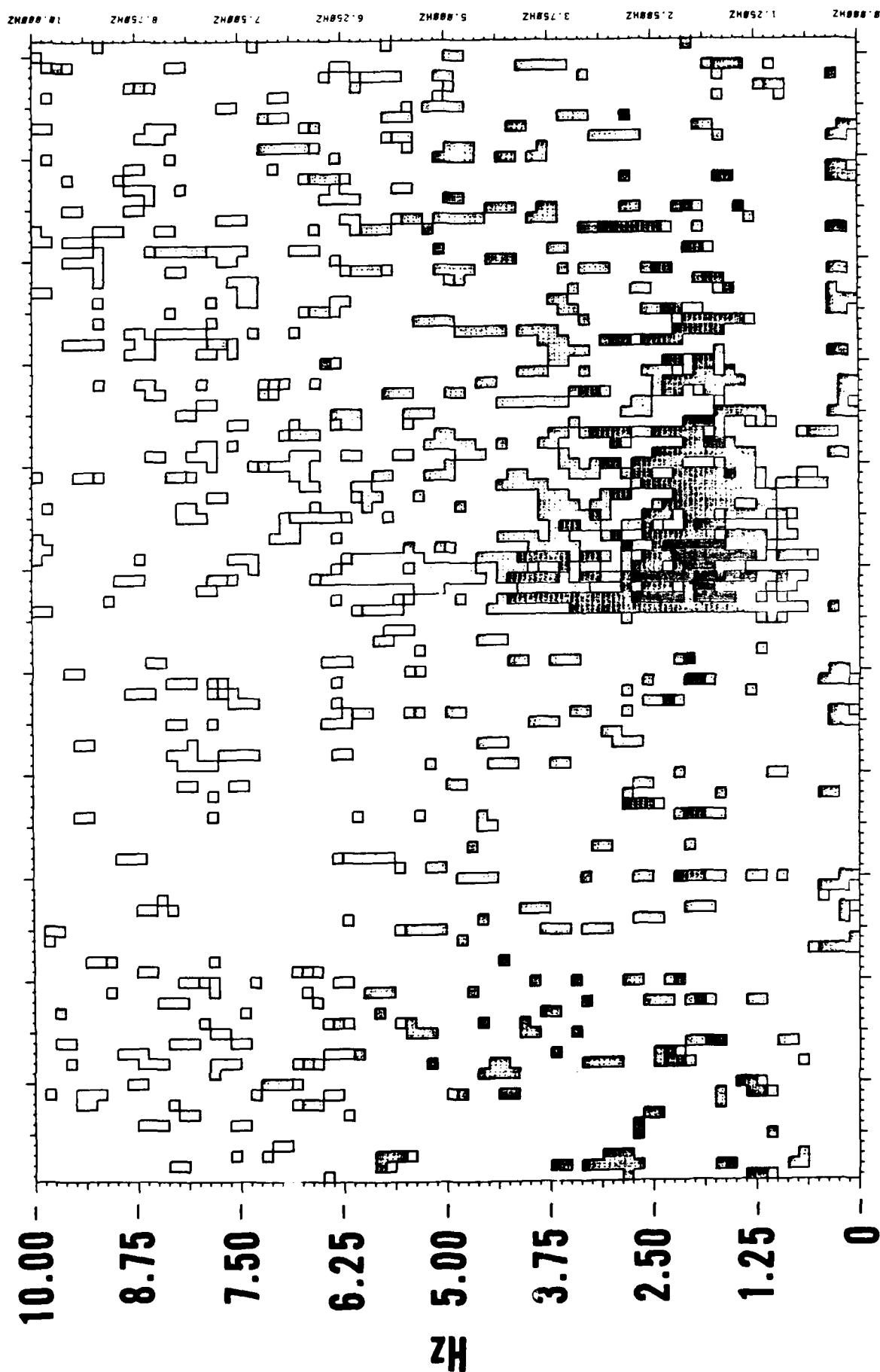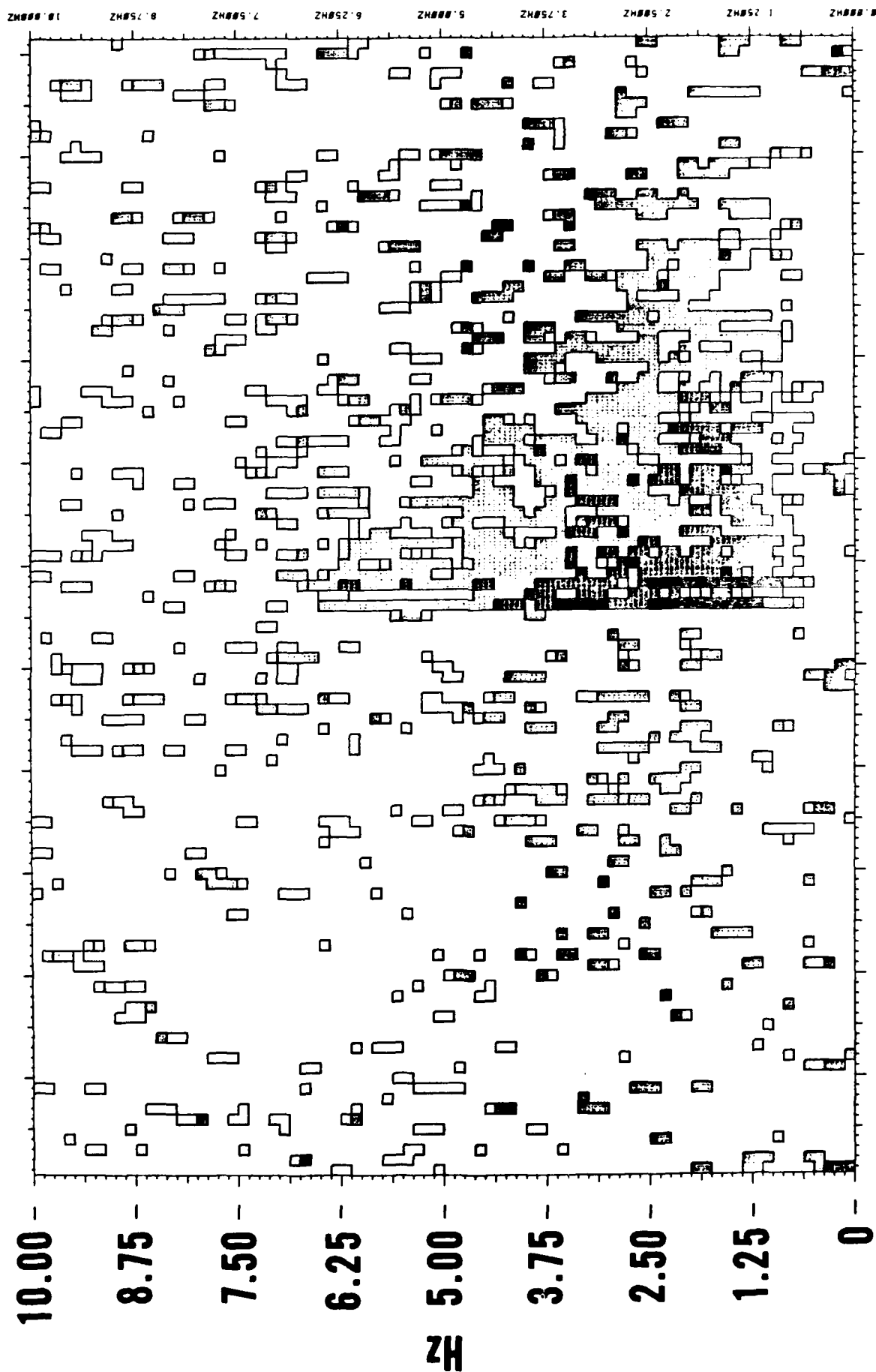
Eastern Kazakh - Discussion

Thirteen events were recorded from this site. With the exception of event # 74 which is only indicated on phones 74 and 76, all were recorded by phones 74, 76, and 2. Unlike the Novaya Zemlya events, the greatest S/N ratios were found on phone 74 - at frequencies generally from 1.5 to 2 Hz. Frequencies often in excess of 5 Hz were observed, with values as high as 7 Hz (e.g. #2608). Event # 2459 appears to have signals in excess of 10 Hz; however, these arrivals are several blocks before the actual onset of the P which is characterized by much lower frequencies. The smallest event recorded was a 5.2 (event # 74; see the noise reduced spectrogram and spectrum for phone 74). Since the noise levels were lower than mean values for this explosion and it was only barely perceptible in the spectral plot for phone 74, but obvious in the noise-reduced spectrogram, it appears that magnitudes much lower than 5.2 might not be generally observable on phone 74 from this site.

```
EVNT ******ORIGIN TIME****** **COORDINATES***   ****
*NO*  YR*MO*DA*JUL*HR*MN*SECS **LAT******LON***   *MB*

SIBERIA

1154 82 10 10 283 04 59 56.8 61 855N 112.833E   5.3
```

SIBERIA

NO	ORIGIN TIME				COORDINATES		DISTANCE (DEG)			SIGNAL LEVELS			NOISE LEVELS			
	YR/MO/DAY	HR	MIN	SEC	N	E	74	76	2	74	76	2	74	76	2	MB
154	82/10/10	4	59	56.8	61.56	112.83	55.05	55.36	57.84	*****	*****	*****	2.0	2.5	4.0	5.3

EVENT: 154

71 –

73 –

74 –

75 –

76 –

1 –

2 –

4 –

112
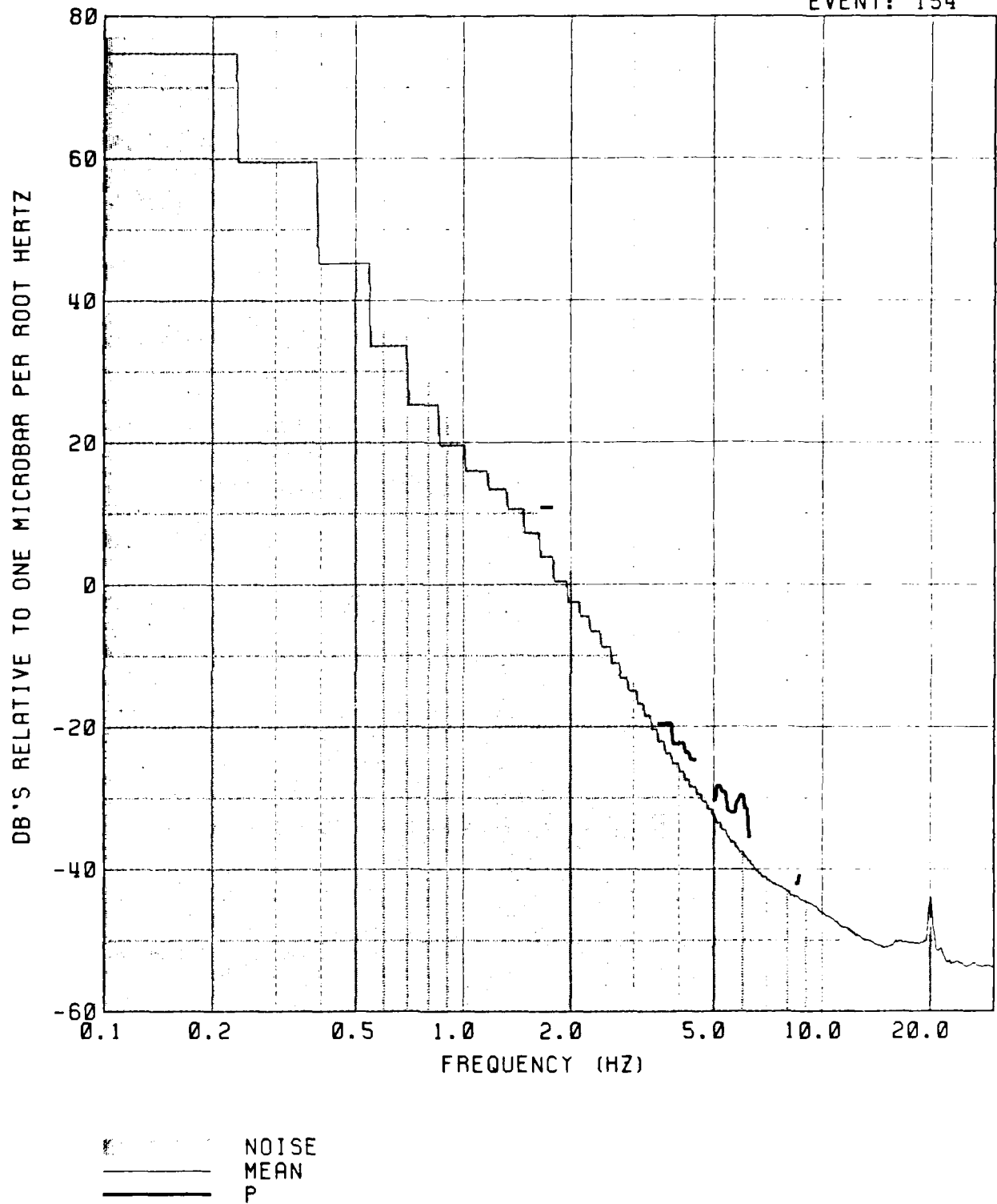
PHONE: 74
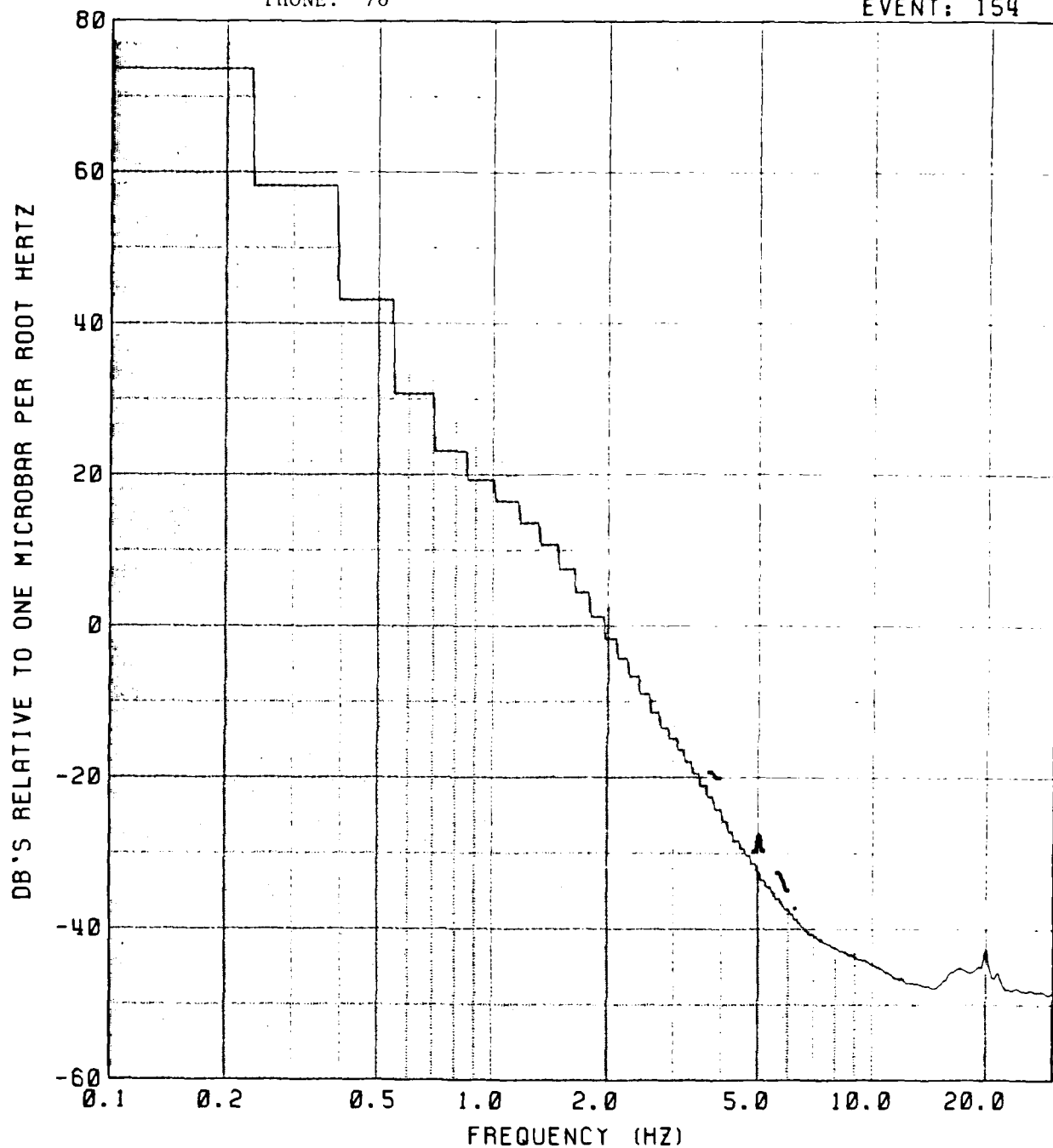
NOISE
MEAN
P

PHONE: 2

NOISE
MEAN
P

EVENT: 154
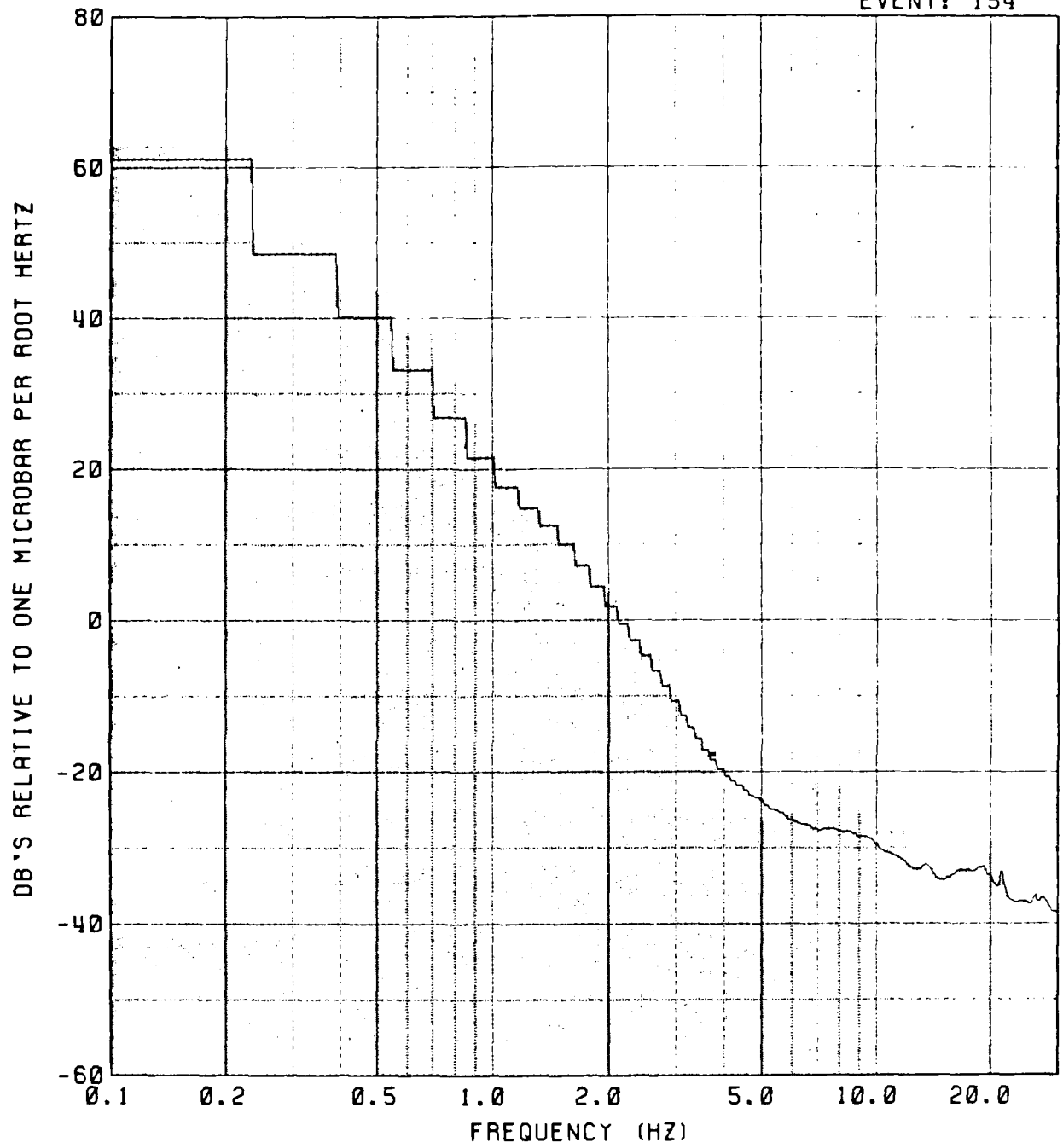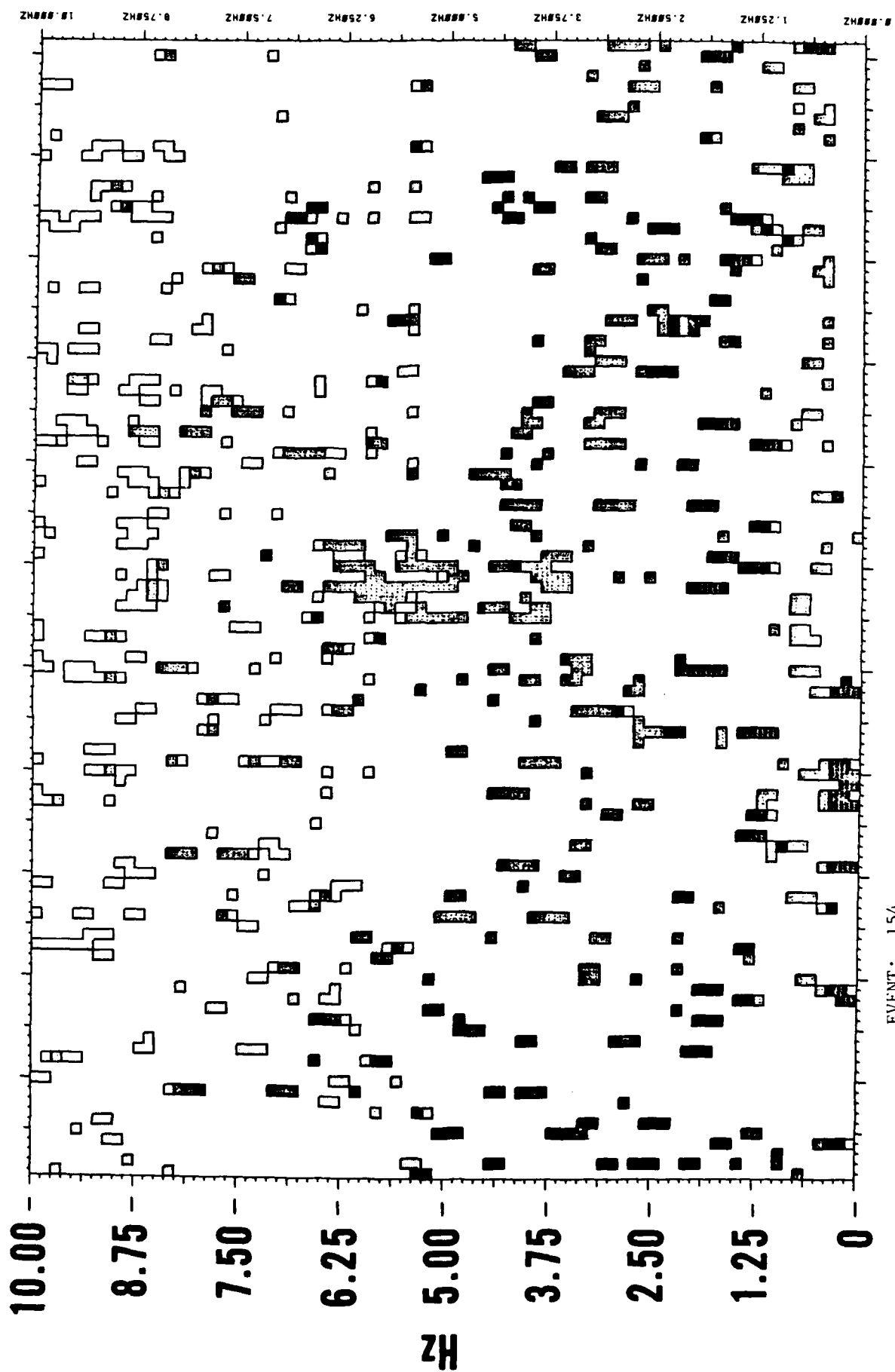
Siberia - Discussion

For this 5.3 event there are indications of a signal on channel 74 of
the time series plot. Frequencies of 3 to 6 Hz are confirmed in the
spectrums and spectrogram. Actually at these higher frequencies, the signal
is well recorded with average background noise. Therefore, it seems likely
that smaller events from this site could be observed on phone 74.
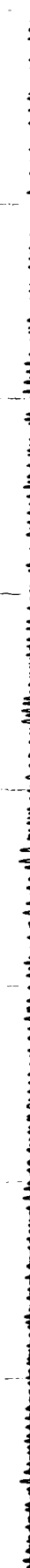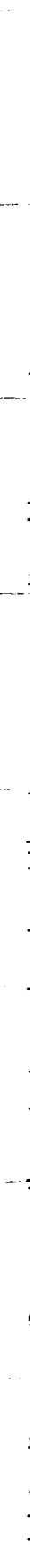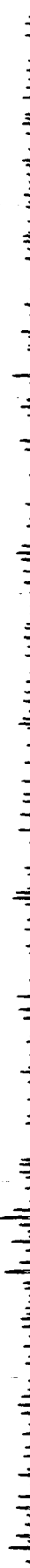
```
EVNT ******ORIGIN TIME****** **COORDINATES***   ****
*NO*  YR*MO*DA*JUL*HR*MN*SECS  **LAT*****LON***   *MB*

CENTRAL SIBERIA

1094 82 09 25 268 17.59.57.0 64.311N  91.859E    5.1
```

CENTRAL SIBERIA

NO	ORIGIN TIME				COORDINATES		DISTANCE (DEG)			SIGNAL LEVELS			NOISE LEVELS			MB
	YR/MO/DAY	HR	MIN	SEC	N	E	74	76	2	74	76	2	74	76	2	
94	82/ 9/25	17	59	57.0	64.31	91.86	64.98	65.29	67.77	*****	*****	2.5	-5.5	-5.5	-2.5	5.1

EVENT: 94

71 -
73 -
74 -
75 -
76 -
1 -
2 -
4 -

120

PHONE: 74   EVENT: 94

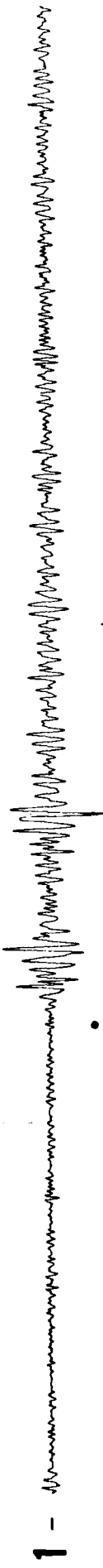PHONE: 76   EVENT: 94

FREQUENCY (HZ)

OB'S RELATIVE TO ONE MICROBAR PER ROOT HERTZ

	NOISE
	MEAN
	P

PHONE: 2   EVENT: 94

PHONE: 2   EVENT: 94

NOISE
MEAN
P

10.000HZ 8.750HZ 7.500HZ 6.250HZ 5.000HZ 3.750HZ 2.500HZ 1.250HZ 0.000HZ

EVENT: 94

Hz

10.00 — 8.75 — 7.50 — 6.25 — 5.00 — 3.75 — 2.50 — 1.25 — 0 —
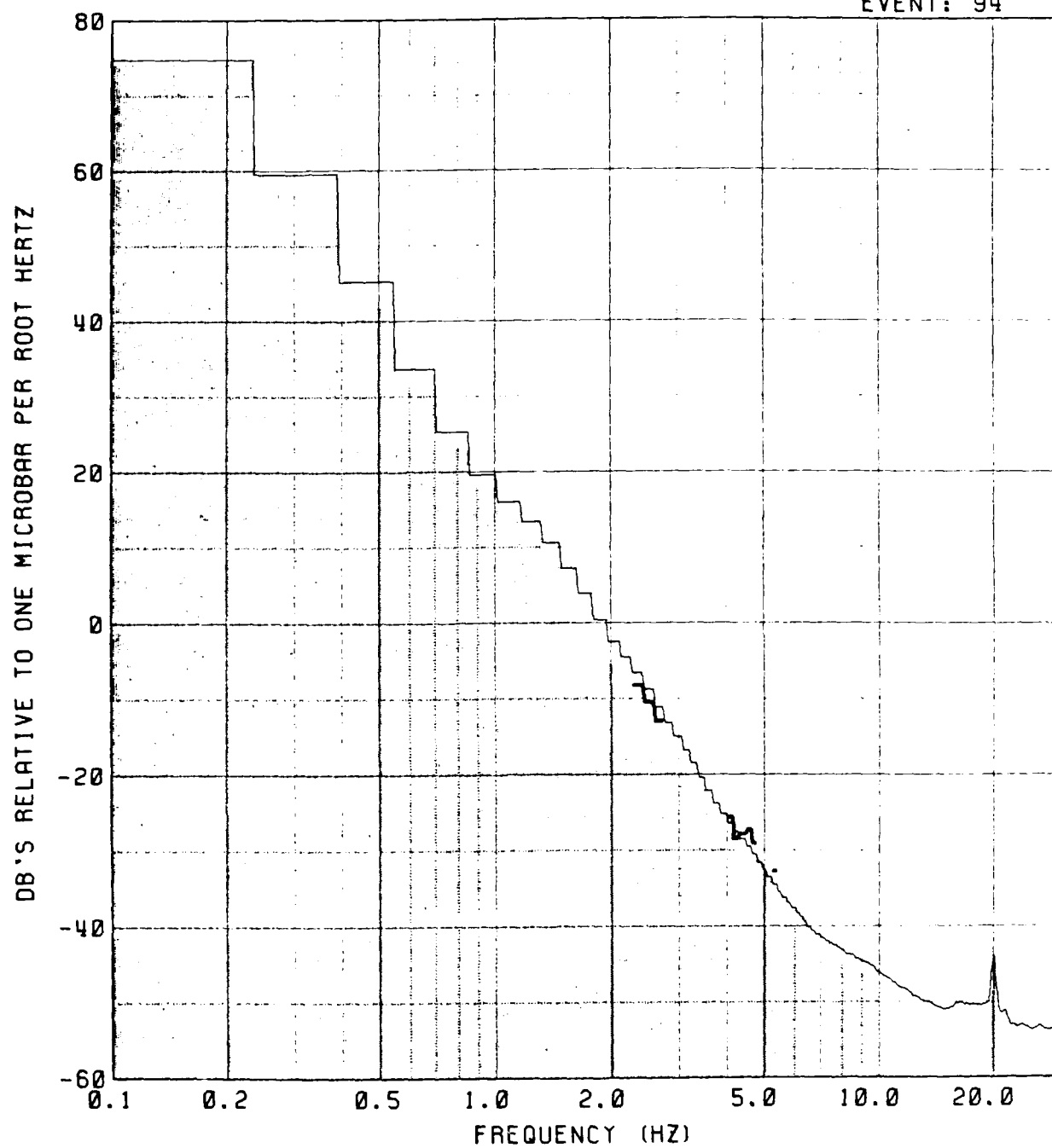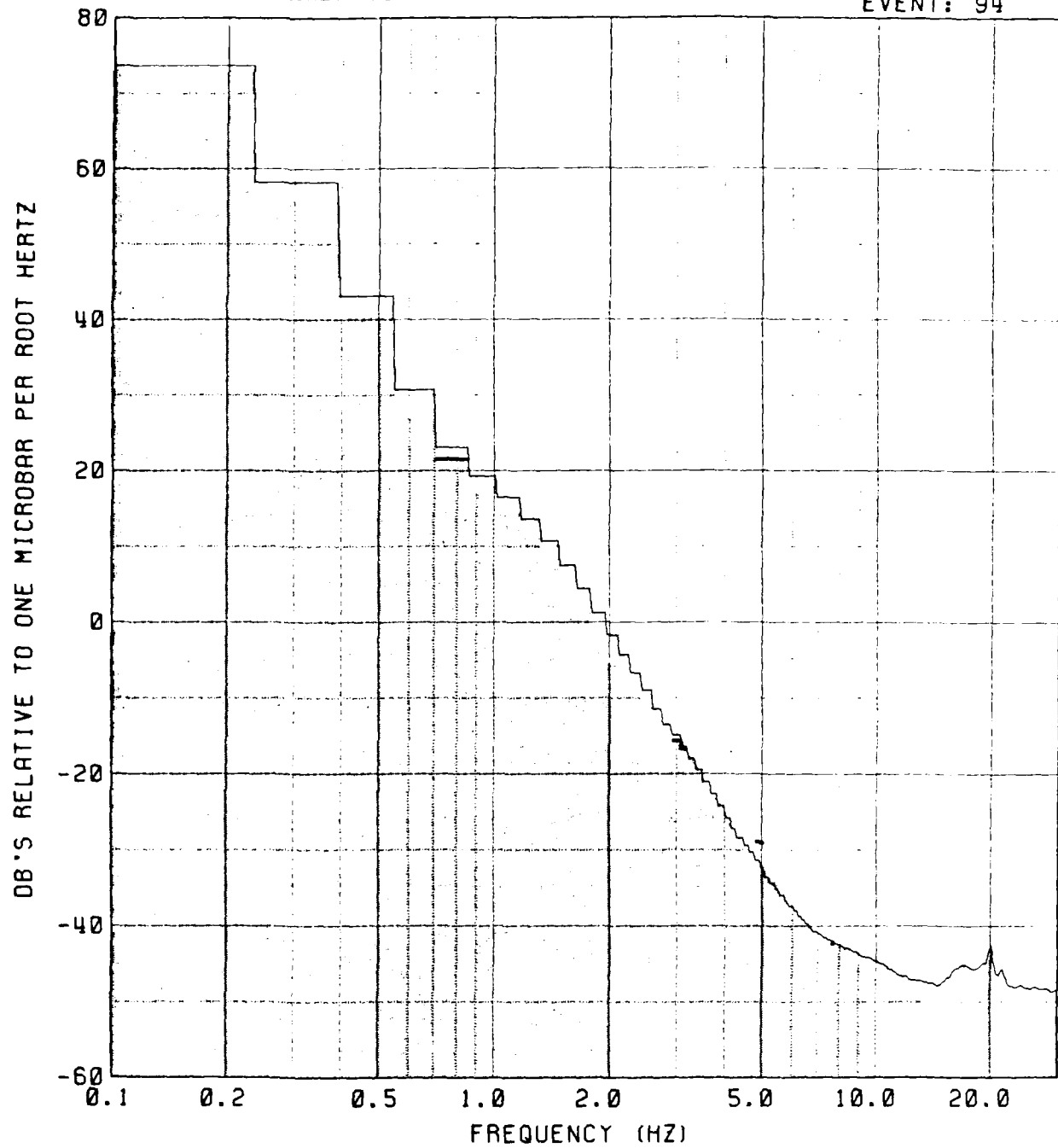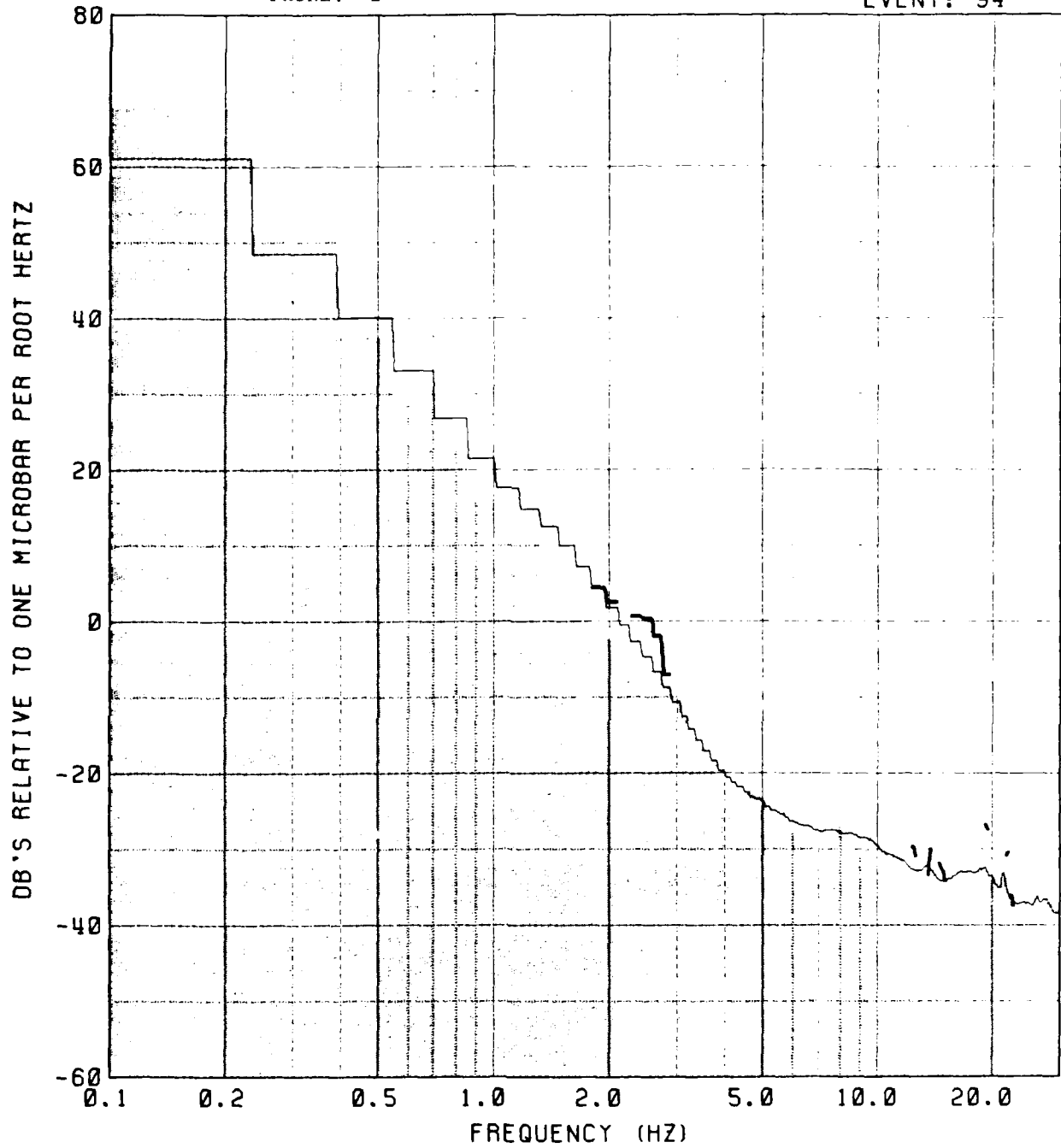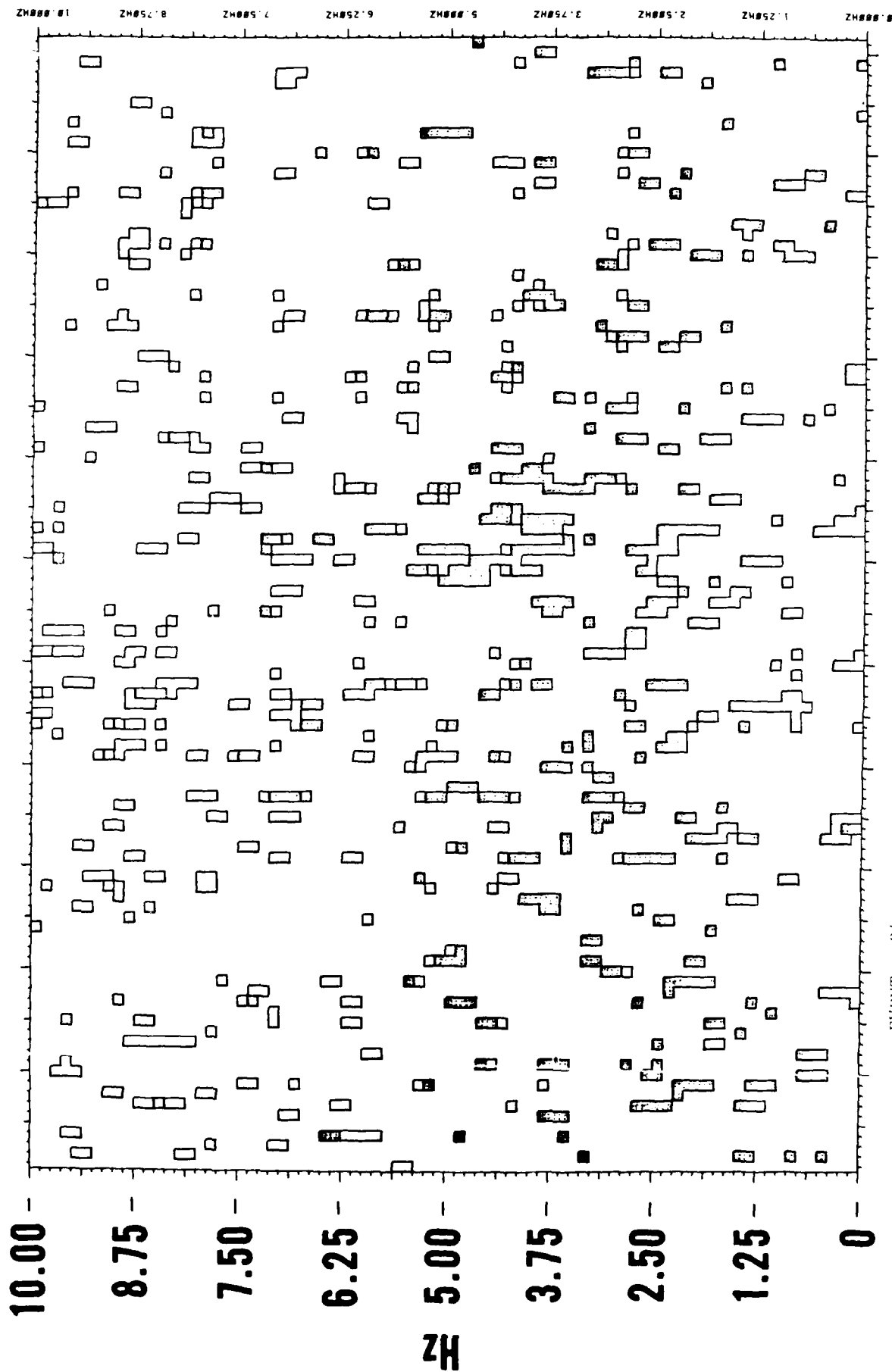
Central Siberia - Discussion

For this 5.1 event, there are indications of a signal on channel 74 and 2 of the time series plot. The signal is best observed in the spectrum for phone 2. Like the previous Siberian explosion, frequencies of 3 to 6 Hz are confirmed in the spectrums and spectrogram. It is doubtful whether this event would have been apparent in the spectrums under average noise conditions.

```
EVNT ******ORIGIN TIME****** **COORDINATES***   ****
*NO* YR*MO*DA*JUL*HR*MN*SECS **LAT*****LON***   *MB*

WESTERN SIBERIA

IRPE 84 08 25 238 18.59.58.5 61.889N  72.149E    5.3
```

127

WESTERN SIBERIA

NO	ORIGIN TIME				COORDINATES		DISTANCE (DEG)			SIGNAL LEVELS			NOISE LEVELS			MB
	YR/MO/DAY	HR	MIN	SEC	N	E	74	76	2	74	76	2	74	76	2	
2992	84/ 8/25	18	59	58.5	61.89	72.15	74.08	74.38	76.86	-13.0	-7.5	*****	-16.0	-17.0	-2.0	5.3

EVENT: 2992

128

71 —
73 —
74 —
75 —
76 —
1 —
2 —
4 —

PHONE: 2

FREQUENCY (HZ)

DB'S RELATIVE TO ONE MICROBAR PER ROOT HERTZ

⊢ —————— NOISE
  —————— MEAN
  —————— P

10.00 — 8.75 — 7.50 — 6.25 — 5.00 — 3.75 — 2.50 — 1.25 — 0 —

HZ
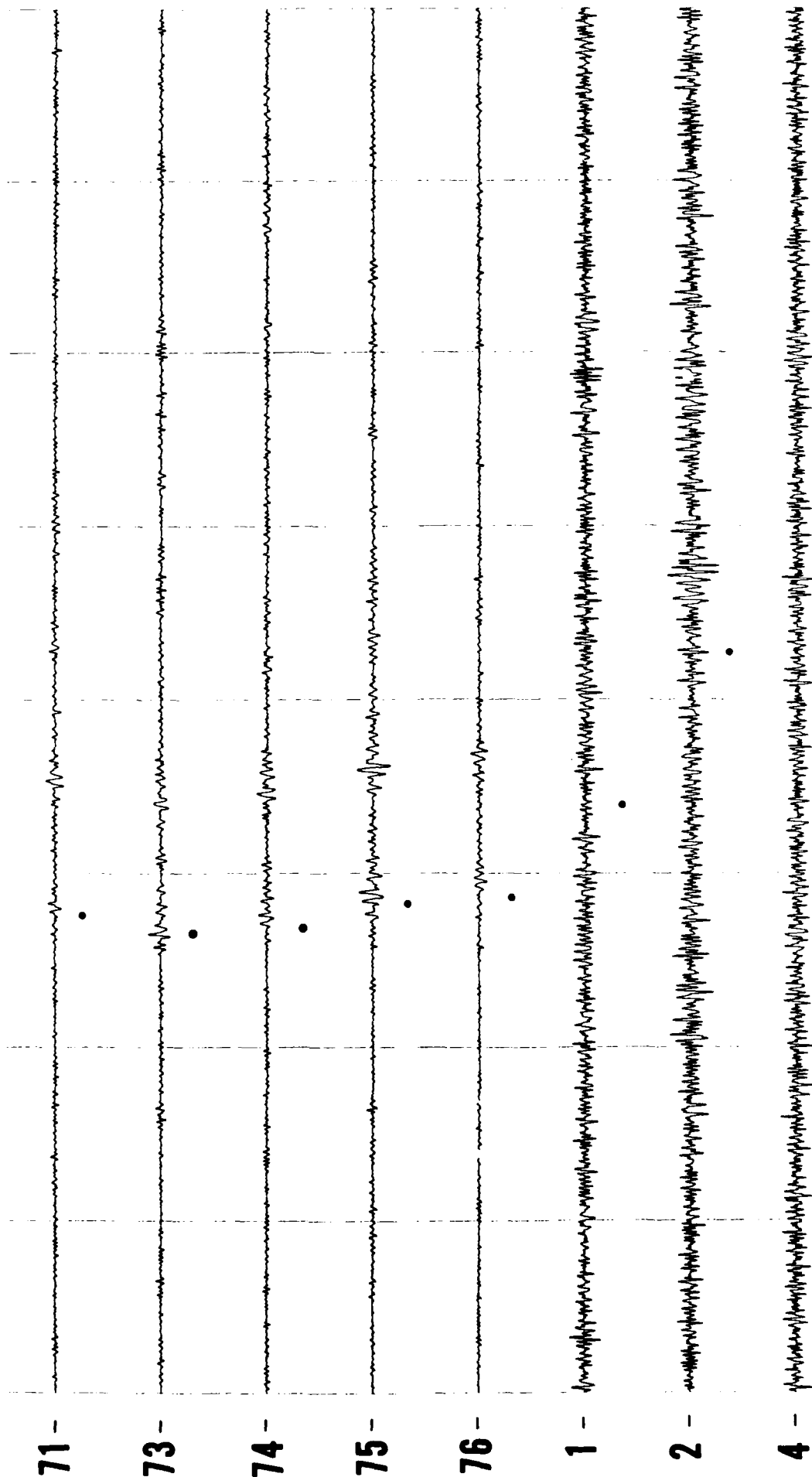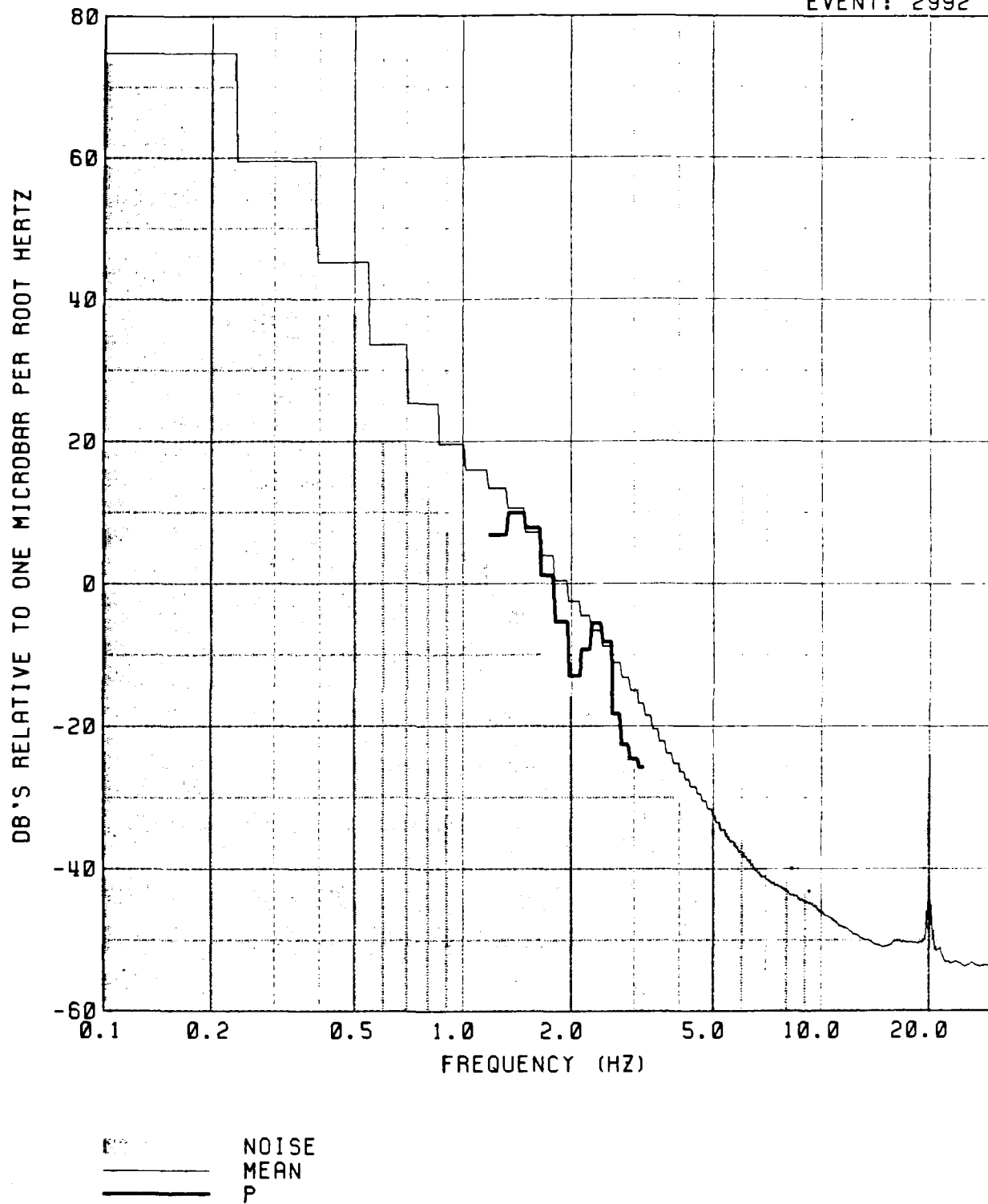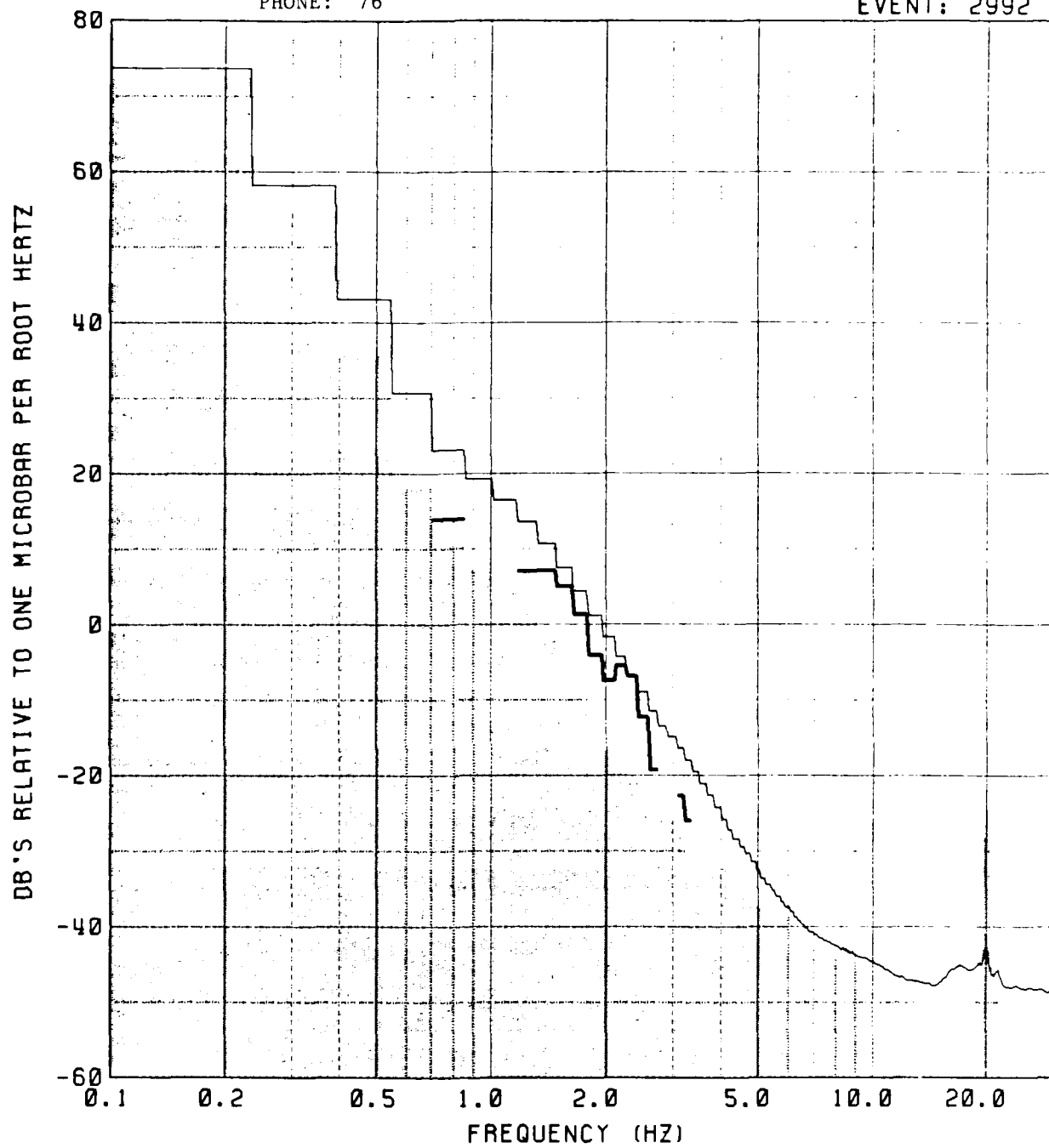
EVENT: 2992
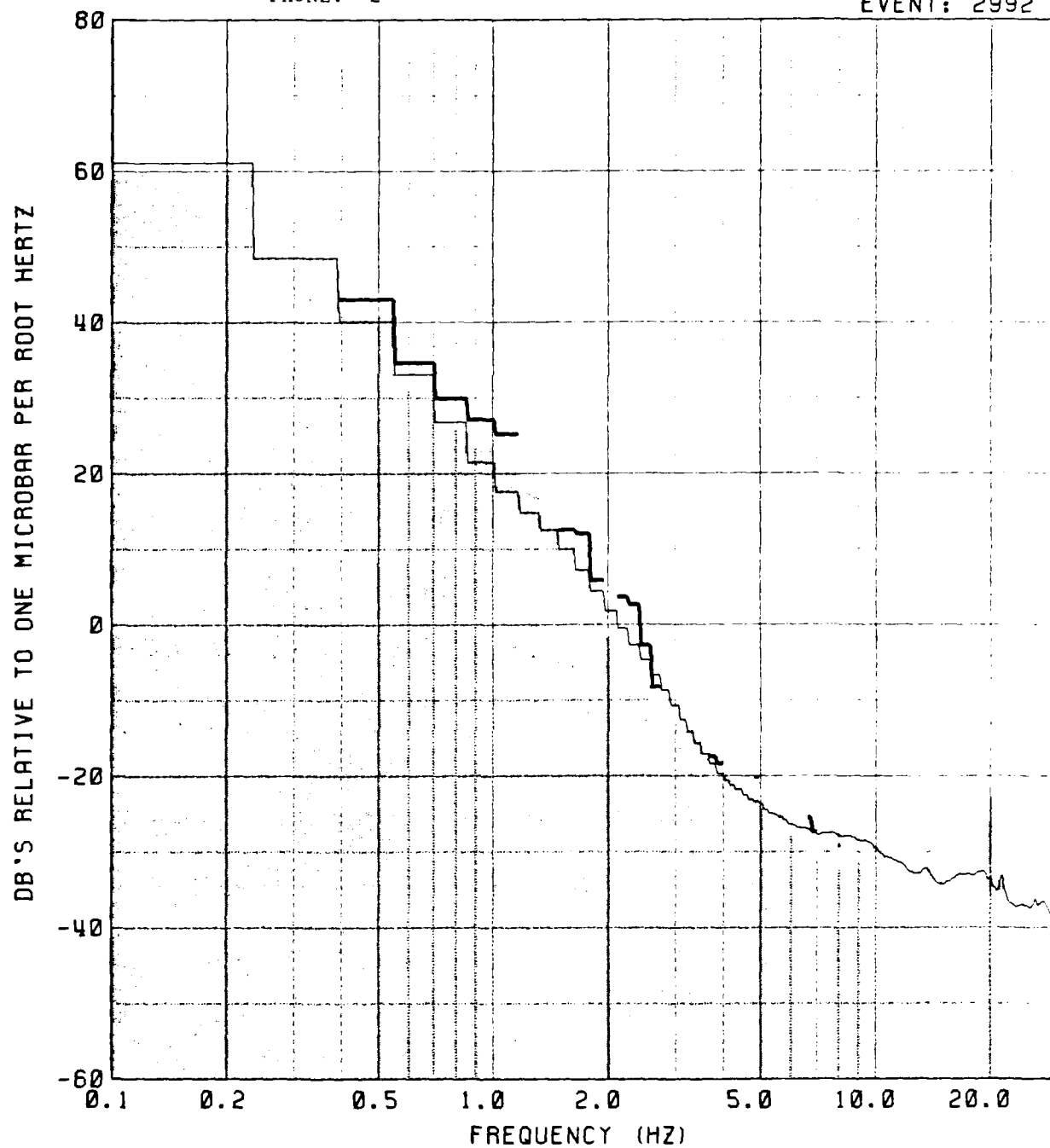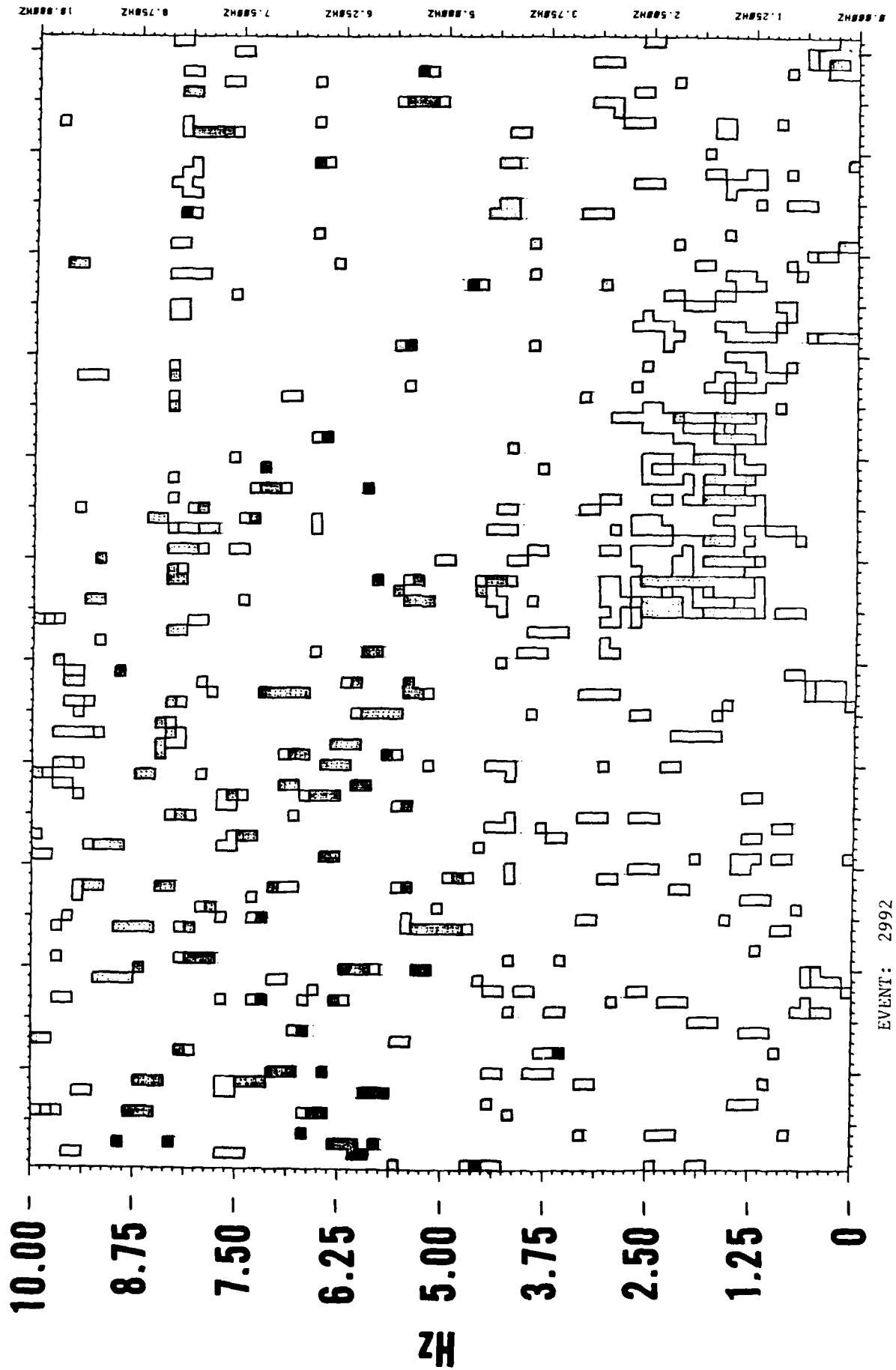
Western Siberia - Discussion

Unlike the previous Siberian and Central Siberian events, this 5.3 explosion has its greatest S/N ratios from 1 to 3 Hz and is fairly well recorded on phones 74, 76, and 2. In terms of frequency content this event is more like the Eastern Kazakh explosions than the Siberian and Central Siberian explosions. In terms of signal strengths on the differing phones (i.e., phones 74 vs. 76), it is more like the Eastern Kazakh explosions than the Novaya Zemlya explosions. This event is obviously well recorded because of extremely low noise conditions. Therefore, it is doubtful whether it would have been observed in the spectrum for phone 74 under average noise conditions.

```
EVNT ***-**ORIGIN TIME****** **COORDINATES***   ****
*NO* YR*MO*DA*JUL*HR*MN*SECS **LAT*****LON***   *MB*

CENTRAL USSR

3052 84 09 17 261 20 59 57.4 55.835N  87.408E   4 9
```

CENTRAL USSR

NO	ORIGIN TIME				COORDINATES		DISTANCE (DEG)			SIGNAL LEVELS			NOISE LEVELS			
	YR/MO/DAY	HR	MIN	SEC	N	E	74	76	2	74	76	2	74	76	2	MB
3052	84/ 9/17	20	59	57.4	55.84	87.41	67.12	67.40	69.82	*****	*****	*****	-6.0	-7.5	-3.5	4.9
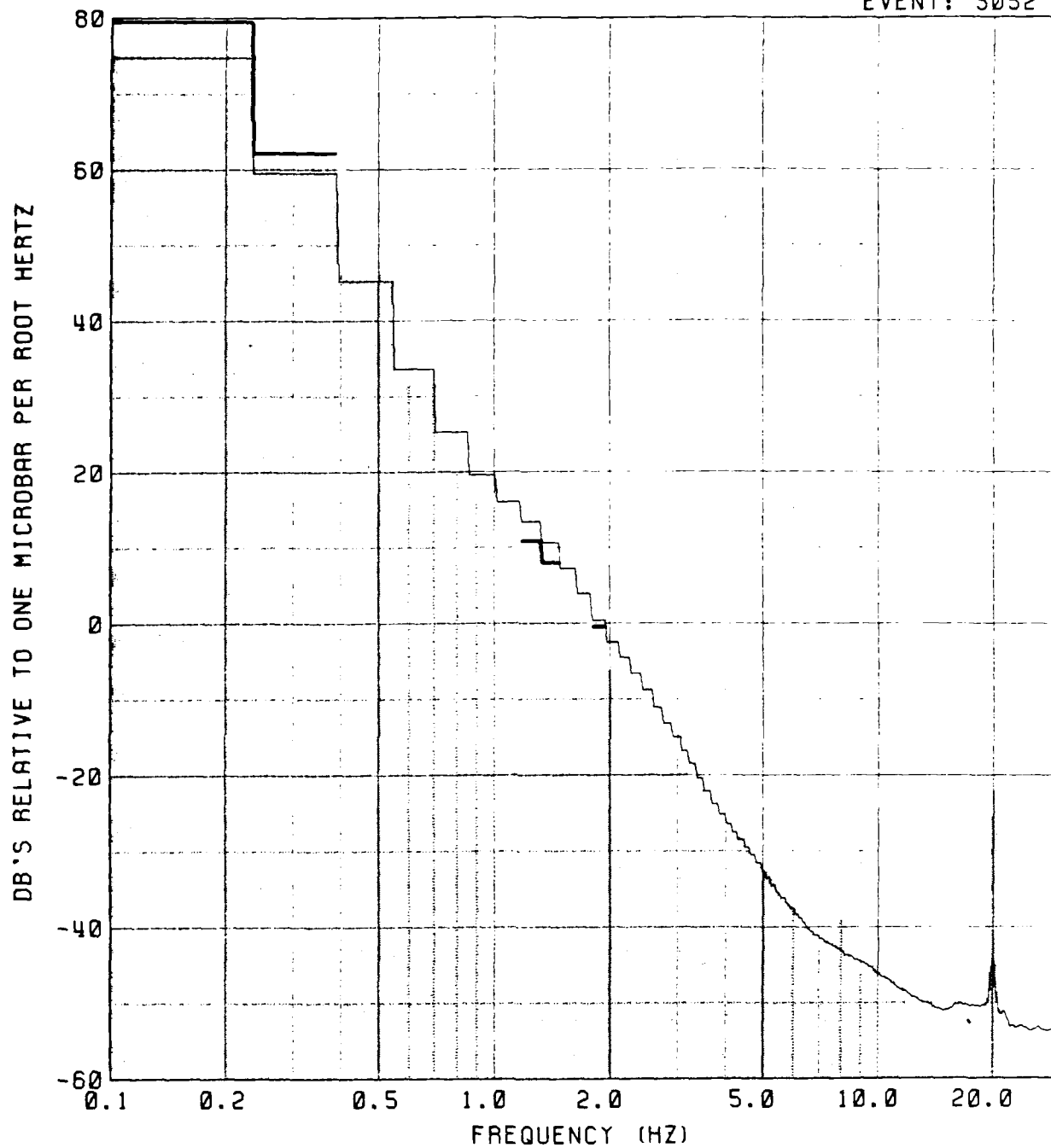
EVENT: 3052

71

73

74

75

76

1

2

4

136

10.00 — 8.75 — 7.50 — 6.25 — 5.00 — 3.75 — 2.50 — 1.25 — 0 —

HZ
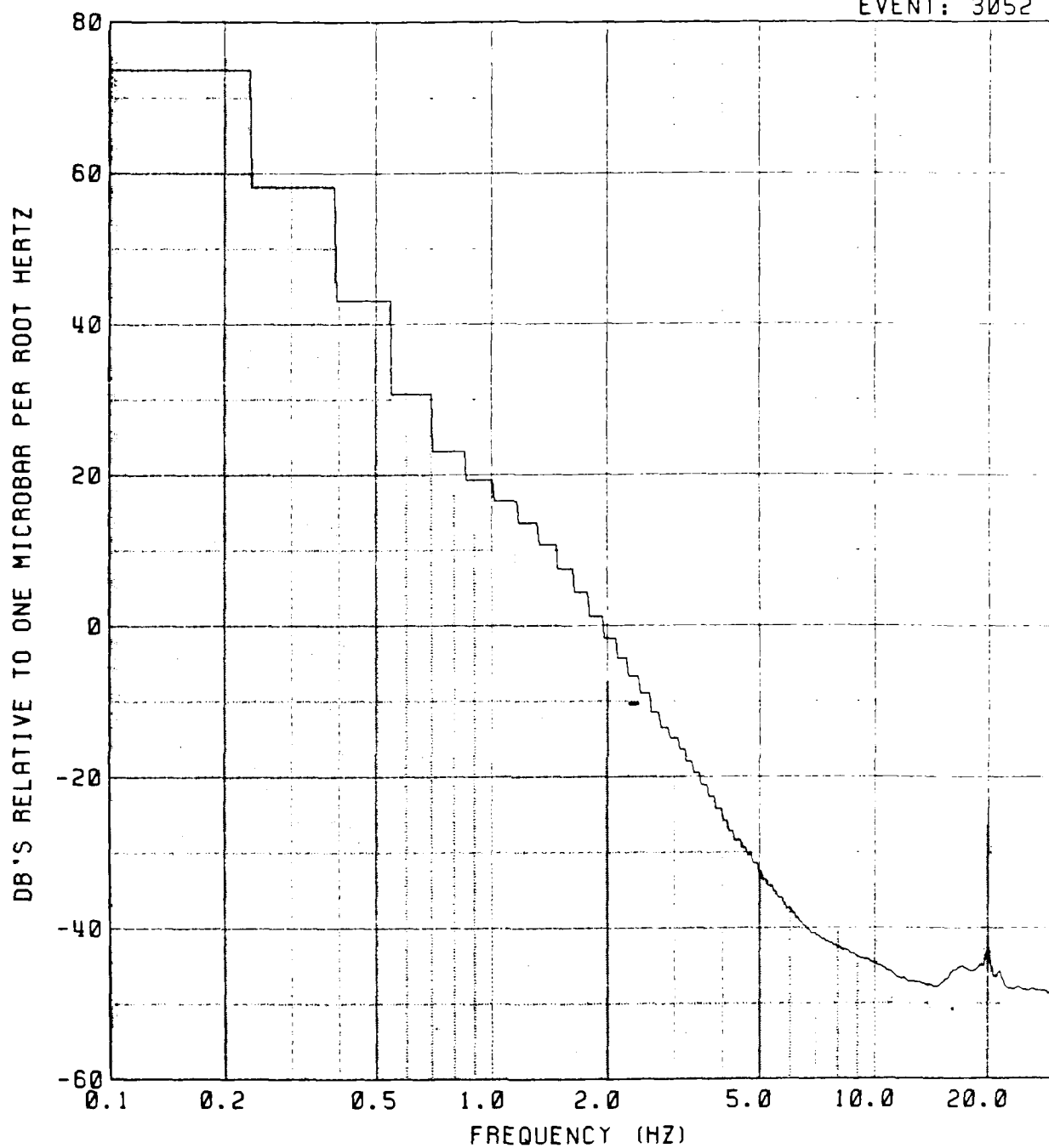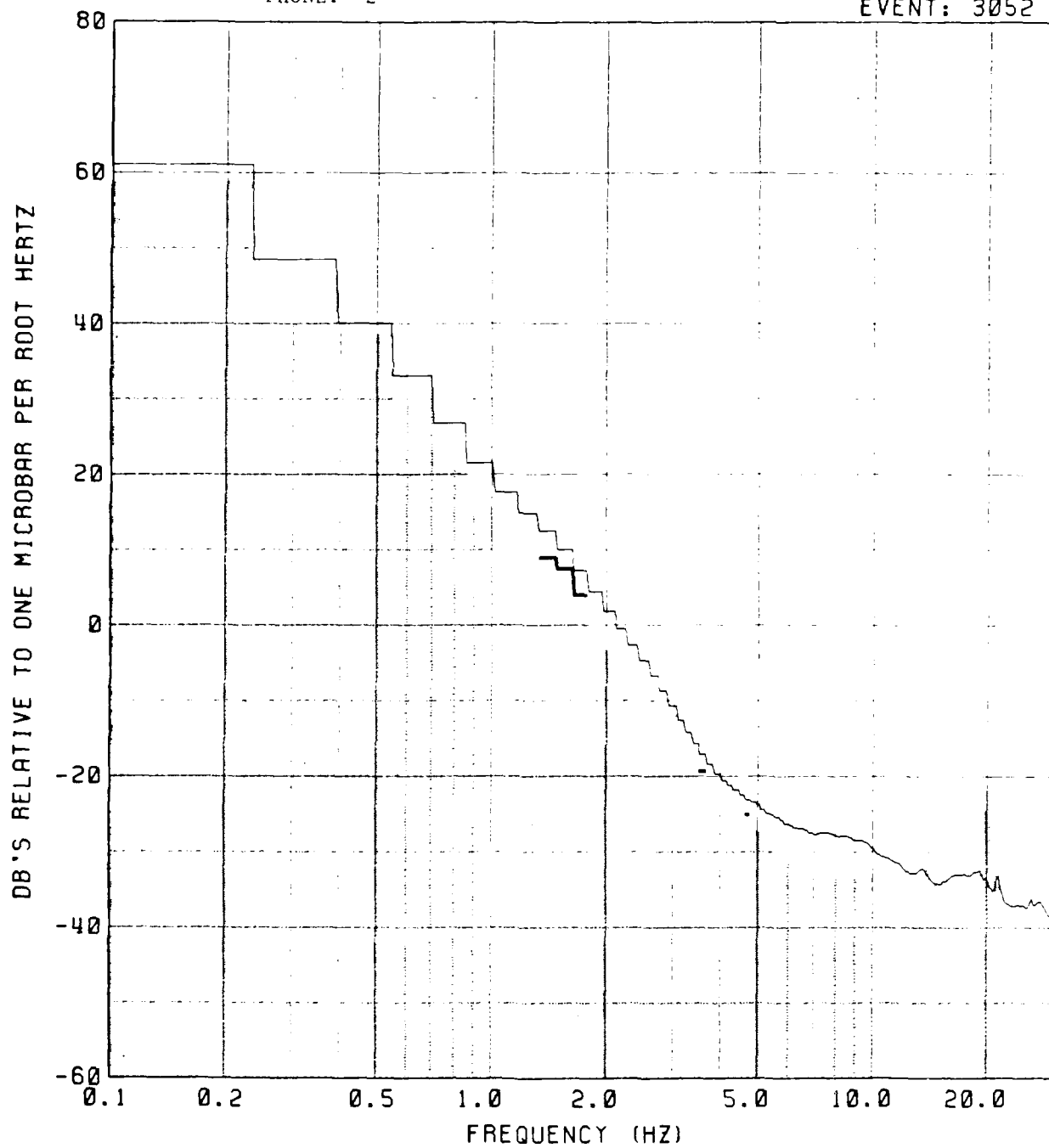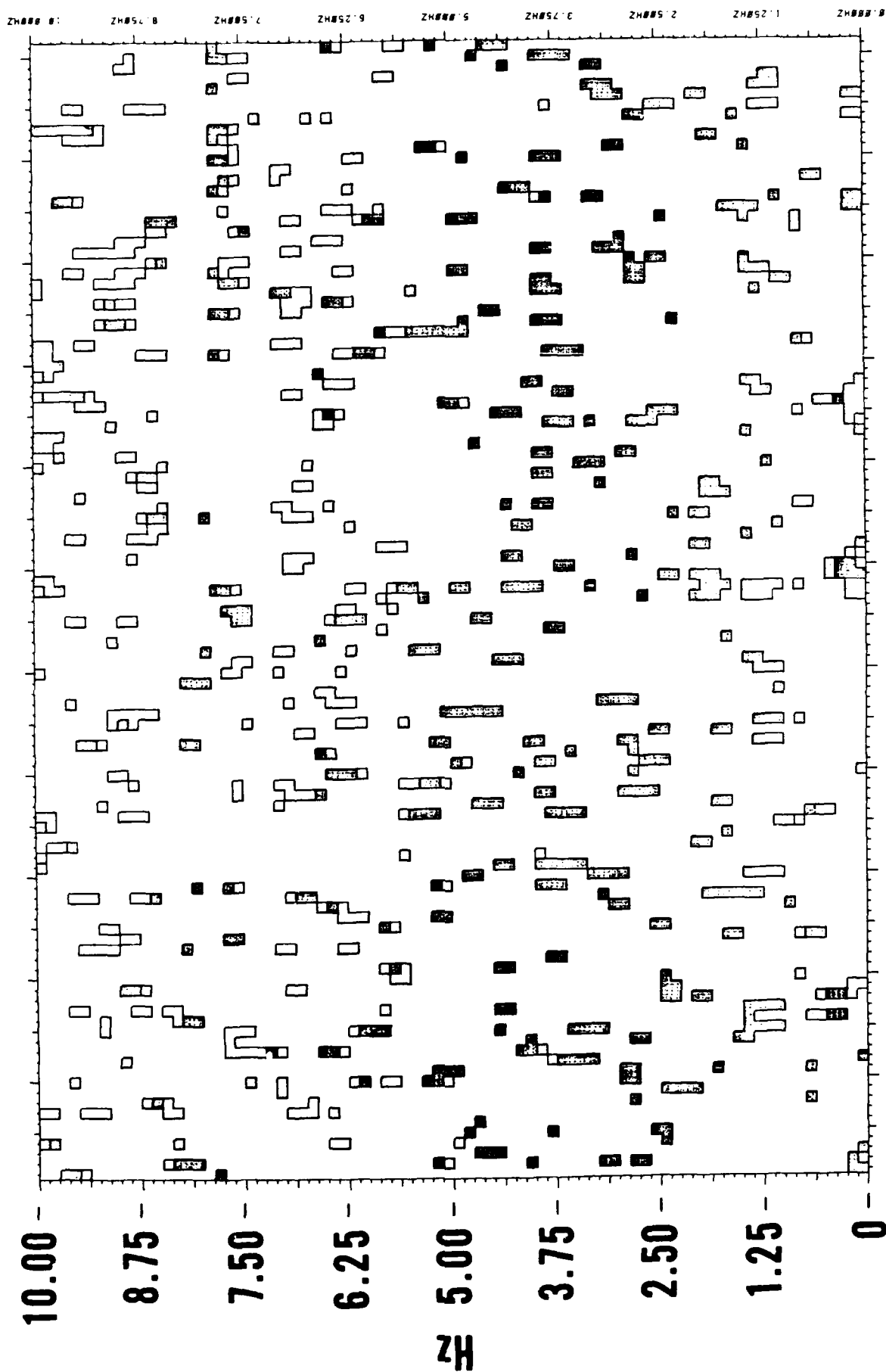
EVENT: 3052

Central U.S.S.R. - Discussion

There is merely a hint of this event on phone 74 and 2 with frequencies of 1 to 2 Hz. This 4.9 explosion is apparent because of lower than average noise conditions.

```
EVNT ******ORIGIN TIME****** **COORDINATES***   ****
*NO* YR*MO*DA*JUL*HR*MN*SECS **LAT*****LON***   *MB*

URAL MOUNTAINS REGION

2927 84 08 11 224 18:59.57.4 65.079N   55.287E    5.2
```

URAL MOUNTAINS REGION

	ORIGIN TIME				COORDINATES		DISTANCE (DEG)			SIGNAL LEVELS			NOISE LEVELS			
NO	YR/MO/DAY	HR	MIN	SEC	N	E	74	76	2	74	76	2	74	76	2	MB
2927	84/ 8/11	18	59	57.4	65.08	55.29	80.03	80.35	82.84	*****	3.0	*****	0.5	-1.0	2.0	5.2

EVENT: 2927

71 —

73 —

74 —

75 —

76 —

1 —

2 —

4 —
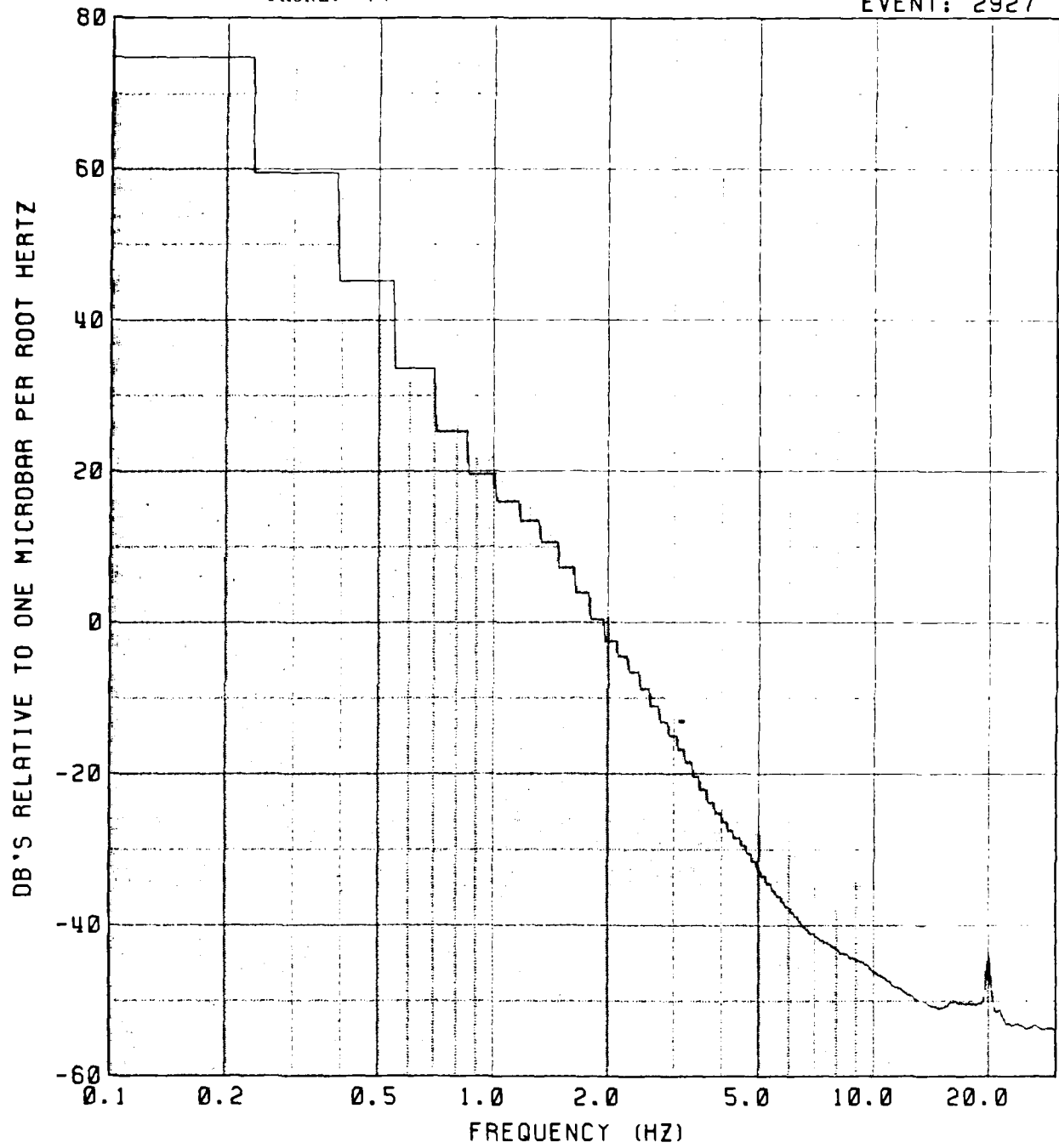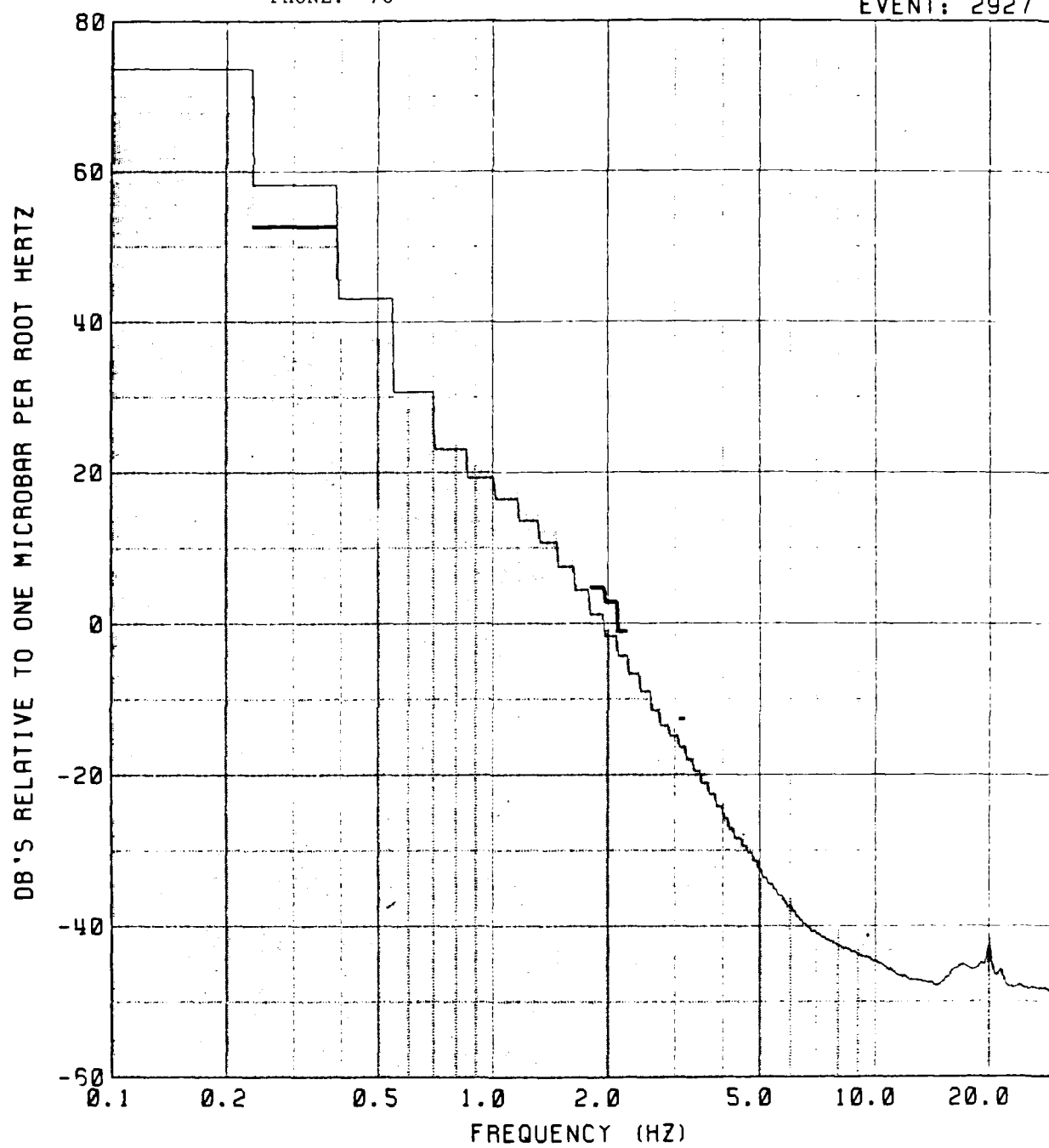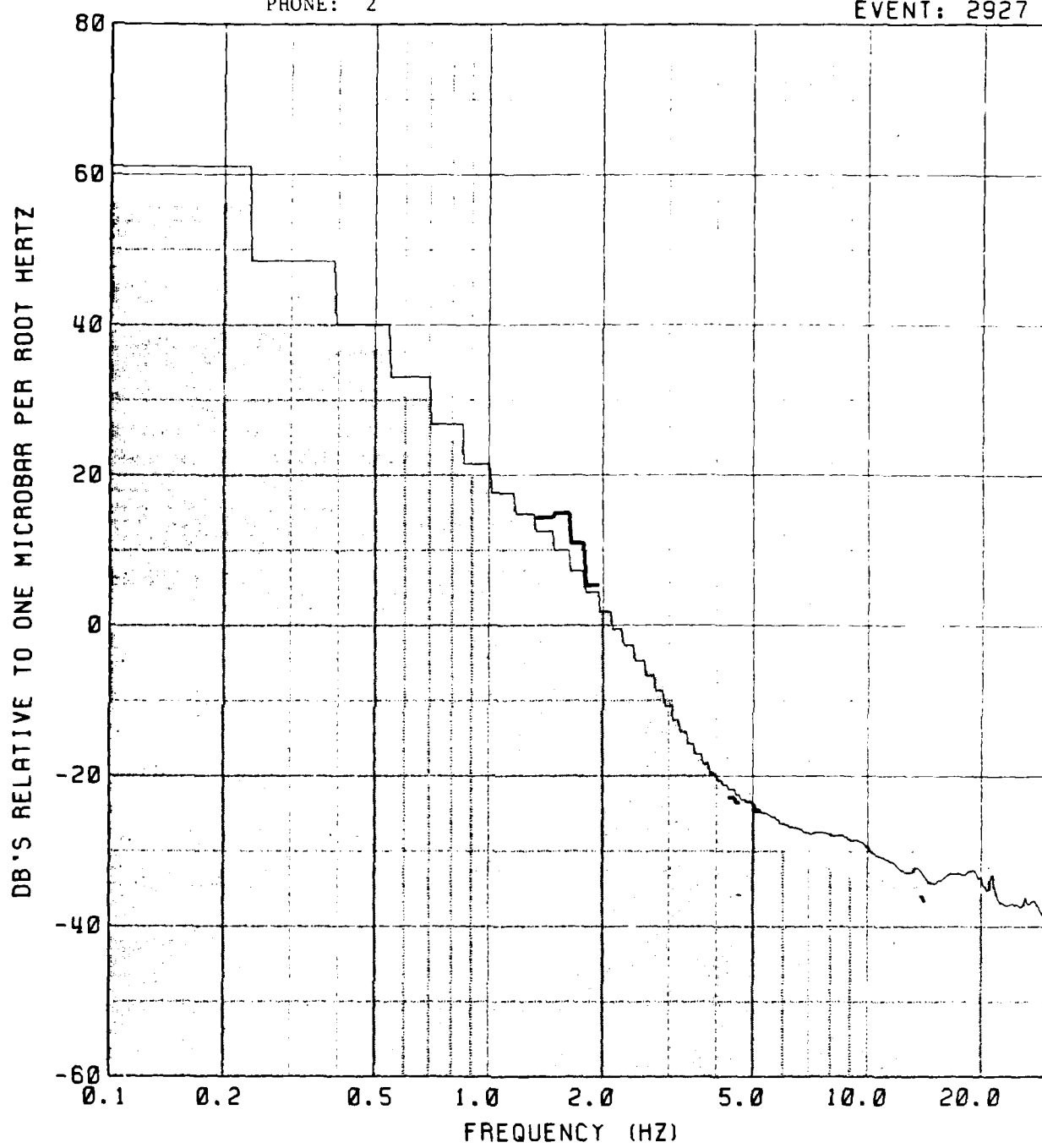
PHONE: 76

NOISE
MEAN
P

EVENT: 2927

HZ
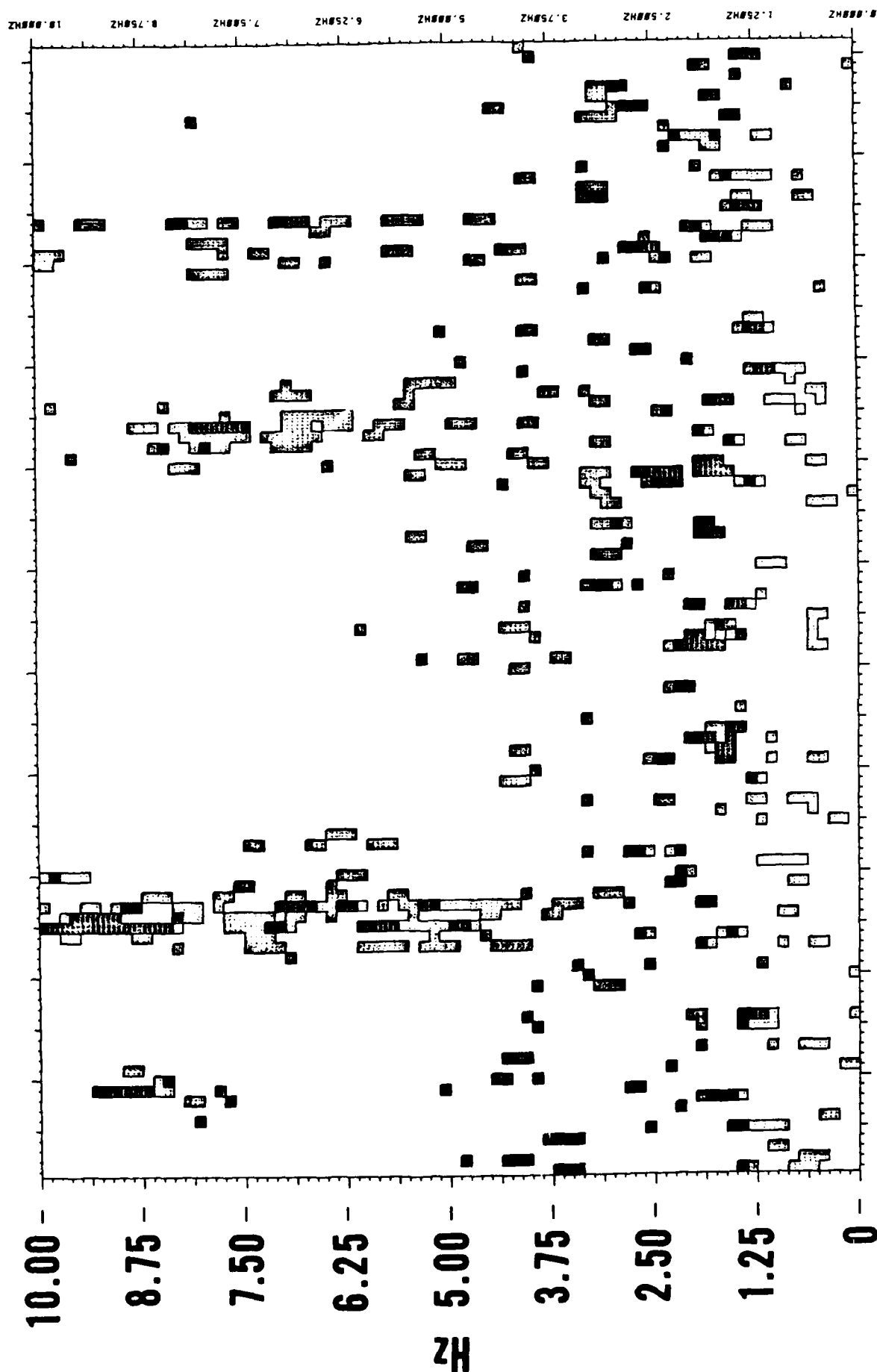
Ural Mountains Region - Discussion

This explosion is not apparent on phone 74 but is suggested on phones 76 and 2, indicating that its recordings at Wake may be similar to those for Novaya Zemlya. Under average noise conditions, this 5.2 event was fairly well recorded on phone 76. At much lower than average noise conditions, it seems likely that magnitudes in the high 4's could be recorded from this site.

```
EVNT ******ORIGIN TIME****** **COORDINATES***   ****
*NO* YR*MO*DA*JUL*HR*MN*SECS **LAT*****LON***   *MB*

EUROPEAN USSR

1312 83 07 10 191 03:59 57.0 51.327N   53.286E   5.3
1313 83 07 10 191 04:04 57.0 51.336N   53.290E   5.4
1314 83 07 10 191 04:09 57.1 51.357N   53.301E   5.2
2348 84 07 21 203 02:59 57.1 51.366N   53.253E   5.3
2349 84 07 21 203 03:04 57.0 51.384N   53.271E   5.2
2350 84 07 21 203 03:09 57.1 51.366N   53.276E   5.3
```

151

```
EVNT ******ORIGIN TIME****** **COORDINATES***   ****
*NO* :R*MO*DA*JUL*HR*MN*SECS **LAT*****LON***   *MB*

EUROPEAN USSR AREA 2

1997 84 08 27 240 05 59 57.5 67.831N  33 450E   4.4
```

```
EVNT ******ORIGIN TIME****** **COORDINATES***   ****
*NO* YR*MO*DA*JUL*HR*MN*SECS  **LAT****LON***   *MB*

SOUTHWESTERN USSR

0170 82 10 16 289 05:59:57.2 46.727N   48.162E    5.2
0171 82 10 16 289 06:04:57.1 46.723N   48.222E    5.3
0172 82 10 16 289 06:09:57.1 46.748N   48.258E    5.2
0173 82 10 16 289 06:14:57.1 46.707N   48.230E    5.4
1623 83 09 24 267 04:59:56.9 46.773N   48.300E    5.1
1624 83 09 24 267 05:04:56.8 46.763N   48.281E    5.0
1625 83 09 24 267 05:09:57.7 46.872N   48.214E    4.9
1626 83 09 24 267 05:14:56.9 46.748N   48.299E    5.1
1627 83 09 24 267 05:19:57.0 46.772N   48.267E    5.2
1628 83 09 24 267 05:24:56.8 46.758N   48.257E    5.2
3127 84 10 27 301 05:59:58.6 47.044N   47.919E    4.8
```

153

European and Southwestern U.S.S.R.

For these sites distances are close to, or beyond, 90°. Therefore, the arrivals at Wake could be expected to be weak or non-existent. Indeed, none were found. Distances to phone 74 are 87.7°, 85.4°, and 93.0° for the European U.S.S.R., European U.S.S.R. Area 2, and Southwestern U.S.S.R. sites, respectively.

EVNT ******ORIGIN TIME****** **COORDINATES***   ****
NO *YR*MO*DA*JUL*HR*MN*SECS **LAT*****LON***   *MB*

SOUTHERN XINJIANG, CHINA

ISPC 84 10 03 277 05 59 57.7 41 633N 88 781E   5.3

SOUTHERN XINJIANG, CHINA

NO	ORIGIN TIME				COORDINATES		DISTANCE (DEG)			SIGNAL LEVELS			NOISE LEVELS			
	YR/MO/DAY	HR	MIN	SEC	N	E	74	76	2	74	76	2	74	76	2	MB
3090	84/10/ 3	5	59	57.7	41 63	88 78	67 62	67 82	69 99	*****	*****	*****	3 0	4 0	4 0	5 3

EVENT: 3090

156

71 –

73 –

74 –

75 –

76 –

1 –

2 –

4 –

PHONE: 76

EVENT: 3090

158

FREQUENCY (HZ)

DB'S RELATIVE TO ONE MICROBAR PER ROOT HERTZ

NOISE
MEAN
P

PHONE: 2

NOISE
MEAN
P

HZ

10.00
8.75
7.50
6.25
5.00
3.75
2.50
1.25
0
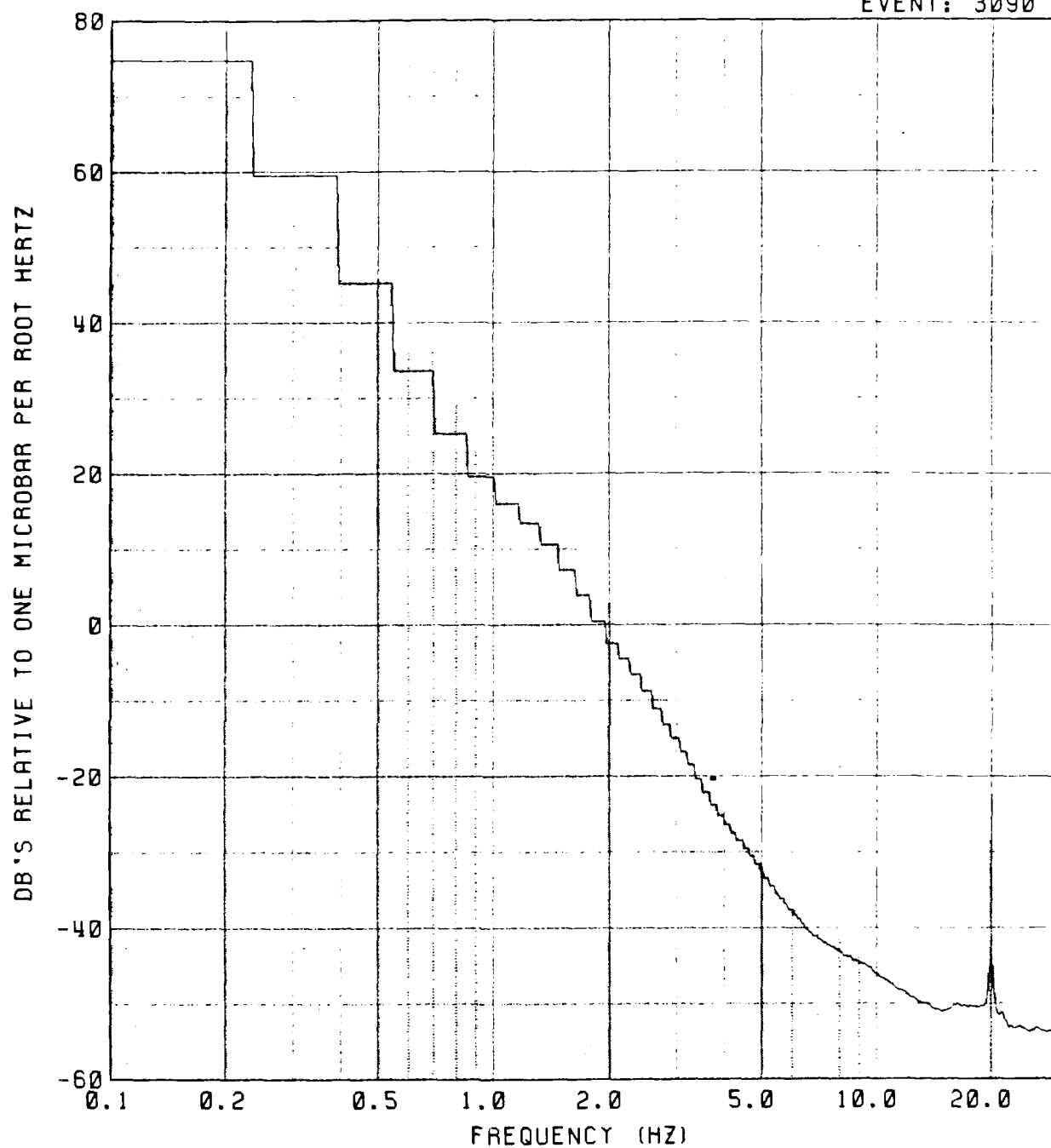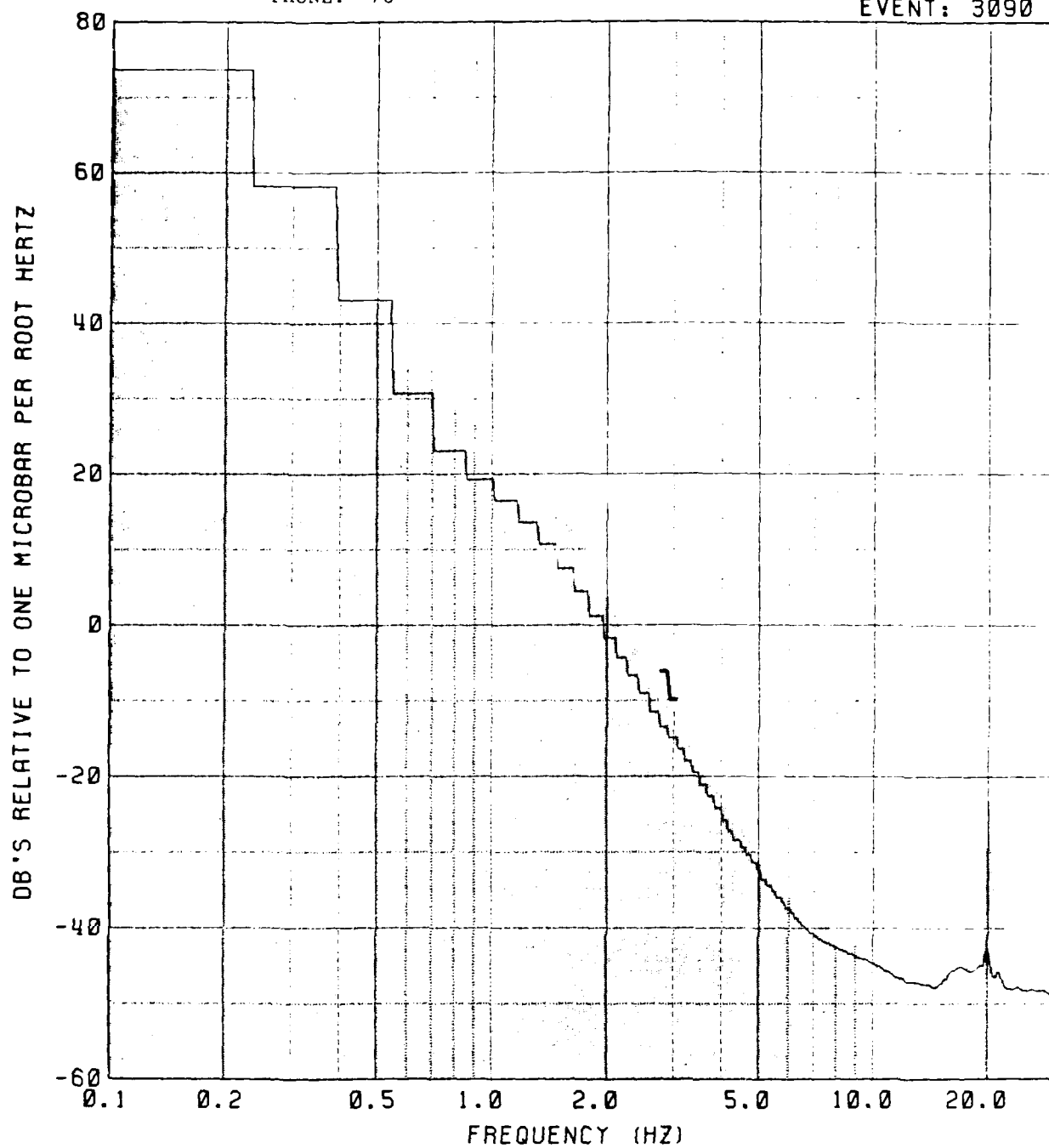
EVENT: 3090
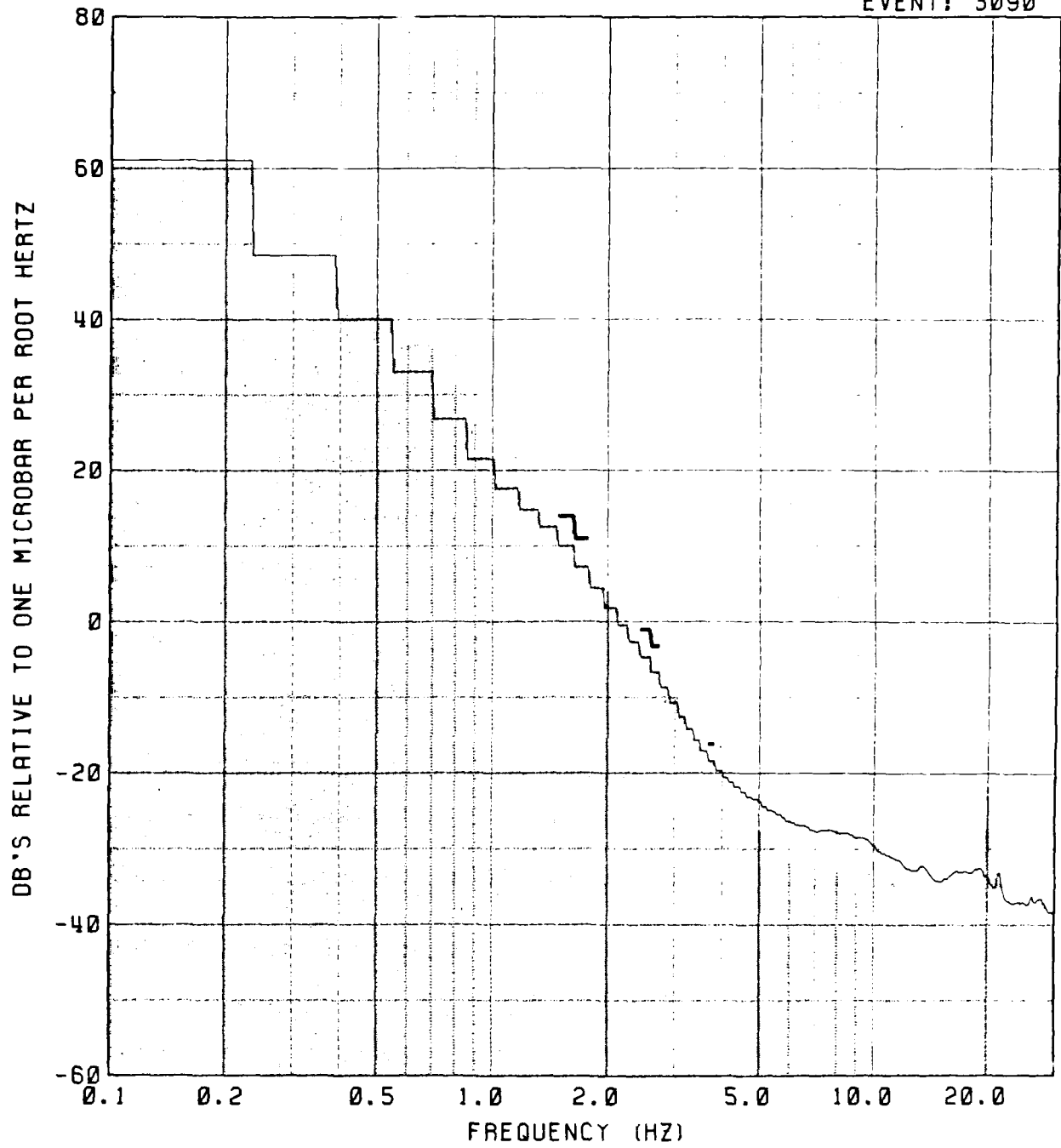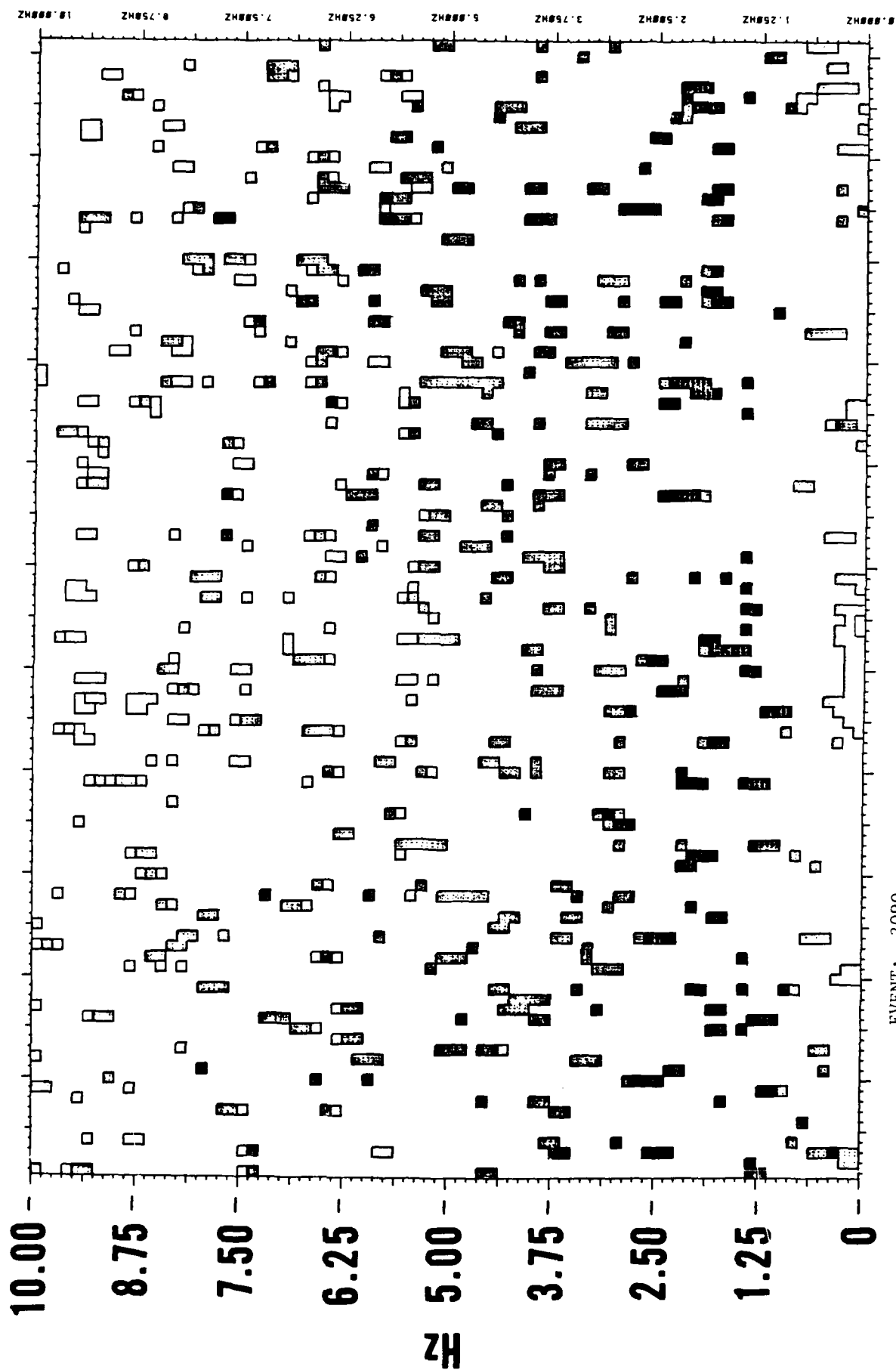
China - Discussion

For this 5.3 event there is a suggestion of a signal on phones 76 and 2. Since the noise levels are higher than average, it seems likely that lower magnitude events could be well recorded at lower than average noise conditions.
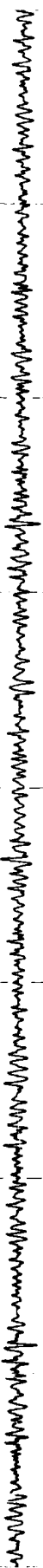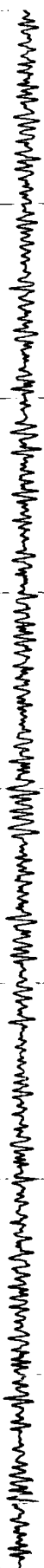
```
EVNT ******ORIGIN TIME****** **COORDINATES***    ****
*NO*  YR*MO*DA*JUL*HR*MN*SECS  **LAT*****LON***   *MB*

TUAMOTU ARCHIPELAGO REGION

0939 83 04 19 109 18:52 58.4 21.864S 138.941W    5.6
1075 83 05 25 145 17:30 58.2 21.912S 138.936W    5.9
1252 83 06 28 179 17:45 58.2 21.815S 138.950W    5.4
2554 84 05 12 133 17:30 58.2 21.808S 139.013W    5.7
2695 84 06 16 168 17:43 57.7 21.932S 139.020W    5.4
3143 84 11 02 307 20:44 58.3 21.904S 139.003W    5.7
3217 84 12 06 341 17:28 58.3 21.890S 138.954W    5.7
```

TUAMOTU ARCHIPELAGO REGION

163

NO	ORIGIN TIME				COORDINATES		DISTANCE (DEG)			SIGNAL LEVELS			NOISE LEVELS			
	YR/MO/DAY	HR	MIN	SEC	S	W	74	76	2	74	76	2	74	76	2	MB
3143	84/11/02	20	44	58.3	21.90	139.00	67.94	67.75	65.64	4.5	*****	*****	1.5	3.5	2.0	5.7
3217	84/12/06	17	28	58.3	21.89	138.95	67.97	67.78	65.67	*****	*****	*****	0.5	0.0	2.0	5.7
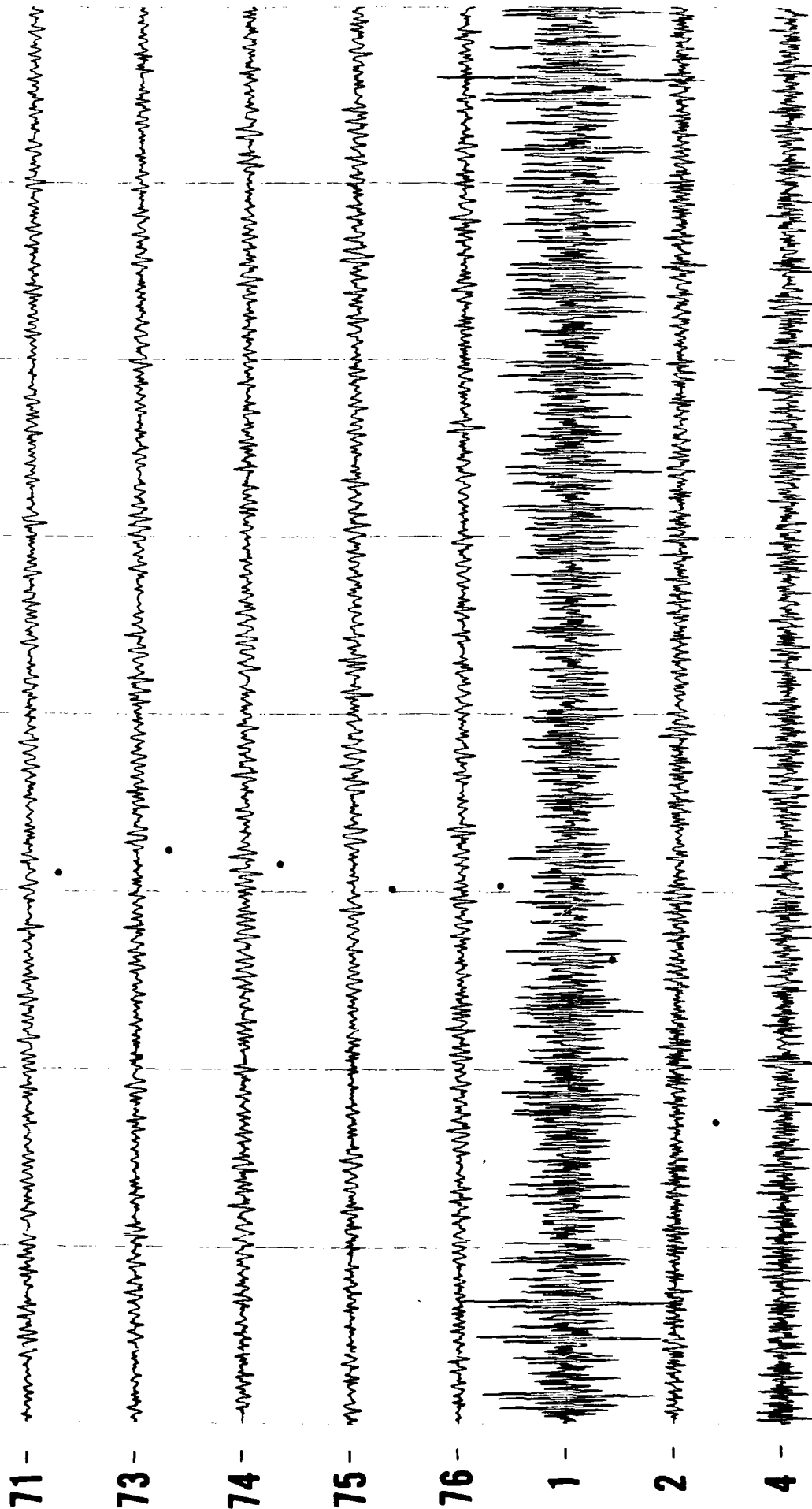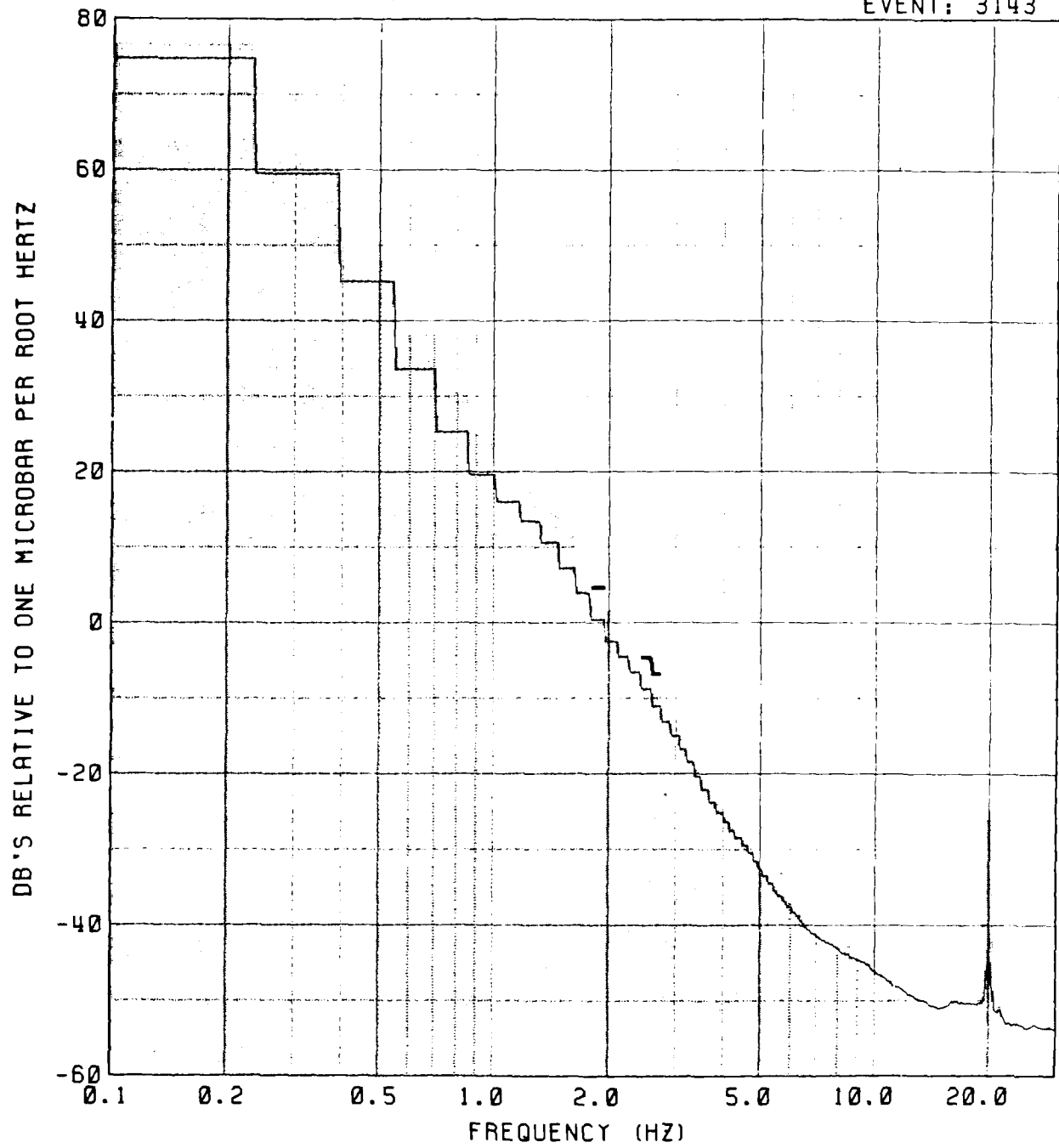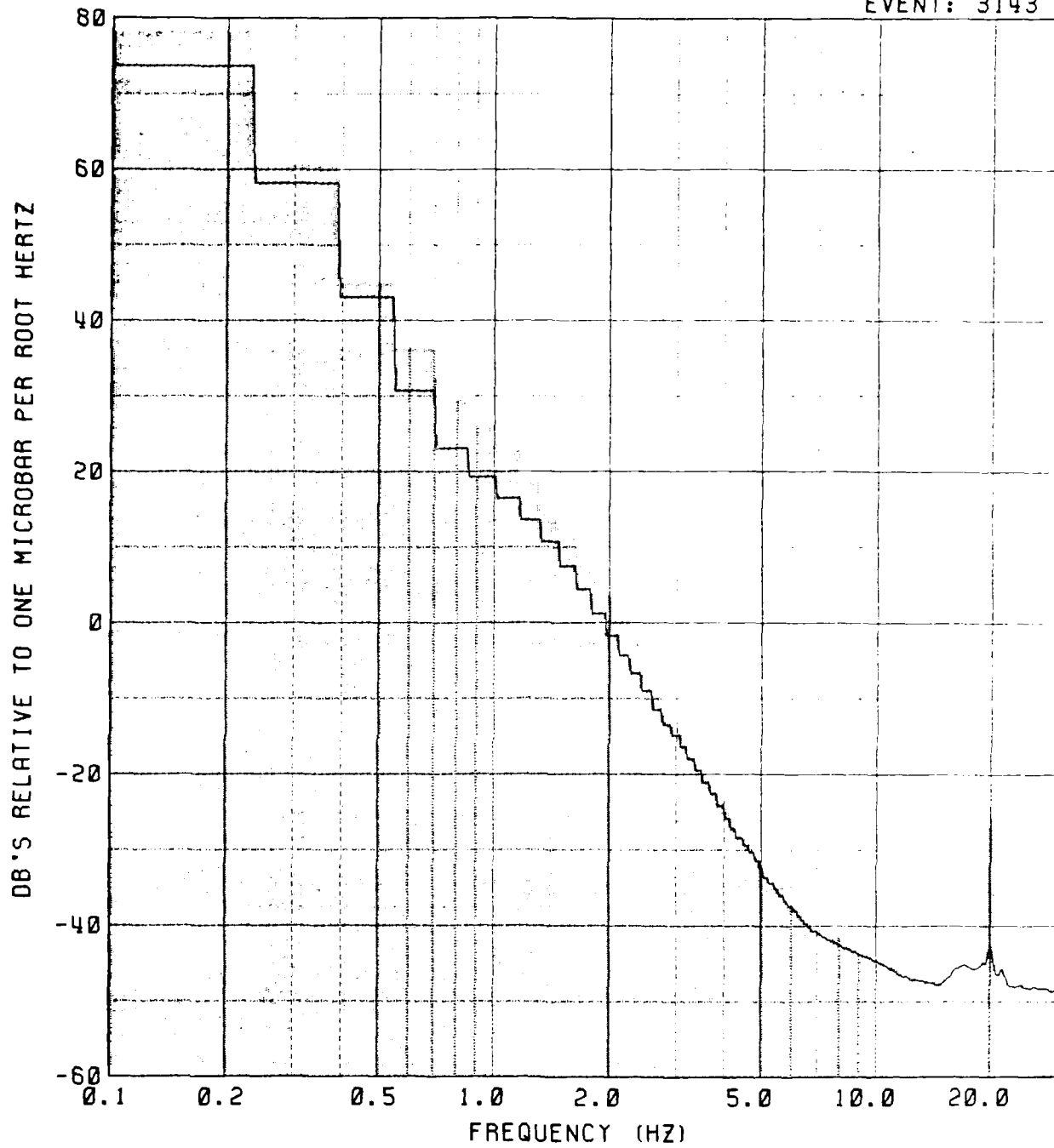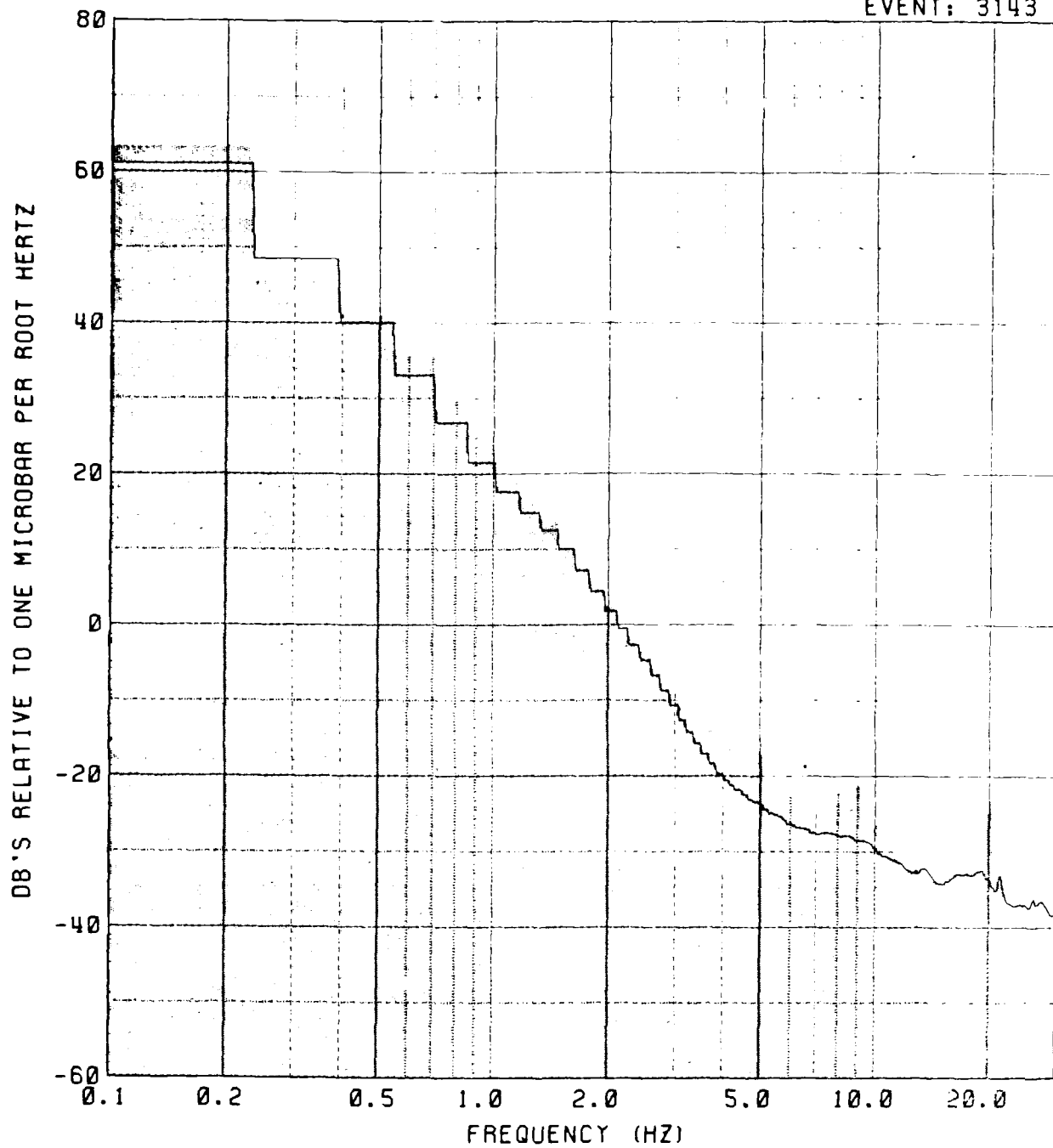
EVENT : 3143

164

71 —

73 —

74 —

75 —

76 —

1 —

2 —

4 —

EVENT: 3217

71

73

74

75

76

1

2

4

165

PHONE: 74   EVENT: 3143

FREQUENCY (HZ)
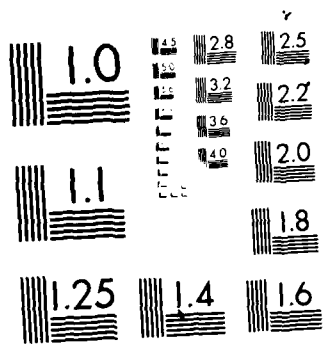
NOISE
MEAN
P

PHONE: 2

NOISE
MEAN
P

MICROCOPY RESOLUTION TEST CHART
NATIONAL BUREAU OF STANDARDS-1963-A
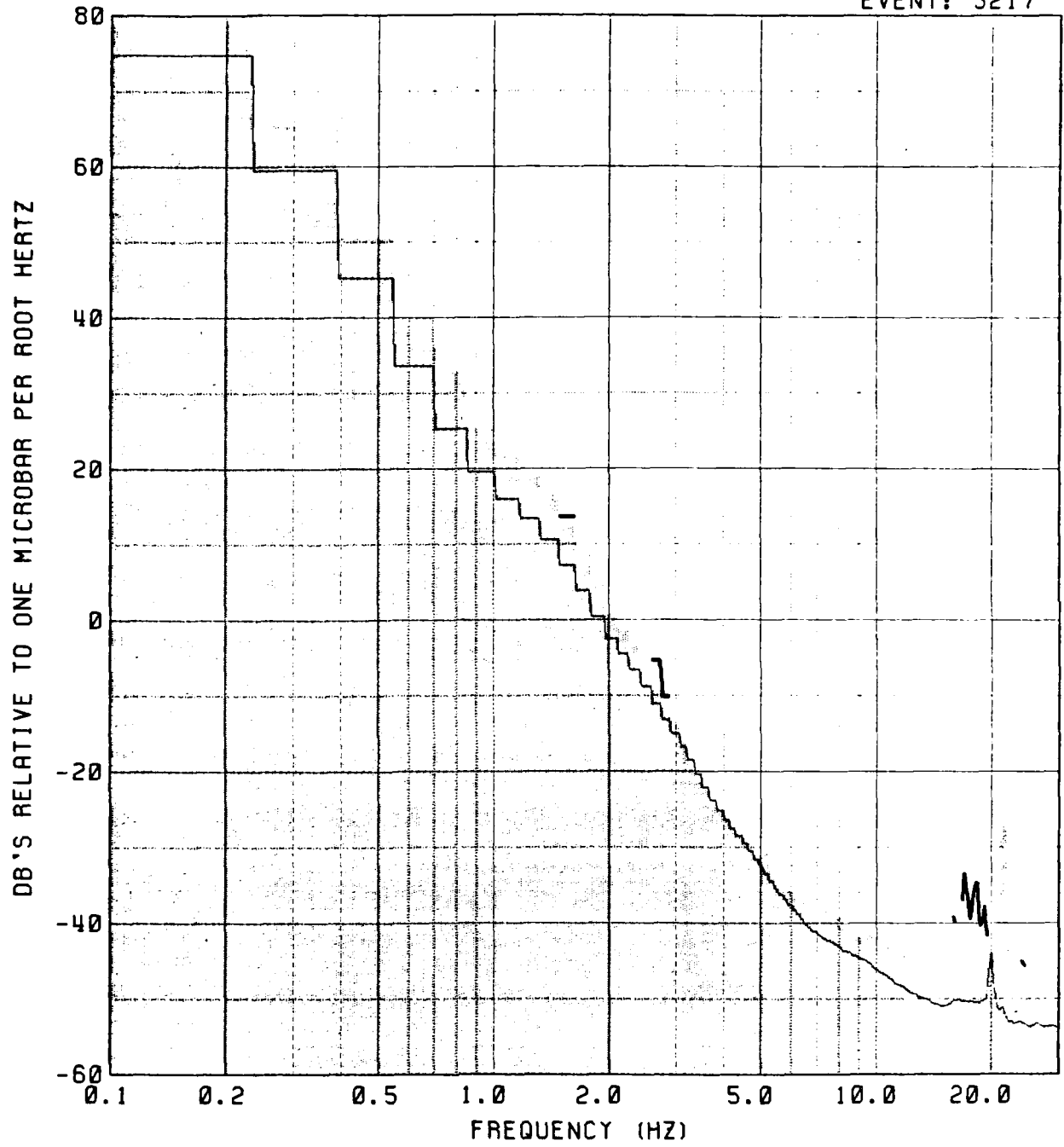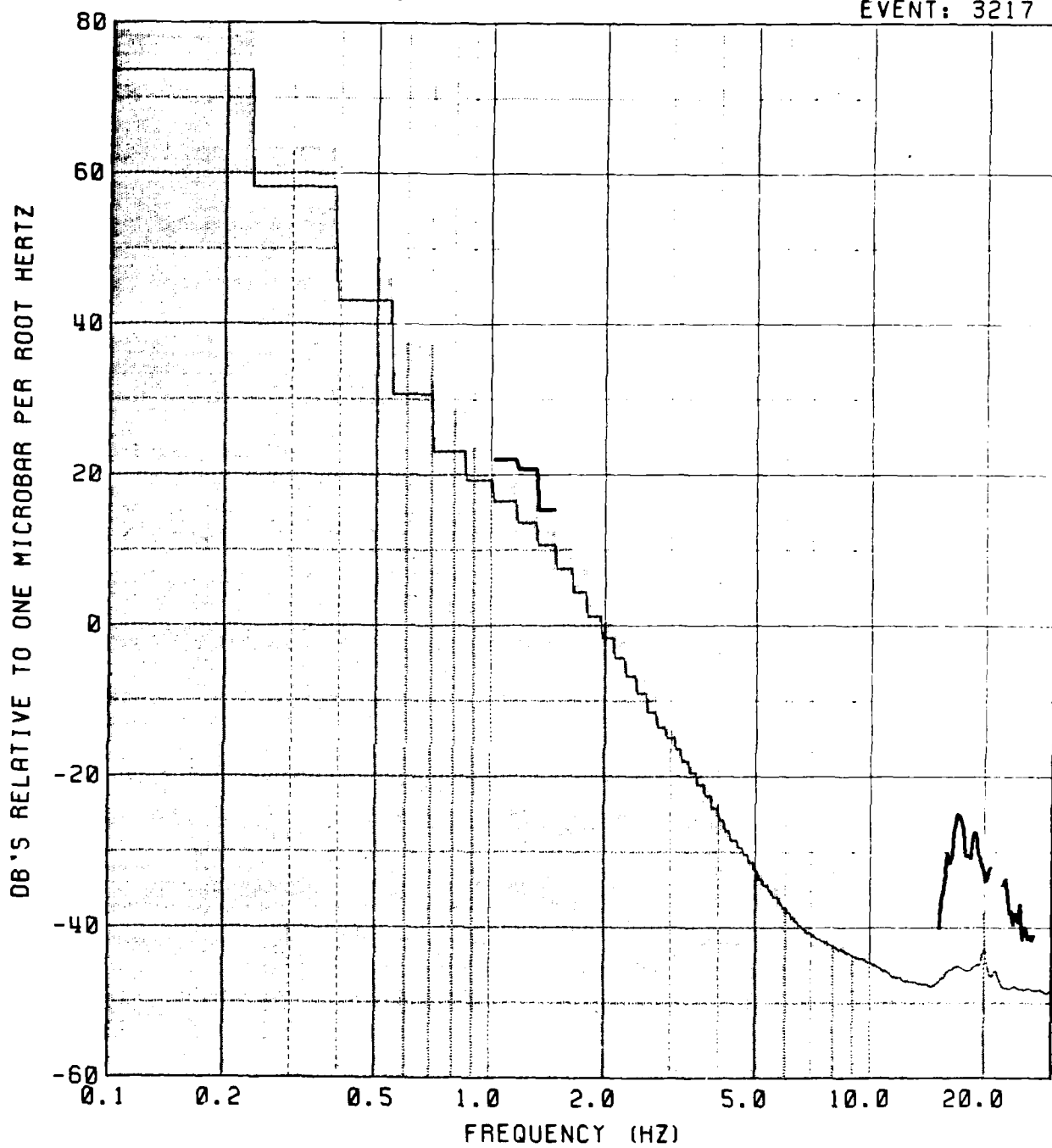
PHONE: 74

NOISE
MEAN
P
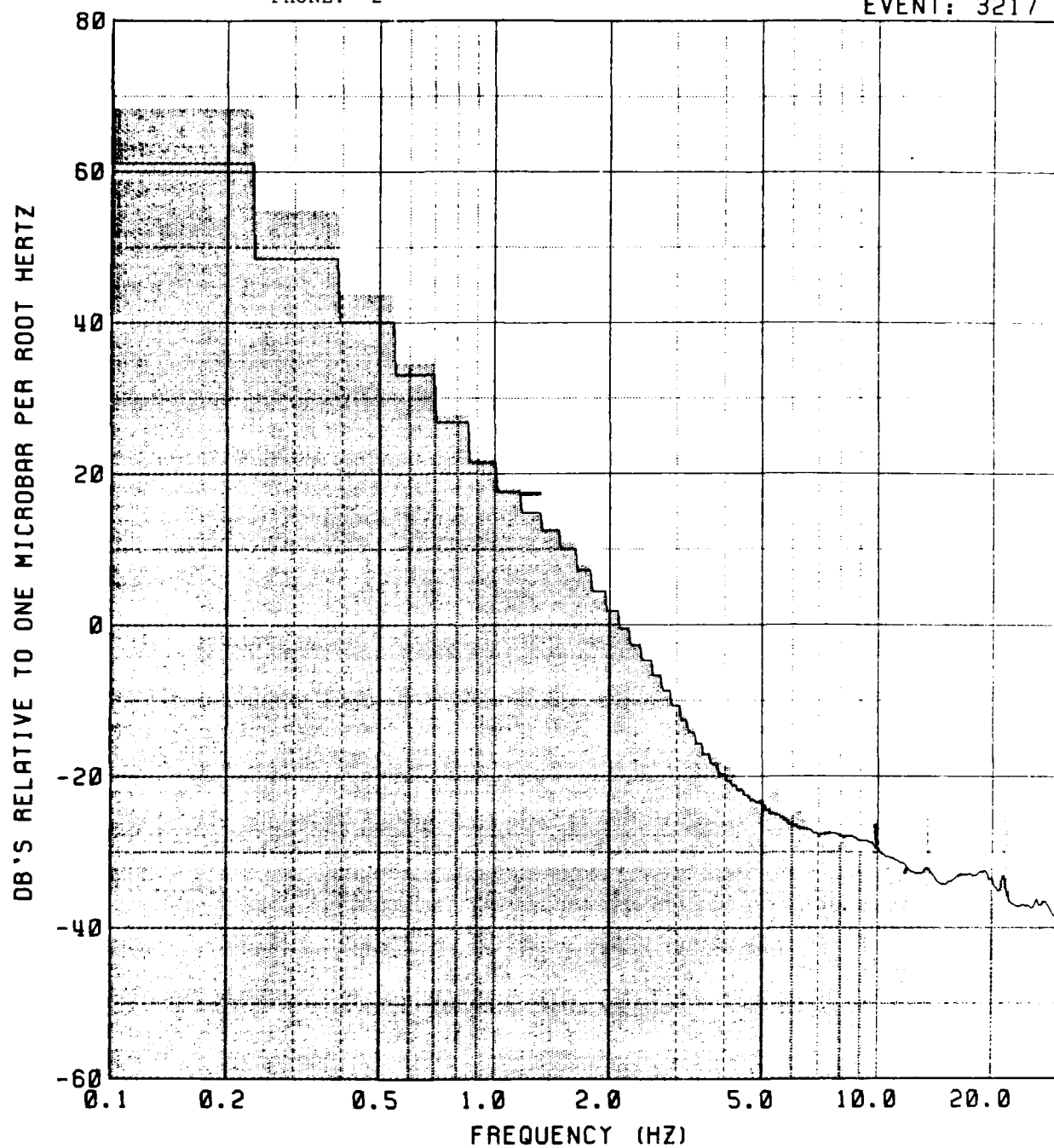
PHONE: 76

NOISE
MEAN
P

EVENT: 3143

172

EVENT: 3217

Tuamotus - Discussion

In the time series plots there are suggestions of a signal on phone 74. The spectrogram for # 3217 provides a stronger suggestion of a signal. For these 5.7 events, noise levels are average or slightly higher than average. It seems unlikely that magnitudes much lower than 5.7 from this site could be well recorded on any of the hydrophones.
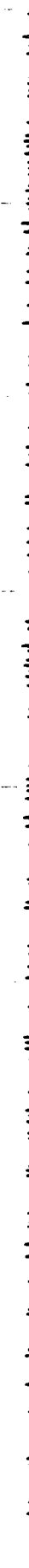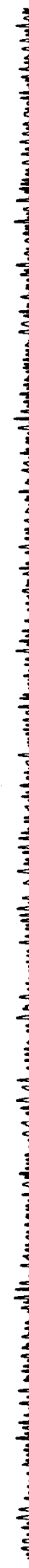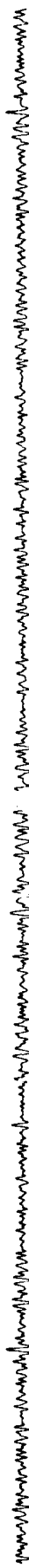
```
EVNT ******ORIGIN TIME****** **COORDINATES***   ****
*NO* YR*MO*DA*JUL*HR*MN*SECS **LAT*****LON***   *MB*

SOUTHERN NEVADA

0082 82 09 23 266 16 00 00.0 37.212N 116.207W   4.9
0083 82 09 23 266 17:00 00.0 37.175N 116.088W   4.9
0110 82 09 29 272 13:30 00.1 37.091N 116.045W   0.0
0248 82 11 12 316 19 17 00 1 37.024N 116.032W   4.4
0343 82 12 10 344 15 20 00.0 37.030N 116.072W   4.8
0649 83 02 11 042 16:00 00.1 37.051N 116.045W   0.0
0674 83 02 17 048 17:00 00.0 37.163N 116.063W   4.0
0826 83 03 26 085 20:20 00.0 37.301N 116.460W   5.1
0912 83 04 14 104 19 05 00.1 37.073N 116.046W   5.7
0951 83 04 22 112 13:53 00.0 37.112N 116.022W   4.0
1010 83 05 05 125 15 20 00.0 37.012N 116.089W   4.5
1084 83 05 26 146 15:00 00.0 37.103N 116.006W   4.3
1157 83 06 09 160 17 10 00.0 37.158N 116.089W   4.6
1424 83 08 03 215 13:33 00.0 37.119N 116.089W   4.2
1541 83 09 01 244 14 00 00.0 37.273N 116.355W   5.4
1607 83 09 21 264 15 00 00.0 37.210N 116.210W   0.0
1610 83 09 22 265 15:00 00.0 37.106N 116.049W   0.0
1913 83 12 16 350 18:30 00.0 37.140N 116.072W   5.1
2157 84 02 15 046 17.00 00.1 37.221N 116.181W   5.0
2223 84 03 01 061 17:45 00.0 37.066N 116.046W   5.9
2372 84 03 31 091 14 30 00.0 37.146N 116.084W   4.3
2523 84 05 01 122 19 05 00.0 37.106N 116.022W   5.3
2529 84 05 31 152 13:04 00.1 37.103N 116.048W   5.7
2709 84 06 20 172 15:15 00.0 37.000N 116.043W   4.8
2876 84 07 25 207 15:30 00.0 37.268N 116.411W   5.4
2898 84 08 02 215 15:00 00.0 37.017N 116.008W   4.8
3011 84 08 30 243 14:45 00.1 37.090N 115.998W   4.4
3047 84 09 13 257 14 00 00.0 37.087N 116.071W   5.0
3222 84 12 09 344 19:40 00.0 37.270N 116.498W   5.5
3229 84 12 15 350 14:45 00.0 37.281N 116.305W   5.4
```

SOUTHERN NEVADA

NO	ORIGIN TIME				COORDINATES		DISTANCE (DEG)			SIGNAL LEVELS			NOISE LEVELS			MB
	YR/MO/DAY	HR	MIN	SEC	N	W	74	76	2	74	76	2	74	76	2	
2223	84/03/01	17	45	0.0	37.07	116.05	68.11	68.34	68.78	*****	*****	*****	-0.5	-1.5	3.0	5.9
2523	84/05/01	19	05	0.0	37.11	116.02	68.13	68.35	68.79	*****	*****	*****	-5.0	-3.0	0.0	5.3
3047	84/09/13	14	00	0.0	37.09	116.07	68.09	68.32	68.76	*****	*****	*****	0.5	-0.5	2.0	5.5
3229	84/12/15	14	45	0.0	37.28	116.31	67.87	68.10	68.55	*****	*****	*****	2.0	3.0	2.0	5.4

EVENT: 2223

71 —
73 —
74 —
75 —
76 —
1 —
2 —
4 —

177

EVENT: 2523

71 -

73 -

74 -

75 -

76 -

1 -

2 -

4 -

EVENT: 3047

71

73

74

75

76

1

2

4

179

EVENT: 3229

180

71 -

73 -

74 -

75 -

76 -

1 -

2 -

4 -
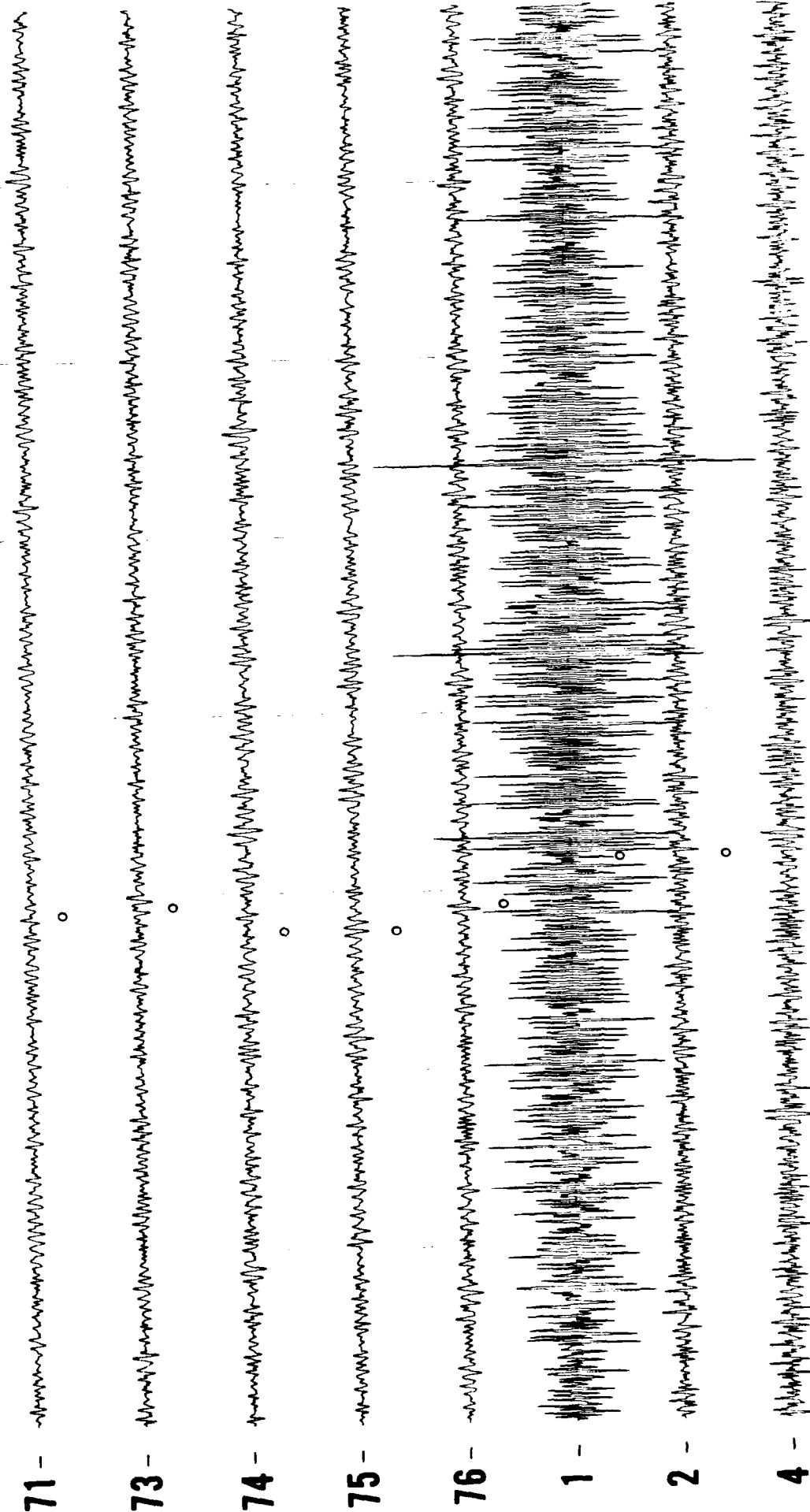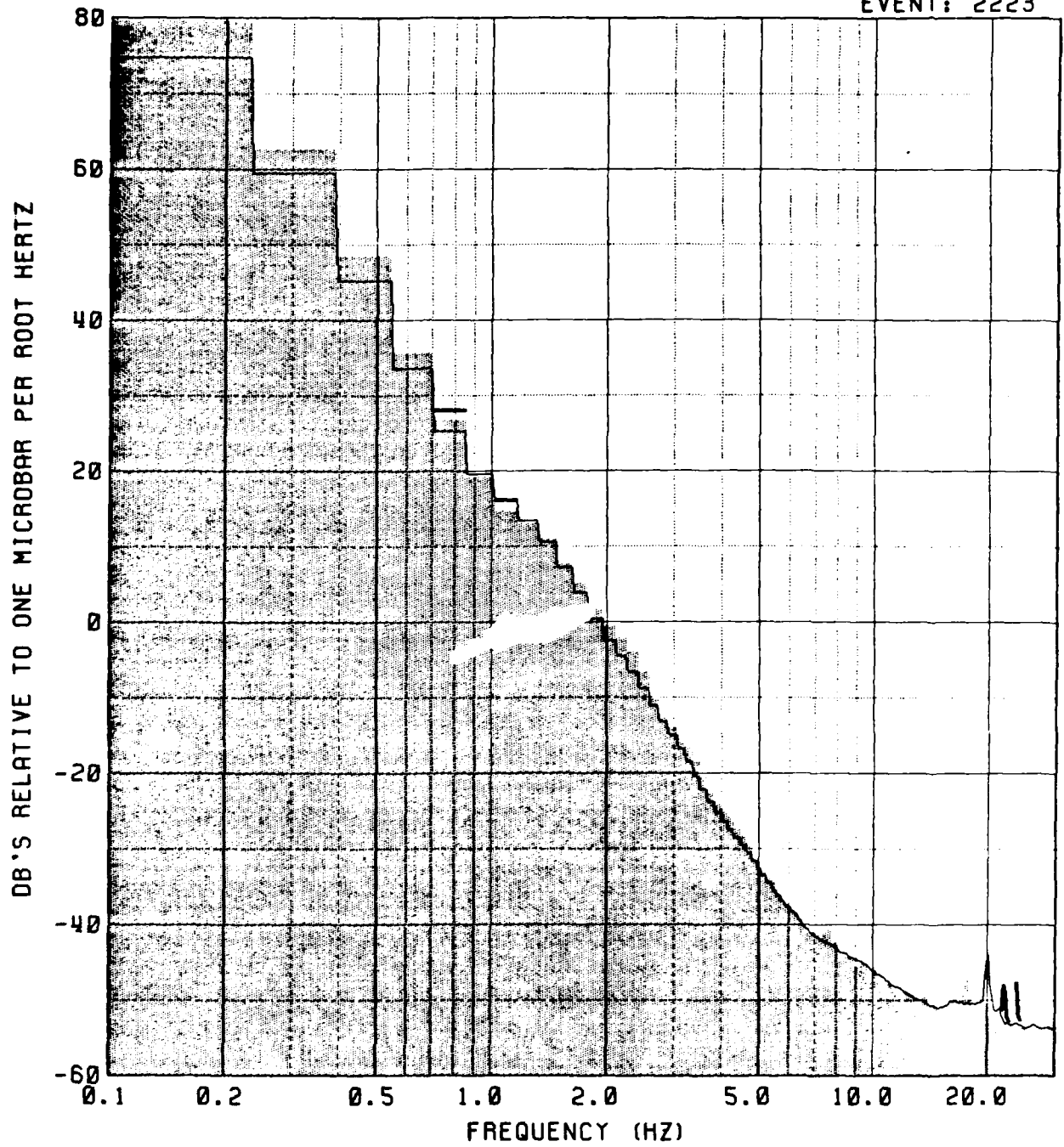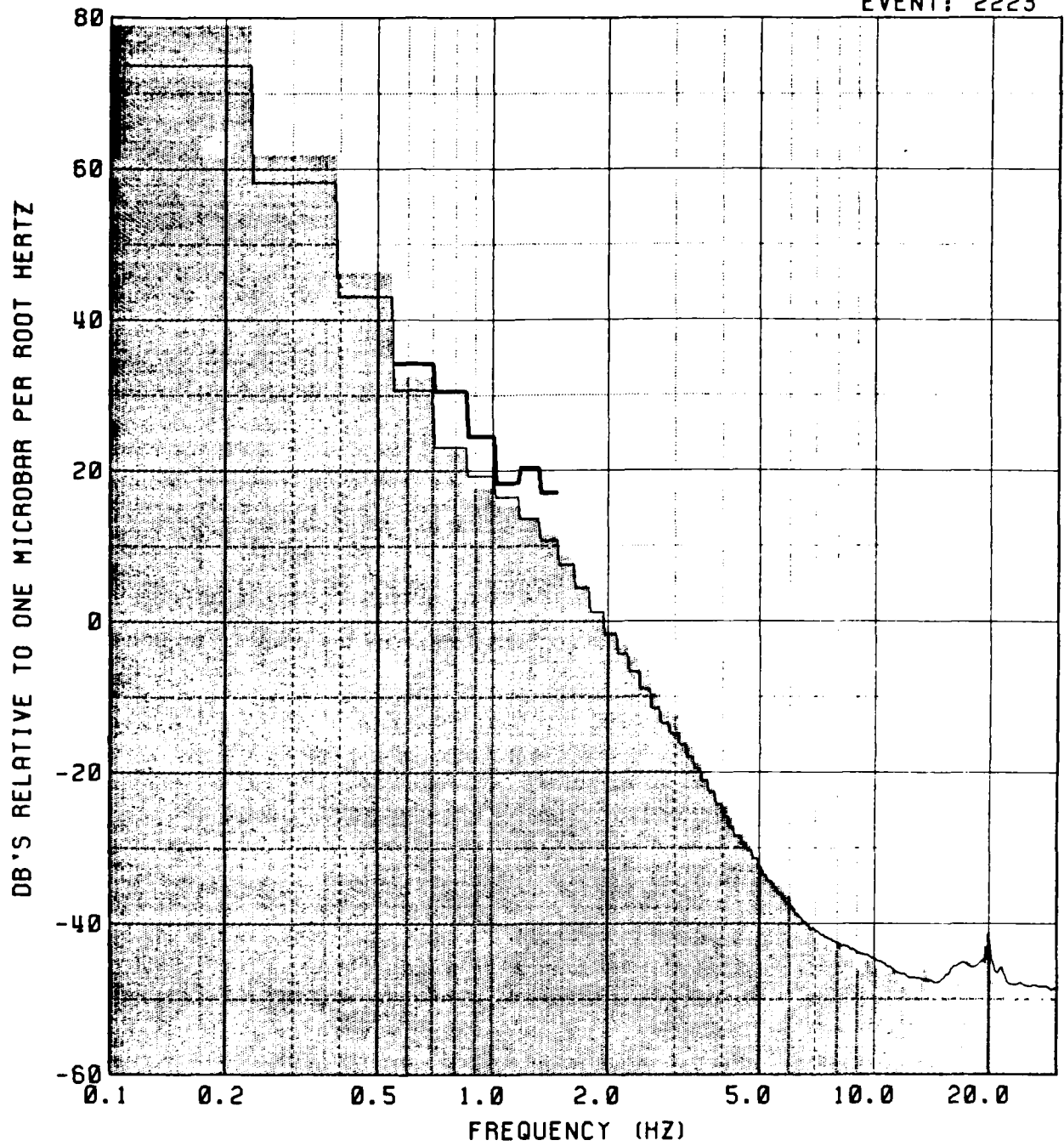
PHONE: 76
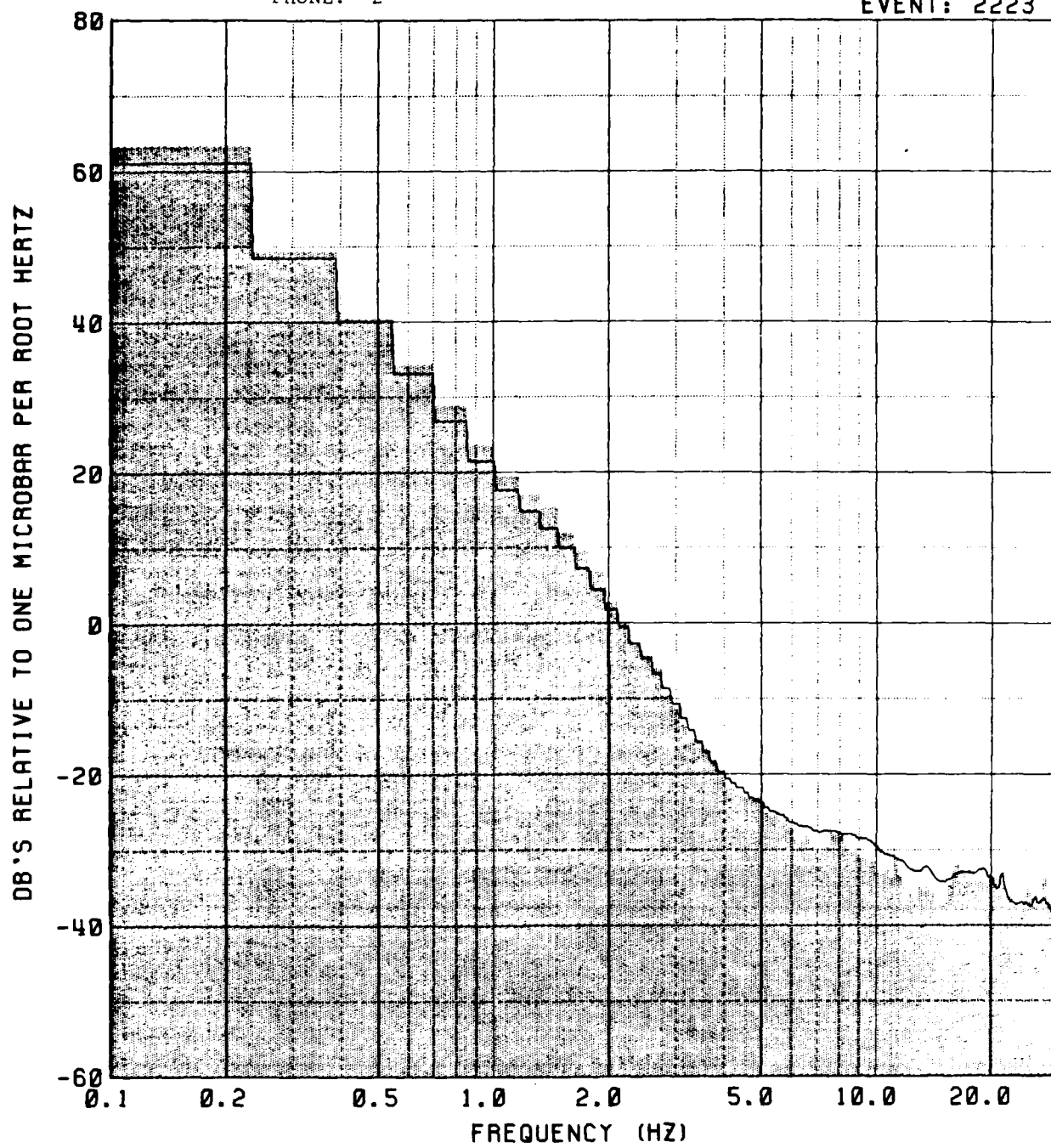
NOISE
MEAN
P
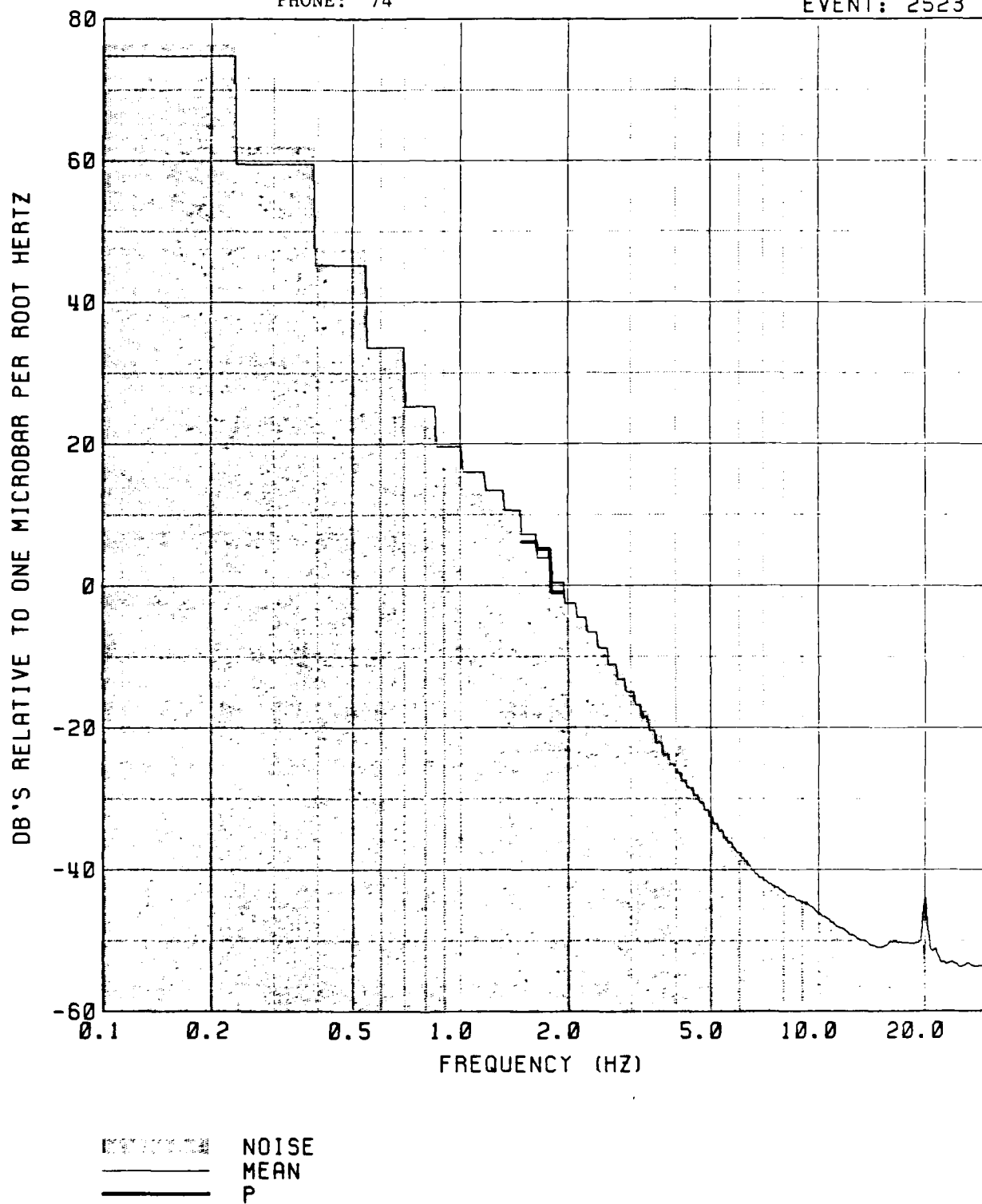
PHONE: 2

NOISE
MEAN
P

PHONE: 74   EVENT: 2523

NOISE
MEAN
P

FREQUENCY (HZ)

DB'S RELATIVE TO ONE MICROBAR PER ROOT HERTZ
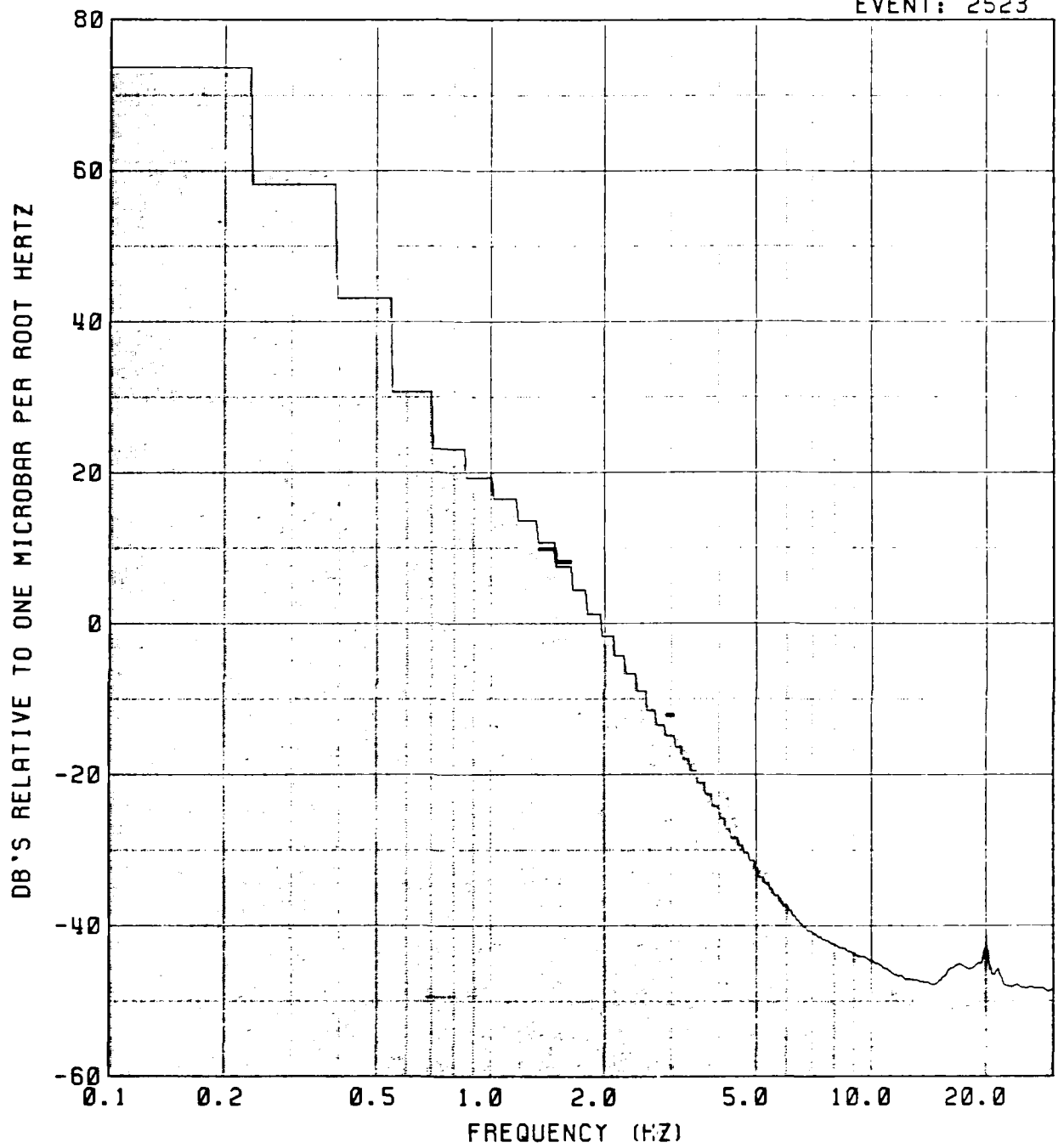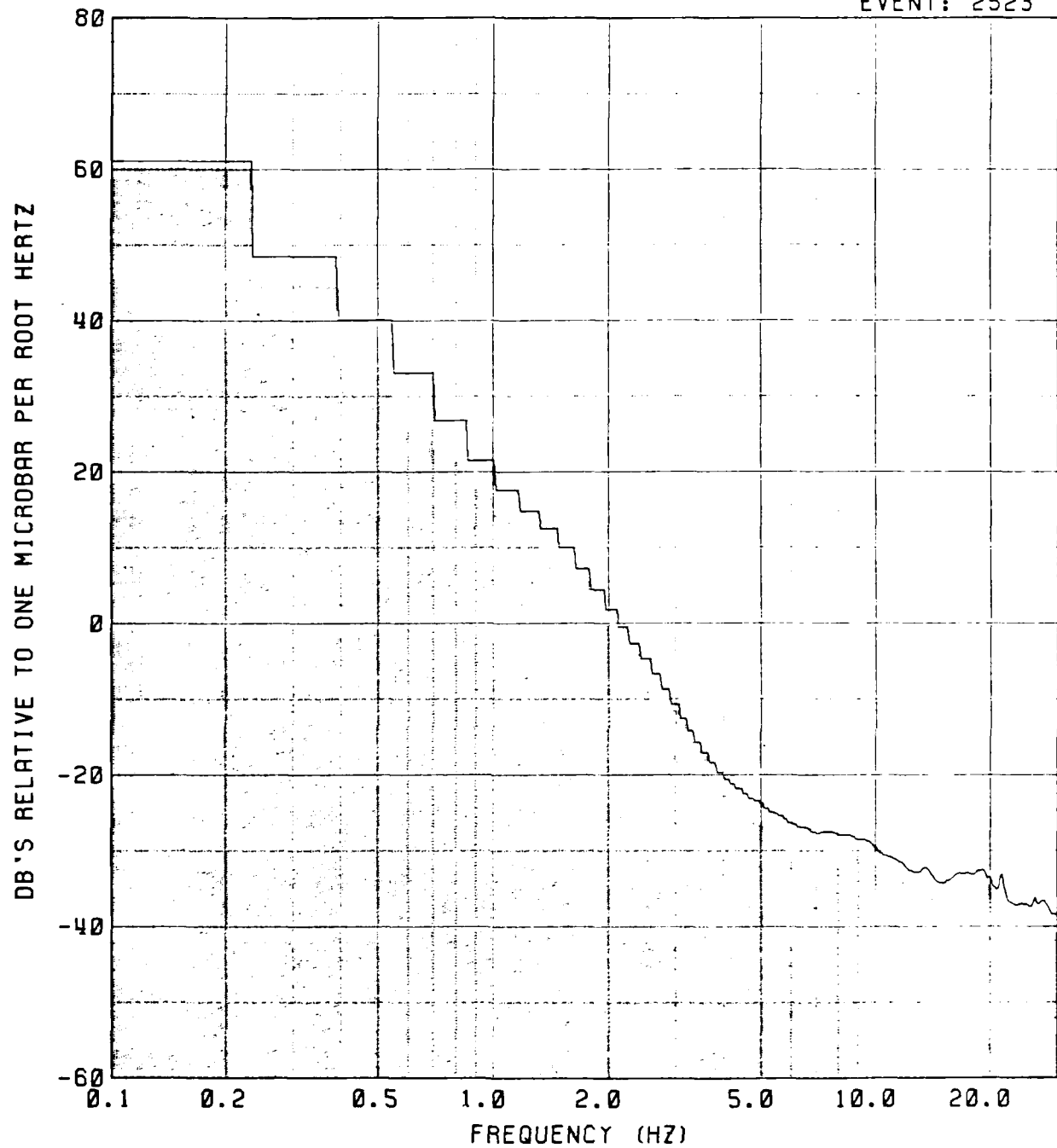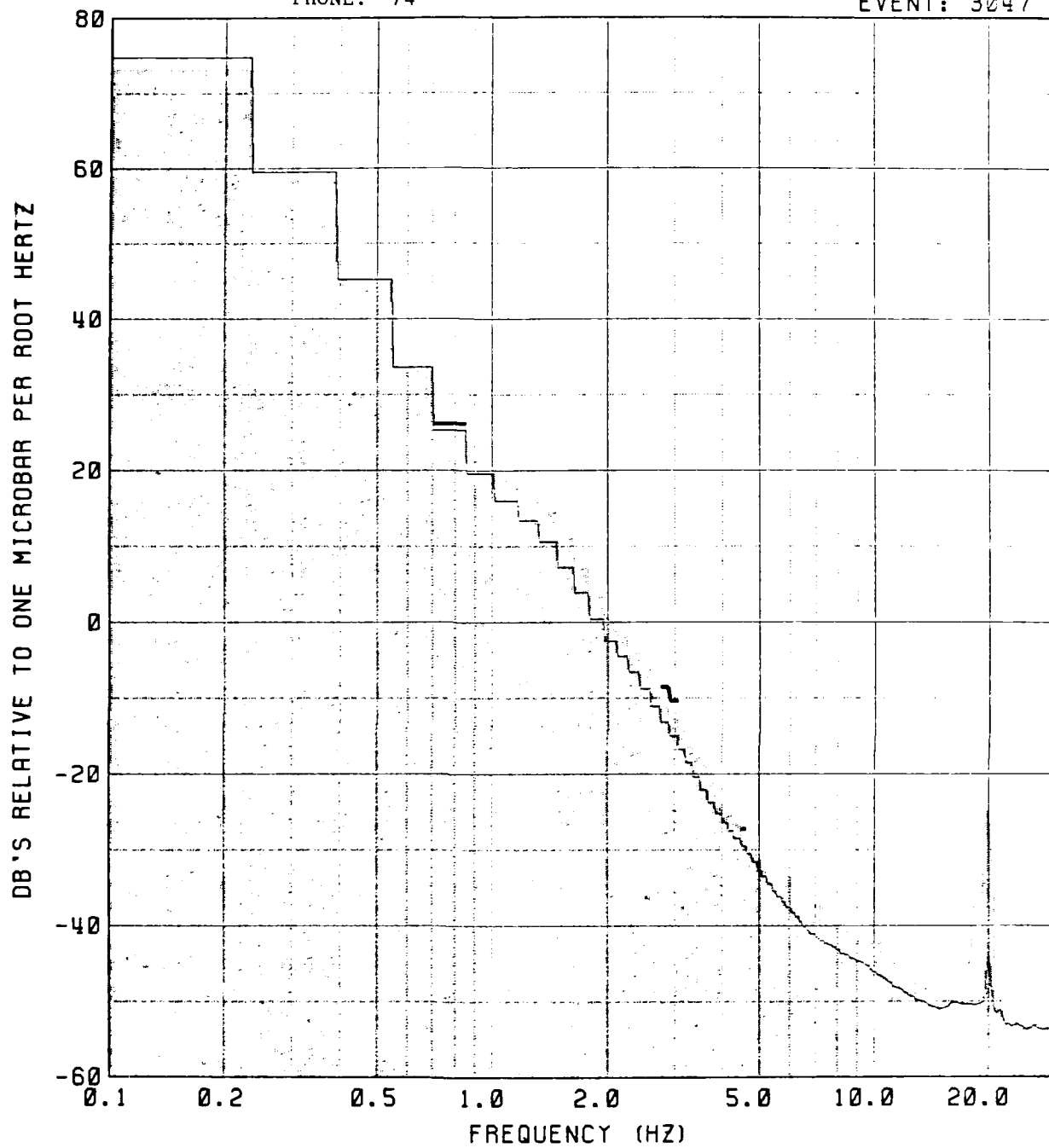
NOISE
MEAN
P

PHONE: 76
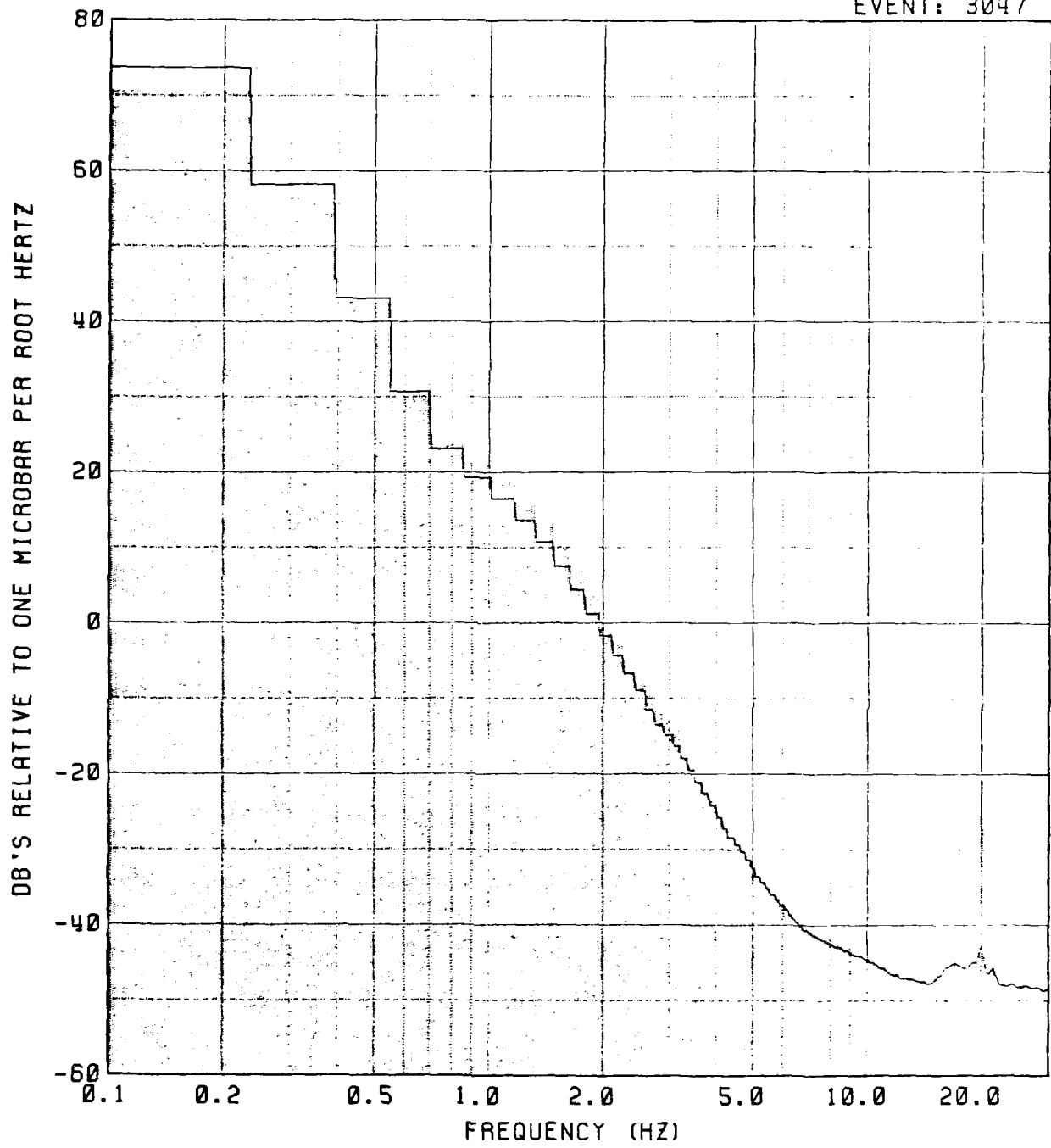
188
EVENT: 3047

NOISE
MEAN
P
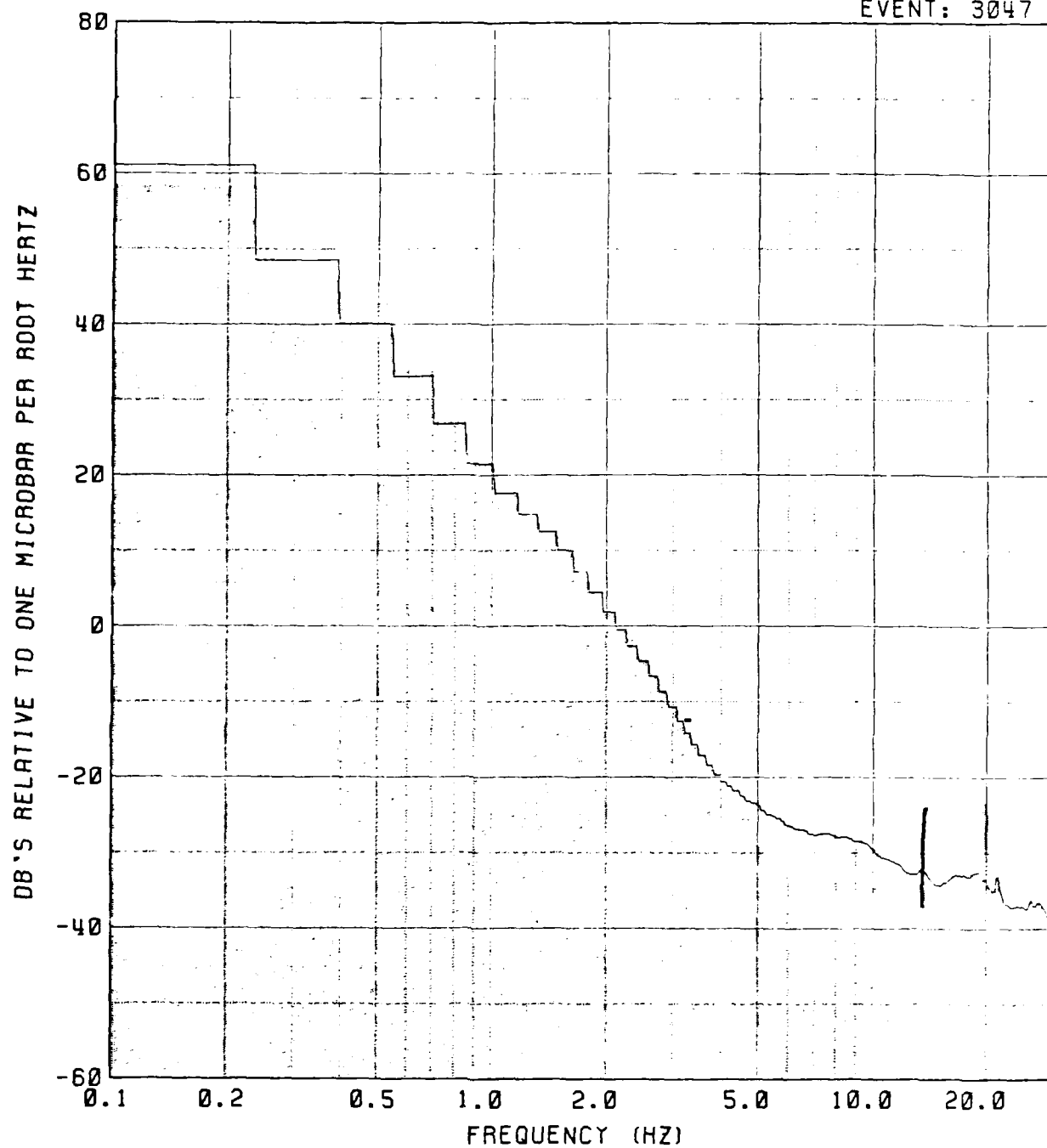
PHONE: 74

190

EVENT: 3229

NOISE
MEAN
P

PHONE: 76
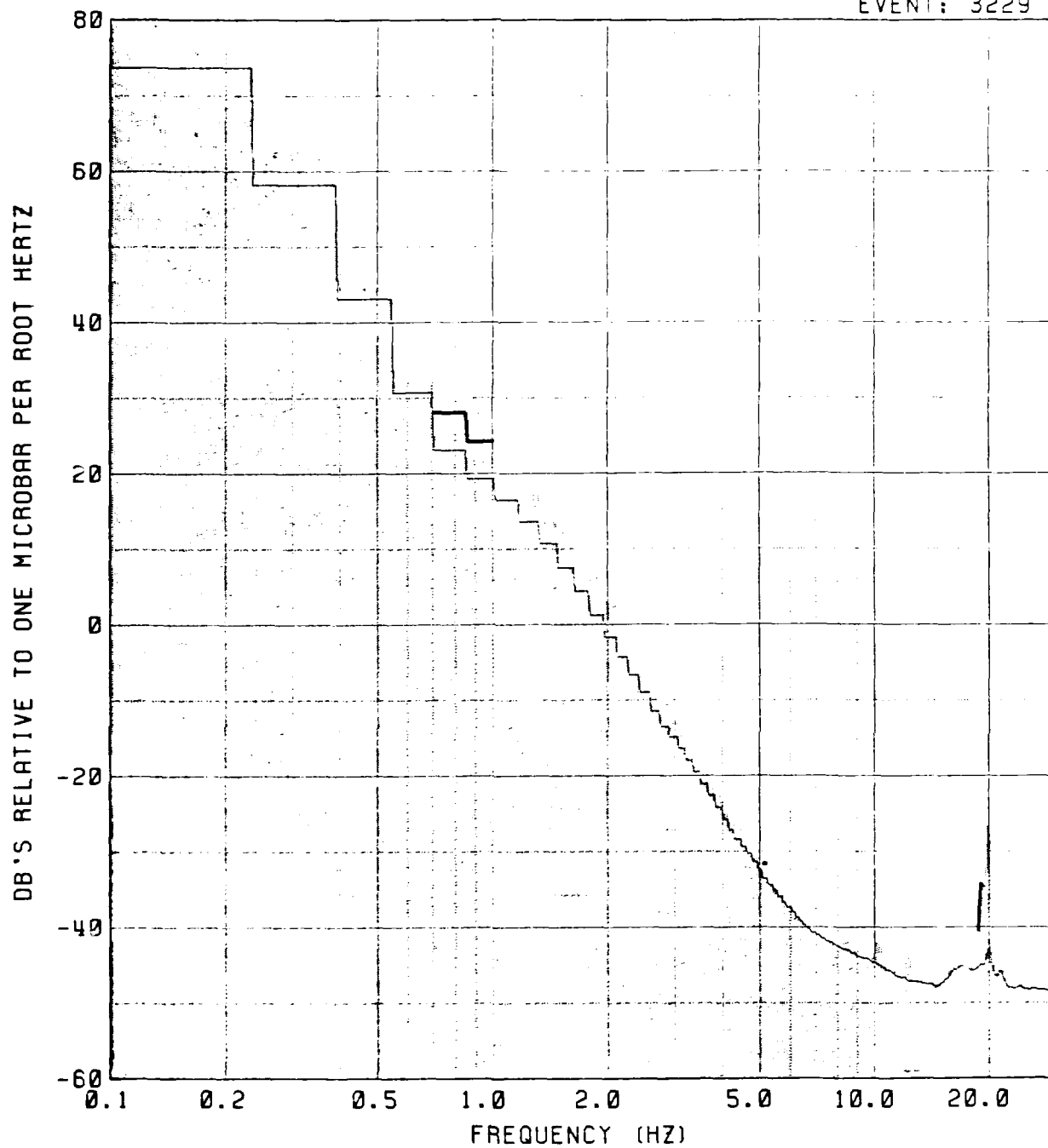
NOISE
MEAN
P

193

EVENT: 2223

Hz
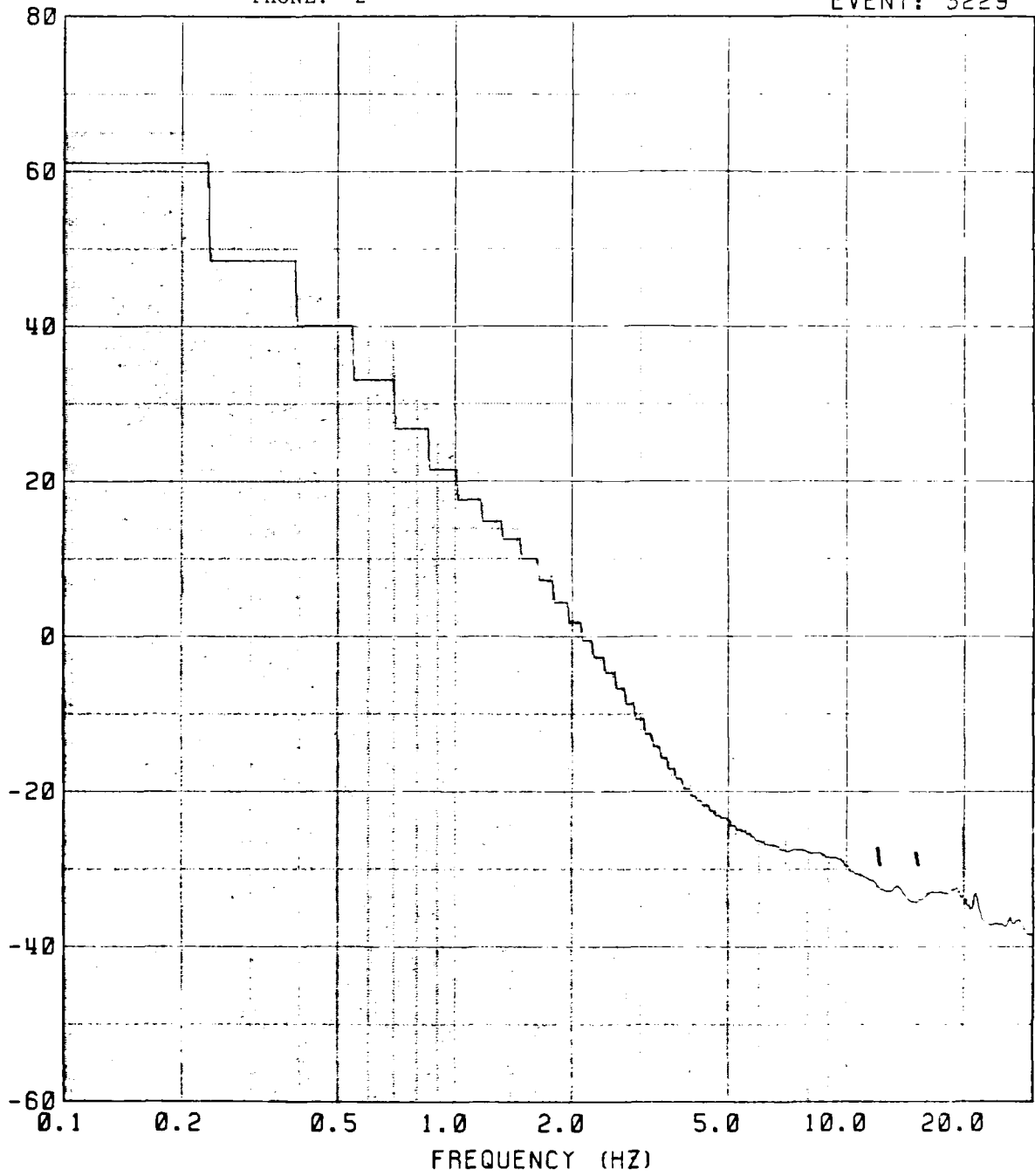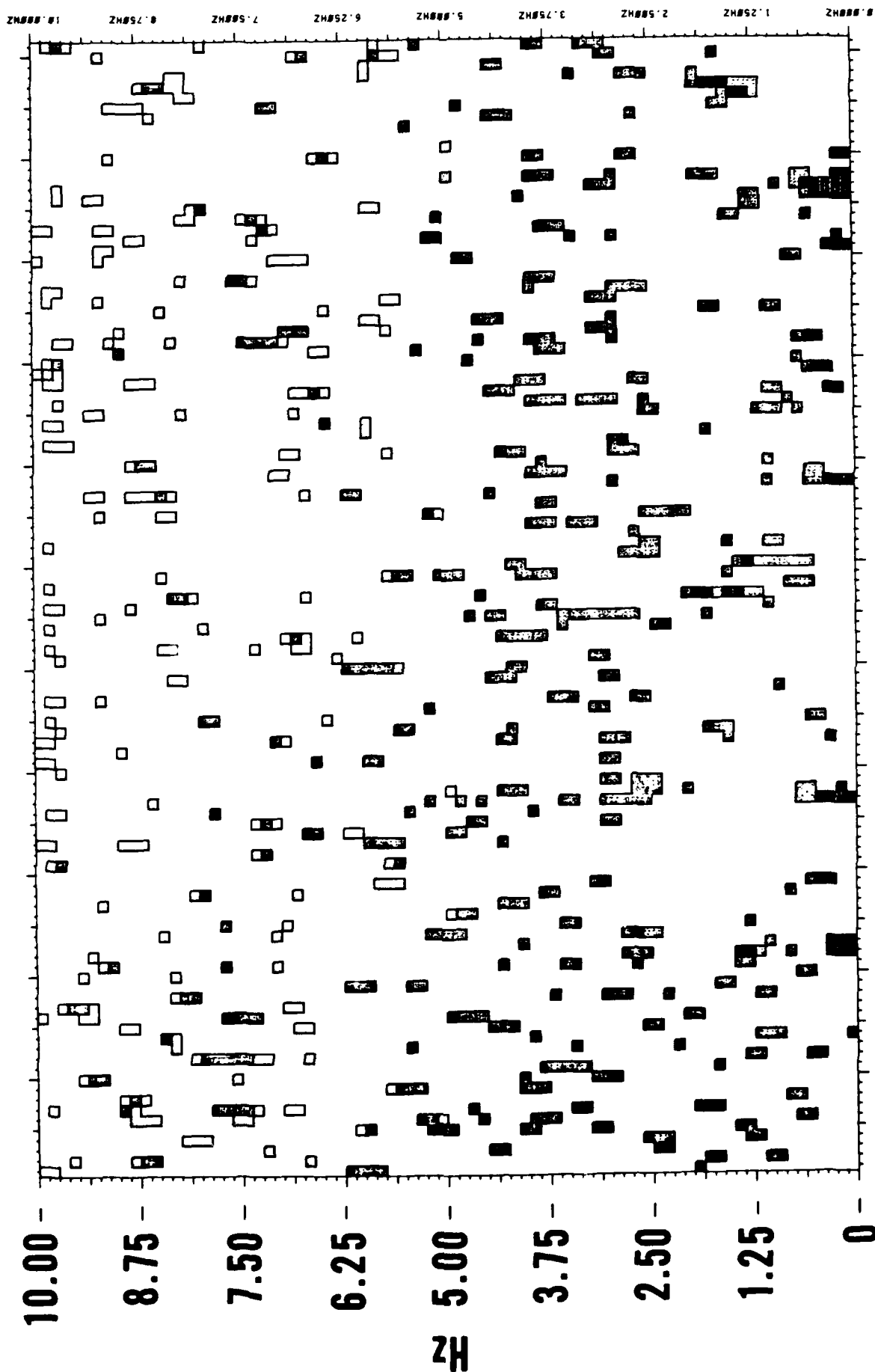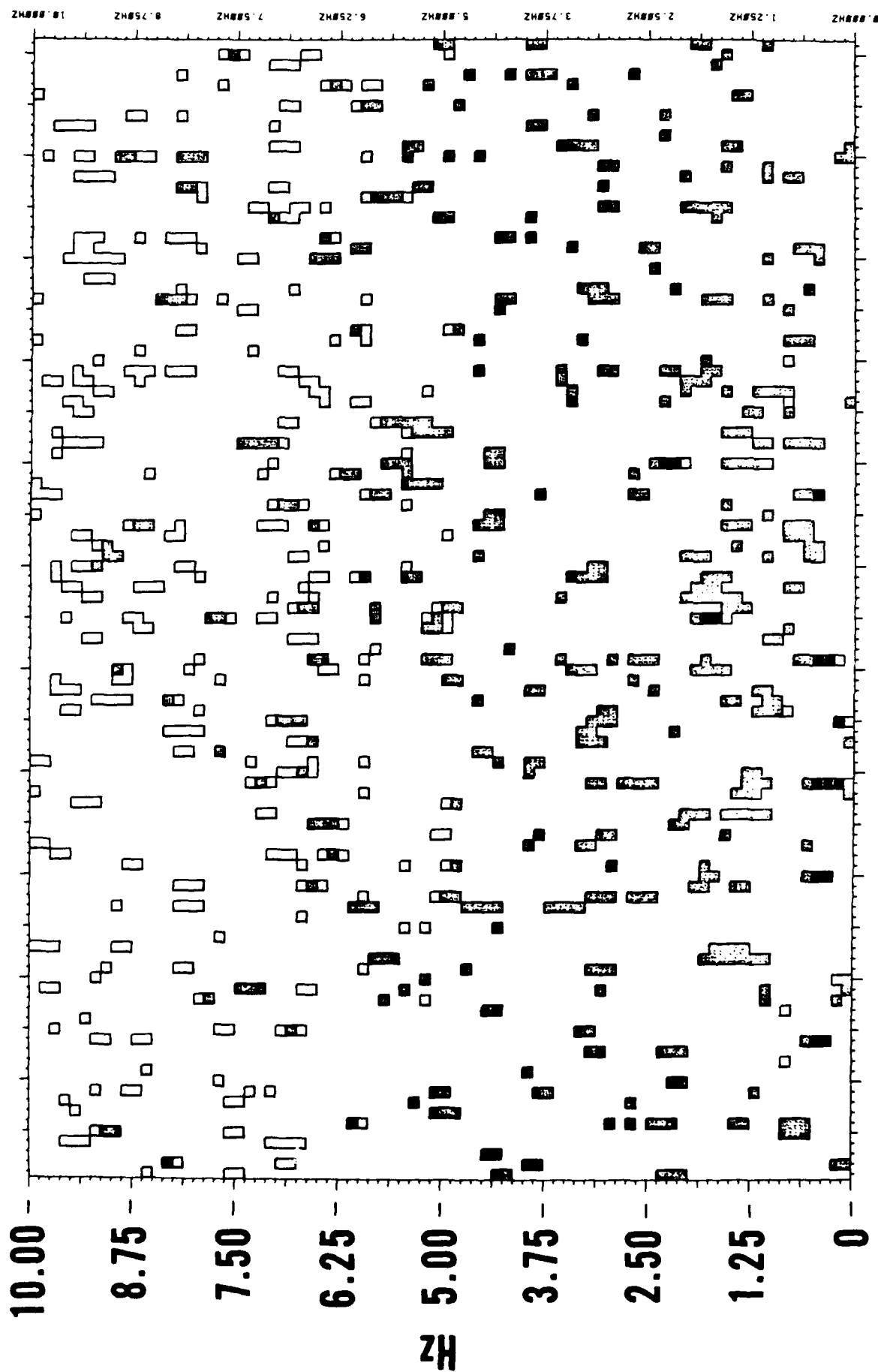
EVENT: 2523

EVENT: 3047

195
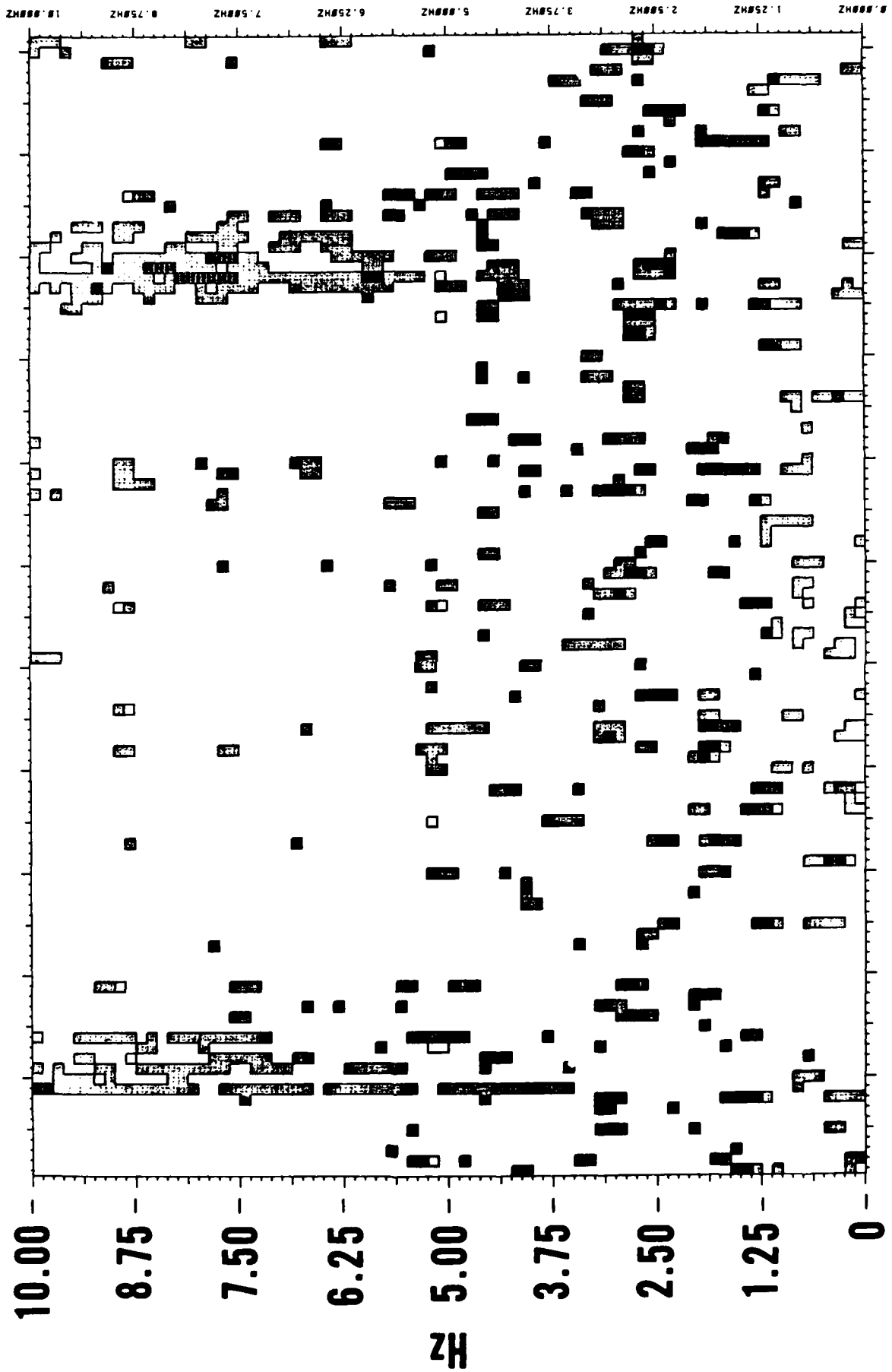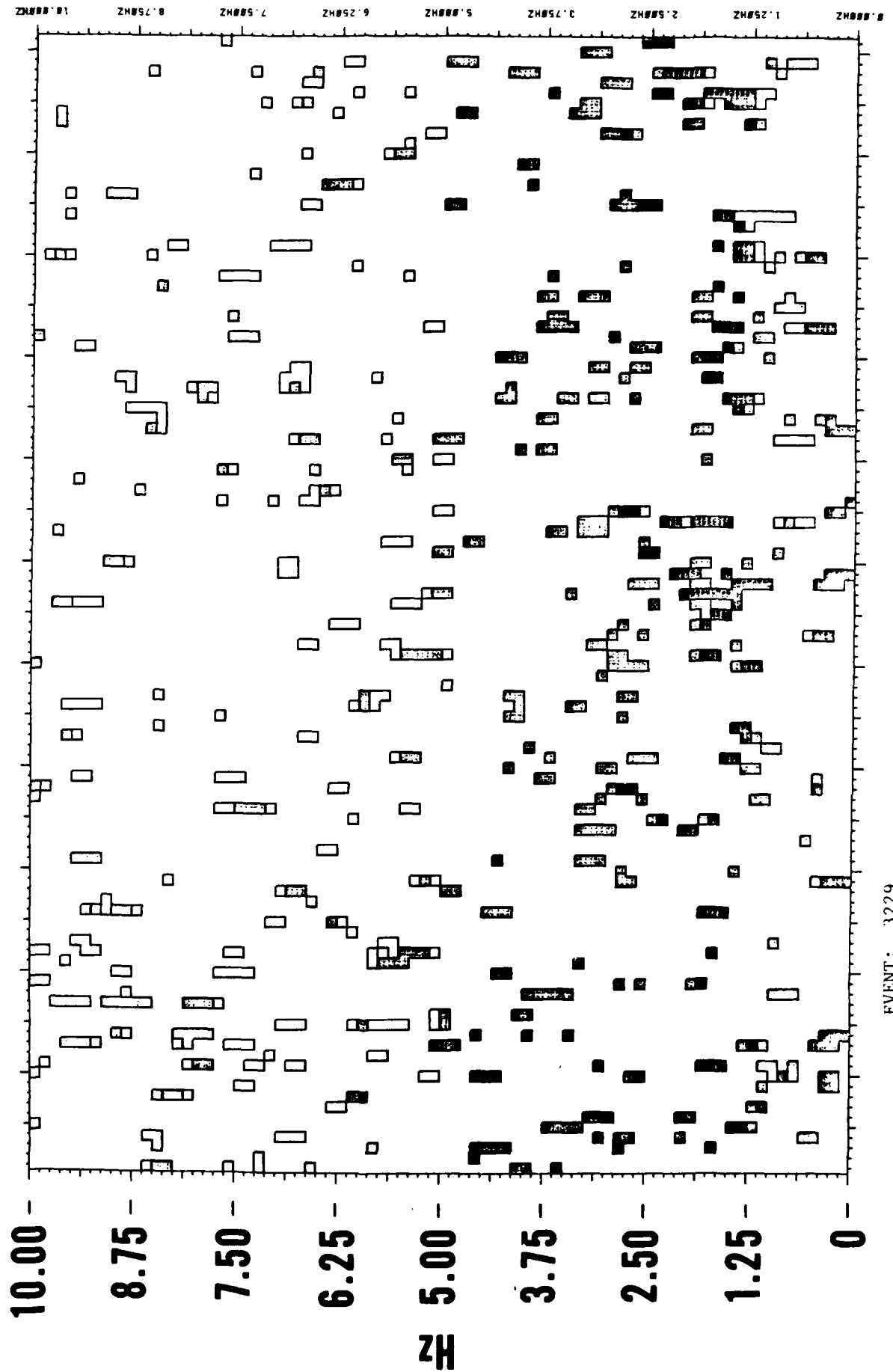
EVENT: 3229

Nevada - Discussion

The 5.9 explosion has its strongest signal on phone 76 under average noise conditions at around 1 Hz. The signal on phone 74 is marginal, suggesting some similarities with Novaya Zemlya, the Ural Mountains site, and possibly the China site. There are some very marginal hints of signals for the three smaller explosions. The 5.3 explosion with low noise conditions seems possible, while the remaining explosions should be viewed with a considerable amount of skepticism pending addition data from this site.

SUMMARY OF OBSERVATIONS

Signals from ten of the thirteen test sites used by various nations from September 1982 through December 1984 were recorded by the Wake array. Distances from all of these sites to phone 74 ranged from 55° to 80° with four sites at nearly identical distances of about 68° (Central U.S.S.R., China, Tuamotus, and Nevada) and three other sites within a few additional degrees (Novaya Zemlya at 76°, Eastern Kazakh at 73°, Western Siberia at 74°, and Central Siberia at 65°). Additional sites in Siberia and the Urals were at 55° and 80°, respectively. It should be noted that all of these distances are highly efficient for the propagation of mantle-refracted P phases since travel paths through low Q regions of the upper mantle are nearly vertical. The three sites for which signals were not observed at Wake had epicentral distances near, or beyond, 90°. Thus, these signals were probably either diminished in amplitude by effects near the mantle-core interface or totally absent due to refractions into the core.

Regarding signal strengths relative to mb values, the poorest recordings are from the Tuamotus and Nevada. Signals from the European and Asian sites generally suggest that mb's in the high 4's might be observed in the spectrums for phones 74, 76, or 2 at times when noise levels are lower than average.

Regarding frequency content, the Eastern Kazakh explosions seem the richest at the widest range of frequencies, with values as high as 7 Hz. The Siberian and Central Siberian signals are peculiar for their strength at high frequencies (i.e., 3 to 6 Hz) relative to their weakness at low

frequencies (i.e., < 3Hz). Signals from the remaining sites are generally confined to frequencies from 1 to 2.5 Hz.

Explosions from Novaya Zemlya, the Ural Mountains, China, and Nevada have larger signal-to-noise ratios on phone 76 than on phone 74, while explosions from Eastern Kazakh, Siberia, Central Siberia, Western Siberia, Central U.S.S.R., and the Tuamotus have larger signal-to-noise ratios on phone 74 than on phone 76. Also, the strongest signal-to-noise ratios on phone 2 were found for explosions from Novaya Zemlya, Eastern Kazakh, Central Siberia, Western Siberia, and the Ural Mountains. Apparent differences in responses to signals from differing sites may be related to: (a) effects near the test sites; and (b) small variations in the azimuths and emergence angles of signals combined with structural irregularities along the mantle-refracted P path near the receivers. These later effects are commonly observed on local arrays.

FINAL REMARKS

The thirteen explosions recorded from the Eastern Kazakh site constitute the largest data set from a single test site recorded at Wake from September 1982 through December 1984. For this same time period, four explosions were recorded from Novaya Zemlya; two from the Tuamotus; possibly four from Nevada; and one each from Siberia, Central Siberia, Western Siberia, Central U.S.S.R., the Urals, and China. Obviously, more data would be required to verify some of the preliminary observations discussed in the previous section of this report. Other observations seem unlikely to change. Signals from differing sites are characterized by very different spectral shapes and signal strengths [C. McCreery and D. Walker, "Spectral

comparisons between explosion P signals from the Tuamotu Islands, Nevada, and Eastern Kazakh", Geophys. Res. Lett., 12, 353-356, 1985.] Also, signals for mb's in the high 4's from European and Asian sites may be observable under low noise conditions in spectrums for phones 74, 76, and 2. This threshold, however, does not take into account any improvements resulting from array processing or the demonstrated potential advantage of dealing with noise reduced spectrograms rather than spectrums or time series.

Larger issues relevant to detection thresholds in general have yet to be addressed. One of these issues is the level and nature of ocean bottom noise. McCreery has shown that ocean bottom noise levels in the frequency range of 0.1 to 30 Hz are strongly related to ocean surface windspeeds [C. McCreery, "Ambient infrasonic ocean noise and wind", in internal review at HIG]. This suggests that the floor of deep ocean basins in regions of low wind may prove to be among the earth's quietest sites for the detection of weak short-period seismic signals. Also, mantle refracted P signals from events between 30° and 90° epicentral distance have corresponding angles of incidence in the water column in the narrow range between 6.9° and 3.6°. Although the directionality of the noise field on the deep ocean bottom has not been estimated from the Wake data since the hydrophones are omni-directional and since the spacings between hydrophones of the bottom array are too large to observe coherent short-period noise, a preliminary analysis of data from two SOFAR hydrophones, separated vertically by only 128 meters, seems to suggest that levels of vertically propagating noise in the water column are substantially smaller than the omni-directional noise level observed on the deep ocean bottom for frequencies between at least 1 and 5 Hz. Thus, additional improvements in signal-to-noise ratios could be expected by using directional hydrophones or more optimally spaced

hydrophone arrays to enhance vertically propagating pressure signals relative to the more omni-directional noise field. Work is in progress to further test this conjecture.

SPECTRAL COMPARISONS BETWEEN EXPLOSION P SIGNALS
FROM THE TUAMOTU ISLANDS, NEVADA, AND EASTERN KAZAKH

Charles S. McCreery and Daniel A. Walker

Hawaii Institute of Geophysics, University of Hawaii

Abstract. A comparison is presented between explosion-generated teleseismic P signals from single events of comparable magnitude in the Tuamotu Islands, Nevada, and E. Kazakh recorded by the Wake Island Hydrophone Array. Spectral analysis of these signals indicates that attenuation (presumably under the source) is greatest for the Tuamotu travel path and least for the E. Kazakh travel path. The high frequencies (> 3 Hz) present in E. Kazakh signals, which enhance the detectability of these signals on the ocean bottom near Wake (where noise levels are low in this range), are generally absent in signals from Nevada and the Tuamotus.

Introduction

In this report we examine the spectral content of teleseismic P from underground nuclear explosions at three different test sites – Eastern Kazakh in the U.S.S.R., Nevada, and the Tuamotu Islands in the South Pacific (Figure 1). The Wake Island hydrophone array is ideally suited for such a comparative study because of (a) low noise in the deep ocean at high frequencies [Walker, 1984], (b) the presence of high-frequency energy (as high as 9 Hz) in P phases from underground explosions at great distances [McCreery et al., 1983], and (c) the general equivalence of epicentral distances to Wake from each of these test sites (73.0° from E. Kazakh, 68.1° from Nevada, and 67.9° from the Tuamotus).

Data

Data from the Wake Island Hydrophone Array have been recorded on a nearly continuous basis since July of 1979 by both analog and digital recording systems. The array consists of eleven hydrophones, six on the ocean bottom (5.5-km depth) in a 40-km pentagonal array, and five at three SOFAR (1-km depth) sites spanning 300 km. The bottom hydrophones are generally the quietest and were primarily used in this investigation. A study of signals from test sites in the USSR has already been made using some of the analog data [McCreery et al., 1983]. In the current study, all the data have been searched for observable P phases from E. Kazakh, Nevada, and the Tuamotus.

Table 1 is a list of events that had body-wave magnitudes greater than 5.5 and that occurred while the recording systems were operational. The analog data were searched for these events by

bandpass filtering a section of record containing the calculated P arrival time. The bands searched were 0.5-1 Hz, 1-2 Hz, and 2-4 Hz, bands within which teleseismic P is usually prominent. The digital data were searched by scanning two-channel, 2-5 Hz filtered drum recordings made simultaneously with the digital tape recordings. In addition, some of the digital recordings were filtered and plotted to search for arrivals. The results are shown in Table 1.

Of the 40 events listed in Table 1, 24 were from E. Kazakh, 10 from Nevada, and 6 from the Tuamotus. Of these the number of events found by the methods described above were 22 (92%) from E. Kazakh, 4 (40%) from Nevada, and 3 (50%) from the Tuamotus. It was desirable, however, to have a signal-to-noise ratio (S/N) of at least 3/1 in order to identify the spectral signatures from each of those test sites. This requirement was met by 21 E. Kazakh events, but by only one event from Nevada (#5, Table 1) and one event from the Tuamotus (#2, Table 1). It is somewhat surprising to find that although a large percentage of E. Kazakh events have been recorded with strong S/N ratios, only a very small percentage of Nevada and Tuamotu events have been similarly recorded. One reason for this may be that the average Eastern Kazakh magnitude is 5.90 whereas the average magnitudes for Nevada and the Tuamotus are smaller at 5.66 and 5.70, respectively. Additional reasons become clear after spectral analyses of the signals and their respective noise levels.

Discussion

The Nevada and Tuamotu events with S/N > 3/1 were recorded by the first configuration of the analog cassette system used at Wake. These two events have been compared with each other and with a single E. Kazakh event (#3, Table 1), recorded by the same recording system. Figure 2 shows the P arrivals for these three explosions, each recorded on the same bottom hydrophone and bandpass filtered between 0.5 and 5.0 Hz. It appears from these playbacks that the signal with the least amount of high-frequency energy is from the Tuamotus, whereas the signal with the most high-frequency energy is from E. Kazakh. This observation is confirmed by the spectra shown in Figure 3. Differences in absolute levels of the signals between about 1.0 and 2.0 Hz generally reflect differences in body-wave magnitudes which were 5.8 at Nevada, 6.0 at the Tuamotus, and 6.1 at E. Kazakh. This is not surprising as those are the frequencies at which body-wave magnitudes are determined from the world-wide data. Below 1 Hz, however, the relationship changes. At a frequency of 0.8 Hz the signal from the Nevada event is nearly as large as the one from the E. Kazakh event, and the Tuamotu signal is more than 8 dB greater than the E. Kazakh signal. Spectral
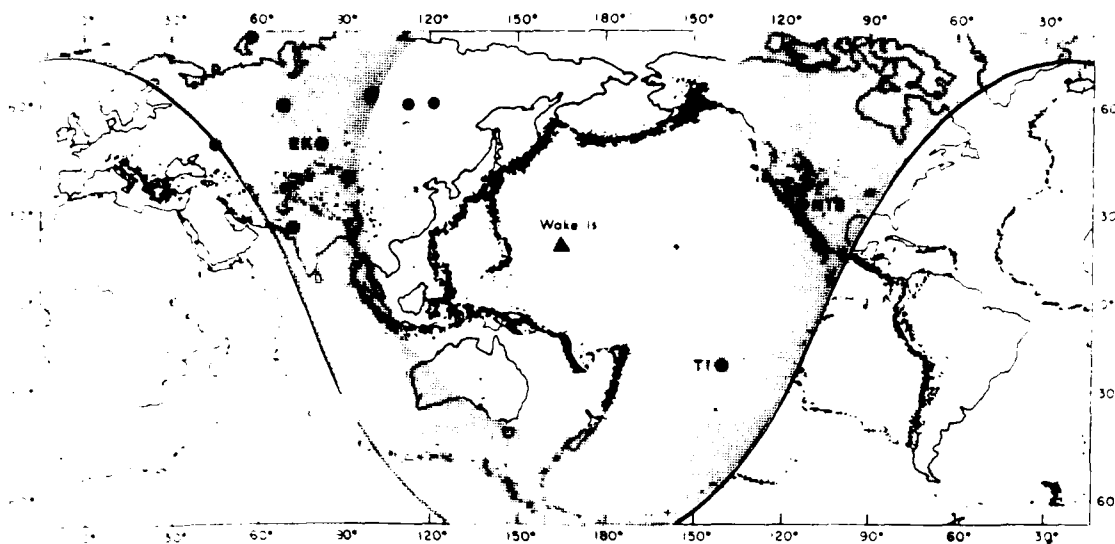
Fig. 1. Map showing the location of Wake Island relative to the world's major nuclear test sites (solid circles), including Eastern Kazakh (EK), the Tuamotu Islands (TI), and Nevada (NTS). The shaded region represents distances to Wake from 60° to 90°. At distances greater than about 60°, only a small portion of the P travel path is in the highly attenuating asthenosphere. At distances beyond 90°, no P energy is observed because of refraction into the core. Earthquake epicenters (small dots) show the world's active seismic zones.

ratios between the 1-Hz smoothed spectra (Figure 4) emphasize the differences in spectral shape between events. The Tuamotus/E. Kazakh ratio decreases at an average rate of around -12 dB/octave. The Nevada/E. Kazakh ratio is also decreasing by an average rate of perhaps -6 dB/octave, although the rate is much higher above about 1.7 Hz. The Tuamotus/Nevada ratio has an apparent droop between about 1.6 and 2.2 Hz, and is on the average also decreasing. All of the

Fig. 2. P arrivals from explosions at the Tuamotu Is., Nevada (NTS), and E. Kazakh recorded from one of the Wake bottom hydrophones. Note the increasing high-frequency content going from the Tuamotus' signal to the E. Kazakh signal.

above observations may be generally explained by attenuation effects which are greatest under the Tuamotu site and least under the E. Kazakh site. This contrasting effect has been previously observed between Nevada and E. Kazakh by other investigators [see, for example, Marshall, 1979].

These limited data present a consistent picture. Differences in amplitude between the three events at about 1 to 2 Hz correspond approximately to the differences in their magnitude. At frequencies below 1 Hz, the Tuamotu event appears to be the richest. At frequencies above 2 Hz, the E. Kazakh event is the most energetic. Under the assumption that differences between the spectral character of these signals are due mostly to attenuation differences under the source, it can be stated that these data support increasing attenuation from E. Kazakh to Nevada to the Tuamotus, in that order. This compares with recent measurements of attenuation under these sites made by Der et al. [1985] based on P-spectra from recordings made at numerous land stations. They found the E. Kazakh site to have the least attenuation, but the Nevada and Tuamotu sites to have essentially the same higher attenuation.

These results are relevant to the observation made earlier regarding the low percentage of Nevada and Tuamotus events recorded at Wake in comparison to E. Kazakh events. In the upper half of Figure 3, an average noise curve from another bottom hydrophone [McCreery et al., 1983] has been superimposed on the data. The standard deviation associated with this noise curve varies from about 4 to 6 dB. Given that (a) the Tuamotu event had the largest magnitude of the Tuamotu events searched for, (b) it is only apparent over a fairly narrow and low-frequency band, and (c) the noise level in that band is often higher
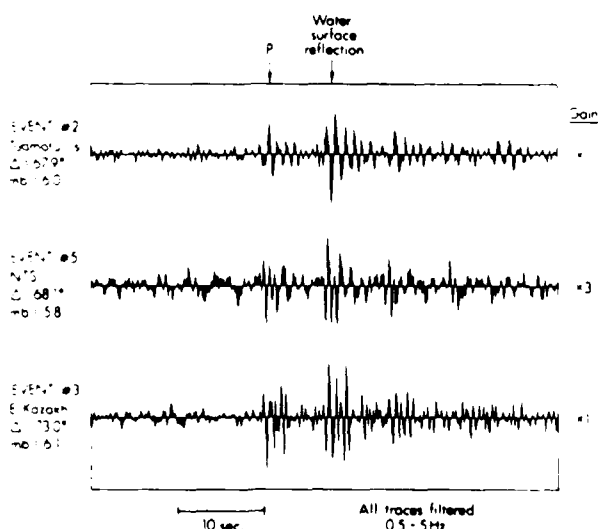
TABLE 1. E. Kazakh, Nevada, and Tuamotu Test
Explosions (mb ≥ 5.5) [from NEIS listings]

No.	Date	Site	mb	System[2]	Quality[3]
1	7 Jul 79	EK	5.8	I	A
2	25 Jul 79	TI	6.0	I	A
3	4 Aug 79	EK	6.1	I	A
4	18 Aug 79	EK	6.1	I	A
5	6 Sep 79	NTS	5.8	I	A
6	26 Sep 79	NTS	5.6	II	C
7	28 Oct 79	EK	6.0	II	A
8	2 Dec 79	EK	6.0	II	A
9	23 Dec 79	EK	6.1	II	A
10	25 Apr 80	EK	5.5	II	A
11	22 May 80	EK	5.5	II	C
12	12 Jun 80	EK	5.6	II	A
13	12 Jun 80	NTS	5.6	II	C
14	16 Jun 80	TI	5.5	II	C
15	29 Jun 80	EK	5.7	II	A
16	19 Jul 80	TI	5.9	II	C
17	25 Jul 80	NTS	5.5	II	C
18	14 Sep 80	EK	6.2	II	A
19	12 Oct 80	EK	5.9	II	C
20	3 Dec 80	TI	5.6	II	B
21	14 Dec 80	EK	5.9	II	A
22	27 Dec 80	EK	5.9	II	A
23	15 Jan 81	NTS	5.6	II	B
24	13 Sep 81	EK	6.0	III	A
25	18 Oct 81	EK	6.0	III	A
26	29 Nov 81	EK	5.6	III	A
27	27 Dec 81	EK	6.2	III	A
28	28 Jan 82	NTS	5.9	III	B
29	12 Feb 82	NTS	5.6	III	C
30	7 May 82	NTS	5.7	III	C
31	24 Jun 82	NTS	5.6	III	B
32	4 Jul 82	EK	6.1	III	A
33	25 Jul 82	TI	5.6	III	B
34	5 Dec 82	EK	6.1	IV	A
35	26 Dec 82	EK	5.7	IV	A
36	14 Apr 83	NTS	5.7	IV	C
37	19 Apr 83	TI	5.6	IV	C
38	12 Jun 83	EK	6.1	IV	A
39	26 Oct 83	EK	6.1	IV	A
40	26 Dec 83	EK	5.5	IV	B

Sites: EK - Eastern Kazakh
       NTS - Nevada Test Site
       TI - Tuamotu Islands

Systems: I - 3-channel analog cassette
              system, configuration 1
        II - 3-channel analog cassette
              system, configuration 2
       III - 3-channel analog cassette
              system, configuration 3
        IV - 8-channel digital system

[3]Quality: A - greater than 3/1 signal to noise
               observed
            B - less than 3/1 signal to noise
               observed
            C - not detected by the search methods
               used
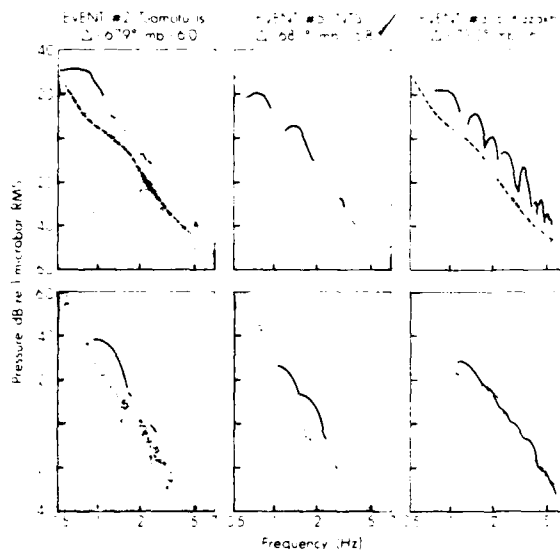
Fig. 3. Spectra of P signals from explosions at
the Tuamotu Is., Nevada (NTS), and E. Kazakh.
These spectra have been computed using a single
1024 point FFT applied to each time series,
digitized at 80 samples/sec, at the time of the P
arrival. Noise spectra have been similarly
computed by averaging the power estimates from
many FFT's taken over an approximate one-minute
section of each time series just prior to the P
arrival. The upper half of the figure shows the
unsmoothed data with a bandwidth of 0.078 Hz
(i.e., [80 samples/sec]/[1024 samples]). The
lower half of the figure shows the same data
smoothed with a 1-Hz boxcar. Noise levels are
indicated by the top surface of the shaded
region. Only signal levels which are at least
4 dB above the noise levels have been plotted.
Also plotted in this figure is an average noise
curve for the Wake bottom hydrophones (dashed
curves in the upper half of figure) and the
average Soviet explosion signal spectrum (dashed
curve in the lower half of the E. Kazakh portion
of the figure); both taken from McCreery et al.
[1983].
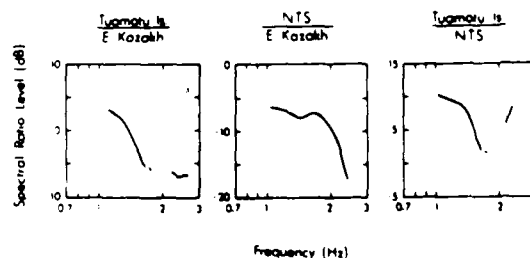
Fig. 4. Spectral ratios between P-signals from
explosions at the Tuamotu Is., Nevada (NTS), and
E. Kazakh. Ratios are only shown at frequencies
where signal levels were at least 4 dB above
noise levels for both of the events.

than the level observed at the time of the studied event, it is not so surprising that no other Tuamotu event was found with S/N > 3/1. Similarly, because (a) the Nevada event was the second largest of the Nevada events searched for, (b) its signal band was also fairly narrow and low, and (c) noise levels at the time it was recorded were substantially lower than average, it also is not surprising that only one Nevada event with S/N > 3/1 was found. On the other hand, the E. Kazakh event studied had a magnitude equalled or bettered by eight other E. Kazakh events and had observable energy over roughly 2.5 octaves including frequencies greater than 3 Hz where ambient noise is very low. It is therefore not surprising that a large percentage of E. Kazakh events are recorded with S/N > 3/1.

In closing, we note that although past studies indicate that the standard deviation of spectral shape for spectra from E. Kazakh explosions is small (generally, less than 3 dB based on an analysis of 12 signals from events 3, 4, 7, 9, 18 and 19 in Table 1 [McCreery et al., 1983]), inferences drawn in this study are valid only if the spectral shapes obtained for Nevada and the Tuamotus are also typical. Additional high-quality data from both Nevada and the Tuamotus need to be collected and analyzed in order to substantiate these findings. In addition we note that: (a) comparisons of spectra from explosions at the Nevada, Tuamotu, and E. Kazakh test sites are important for understanding the nature of explosions from these sites; (b) Wake, in being essentially equidistant from these sites, is unique for such studies; and (c) the low noise of the deep oceans at high frequencies presents an opportunity for recording broader spectra than are possible with many continental stations. Because of these factors and because data sufficient for a comprehensive analysis may not be forthcoming for several years, we feel justified in presenting the preliminary indications of this study.

References

Der, Z., T. McElfresh, R. Wagner, and J. Burnetti, Spectral characteristics of P waves from nuclear explosions and yield estimation, Bull. Seismol. Soc. Am., 75, 379-390, 1985.

Marshall, P. D., D. L. Springer, and H. C. Rodean, Magnitude corrections for attenuation in the upper mantle, Geophys. J., 57, 609-638, 1979.

McCreery, C. S., D. A. Walker, and G. H. Sutton, Spectra of nuclear explosions, earthquakes, and noise from Wake Island bottom hydrophones, Geophys. Res. Lett., 10, 59-62, 1983.

Walker, D. A., Deep ocean seismology, EOS, 65, 2-3, 1984.

C. S. McCreery and D. A. Walker, Hawaii Institute of Geophysics, 2525 Correa Road, Honolulu, HI 96822

Ambient Infrasonic Ocean Noise and Wind

by

Charles S. McCreery

ABSTRACT

Analysis of one-year of ambient infrasonic acoustic noise data from four hydrophones of the Wake Island Array in the northwestern Pacific, two on the ocean bottom at 5.5-km depth and two in the SOFAR channel at 1-km depth, clearly shows a direct relationship between noise levels and windspeed. At least three different types of wind-related noise are apparent. Between about 0.4 and 6 Hz, on both of the bottom hydrophones and on one of the SOFAR hydrophones, noise increases with wind at rates up to 1 dB per mph until a well-defined saturation level is reached. The spectral slope of that saturation level, about -27 dB per octave and its position in frequency suggest that it is related to the saturation level of the ocean surface wind waves. The second type of noise, at frequencies between 4 and 30 Hz (and possibly higher), apparent on at least the two bottom hydrophones, also increases with wind speed at rates up to 1 dB per mph. However, this noise has a spectral slope which is markedly less steep than the noise below 4 Hz, and does not exhibit any saturation level but in fact overrides the previously mentioned saturation level between 4 and 6 Hz. The third type of noise dominates the SOFAR hydrophone which is anchored in the water along the slope descending from Wake Island. This noise also increases with wind speed at rates up to 1 dB per mph, however, absolute levels are significantly higher than on the other three hydrophones and no obvious saturation level is

observed. The source for this higher noise is presumably related to the interaction of wind-waves with Wake Island. The estimated absolute noise levels on the ocean bottom, and their demonstrated relationship to wind speed suggest that some of the world's best sites for the detection of short period seismic signals may yet be found on the deep ocean bottom in regions with low average wind conditions.

Introduction

Although studies of ambient acoustic noise levels in the ocean and
their relationship to wind and waves have primarily been the work of
acousticians and physical oceanographers, seismologists also have a special
interest these signals, especially in the infrasonic range (a summary of
previous work is found in Nichols, 1981). Much work has already been done
establishing relationships between ocean wind waves and long period
microseisms observed on continents (for example, Haubrich et al., 1963).
But much still needs to be learned about the characteristics of seismic
noise within the oceans themselves, especially with the ever-increasing need
for deployment of seismometers in the world's oceans. Most investigators
agree that there are too few data in the infrasonic frequency range.
Therefore, it is the goal of this report to present much of what we have
learned about these noise levels based upon a unique long-term set of
hydrophone data recently analyzed.

Data

Since September 1982, the Hawaii Institute of Geophysics (HIG) has
digitally recorded, on a continuous basis, signals from eight hydrophones in
an eleven element array located near Wake Island in the northwestern Pacific
Ocean. Six elements of the Wake Island Array (WIA) are located on the ocean
bottom (5.5-km depth) at the center and vertices of a 40-km pentagon, and
the other five are located at three sites in the SOFAR channel (1-km depth).
A general location map is given in Figure 1. The hydrophones themselves are

passive, moving-coil type and are cabled directly to Wake Island. Although originally designed to record signals at frequencies greater than 20 Hz, the hydrophones have proven to be quite sensitive to frequencies in the short period seismic band and have detected frequencies at least as low as 0.05 Hz from some larger earthquakes. Unfortunately, the size of the electrical signals in the seismic bands is very small and requires very low-noise preamps to detect. This problem makes itself apparent in our study and will be discussed further later on. After amplification, pre-whitening and anti-aliasing, signals from eight of the eleven elements are digitized multiplexed, and recorded on 9-track computer tapes which are shipped regularly to HIG. The digitization rate is 80 samples per second per channel with 16 bits of resolution per sample. Figure 2 shows the combined hydrophone-cable-amplifier-filter-digitizer response curve. The amplifier-filter-digitizer response was measured in situ. The hydrophone response is only an estimate extrapolated from a response curve at higher frequencies using knowledge of the hydrophone design (Thanos, 1966). Cable response is unknown and was assumed to be zero dB.

At HIG, three-minute ambient noise samples are extracted from the original tapes at an average rate of one per hour. The exact spacing between samples is made random to minimize the possibility of electrical signal contamination by unknown sources at Wake (such as RF) which might also be on an hourly schedule. Fiscal and temporal considerations prevented the analysis of every noise sample collected from every hydrophone for the entire time period (now greater than three years). Instead, a subset consisting of the 3-minute noise samples from two bottom hydrphones, 74 and 76, and two SOFAR hydrophones, 10 and 20, spaced approximately every six hours over the first year of operation at Wake has been studied.

Spectral Computation

The first major step in the analysis of these data was transformation from the time domain to the frequency domain. Each 3-minute time series was divided into 27 adjacent 512-point segments which were each demeaned, deskewed, Lancoz windowed (to approximately preserve absolute amplitudes), and then Fourier transformed with a 512-point FFT. Mean power spectral levels at each of the 256 frequencies were then computed from the 27 segments. The end result of this transformation was four data sets (one for each hydrophone), each consisting of 256 time series, 1460 samples long (i.e., 4 samples/day x 365 days), representing the ambient noise level fluctuations with time over one year in each frequency band. Only the first 192 of each 256 time series, representing 0 to 30 Hz, was actually used to avoid any possible contamination by aliasing near the 40 Hz Nyquist frequency.

Removal of Transients

An attempt was made to remove transients which were present in each of these time series. Sources for these transients are primarily earthquake phases, ships passing nearby, and signals from man-made underwater explosions. A transient was defined as any individual sample which had a power level at least 3 dB greater than both of its adjacent samples. Transients were replaced by the mean value of the two adjacent samples, Figure 3 shows the effects of this procedure on a sample time series. Most of the underlying character of the original time series remains. Figure 4

shows that at a maximum only about 10% of the data points of any time series were modified by this procedure.

Yearly Mean Noise Levels

Figure 5 shows yearly mean noise levels with associated standard deviations for each of the four hydrophones. The standard deviations should be interpreted with caution since the actual distribution of data points about the mean at any frequency is often highly non-Gaussian as will be illustrated later. The prominent peak at 20 Hz on the curves for hydrophones 74 and 76 is due to a large 60 Hz spike in the analog data which has been aliased. A rise in level at about 17 Hz on all curves is due to whales. Figure 6 shows differences between the four yearly means using hydrophone 74 as the reference at zero dB. The two bottom hydrophones, 74, and 76, have means which are nearly identical as might be expected due to their close proximity. Differences in these two curves at frequencies above about 10 Hz are probably due to differences in their respective cable responses. SOFAR hydrophone 20 is quieter than 74 below 0.7 Hz, and noisier above 0.7 Hz. Increased noise levels at the high frequencies are probably due to its location within the SOFAR waveguide. Low levels at long periods may be the result of its proximity to the oceans's free surface (e.g., 0.5 Hz has a wavelength of 3 km compared to hydrophone 20's depth of 1 km). SOFAR hydrophone 10 is noisier than 20 at all frequencies. This is presumably the result of its location on the slope of Wake Island and hence its proximity to an additional noise source. Figure 7 compares the yearly mean of hydrophones 74 and 20 to an assortment of other ambient ocean noise measurements compiled in _Principles of Underwater Sound_ (Urick, 1983). It

appears that both the Wake bottom and SOFAR hydrophone noise levels are in general higher below about 2 Hz and lower above about 4 Hz than the other noise level measurements. It is not known whether these differences imply actual differences in the ambient noise field near Wake or simply reflect uncertainties in our calibration.

Temporal Variations of the Noise and Wind Speed

In order to more easily view the information contained in the 192 time series associated with each hydrophone, the data were reduced into only 15 time series for each hydrophone, representing ambient noise level fluctuations in each contiguous 2-Hz band from 0 to 30 Hz. Computation of these new time series was made by summing the power of the original time series in each 2-Hz band of interest.

Figure 8 shows each of these series from hydrophone 74 for the entire year. It is clear than many features correlate across numerous frequency bands. It is also apparent that there are significant differences in the general character of these time series. For example, the 2-4 Hz time series appears flat-topped, and exhibits noise holes which are as much as 15 dB below the apparent noise ceiling. Similar features in the ambient noise data from a long-term deployment of HIG's Ocean Sub-bottom Seismometer down a deep-sea drill hole near the Kuril Islands has also been reported by Duennebier et al. (1986). The time series for frequencies above 6 Hz, on the other hand, appear flat-bottomed and exhibit noise peaks which may be 20 dB or more above the apparent noise floor. The 4-6 Hz time series seems to be a transition between the 2-4 and 6-8 Hz bands, and is flat-middled with some holes and some peaks. Only the 0-2 Hz curve appears to have a full and

continuous dynamic range. A few signals with maximum signal-to-noise around 17 Hz are due to whales.

Figure 9 shows 100 days of ambient noise in 6 of the 15 2-Hz bands for all hydrophones studied. Note that the bottom hydrophones, which are only about 40 km apart, have a high degree of correlation at all frequencies. Correlation between the bottom hydrophones and the SOFAR hydrophones, however, is not nearly as strong, although some features do appear coherent, especially in the 0-2 Hz range where absolute noise levels are similar. Above 2 Hz, the SOFAR hydrophones become increasingly noisy with respect to the bottom hydrophones, and also become decreasingly coherent. Correlation between the two SOFAR hydrophones is also weak at the higher frequencies where hydrophone 10 is consistently noisier than hydrophone 20.

Figure 10 compares the ambient noise data from hydrophone 74 in 6 2-Hz bands with the daily mean wind speed measurements made at Wake Island by the National Weather Service and published in their "Local Climatological Data" monthly summaries. At 0-2 Hz, the two data sets are remarkably similar. At 2-4 Hz and 4-6 Hz, noise holes nearly always correspond with low wind, and above 6 Hz the noise peaks nearly always correspond with high wind. From these data, there can be no question that wind speed plays an important role either directly or indirectly in the generation of infrasonic ambient ocean noise.

Nonlinear Wave-Wave Interaction

The most widely accepted theory regarding the generation of infrasonic ocean noise and closely related microseism levels, is that of non-linear wave-wave interaction of the ocean wind-waves, discovered by Miche (1944)

and developed by Longuet-Higgins (1950) and many others. In a recent paper,
Kibblewhite and Ewans (1985) report the observance of significantly
increased microseism levels at the time of shifts in wind direction in even
a moderate wind field due to this wave-wave interaction. To look for these
effects, wind direction at Wake has also been plotted in Figure 10.
However, it does not appear that our data reflect this effect since there
are many shifts in wind direction which are unaccompanied by increased noise
levels.

<div align="center">Noise Spectra Versus Wind Speed</div>

Figure 11 shows mean noise spectra for eight wind speed ranges from
each of the four hydrophones studied. (Refer to Figure 12, which shows the
distribution of mean daily wind speeds at Wake, to determine the number of
observations at each wind speed range.) The spectra have been rotated
counterclockwise about 1 Hz by 18 dB per octave in order to visually clarify
the differences between them (which remain the same). These spectra present
a remarkably clear picture showing the effects of wind speed on ambient
infrasonic ocean noise levels.

Sets of spectra from the two bottom hydrophones are nearly identical.
Between about 0.4 and 5 Hz, noise levels increase regularly with wind speed
at rates up to 1 dB per mph until a saturation level is reached. This
saturation level is clearly apparent between about 1.5 and 6 Hz and has a
slope of about -27 dB per octave (-9 dB per octave on the plot). It should
be noted that this saturation level is not instrumental, since higher noise
levels were actually observed in the transients, previously discussed, which
were removed from these data. Between about 0.3 and 0.8 Hz, noise levels

rise up from a minimum level with a slope of about -33 dB per octave (-15 dB per octave on the plot). Between about 6 and 30 Hz, there is a noise level minimum which corresponds to an estimate of the equivalent hydrophone, cable, amplifier, and recording system noise, also shown on the plot. When wind speed exceeds about 16 mph noise levels rise out of this basement at rates up to 0.8 dB per mph. Between 4 and 6 Hz these increasing levels actually rise above the saturation level mentioned earlier. All of these observations are consistent with the time series data discussed earlier which were flat-topped between 2 and 4 Hz, flat-middled between 4 and 6 Hz, and flat-bottomed greater than 6 Hz.

Thus it would appear from these data that at least two distinct wind-related noise generating mechanisms are at work on the ocean bottom in this frequency range. The first, from roughly 0.4 to 6 Hz is characterized by noise levels that increase with wind speed to a sharply defined saturation level. The second, above 4 Hz, which is also characterized by noise levels that increase with wind, at least above 16 mph, produces a markedly different spectral slope. At the wind range of 28-32 mph, for instance, this change in slope, which occurs at about 4 Hz, has a magnitude of around 24 dB per octave. Additionally, the second mechanism actually appears to overide the saturation level of the first mechanism between 4 and 6 Hz.

The noise spectra of SOFAR hydrophone 20 resembles, in many respects, those of the bottom hydrophones. Noise levels regularly increase with wind speed between 0.4 and 4 Hz at rates up to 1 dB per mph. A noise saturation level is clearly visible between about 1.5 and 4 Hz with a slope of about - 25 dB per octave. Above 4 Hz there is again a sharp difference in spectral slope, however, the magnitude of increases in noise level with wind speed is less than 0.2 dB per mph. Instrumental noise does not seem to be a factor

in these spectra due to generally increased absolute levels at the higher frequencies in the SOFAR channel.

Hydrophone 10 has spectra which are also clearly wind related. At virtually all the frequencies shown, from 0.1 to 30 Hz, noise increases with increasing wind speed at rates up to 1 dB per mph. However, there is no saturation level apparent in these spectra, nor is there such an abrupt change in spectral slope at around 4 Hz, but only a more gradual change between about 1 and 10 Hz. In addition, as noted previously, absolute noise levels are generally higher than the other three hydrophones. These differences are probably the result of hydrophone 10's proximity to Wake, and hence its proximity to noise generated by interaction of wind waves with the island itself.

Figure 12 shows the distribution of daily mean wind speeds at Wake for the year studied. The yearly mean wind speed in 14.0 mph. It is easy to see that each of the spectra shown in the previous figure do not represent an equal amount of dat. For example, there are only 3 days with wind speeds between 12 and 16 mph. In spite of this fact, it is interesting to note that the 28 to 32 mph spectrum is clearly noisier than the lower wind speed spectra on all of the hydrophones. This would seem to indicate that there is not a large amount of scatter in these data.

Figure 13 shows the actual level of this scatter. It is a plot of the 1460 individual noise measurements, as a function of wind speed, at 3 discrete frequencies (of the 256 out of the FFT) from hydrophone 74. At 1.6 Hz there is the most dynamic range although the saturation level is clearly visible. Scatter varies from about 20 dB at the lower windspeeds to less than 5 dB at the higher wind speeds. At 2.5 Hz the saturation level is dominant over a wider wind speed range, as can be seen in the spectra of

figure 11. Scatter is similar to that observed at 1.6 Hz. At 10 Hz, the instrumental noise level dominates at the lower wind speeds. Scatter is generally less than 10 dB throughout the plot. Refering back to figure 5, which shows the yearly mean noise levels, it is clear from these data that their distribution is non-Gaussian and therefore the standard deviations shown in figure 5 must be interpreted with caution.

Interpretation of the Saturation Level

Duennebier et al. (1986) has proposed that the saturation level observed in downhole seismic noise is related to saturation of the ocean wind waves. Figure 14 shows the observed saturation level of wind wave heights as a function of frequency from Phillips (1977). It is well established that these waves generate microseisms (and probably acoustic energy) at twice the frequency of the wind waves (Haubrich et al., 1963). Saturation of the wind waves between 0.2 and 3 Hz might translate then to a saturation in acoustic energy between 0.4 and 6 Hz. Furthermore, if the acoustic amplitudes are proportional to the square of the wind-wave amplitudes (as they are in non-linear wave-wave interactions) then the slope of the ambient noise saturation level should be twice that of the wind wave saturation level. This is almost precisely the case since the wind-wave slope is around -15 dB per octave and the ambient noise slope averages around -26 dB per octave in our data. These facts lead us to conclude that the saturation level observed in the ambient noise data between about 1.5 and 6 Hz is probably a manifestation of the saturation level of the wind waves on the ocean's surface.

Potential Low Noise Sites for Seismic Detection

One implication of this study is that when planning the placement of seismic sensors in the oceanic environment it is probably worthwhile to look for low-wind sites. Near 1 Hz, the frequency of teleseismic P, these data show that noise levels can vary by at least 20 dB with wind speed. During low wind at Wake the detectability of P may therefore be enhanced by one magnitude or more relative to high wind conditions. Figure 15 shows potential low-noise sites around the world based strictly on mean scalar wind speed data. Other factors such as shipping, currents, bathymetry and nearby coastlines may also contribute to the noise level. Considering that noise levels on the ocean bottom near Wake are comparable with levels at quiet continental sites at frequencies above 3 Hz (McCreery et al., 1983); that only a minuscule percentage of the ocean has yet been sampled in terms of ambient infrasonic noise; and that this noise is clearly wind related, it may be that some of the world's best sites for the detection of seismic signals are yet to be found in low-wind regions of the world's oceans.

Acknowledgments

Reference

Duennebier, F. K., R. K. Cessaro, and P. Anderson (1986). Geo-acoustic noise levels in a deep ocean borehole, _Ocean Seismo-Acoustics; Low-Frequency Under Water Acoustics_, Plenum Publishing Corporation, New York, New York, (in press).

Haubrich, R. A., W. H. Munk, and F. E. Snodgrass (1963). Comparative spectra of microseisms and swell, _Bull. Seism. Soc. Am._, 53, 27-37.

Kibblewhite, A. C. and K. C. Ewans (1985). Wave-wave interactions, microseisms, infrasonic ambient noise in the oceans, Appl. Res. Labs., Univ. Texas, Austin TX, Pp. 87 (technical report).

Longuet-Higgins, M. S. (1950). A theory of the origin of microseisms, _Philos. Trans. R. Soc. London A243_, 1-35.

McCreery, C. S., D. A. Walker, and G. H. Sutton (1983). Spectra of nuclear explosions, earthquakes, and noise from Wake Island bottom hydrophones, _Geophys. Res. Lett._, 10, 59-62.

Miche, M. (1944). Mouvements ondulatoires de la mer en profondeur constante on decroissante, _Ann. Ponts Chaussees_, 114, 25-87.

Nichols, R. H. (1981). Infrasonic ambient ocean noise measurements: Eleuthera, _J. Acoust. Soc. Am._, 69, 974-981.

Phillips, O. M. (1977). _The Dynamics of the Upper Ocean_, Cambridge University Press, Cambridge, England, p. 336.

Thanos, S. N. (1966). _OBS Calibration Manual_, Lamont Geological Observatory, Columbia, New York.

Urick, R. J. (1983). _Principles of Underwater Sound_, McGraw-Hill Book Company, New York, p. 423.

FIGURE CAPTIONS

Fig. 1. Map showing the position of Wake Island in the northwestern Pacific Ocean, and the relative position of hydrophones in the Wake Island Array. Hydrophones 71-76 are on the ocean bottom at about 5.5-km depth, while hydrophones 10, 11, 20, 21, and 40 are in the SOFAR channel at about 0.8-km depth.

Fig. 2. Estimated response curve for the hydrophones and recording system of the Wake Island Array.

Fig. 3. An example time series of ambient noise fluctuations before (upper) and after (lower) the removal of transient signals.

Fig. 4. The percent number of transients removed from the hydrophone 74 noise data as a function of frequency.

Fig. 5. Yearly mean ambient noise plus and minus one standard deviation.

Fig. 6. Differences between the yearly noise means of hydrophones 76, 10, and 20 relative to the yearly noise mean of hydrophone 74 (zero dB).

Fig. 7. A comparison between some ambient infrasonic noise levels compiled in Principles of Underwater Sound (Urick, 1983) and the yearly mean noise level of Wake hydrophone 74.

Fig. 8. A one-year plot of the temporal variation in ambient noise for 15, 2-Hz bands from Wake bottom hydrophone 74.

Fig. 9. Comparison in six frequency bands between temporal noise level fluctuations of the four hydrophones studied.

Fig. 10. Comparison between the temporal characteristics of the ambient ocean noise on hydrophone 74 in 6 frequency bands (think lines), and the daily mean wind speed at Wake Island (thin lines). Also plotted (top) is the mean daily wind direction.

Fig. 11. Noise spectra from each hydrophone averaged into 8 wind speed groups. Also shown are estimated spectra of the instrumental noise (dashed lines).

Fig. 12. The distribution of daily mean wind speed at Wake Island for the one-year period from 8 September 82 to 8 September 83. The yearly mean wind speed for these data is 14.0 mph (6.3 m/s).

Fig. 13. Each of the 1460 noise level measurements at 3 discrete frequencies from hydrophone 74 plotted as a function of wind speed to show the level of scatter in the data.

Fig. 14. The saturation level of ocean wind-generated waves from The Dynamics of the Upper Ocean by O. M. Phillips (1977).

Fig. 15. World map showing the mean wind speed over the oceans based on 80 years of data. (Map provided through the courtesy of the University of

Hawaii, Department of Meterology.)

Fig. 1
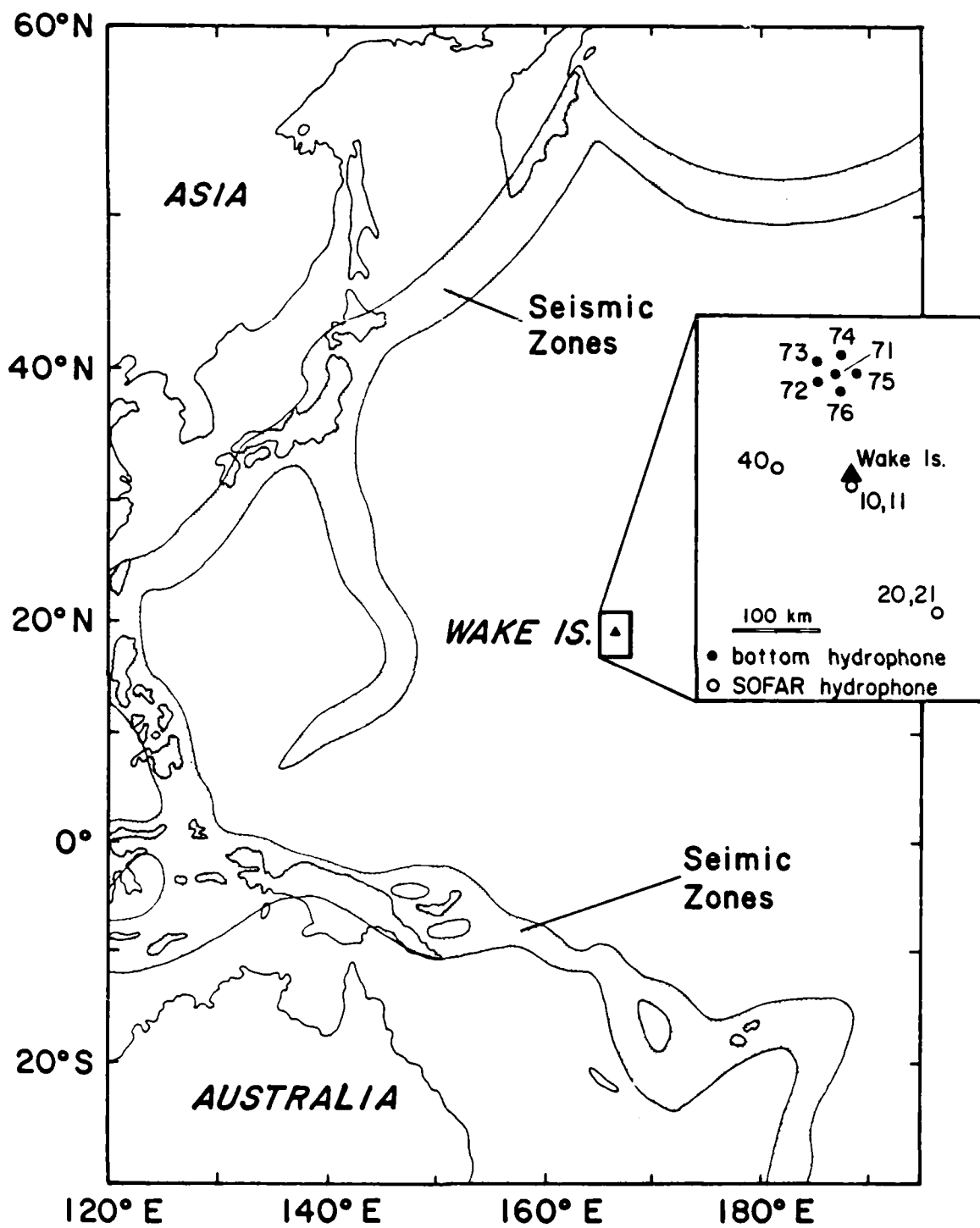
Fig. 2

Fig. 3

Fig. 4

Fig. 5

Fig. 6

Fig. 7

WAKE PHONE 74

Talpey and Worley
15.5 kn, site 1

Talpey and Worley
5.1 kn, site 2

Nichols
7-16 kn
(ss 3-4)

Perrone
38-24 kn

Perrone
8-12 kn

McGrath

Spectrum level, dB re 1 μPa /$\sqrt{Hz}$

Frequency, Hz
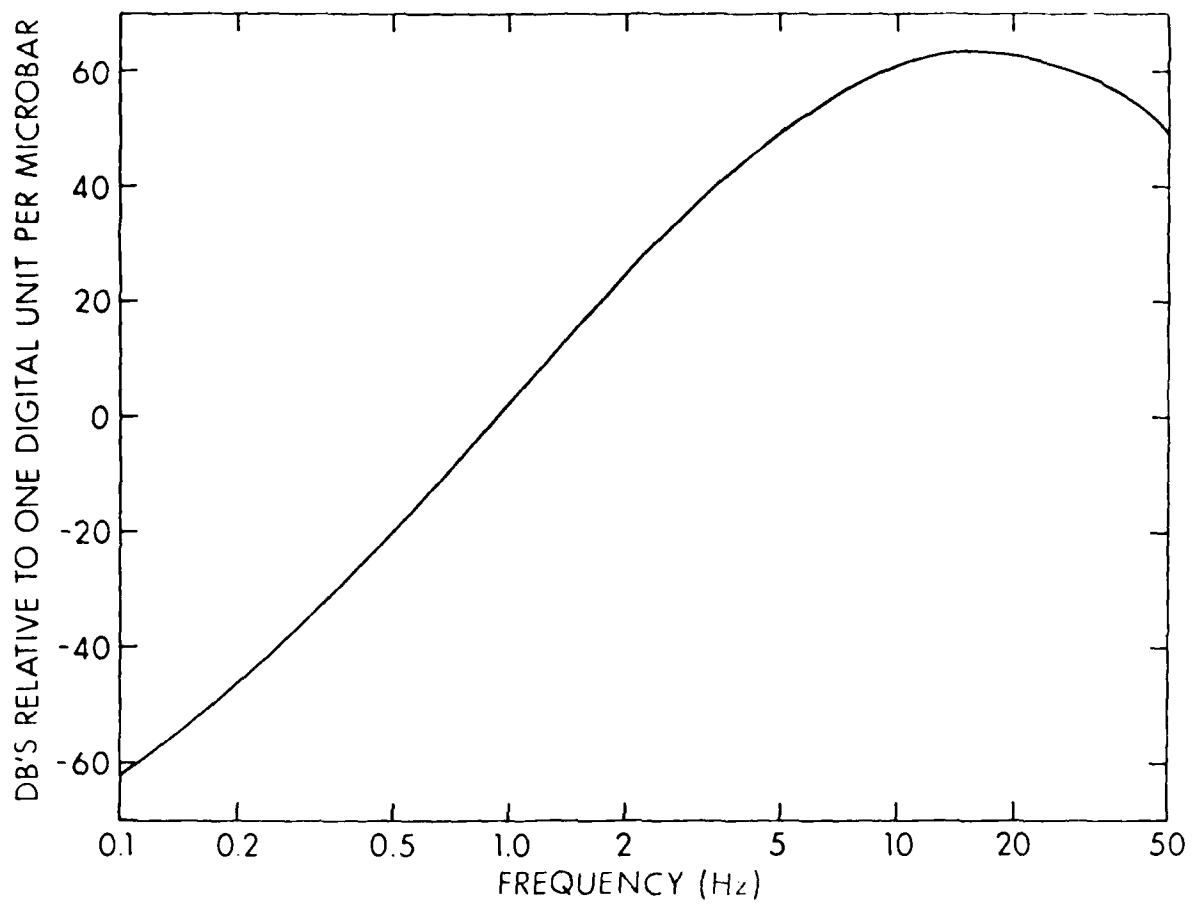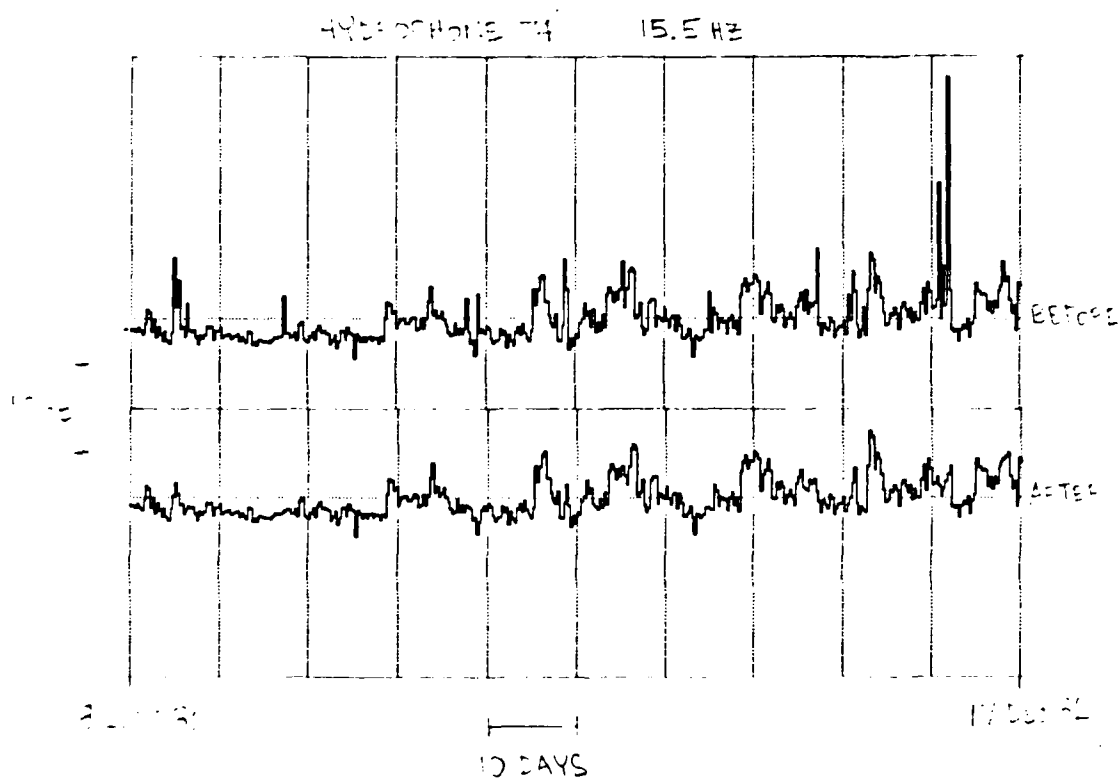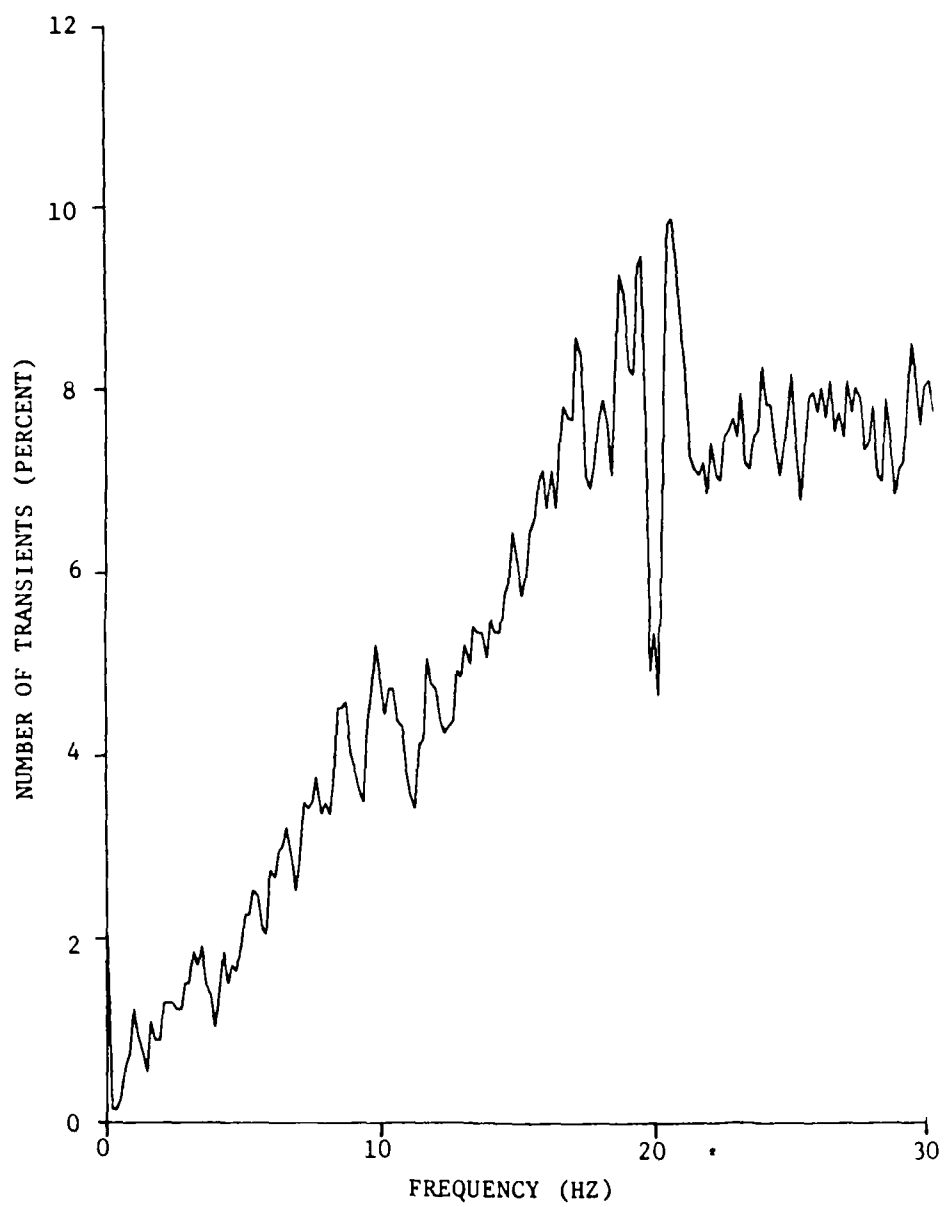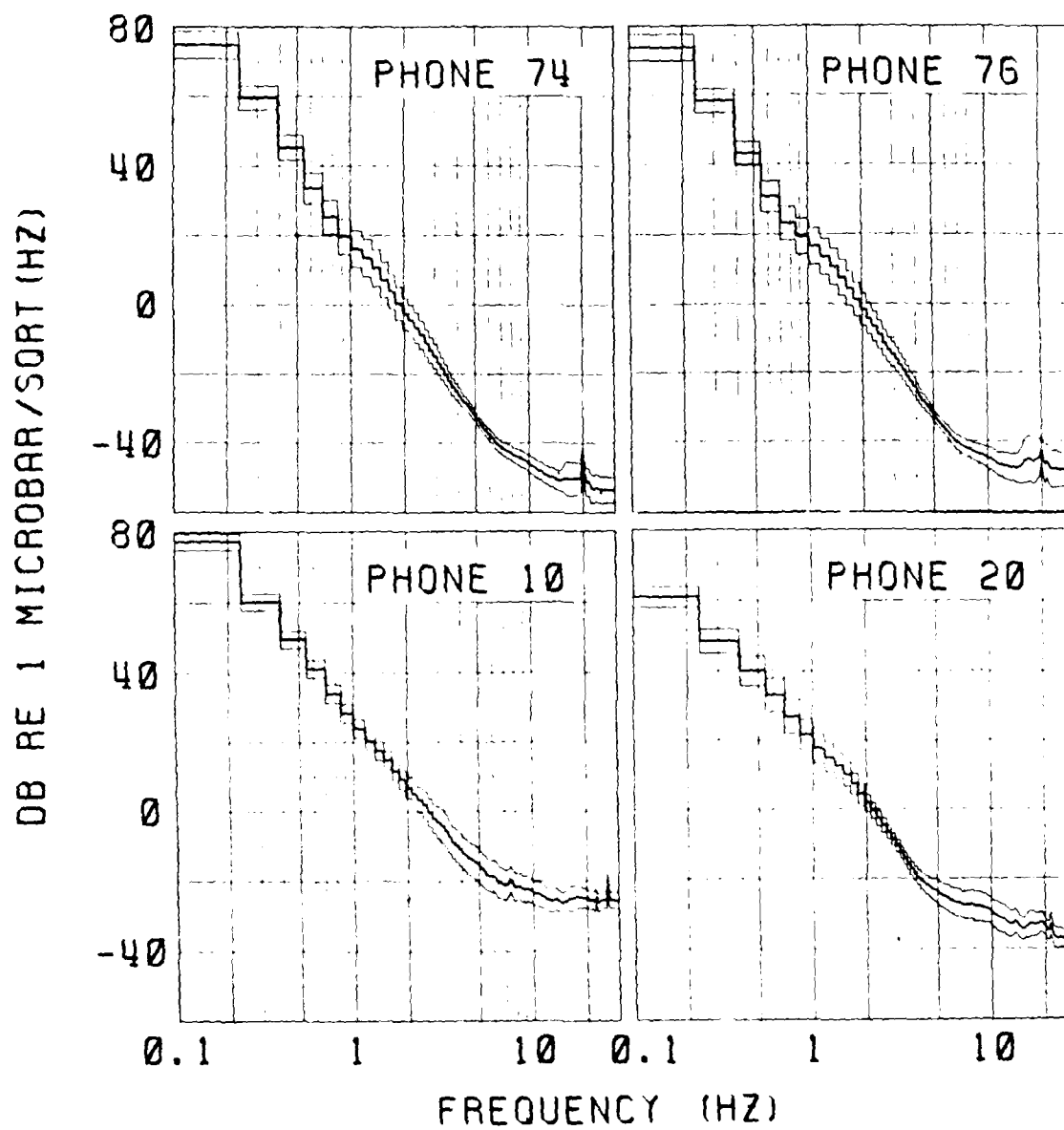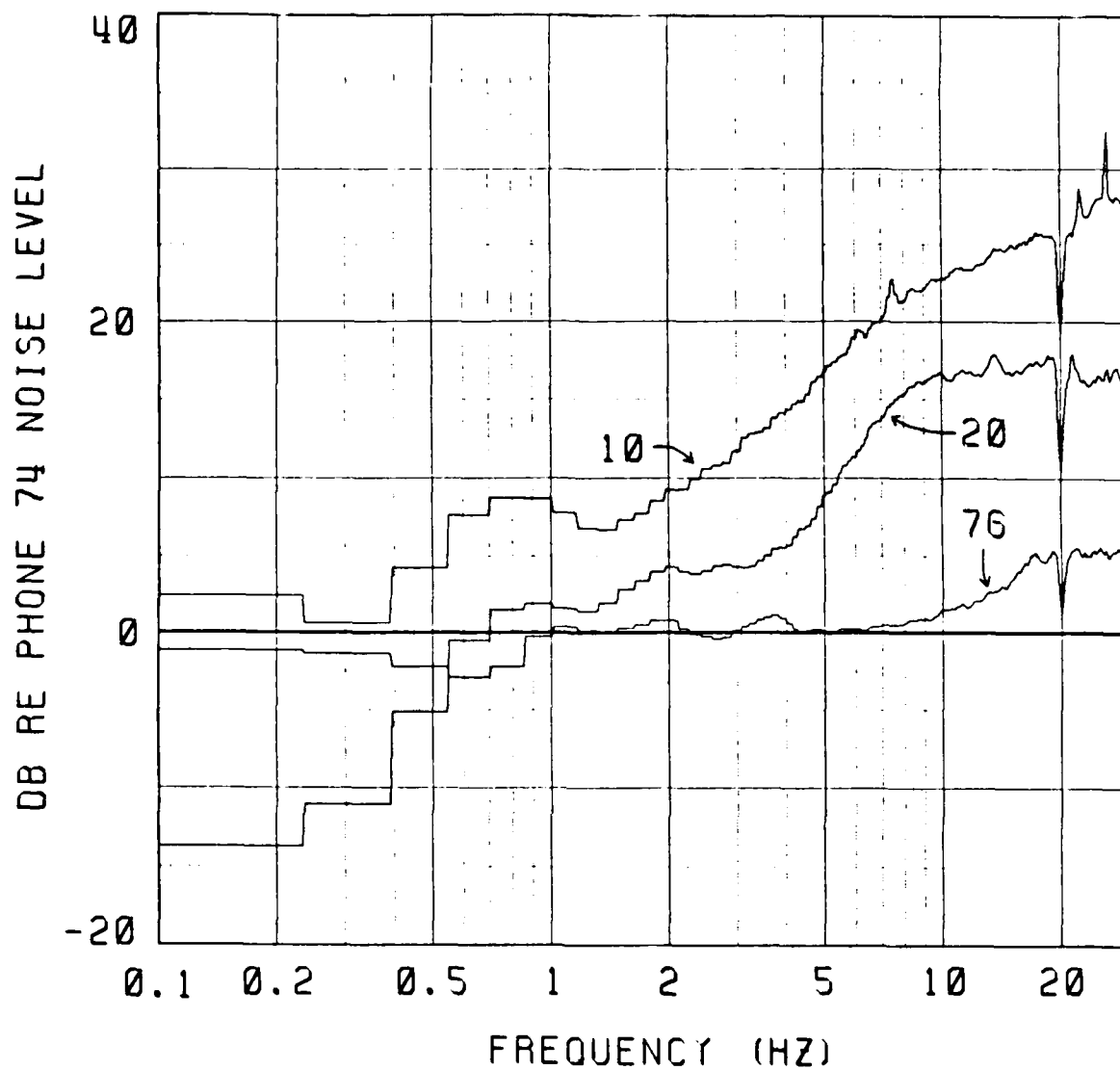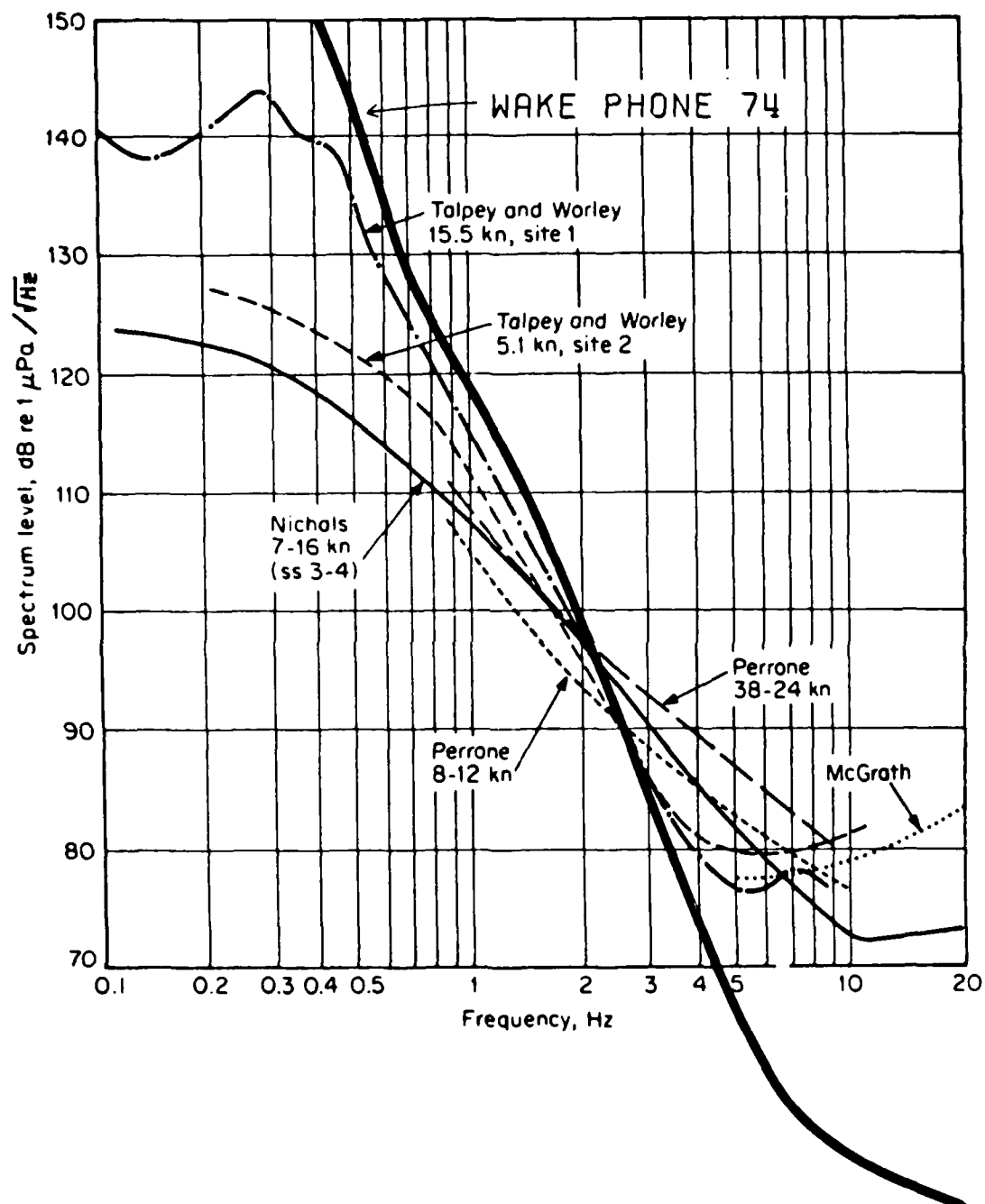
Fig. 8
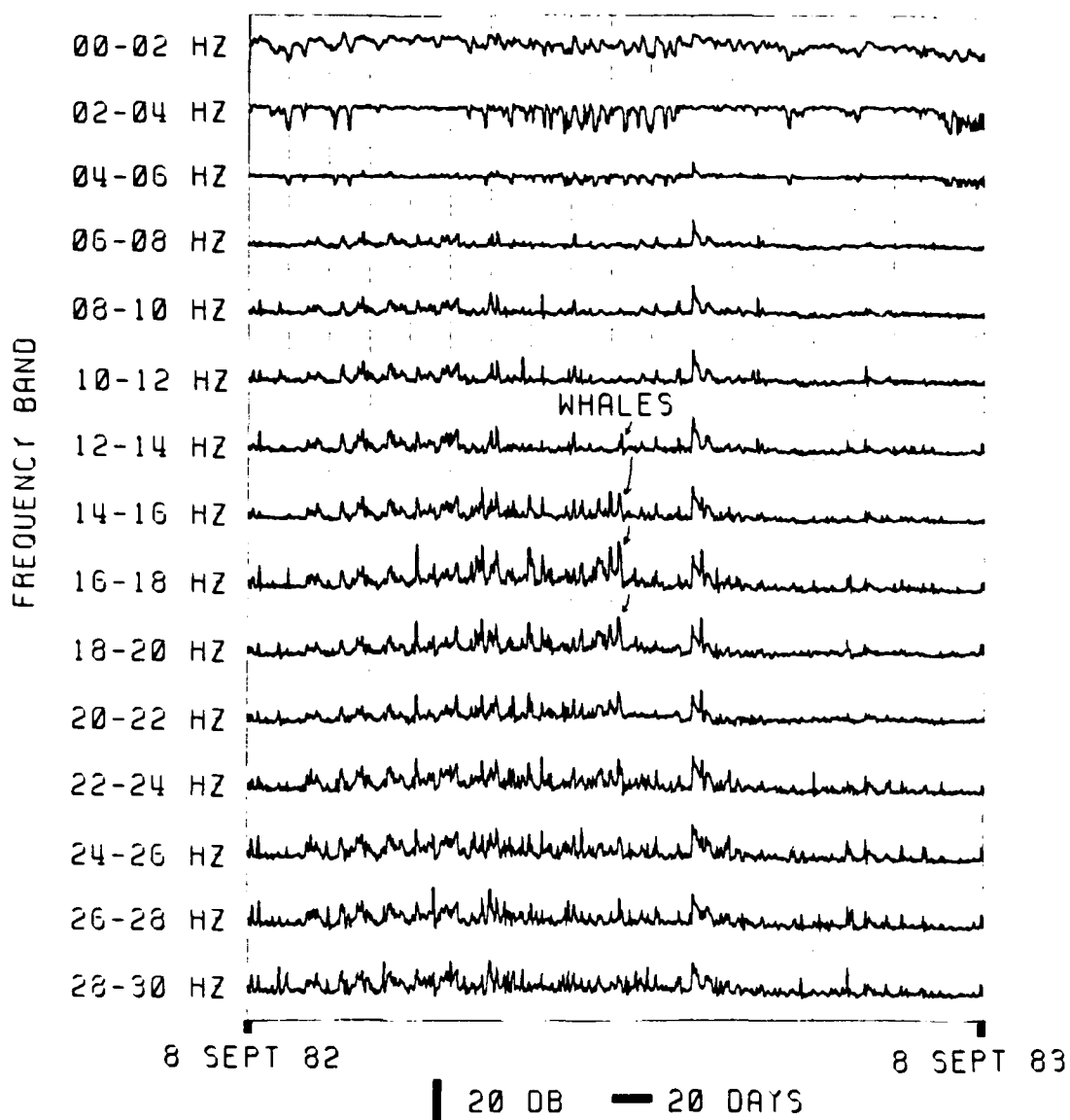
Fig. 9
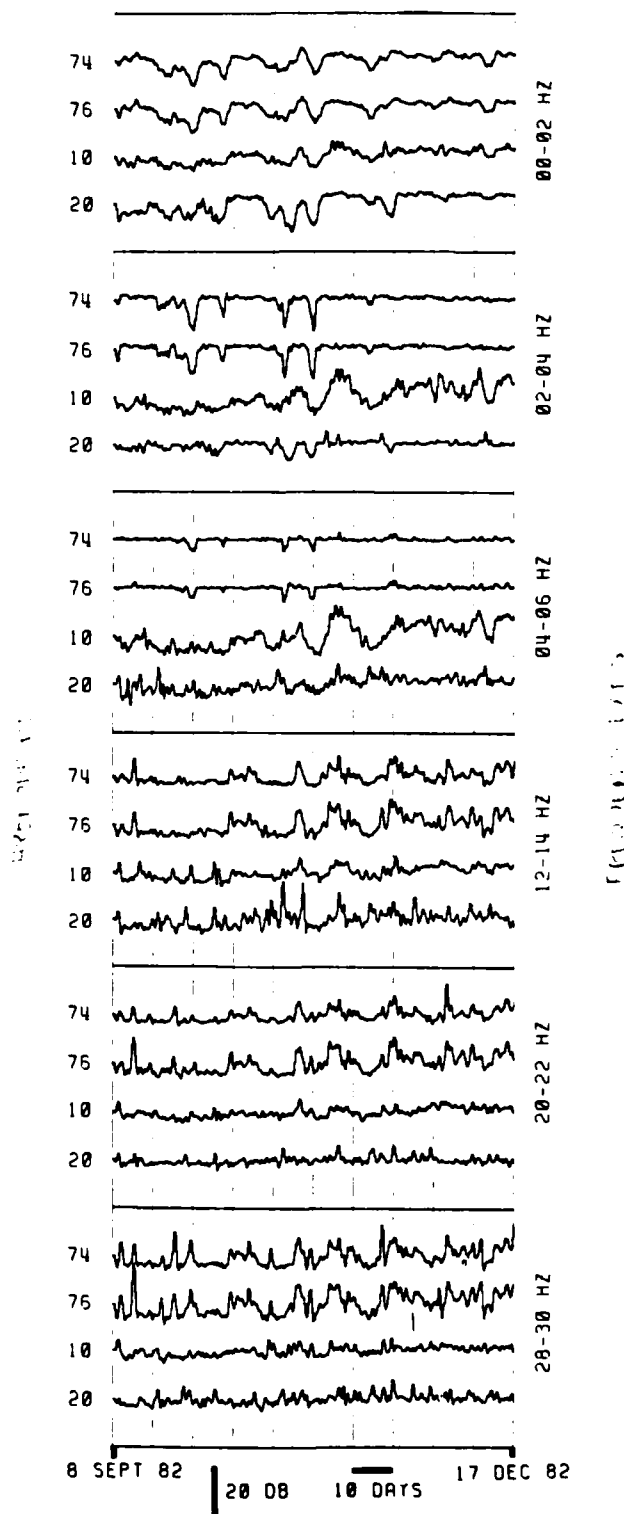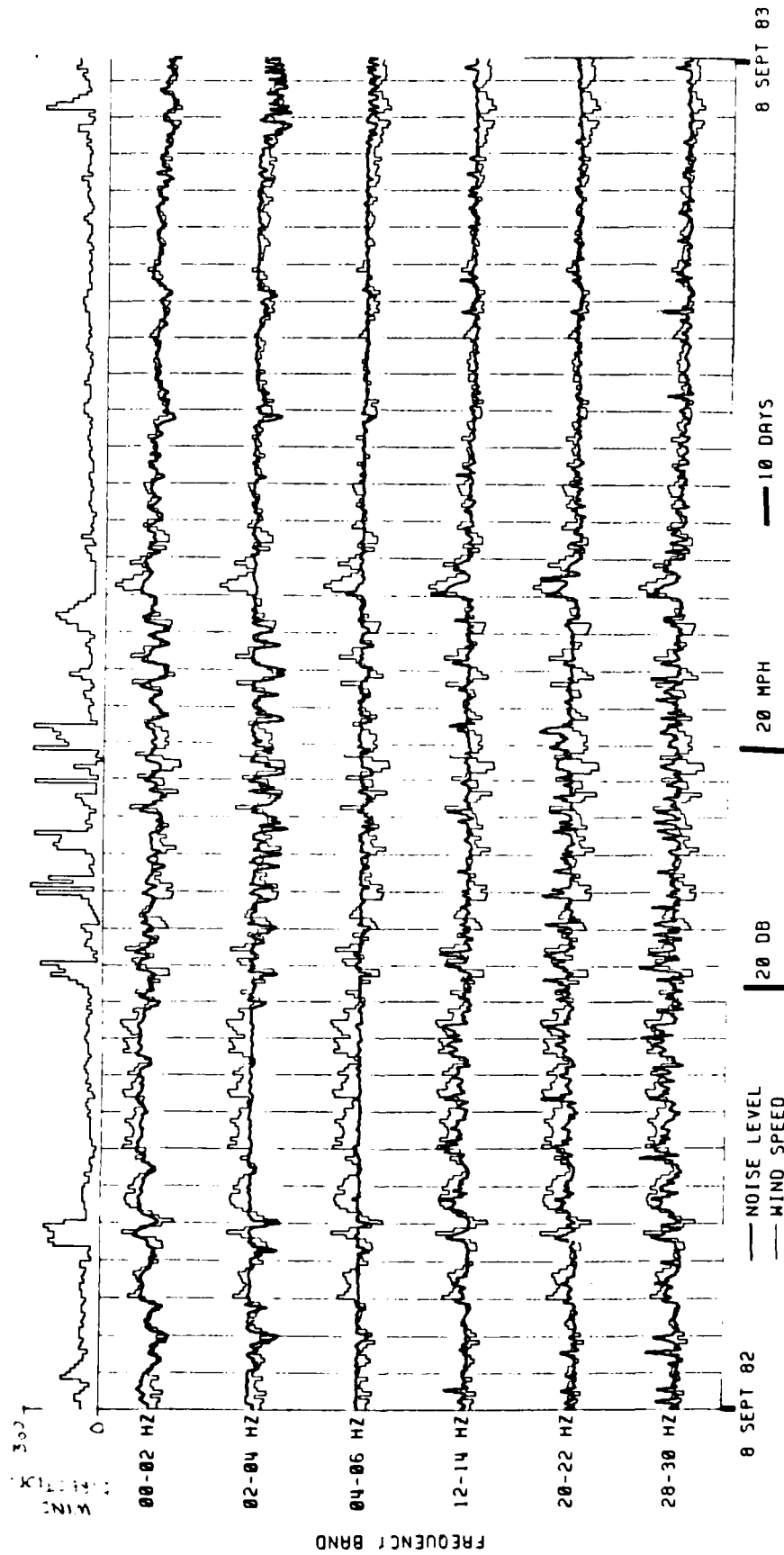
Fig. 10

Fig. 11
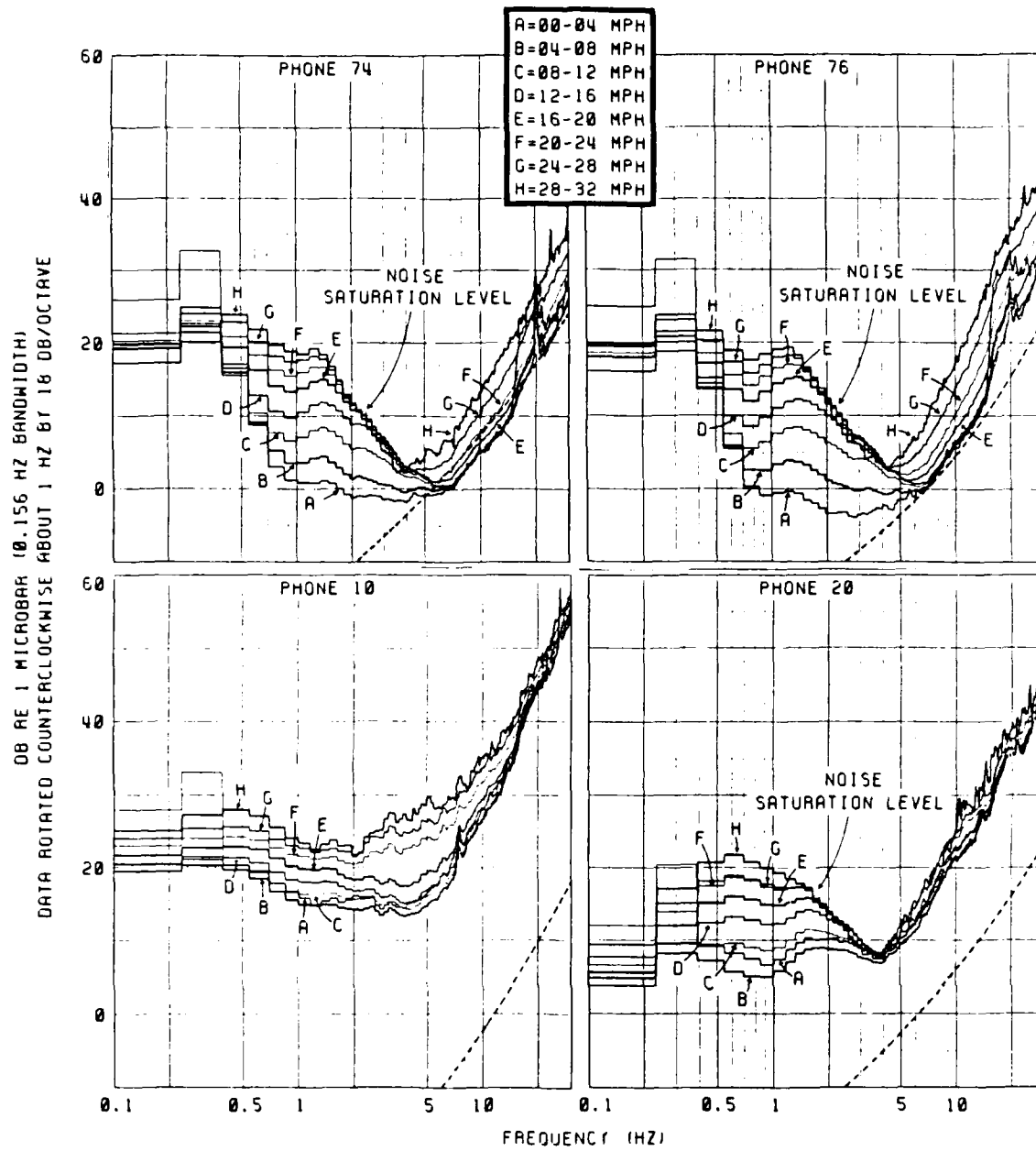
Fig. 12
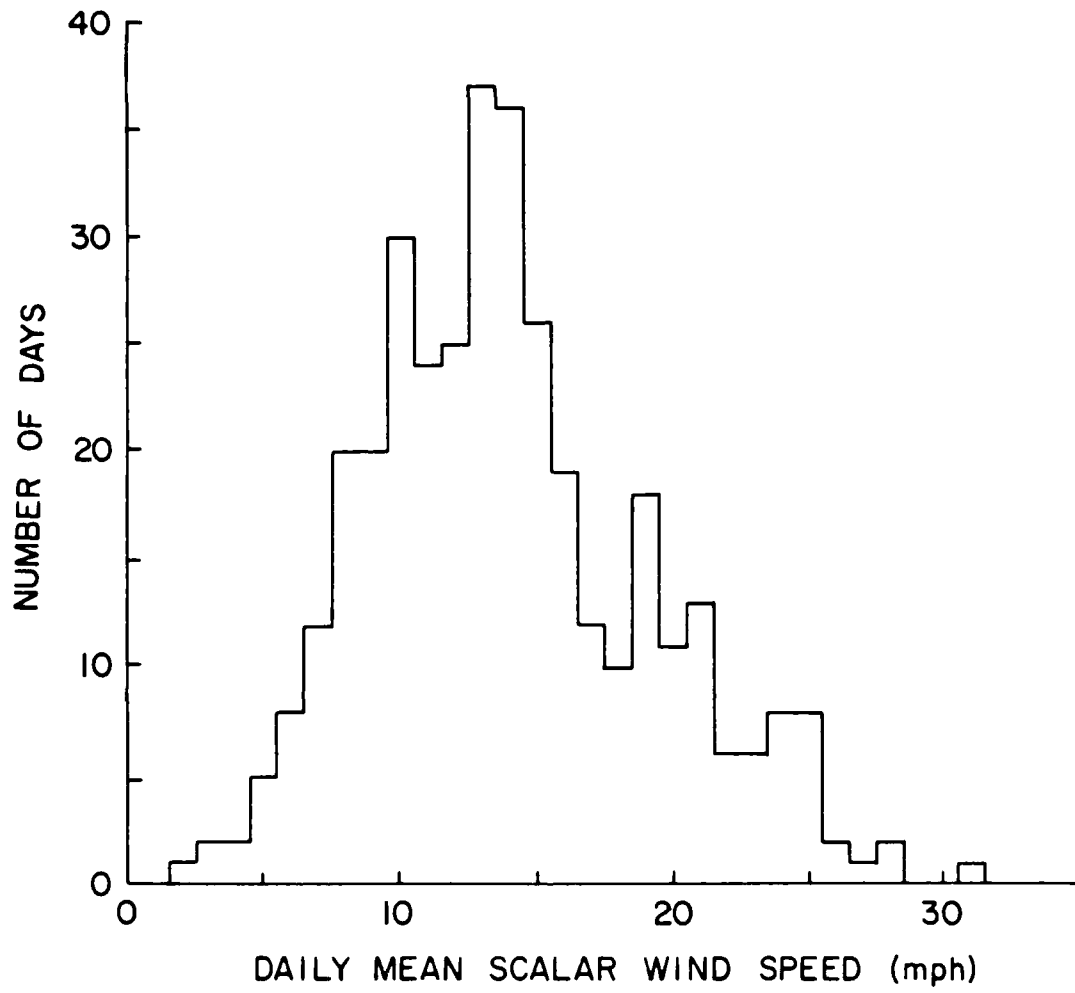
Fig. 13
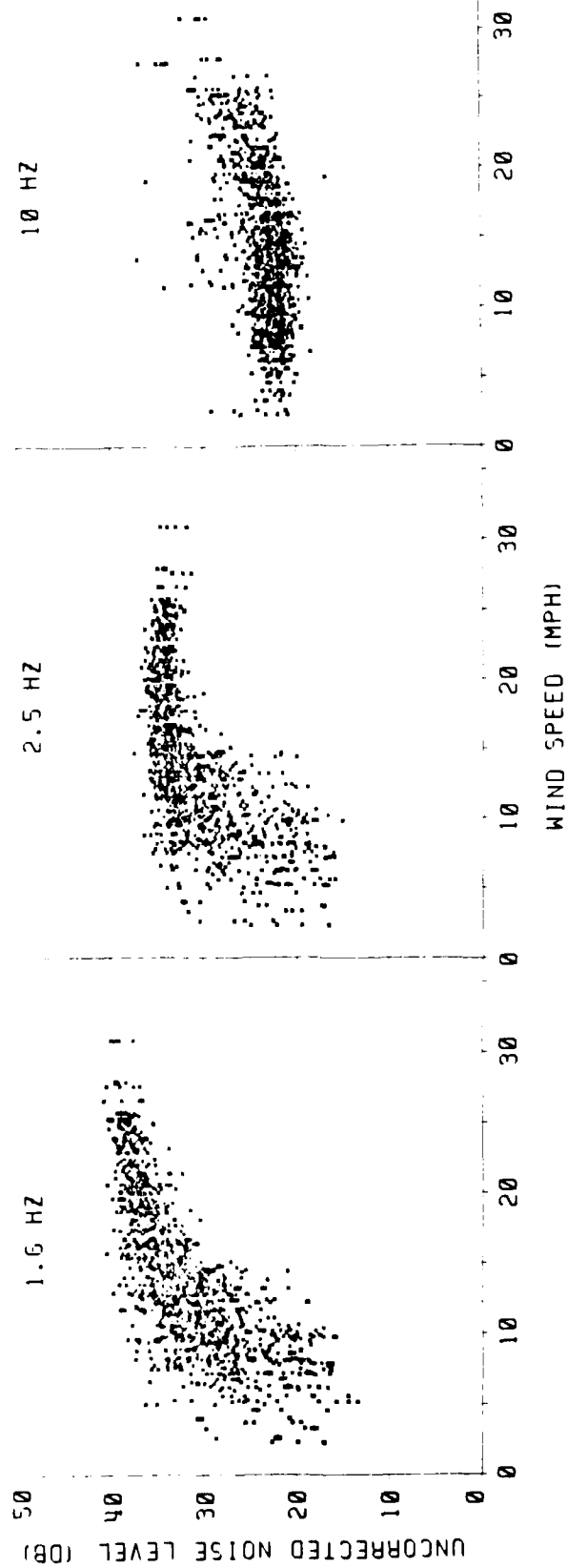
Fig. 14
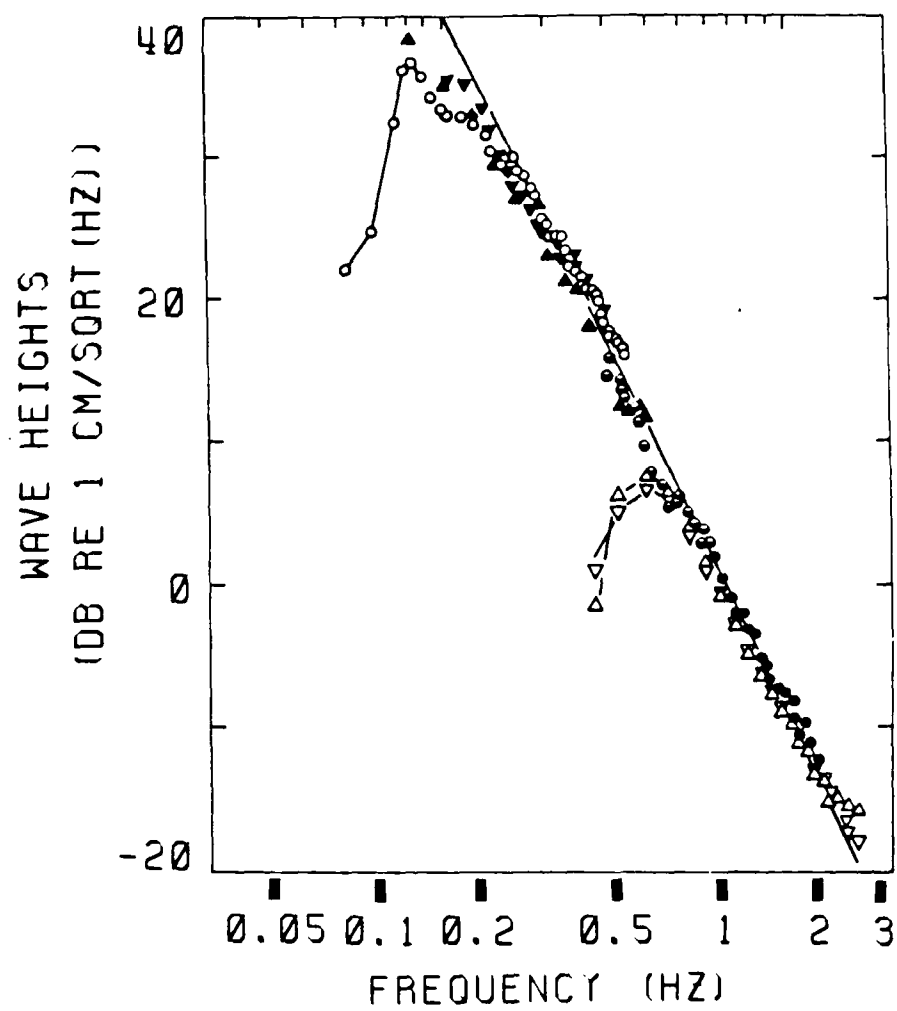
Fig. 15
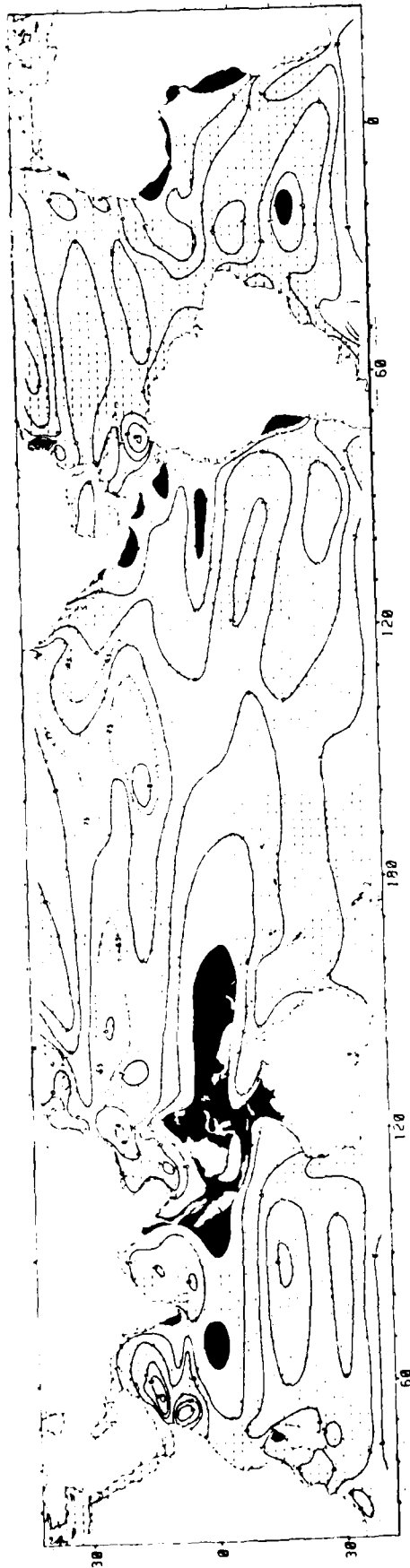
The Oceanography Report

Editor: Arnold L. Gordon, Lamont-Doherty Geological Observatory, Palisades, NY 10964 (telephone 914-359-2900, ext 325)

Deep Ocean Seismology

Daniel A. Walker

Recent measurements of seismic noise on the ocean bottom have revealed surprisingly low levels at frequencies greater than 3 Hz (Figure 1). In some instances values for frequencies of 3 to 15 Hz are comparable to, or lower than, values from the best continental seismic stations. This would be of little significance if, as is generally observed with most continental instruments, the only phases to have such frequencies were the result of local earthquakes. Actual observations, however, indicate that two classes of teleseismic (distant) phases have substantial signal-to-noise (S/N) ratios at high frequencies when observed in the low noise environment of the deep oceans.

The first class consists of Po/So (i.e., ocean P/ocean S) phases from earthquakes occurring under oceans or along ocean margins. First arriving Po/So phases travel with fairly constant apparent velocities of about 8.0 and 4.6 km s⁻¹, respectively, while peak arrivals have velocities about (7.6 and 4.5 km s⁻¹) comparable to basal crustal rates (Figure 2). At distances of about 18° (approximately 2000 km), highest observed frequencies of Po and So are greater than 20 Hz (actually as high as 30 and 35 Hz, respectively) and, at distances of about 30°, as high as 15 and 20 Hz, respectively (Figure 3). The S/N ratios for Po/So phases are generally at least 10 times greater than the ratios of their respective normal, mantle-refracted P and S phases; and in many instances no P's or S's can be found in spite of the presence of very strong Po's and So's (Figures 2 and 3).

Po/So phases have thus far been observed extensively in the North Atlantic, the North and Central Pacific, and across the Gulf of Mexico. Other observations have been made across portions of the Cocos plate, the Philippine Sea, and the Fiji-Tonga region. References for most of these studies may be found in *Molnar and Oliver* [1969] and/or *Walker* [1977]; others are *McCreery* [1981], *Talandier and Bouchon* [1979], *Ouchi* [1981], *Ouchi et al.* [1981], and *Bibee* [1983]. The second class of teleseismic phases having substantial amounts of high-frequency energy when observed in the low noise environment of the deep oceans consists of normal, mantle-refracted P phases from earthquakes and underground nuclear explosions at great distances. For these phases frequencies of 6 Hz (and up to 9 Hz) have been observed at distances greater than 60° (Table 1 and Figure 4).

These observations have significance in terms of applied, as well as basic research. Obviously, aside from the SOFAR channel of the world's oceans, the Po/So waveguide would appear to be the earth's most efficient acoustical waveguide. Thus far, however, no comprehensive explanation has been given for Po/So frequencies as high as 30 Hz at distances in excess of 2000 km, or for So phases often having more energy at high frequencies and great distances than Po. Such an explanation would contribute to our understanding of the crust and uppermost mantle under the world's oceans and marginal seas and eventually provide a basis for large-scale mapping of those regions.

The broad frequency content of ocean bottom recordings of these two classes of teleseismic phases (i.e., normal, mantle-refracted P phases recorded at great distances and Po/So phases) would also be useful in studies of the frequency dependence of Q, with concomitant advances in understanding the earth's deep mantle, as well as the crust and upper mantle under the world's oceans and marginal seas. S/N ratios for Po/So phases at their dominant frequencies (about 4 to 8 Hz) are generally from 5 to 10 times greater than
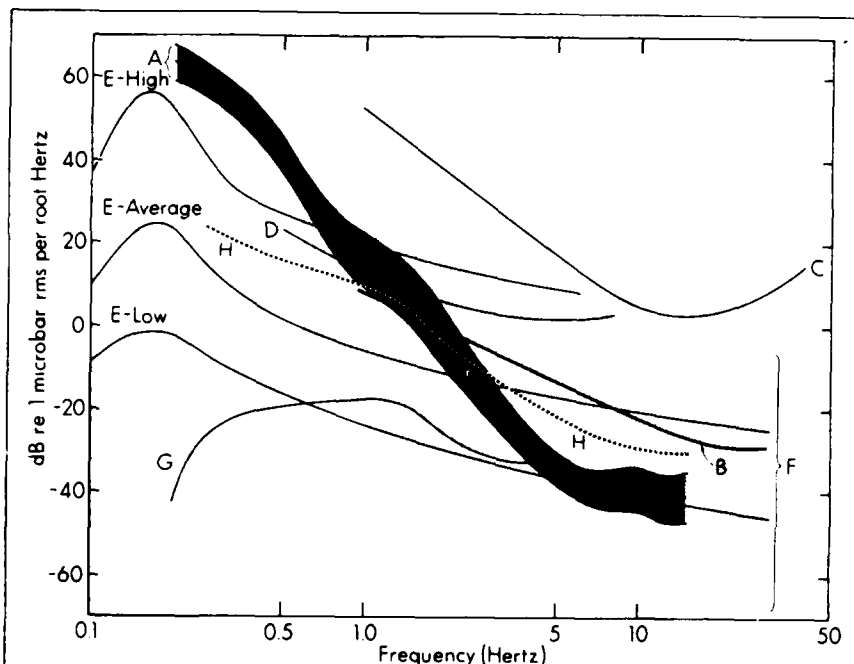
Fig. 1. The average spectrum ± 1 standard deviation of 52 samples of background noise over 18 months from hydrophones located near Wake Island is labeled A. Also shown are some published noise curves for both ocean bottom (B, C, D, and H) and continental (E, F, and G) environments, which have been converted from an assortment of units to the scale shown. B is a hypothetical "sample spectrum of deep-sea noise" [*Urick*, 1975, p. 188]. C is a vertical seismometer measurement made in the Mariana basin [*Asada and Shimamura*, 1976]. D is a vertical seismometer measurement made at 4.6-km depth between Hawaii and California [*Bradner and Dodds*, 1964]. H is a noise curve for a hydrophone bottomed off Eleuthera Island at 1200-m depth [*Nichols*, 1981]. E represents low, average, and high noise levels estimated from curves compiled by *Brune and Oliver* [1959]. F is an area bounded by the limits of noise curves measured in vertical seismometers for 16 locations within the United States and Germany [*Frantti et al.*, 1962]. G is the noise curve for the Over subarray of the Norwegian seismic array measured during a period "when most of the North Atlantic Ocean was very quiet" [*Bungum et al.*, 1971]. Some of the noise on the Wake hydrophones at frequencies of more than 3 Hz may be system generated; thus actual levels of background noise may be lower than indicated estimates. This figure, as well as Figures 4 and 5, have been taken from *McCreery et al.* [1983].
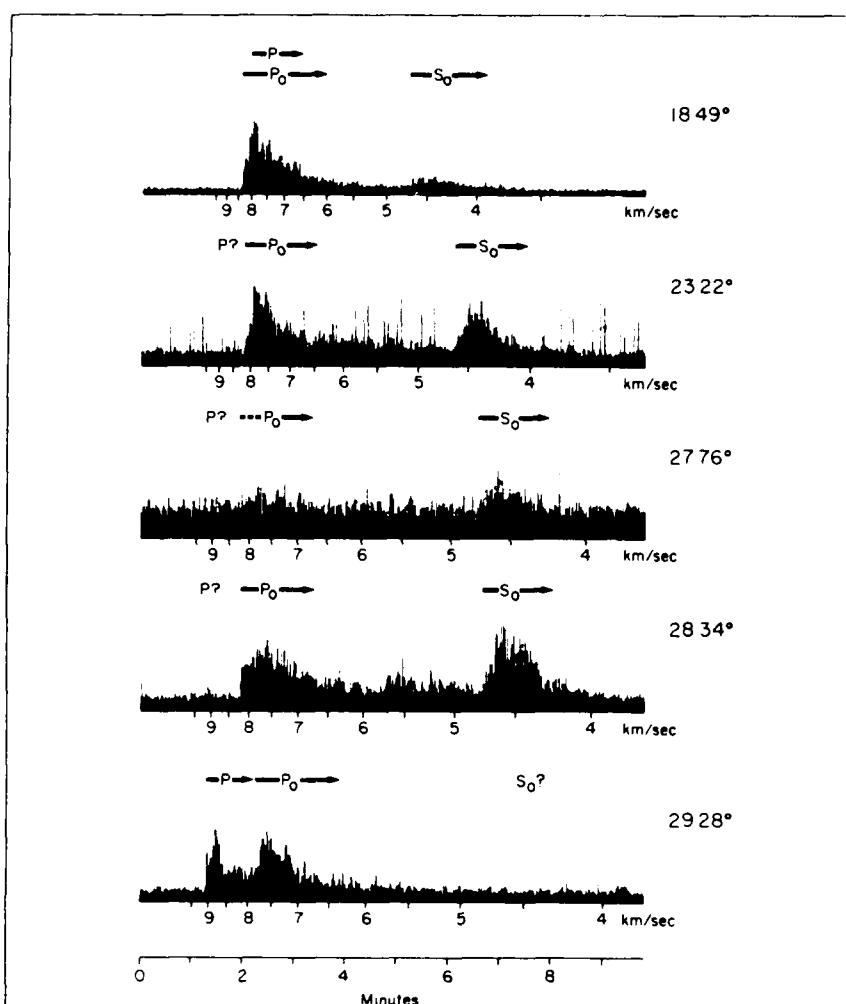
Fig 2 Digitally rectified and compressed plots of Po/So phases recorded by the Wake hydrophones [from *Walker et al.*, 1978]. Scales beneath each plot indicate epicentral distance divided by travel time in kilometers per second.

significance of this is compounded by the general belief that explosions with smaller yields are relatively richer at higher frequencies than explosions with greater yields. Another noteworthy advantage of ocean bottom recordings of near vertically incident phases is that ocean surface reflections can be used for signal enhancement (Figure 5).

Since the pioneering work of Maurice Ewing and his associates, many advances have been made in the instrumentation available for deep ocean recordings. Recent experiments have included the deployment of ocean bottom arrays of hydrophones and seismometers with dimensions of up to 1500 km and recording times of up to 60 days; the emplacement in, and successful retrieval from, deep ocean core holes with recording times of up to 60 days; and the continuous digital recording of deep ocean hydrophone arrays (40 km and 300 km apertures) since October 1982. (Data from the deep ocean hydrophone arrays is sent to the Defense Advanced Research Projects Agency Center for Seismic Studies for use by interested investigators.)

In conclusion, the combined effects of (1) the low noise environment of the deep oceans at frequencies above 3 Hz; (2) the presence of significant amounts of high-frequency energy in Po/So phases and mantle-refracted P phases from earthquakes and explosions at great distances; and (3) technological advances in deep sea instrumentation offer unique opportunities for advancing our knowledge of the earth's interior and for contributing to the verification of nuclear test ban treaties.

Acknowledgments

the S/N ratios for normal, mantle-refracted P phases at their dominant frequencies (about 1.5 to 2.5 Hz), suggesting that regional detection and discrimination of underground explosions with seismic instrumentation in an ocean environment may in large part be based on Po/So recordings.

The ability of deep ocean instruments to record high frequencies in the P phases of nuclear explosions at great distances provides another reason for increased interest in deep ocean seismology. Deep ocean recordings reveal explosion P phases with higher corner frequencies (approximately 2.2 Hz) than earthquake P phases (less than or equal to 1 Hz) at comparable distances (Figure 4); the

References

Asada, T., and H. Shimamura, Observation of earthquakes and explosions at the bottom of the western Pacific: Structure of oceanic lithosphere revealed by Longshot experiment, in *The Geophysics of the Pacific Ocean Basin and Its Margin, Geophys. Monogr.*

TABLE 1. Description of Events Used in Figure 4

Event Number	Date	Location	Distance, degrees	Depth, km	Magnitude, mb	Type	Number of Hydrophones
1	July 24, 1979	S. of Java	65.7	31	6.3	earthquake	3
2	August 4, 1979	E. Kazakh	73.2	0	6.1	explosion	3
3	August 18, 1979	E. Kazakh	73.2	0	6.1	explosion	3
4	September 24, 1979	Novaya Zemlya	76.7	0	5.7	explosion	1
5	September 29, 1979	N. Sumatera	72.9	27	6.2	earthquake	1
6	October 18, 1979	Novaya Zemlya	76.8	0	5.8	explosion	1
7	October 28, 1979	E. Kazakh	73.2	0	6.0	explosion	1
8	December 23, 1979	E. Kazakh	73.3	0	6.1	explosion	1
9	July 29, 1980	Nepal	76.4	18	6.1	earthquake	2
10	September 14, 1980	E. Kazakh	73.2	0	6.2	explosion	2
11	October 12, 1980	E. Kazakh	73.2	0	5.9	explosion	2
12	November 19, 1980	Sikkim	70.4	17	6.0	earthquake	2

Fig. 4 Sample spectra of normal, mantle-refracted P phases recorded between 60° and 90° epicentral distance by the Wake hydrophones from shallow focus earthquakes and nuclear explosions are shown in the upper portion of this figure. Numbers refer to the events as described in Table 1. The composite spectrum of each group, an average with ± 1 standard deviation, is shown in the lower portion of the figure. Before standard deviations were computed, individual spectrums were normalized by subtracting the difference between their mean dB value over the range 1.5–3.0 Hz and the mean dB value for all spectra over the same frequency range.

Fig. 3 Spectrograms for Po/So phases recorded by the Wake hydrophones. Expected times of arrivals are based on either the *Jeffreys and Bullen* [1958] tables for P or Po/So travel time curves from *Walker* [1977]. These spectrograms were made by dividing the time series into adjacent, 512-point segments, Lanczos-squared windowing the segments, and performing a fast Fourier transform (FFT) on each segment. In the horizontal direction, the width of each shaded block corresponds to one of the 512-point segments in the time series. In the vertical direction, each block is the average of two adjacent power spectral estimates out of the FFT. Only frequencies from 0 to ½ Nyquist are shown. The contour interval is 8 dB. The line at 10 Hz is due to time code cross talk. Instrument responses have not been removed. This figure has been taken from *Walker et al.* [1983].

Fig. 5 Sample time series of normal, mantle-refracted P phases, filtered to maximize signal noise, from two nuclear explosions recorded on the Wake hydrophones. The upper trace is from a single hydrophone and shows the direct arrival and its first water surface reflection. The lower trace is a composite of signals from two hydrophones with 40-km separation, obtained as follows: The filtered (1.5–5.0 Hz) time series from each hydrophone was inverted, shifted in time by the water surface reflection time, weighted to maximize the increase in signal/noise, and added to itself; the two resulting time series were then added with the appropriate propagation delay and weighted to maximize the increase in signal noise. Signal/noise was increased by 90% of the theoretical maximum with this method, indicating a high level of coherence between the signals added.

Ser., vol. 19, pp. 135–153, edited by G. H. Sutton, M. H. Manghnani, and R. Moberly, AGU, Washington, D. C., 1976.

Bibee, L., Propagation studies in the West Philippine Sea: A long line refraction experiment, *Ocean Acoustics Program Program Summary for FY82*, edited by J. M. McKisic, pp. 88–89, Environmental Sciences Directorate, Office of Naval Research, Washington, D. C., 1983.

Bradner, H., and J. Dodds, Comparative seismic noise on the ocean bottom and land, *J. Geophys. Res.*, 69, 4339–4348, 1964.

Brune, J., and J. Oliver, The seismic noise of the earth's surface, *Bull. Seismol. Soc. Am.*, 49, 349–353, 1959.

Bungum, H., E. Rygg, and L. Bruland, Short-period seismic noise structure at Norwegian seismic array, *Bull. Seismol. Soc. Am.*, 61, 357–373, 1971.

Frantti, G. D. Willis, and J. Wilson, The

spectrum of seismic noise, *Bull. Seismol. Soc. Am.*, 52, 113–121, 1962.

Jeffreys, H., and K. Bullen, *Seismological Tables*, Office of the British Association, Burlington House, London, 1958.

McCreery, C., High-frequency Pn, Sn phases recorded by ocean bottom seismometers on the Cocos Plate, *Geophys. Res. Lett.*, 8, 489–492, 1981.

Molnar, P., and J. Oliver, Lateral variations of attenuation in the upper mantle and discontinuities in the lithosphere, *J. Geophys. Res.*, 74, 2648–2682, 1969.

Nichols, R. H., Infrasonic ambient ocean noise measurements: Eleuthera, *J. Acoust. Soc. Am.*, 69, 974–981, 1981.

Ouchi, T., Sprectral structure of high frequency P and S Phases observed by OBS's in the Mariana Basin, *J. Phys. Earth*, 29, 305–326, 1981.

Ouchi, T., S. Nagumo, and S. Koresawa,

Ocean bottom seismometer study on the seismic activity in the Mariana Island arc region. *Bull. Earthquake Res. Inst. Univ. Tokyo*, 56, 43–65, 1981.

Talandier, J., and M. Bouchon, Propagation of high frequency Pn waves at great distances in the Central and South Pacific and its implications for the structure of the lower lithosphere. *J. Geophys. Res.*, 84, 5613–5619, 1979.

Urick, R., *Principles of Underwater Sound*, McGraw-Hill, New York, 1975.

Walker, D., High frequency Pn and Sn phases recorded in the Western Pacific. *J. Geophys. Res.*, 82, 3350–3360, 1977.

Walker, D., C. McCreery, G. Sutton, and F. Duennebier, Spectral analyses of high frequency Pn and Sn phases observed at great distances in the Western Pacific, *Science*, 199, 1333–1335, 1978.

Walker, D., C. McCreery, and C. Sutton, Spectral characteristics of high frequency Pn, Sn phases in the Western Pacific. *J. Geophys. Res.*, 88, 4289–4298, 1983.

Daniel A. Walker is with the Hawaii Institute of Geophysics, University of Hawaii at Manoa, Honolulu, HI 96822.

SIGNIFICANT UNREPORTED EARTHQUAKES IN "ASEISMIC" REGIONS
OF THE WESTERN PACIFIC

Daniel A. Walker and Charles S. McCreery

Hawaii Institute of Geophysics, University of Hawaii

Abstract. With data recorded by a deep-ocean hydrophone array centrally located in the Northwestern Pacific Basin near Wake Island, significantly large earthquakes were found to have their epicenters within the interior of the Pacific plate. The signal/noise ratio of the largest is about 40/1 at a distance of 2268 km. Although all of these earthquakes were unreported in National Earthquake Information Service (NEIS) listings, comparisons with the Po/So phases of other earthquakes reported by NEIS indicate that these earthquakes could have body-wave magnitudes in excess of 5.0.

Introduction

The Hawaii Institute of Geophysics has operated an array of ocean bottom hydrophones near Wake Island since September 1982. The 300-km array consists of eleven elements, six on the ocean floor and five in the SOFAR channel. One element from each of three SOFAR sites and five bottom elements are recorded on a computer-controlled digital tape system. Of particular interest are Po/So phases from subducting margins of the Western Pacific and teleseismic P phases from earthquakes and underground explosions. Results of this investigation suggest that seismic activity within supposedly aseismic interiors of oceanic plates is an additional topic of special importance.

From September 1982 through December 1983, thirty-three events were recorded on the array that were not reported in NEIS monthly listings. As it was well known from experiments in the Western Pacific dating back to the early 1960's that small earthquakes (mb's < 5.0) in the Marianas were well recorded on deep ocean hydrophones, these unreported events were assumed to be from that area. Arrival times at differing elements of the array revealed that seven of the unreported events were actually located in regions generally considered to be aseismic (Figure 1). Po, So, and T phases observed for these events are shown in Figure 2. Recordings for one of the events (No. 7) on all of the elements of the array are shown in Figure 3.

Epicenters and origin times were determined by comparing observed Po, So, and T arrival times with corresponding calculated Po, So, and T arrival times from points located at the intersections of a one-half by one-half degree grid covering the estimated region of the epicenter. Velocities used for Po, So, and T were 7.96, 4.57, and 1.48 km/sec, respectively. Contours shown in Figure 1 are the loci of 3-sec

values of standard deviations between calculated and observed arrival times. The quality of the data requires actual epicenters within these 3-sec contours. Also, standard deviations were minimized with respect to origin time, thus determining a best origin time at each point. Times and epicenters given in Table 1 represent the point on each grid with the smallest standard
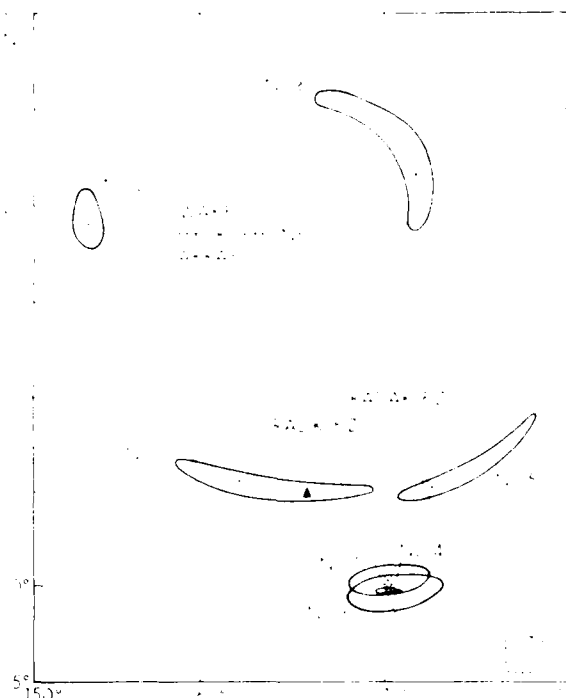
Fig. 1. The Wake array and contours indicating source locations of unreported earthquakes from September 1982 through December 1983. Event numbers as taken from Table 1 are shown next to each contour, and epicenters also taken from Table 1 are shown by an "X" within each contour. Note that Event Nos. 3 and 4 have the same epicenter. For an explanation of contours see text. Also shown are seamount locations (shaded circles) (i.e., features extending upward from the ocean floor to depths of less than 2000 fathoms with circular-like bathymetry contours), the Ralik and Radak fracture zones (F.Z.'s), the approximate locations (shaded square) of a rare swarm of earthquakes at the southernmost extension of the Gilbert Islands (Lay and Okal, 1983), and a hotspot location (solid triangle) from Keating et al. (1981). Bathymetry is taken from Chase, Menard, and Mammerickx (1977); tectonics from Kroenke and Woodward (1984), and Handschumacher and Kroenke (in prep.).

EVENT NO. 1
Δ = 1698 km (76)/
1488 km (2)   NR

1 min

2
1314/1429

3
2268/2000

4
2268/2000

5
1734/1458

6   NA
542/576

7
2214/1945

Po/So PHASES ON PHONE #76   T PHASES ON PHONE #2
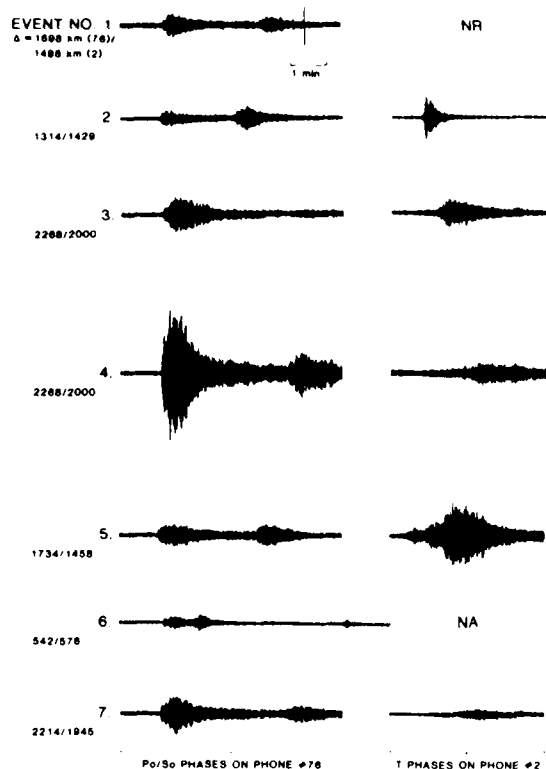
Fig. 2. Po, So, and T arrivals for the seven unreported earthquakes. Po/So recordings are from phone 76, a bottom-mounted hydrophone of the pentagonal array. T recordings are from phone 2, a hydrophone suspended in the SOFAR channel. Numbers to the left of the arrivals are distances in km from the epicenters of the events (as given in Table 1) to phones 76 and 2, respectively. For event no. 1, no records (NR) are available for times at which T would be expected to arrive. For event no. 6, a T was recorded on phone 76, but was not apparent (N/A) on phone 2.

deviation. A comprehensive description of this method is available from the authors.

Discussion

The largest of the intra-plate earthquakes (No. 4) occurred near the equator on 29 June 1983. An attempt to estimate the magnitude of this event may be made through comparisons of its Po/So amplitudes to those at comparable distances from earthquakes in the Marianas. [We recognize that differences in source mechanisms and focal depths may be important considerations in these comparisons. At this time, however, the effects on Po/So propagation of differing source mechanisms and focal depths in subducting zones as well as aseismic interiors of oceanic plates is not well understood.] Twenty-one events from the Marianas at similar distances have been observed from September 1982 through December 1983. Comparisons of some of these Po/So phases to those of No. 4 are shown in Figure 4. On the

basis of comparisons, the body-wave magnitude of No. 4 is estimated to be in the range of 5.0 to 6.0. It also is possible that some of the other earthquakes have magnitudes as large as 5.0.

Although Po/So phases for all of the NEIS reported earthquakes of Figure 4 are smaller than the Po/So phases of No. 4, a large number of stations (120, 99, and 120) were used in calculating the NEIS epicenters. This fact makes No. 4's absence from the NEIS listings even more remarkable. Therefore, possible explanations for the cause of this omission should be considered.

One consideration is the exclusive areal coverage of the Wake array. This array is the only continuously operating seismic station in an area as large as the entire North American continent. Although this could explain why the smaller "local" events (Nos. 2 and 6) were recorded only by the Wake array, such explanations would not be reasonable for the larger events. Earthquakes with body-wave magnitudes of 5.0 or greater in seismically active regions of the earth are well recorded by numerous stations at great distances. Although most of these events occur in subducting margins of plate edges, other events well recorded at great distances include those from rising plate edges and those within the margins of continental plates. Therefore, results presented here suggest that some earthquakes originating in aseismic interiors of oceanic plates are deficient in teleseismic P-phase energy. Furthermore, this deficiency is relative, in that the Po/So energy of these events is comparable to the Po/So energy observed from earthquakes along the subducting margins of oceanic plates, which are well recorded worldwide on the basis of teleseismic, mantle-refracted P phases. The great strength of Po/So phases relative to their respective mantle-refracted P phases may be a function of: (a) source mechanism, (b) focal depth, (c) the nature of the Po/So waveguide, and (d) properties along the P travel path. At this time, one reasonable hypothesis would be that, for earthquakes originating in or above the Po/So waveguide, most or all of the rays that would normally become teleseismic P's (or S's) are, instead, trapped within the waveguide and, in fact, become Po (or So) phases. Another hypothesis is that the P energy is highly attenuated under the source, similar to that observed under the Tuamotus for explosions (Der et al., 1985; and McCreery and Walker, 1985).

Another consideration is that Po/So phases from the unreported earthquakes may not have been recorded by stations bordering the Western Pacific. Studies have shown that although these phases propagate to great distances (often > 3000 km) with little attenuation in oceanic lithosphere underlying deep ocean basins [Walker et al., 1978], severe attenuation can occur when paths cross subducting margins or large sections of island archipelagos [Walker, 1977]. In other words, Po/So phases are more likely to be well recorded by instruments located on the deep-ocean floor than by instruments either on the continental side of subducting margins or on islands. Also compounding the favorability of the deep-ocean environment is its low noise at
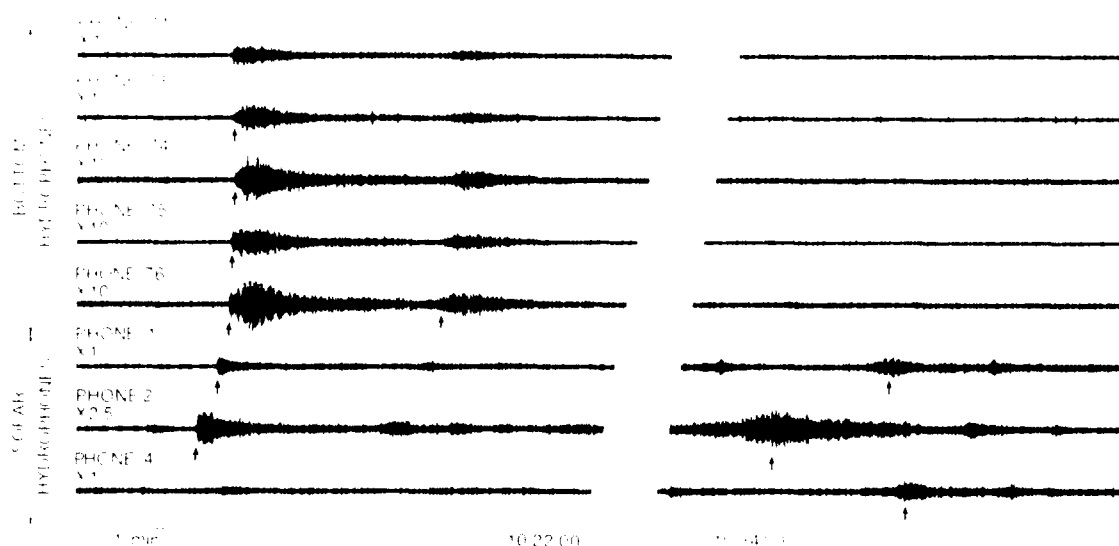
Fig. 3. Recordings from all elements of the array for event no. 7. Arrows indicate "picks" used in the determination of the source location. Phone numbers and relative gain levels are shown above the beginning of each trace. As indicated by these recordings, bottom phones are generally better receptors of Po/So phases, and SOFAR phones are generally better receptors of T-phases.

frequencies where Po/So phases have great strength [Walker, 1984].

Tectonic adjustments within seamounts may be possible explanations for some of the events (especially No. 6 and, possibly No. 2). Although similar explanations may apply to the other events, signal amplitudes and distances to the hydrophones suggest that alternate explanations should be investigated. The proposed "hotspot" extension of the Caroline Archipelago [Keating et al., 1981; Keating et al., 1984] lies within the 3-sec contour solution of No. 1 (Figure 1); No. 5 is near the Radak F.Z.; and Nos. 3, 4, and 7 are near the Ralik F.Z.

Nos. 3, 4, and 7 could all have the same source location. The closeness in the times of occurrence further suggests a common origin (Table 1). It may be significant that No. 5 occurred within the same four-month period during which Nos. 3, 4, and 7, occurred on, or near, the adjoining Ralik F.Z.—only nine days after the largest of these three events. Earthquakes on the Ralik and Radak fracture zones, as well as the proposed Caroline hotspot event, occurred during, or shortly after, a rare swarm of earthquakes at the southernmost extension (3.5°S, 177.5°E) of the Gilbert Islands [Lay and Okal, 1983]. From December 1981 through March 1983, 217 events were located by NEIS in this region previously believed to be aseismic.

Concluding Remarks

The results of this investigation suggest that regions of the world's oceans previously considered to be aseismic may, in fact, have substantial numbers of significant, yet unreported earthquakes. Possible explanations

for the absence of these events in published listings of earthquakes are the lack of high-frequency instruments in deep oceans and relatively low energy levels of mantle-refracted, teleseismic P phases generated by some earthquakes in the interiors of oceanic plates.

After the completion of this report, a recent event of special significance was brought to our attention. On 10 January 1985, the residents of Kosrae (Figure 1; circle closest to the "X" for event No. 1 of 5 November 1982) felt an earthquake at about 1015Z and requested information from the Pacific Tsunami Warning Center (PTWC). They were advised that "neither PTWC nor U.S. Geological Survey seismic records confirm any noticeable earthquake activity in southwest Pacific on 10 January [teletype message from PTWC to Kosrae via RCA Global Communications on 11 January 1985 at 1320Z]. Subsequently, NEIS's "Preliminary Determination of Epicenters"

TABLE 1. Origin Times and Locations of North-western Pacific Intra-Plate Earthquakes

NO	ORIGIN TIME				COORDINATES	
	YR/MO/DAY	HR	MIN	SEC	°N	°E
1	82/11/05	16	26	06	5.5	162.0
2	83/03/24	00	24	08	19.0	154.0
3	83/05/28	23	21	41	0.0	170.0
4	83/06/29	16	15	01	0.0	170.0
5	83/07/08	14	39	35	5.5	172.0
6	83/08/26	01	17	32	21.5	171.5
7	83/09/19	10	14	47	0.5	170.0

21 JAN 1984 12.96° N 145.31° E 46km 5.4mb 120 STATIONS

3 FEB 1984 17.48° N 147.39° E 51km 5.2mb 99 STATIONS

8 JULY 1984 13.31° N 145.93° E 49km 5.7mb 120 STATIONS

EVENT No. 4 (see table 1)   —   UNREPORTED BY NEIS
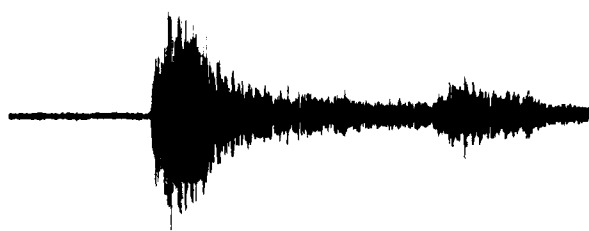
Fig. 4. Comparison of Po/So phases from the
Marianas to the Po/So phases of event no. 4. All
recordings are at the same gain level. Data are
taken from NEIS monthly listings. Numbers of
stations used by NEIS are shown at the top right-
hand side of each event.

network of seismic stations is incapable of
detecting some large earthquakes within the
interiors of oceanic plates.

References

Chase, T. E., H. W. Menard, and J. Mammerickx,
    Topography of the North Pacific, Scripps
    Institution of Oceanography, 1977.
Der, Z., T. McElfresh, R. Wagner, and J.
    Burnetti, Spectral characteristics of P waves
    from nuclear explosions and yield estimation,
    Bull. Seismol. Soc. Am., 75, 379-390, 1985.
Keating, B., D. Mattey, J. Naughton, D. Epp, and
    C. Helsley, Evidence for a new Pacific
    hotspot, Trans. Am. Geophys. Union, 62, 381,
    1981.
Keating, B., D. Mattey, C. Helsley, J. Naughton,
    D. Epp, A. Lazarewicz, and D. Schwank,
    Evidence for a hotspot origin of the Caroline
    Islands, J. Geophys. Res., 89, 9937-9948,
    1984.
Kroenke, L. W., and P. Woodward, Tectonic
    Elements of the Southwest Pacific, Chart 2 of
    the Geophysical Atlas of the Southwest
    Pacific, CCOP/SOPAC, 1984.
Lay, T., and E. Okal, The Gilbert Islands
    (Republic of Kiribati) earthquake swarm of
    1981-1983, Phys. Earth Planet. Inter., 33,
    284-303, 1983.
McCreery, C. S., and D. A. Walker, Spectral
    comparisons between explosion P signals from
    the Tuamotu Islands, Nevada, and Eastern
    Kazakh, Geophys. Res. Lett., in press, 1985.
Walker, D. A., High-frequency Pn and Sn phases
    recorded in the Western Pacific, J. Geophys.
    Res., 82, 3350-3360, 1977.
Walker, D. A., Deep ocean seismology, Eos, 65, 2-
    3, 1984.
Walker, D., C. McCreery, G. Sutton, and F.
    Duennebier, Spectral analyses of high-
    frequency Pn and Sn phases observed in the
    Western Pacific, Science, 199, 1333-1335,
    1978.

for 10 January 1985 (No. 2-85, published on
31 January 1985) contain no entries that could
explain the vibrations on Kosrae. Nonetheless,
the Wake array recorded strong Po, So, and T
phases at around 1017Z. The signal-to-noise
ratio of the Po phase is about 20/1, larger than
the 8/1 ratio observed for the Po of event No. 1.
The 3-sec contour for the 10 January earthquake
fits well within the 3-sec contour of No. 1, and
the best solutions for each are nearly identical
(5.5 N, 162.0 E for No. 1 and 5.5 N, 163.0° E for
the 10 January earthquake).

    These comments are not intended as criticism.
The Kosrae incident is additional evidence of the
important fact that the existing worldwide

    D. A. Walker and C. S. McCreery, Hawaii
Institute of Geophysics, 2525 Correa Road,
Honolulu, HI 96822.

Marine Geophysics Posters

Room Main Arena Tues AM
Presider. K. McNally,
Univ. of California, SC

Thermal Observations At An Arctic Shoreline: Heat Flow, Permafrost Growth and Emergence History

ALAN JUDGE, Earth Physics Br., EMR, 1 Observatory Cres., Ottawa, Ontario, K1A 0Y3)

The earliest heat flow determination in Arctic Canada of 121 mWm^{-2} reported by Misener (1955) at Resolute Bay caused considerable speculation about arctic tectonic processes. As Lachenbruch (1957) subsequently showed, the measured heat flow could be over 30% greater than the actual flux from the crust of the earth due to lateral thermal effects related to proximity to an arctic shoreline. Recent onshore and offshore exploratory drilling at the Polaris mine site on Little Cornwallis Island in the Canadian Arctic has provided the opportunity to examine these thermal effects and the distortion to the heat flow in some detail.

Some 15 surface mining exploration holes have been instrumented for temperature measurements to depths exceeding 150 m and an additional angled underground

hole provides further information at the shoreline. In total the holes span the shoreline ranging from a distance of 500 m offshore to 1000 m onshore with a higher hole density in the vicinity of the present shoreline. Measured temperatures illustrate the very different thermal environments onshore and offshore. Offshore and remote from the shoreline, temperatures, range from 1.7°C at the seafloor to 1.1°C at 300 m; at the shoreline the values range form 10°C to 7.5°C and 1000 m onshore from 16°C to 8°C. Corresponding permafrost thicknesses increase progressively from 150 m through 350 m to in excess of 700 m. The apparent heat flux determined for the onshore holes, using the borehole temperatures and the thermal conductivity measurements on 300 typical core samples, yield values ranging from 106 to 169 mWm^{-2}. Offshore the apparent heat flux is as low as 33 mWm^{-2}. The onshore values decrease with increasing elevation and increasing distance from the present shoreline. Simple mathematical modelling of the results suggests a shoreline which is emerging from the ocean at about 1 cm per year. The undisturbed crustal heat flux in the region of the Boothia Arch is 60 to 70 mWm^{-2}.

T21C-87   POSTER

Long-Term Temporal Variation in Ambient Ocean Noise, 0.1-10 Hz, from Wake Hydrophones

CHARLES S. McCREERY, DANIEL A. WALKER and FIRMIN J. OLIVEIRA (all at   Hawaii Institute of Geophysics, 2525 Correa Rd., Honolulu, HI 96822)
GEORGE H. SUTTON (Rondout Associates, P.O. Box 224, Stone Ridge, NY 12484)

Three-minute ambient noise samples, taken at 6-hour intervals over an entire year, from four hydrophones of the Wake Hydrophone Array, two on the ocean bottom at 5.5-km depth and two in the SOFAR channel at 0.8-km depth, have been spectrally analyzed to examine the temporal variation in ambient noise level for discrete frequency bands between 0.1 and 30 Hz. These data have been compared with the daily scalar mean wind speed measured at Wake Island over the same time period. Some results of this comparison were   (1) a high degree of correlation exists at frequencies less than 2 Hz with a correspondence on the order of 1 dB per 1 mph between noise level and wind speed; (2) an apparent non-instrumental noise level ceiling is clearly visible for frequencies between 2 and 6 Hz on the bottom hydrophones, and in this range a correspondence exists between noise level drops and low wind; (3) conversely, an instrumental noise floor is visible for frequencies above 6 Hz on the bottom hydrophones, and in this range a correspondence exists between noise level peaks and high wind, and (4) correlation is weakest for frequencies above 6 Hz on the SOFAR hydrophones, where absolute noise levels are higher than those measured on the bottom hydrophones by 15-20 dB. Absolute noise levels averaged over the entire year indicate that for frequencies above about 4 Hz, the ocean bottom near Wake is probably as quiet as or quieter than the best land sites. Since noise levels during low wind conditions at Wake (5 mph) were 5-15 dB less than for average wind conditions (14 mph), the world's most sensitive sites for the detection of short period seismic signals may be on the deep ocean bottom in regions with low average wind conditions. Such sites have been identified in the Pacific, Atlantic, and Indian Oceans using yearly mean scalar wind speed contour maps of these regions.

T21C-88   POSTER

Significant Unreported Earthquakes Along the Subducting Margins of the Western Pacific Basin, Within Its Interior, and Along the Recently Postulated Micronesian Trench

DANIEL A. WALKER, CHARLES S. McCREERY and MICHAEL H. IWATAKE (Hawaii Institute of Geophysics, 2525 Correa Rd., Honolulu, HI 96822)

Using a 300-km aperture array of ocean bottom and SOFAR channel hydrophones near Wake Island, numerous earthquakes have been located which are unreported in listings of the National Earthquake Information Service (NEIS). Epicentral determinations of the unreported earthquakes are based on the arrival times of Po, So, and T phases on the differing elements of the array. Many of the unreported earthquakes were located along the subducting margins of the Western Pacific basin, some were located well within the interior of the basin, and several were along the recently postulated Micronesian trench. Although all were unreported in NEIS listings, comparisons with the Po/So phases of other earthquakes which were reported by NEIS indicate that many of the unreported events could have body-wave magnitudes in excess of 5.0. Po/So phases travel with great efficiency in the crust and uppermost mantle underlying the earth's deep ocean basins and are well recorded on the floor of the deep oceans where low ambient noise levels at frequencies greater than 4 Hz combine with the relative richness of Po/So energy at these frequencies to produce large signal-to-noise ratios. Po/So phases do not efficiently propagate across subducting margins and are often poorly recorded at islands. These unreported earthquakes, while strong in Po/So energy, appear to be relatively weak (or totally deficient) in mantle-refracted P energy

normally recorded by the worldwide network. These characteristics serve to exacerbate the current situation of the oceans being highly undersampled for the detection of seismic events. Almost certainly, many features related to the dynamics of ocean plates are being missed. In addition, underground nuclear tests could be conducted illegally permitting in oceanic regions without any evidence of those tests appearing in the existing conventional network of worldwide seismic stations.

T21C-89   POSTER

Deformation above the Juan de Fuca Subduction Zone: Some Enigmas with Bearing on Great Earthquake Risk

JOHN ADAMS, (Division of Seismology and Geomagnetism, Earth Physics Branch, Ottawa, Ontario K1A 0Y3 Canada)

First order levelling and tide gauge data of the coast ranges between central Vancouver I. and Cape Blanco reveals their systematic landward tilting at about 1 × 10^{-6} rad/yr (OR 84 3023, JRL 84). Tectonics 1 449). Second order features superposed on the linear tilt reflect tilting in local structures that also control long term (10^{5}yr) terrace deformation. 10^5 yr terraces are high on coastal salients like C. Blanco, and low in northern Oregon. When projected onto profiles normal to the volcanic arc or to the continental slope, the terraces indicate landward tilting at 1.4 or 1.4 × 10^{-6} rad/yr for the coast, substantially augmenting the 10 yr geodetic tilt rate for the entire range.
The enigmas are these   Cascadia tilt 10 yr is closely similar to terrace 10^{5}yr tilt. Washington is rising at 2.4 mm/yr (for 10^4 yr) but <0.1 mm/yr (for 10^{5}yr). Cinser Bay at C. Arago is rising at 0.1-0.5 mm/yr of 1 10^{5}yr but 1-3 mm/yr old drowned trees are at mean sea level 1-2 mm/yr. One dated (3010 yr), raised beach at C. Blanco emerged 2.5 m. The terraces define a zero isobase near 123.7°W with subsidence inland, for the levelling the zero isobase is near 123.7°W. Perhaps these enigmas might be explained by an earthquake cycle of long duration. Heaton and Kanamori, BSSA 74 933) suggest that M 8.3 earthquakes are possible, but none has occurred in the 150 yr of settlement. However, there were 13-16 turbidites in the Cascadia Channel off Oregon in the last 5600 yr, a few of the 16 are missing at the far end of the channel. Significantly, two independent tributaries have 15 and 16 turbidites each, and there are only 13 (and not 31 or 316) turbidites below their junction. Hence tributary turbidites occurred synchronously and so had a common cause great earthquakes every 410 yr?

T21C-90   POSTER

Deep Seismic Profiling Along the Middle America Trench. A Joint Mexico-U.S. Interim Project of PASSCAL

McNALLY, KAREN C (Charles F. Richter Seismological Laboratory, University of California, Santa Cruz, CA 95064)
ALEJANDRO NAVA (Instituto de Geofisica, U.N.A.M., Mexico 14)
G. W. SIMILA (California State University Northridge, CA 91330)
JAIME R. GONZALEZ-RUIZ (Charles F. Richter Seismological Laboratory, University of California, Santa Cruz, CA 95064)
JAVIER GONZALEZ-GARCIA (C.I.C.E.S.E. Ensenada Baja California)
AND THE INTERINSTITUTIONAL WORKING GROUP FOR SEISMIC PROFILING IN GUERRERO, MEXICO

A major international cooperative project was conducted in March-April 1985 to develop high resolution seismic profiles of the continental crust, subducting sea floor and upper mantle structure along the Middle America Trench in southern Mexico. The National University of Mexico coordinated the project with support from CONACYT. U.S. participation was by the University of California, Santa Cruz with equipment mostly on loan from operating institutions as an NSF interim project of PASSCAL. The seismic refraction experiment was conducted along 240 kms between Puerto Vallarta, Nacional Oaxaca and Acapulco Guerrero. The Mexican Navy's Oceanographic Institute of Manzanillo detonated 13 shots 400 - 300 kg each at 15 offshore locations along the profile. Digital recorders were operated at 15 km intervals effective 2.5 km spacing and stationed by 2.5 km. Shot firing positions with duplicate shots at each point. All recording positions were measured to within 40 meters using a new satellite positioning system (GPS) lent by the U.S. Navy. Each instrument recorded a WWV or a satellite rebroadcast set time signal to within timing accuracy of better than 5 seconds. The shot positions were located by both the GPS and the ship navigation systems. The station and shot profiles parallel the strike of the Middle America Trench and provide good regional sampling of the crust and upper mantle and are also tied to a previous refraction profile which extended in and to the north of Puo trera Nacional. At least all 13

T21C-91   POSTER

Evidence for Active Convergence Along the South Panama "Strike-slip" Margin

D. KELLOGG, G. MOORE (both at: Dept. Geosci., Tulsa Univ., Tulsa, OK 74104), T. SHIPLEY (Inst. for Geophysics, Univ. Texas, Austin, TX 78751), E. SILVER, J. FAGUDIN, D. HEIL (all at Earth Sciences, Univ. Calif., Santa Cruz, CA 95064), D.HUSSONG (Hawaii Inst. Geophysics, Honolulu, HI 96822)

Migrated seismic reflection profiles and

Significant Unreported Earthquakes Along the Subducting
Margins of the Western Pacific Basin, Within Its
Interior, and Along the Recently Postulated Micronesian
Trench

DANIEL A. WALKER, CHARLES S. McCREERY and MICHAEL M.
  IWATAKE (Hawaii Institute of Geophysics, 2525 Correa
  Rd., Honolulu, HI 96822)

Using a 300-km aperture array of ocean bottom and
SOFAR channel hydrophones near Wake Island, numerous
earthquakes have been located which are unreported in
listings of the National Earthquake Information Service
(NEIS). Epicentral determinations of the unreported
earthquakes are based on the arrival times of Po, So,
and T phases on the differing elements of the array.
Many of the unreported earthquakes were located along
the subducting margins of the Western Pacific basin,
some were located well within the interior of the
basin, and several were along the recently postulated
Micronesian trench. Although all were unreported in
NEIS listings, comparisons with the Po/So phases of
other earthquakes which were reported by NEIS indicate
that many of the unreported events could have body-wave
magnitudes in excess of 5.0. Po/So phases travel with
great efficiency in the crust and uppermost mantle
underlying the earth's deep ocean basins and are well
recorded on the floor of the deep oceans where low
ambient noise levels at frequencies greater than 4 Hz
combine with the relative richness of Po/So energy at
those frequencies to produce large signal-to-noise
ratios. Po/So phases do not efficiently propagate
across subducting margins and are often poorly recorded
on islands. These unreported earthquakes, while strong
in Po/So energy, appear to be relatively weak (or
totally deficient) in mantle-refracted P energy
normally recorded by the worldwide network. These
characteristics serve to exacerbate the current
situation of the oceans being highly undersampled for
the detection of seismic events. Almost certainly,
many features related to the dynamics of ocean plates
are being missed. In addition, underground nuclear
tests could be conducted (technology permitting) in
oceanic regions without any evidence of those tests
appearing on the existing conventional network of
worldwide seismic stations.

AUSTRALIA

PAPUA
NEW GUINEA

SOLOMON

ONTONG

JAVA

PLATEAU

NEW
CALEDONIA

VANUATU

FIJI

TONGA

NIUE

WESTERN
SAMOA

TUVALU

NAURU

KIRIBATI

FEDERATED STATES OF MICRONESIA

RIDGE

140°E

150°

160°

170°

180°

170°W

10°
N

0°

10°
S

20°
S
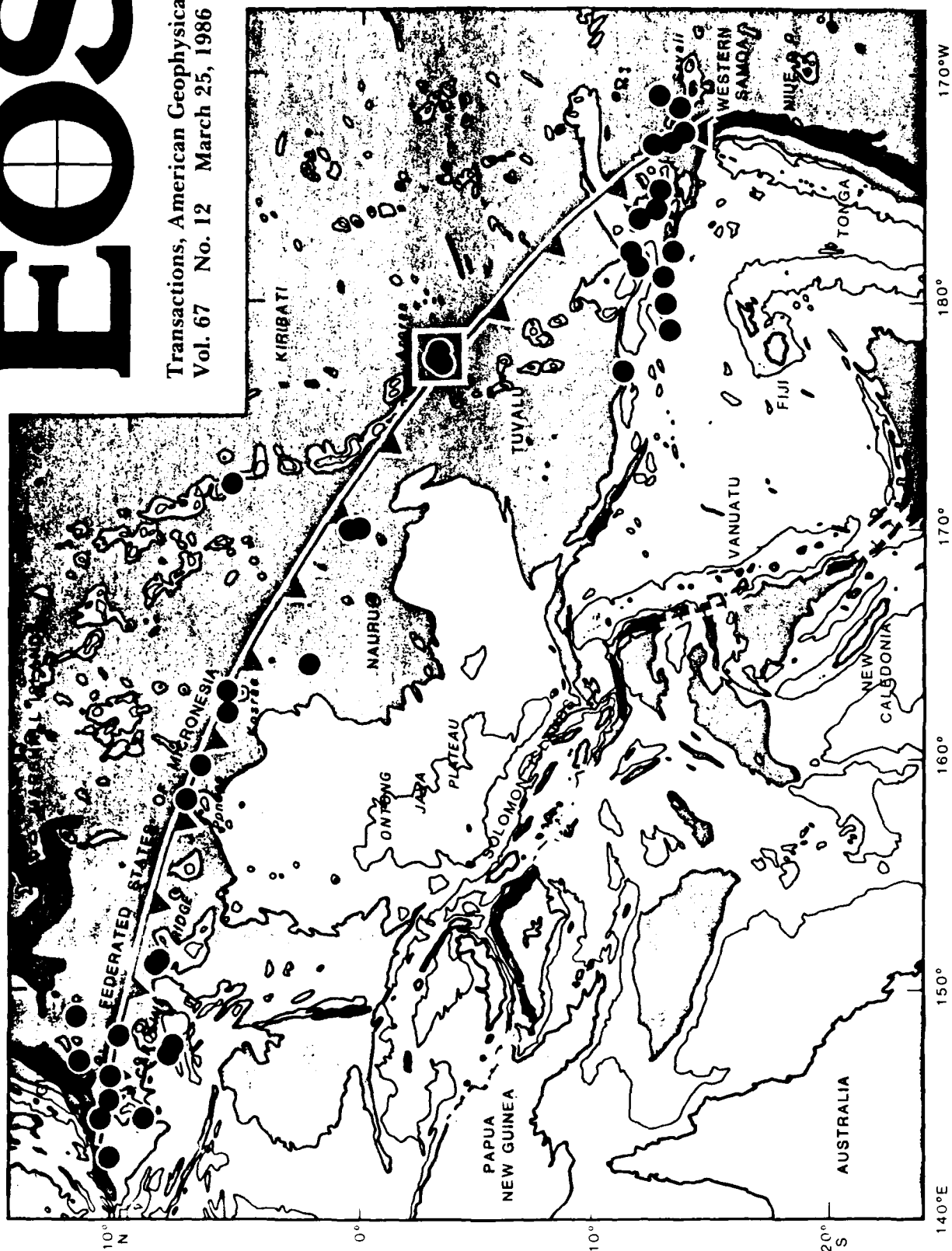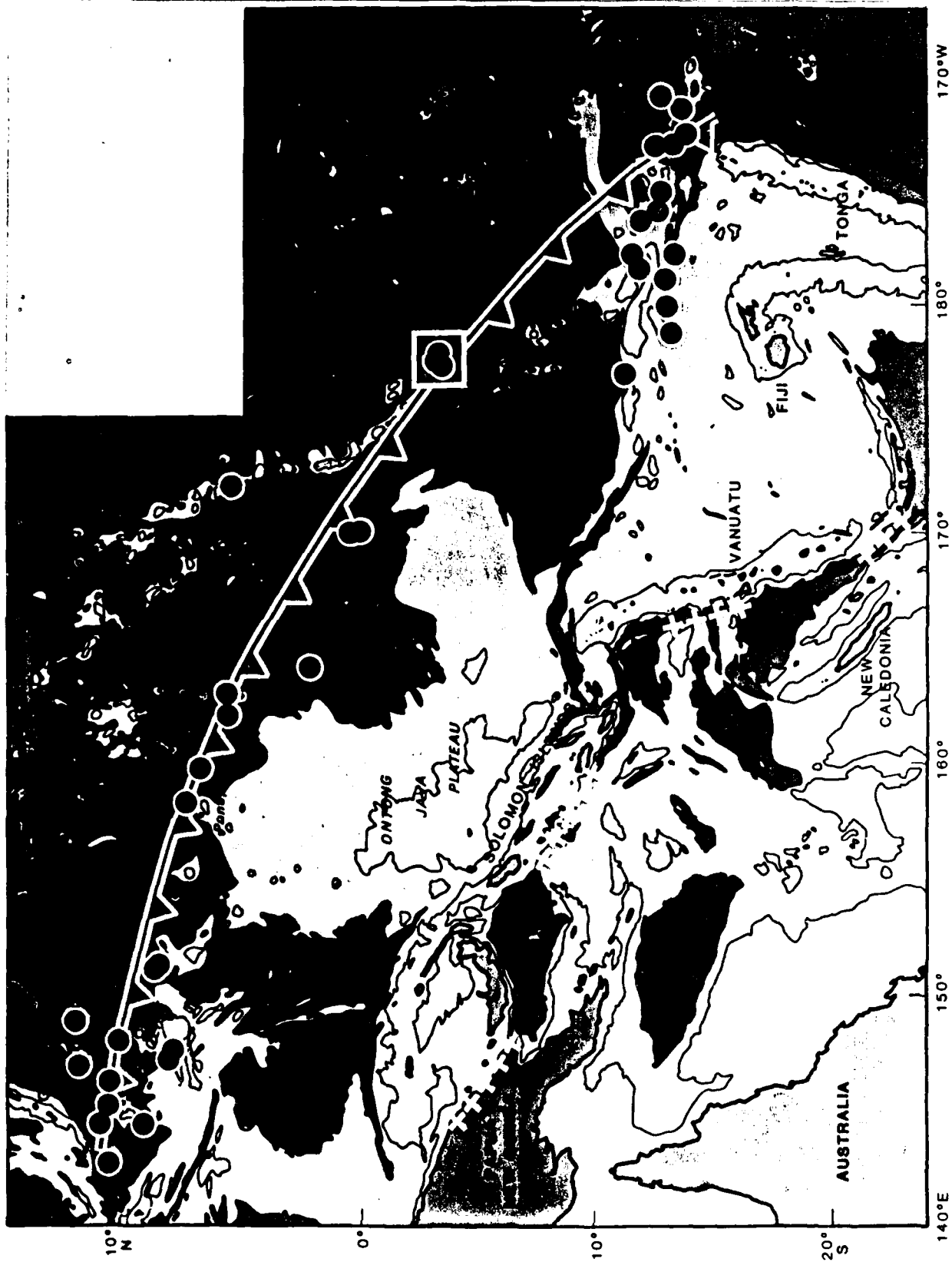
Preprint

EVIDENCE FOR THE FORMATION OF A NEW TRENCH
IN THE WESTERN PACIFIC

Loren W. Kroenke

Daniel A. Walker

Introduction

Shallow intraplate earthquakes, detected along an arcuate zone
extending from the northern side of the Caroline Ridge across the western
Pacific to the southern end of Kiribati (cover illustration), may portend a
northward shift in convergence between the Indo-Australia and Pacific
plates. Low-amplitude sea floor structures along this zone indicate recent
deformation and, in places, suggest trench-forearc morphology. These
earthquakes and sea floor structures may provide evidence for the formation
of a new subduction zone--the Micronesian trench. The western end of the
postulated trench seems to be part of a complex triple junction at the
concurrence of the Yap, Mariana, and Micronesian trenches. The eastern end
joins the Tonga trench south of Savaii, Western Samoa.

Background

The modern southwest Pacific is a clutter of rifted continental
fragments, abandoned arcs, and oceanic plateaus (Glaessner, 1950; Hess and
Maxwell, 1953; Officer, 1955; Karig, 1970 and 1972; Moberly, 1972; Packham,
1973; Packham and Andrews, 1975; Coleman and Packham, 1976; Shaw, 1978;
Falvey and Mutter, 1981). A recent tectonic analysis, synthesizing previous
geological investigations of this region, documents the recurrent shifts in

the convergent boundary between the Indo-Australia and Pacific plates
and attests to the large-scale tectonism rampant in the past (Kroenke,
1984). Collision tectonism is obvious today along much of the length of the (Cover)
New Britain-San Cristobal-New Hebrides trench (cover figure and Fig. 1) and (Fig 1)
subduction, it seems, is being obstructed. For example, arc-continent
collision is occurring along the northeastern side of Papua New Guinea
(Jaques and Robinson, 1977; Kroenke, 1984) and has resulted in uplift of
flights of Quaternary coral terraces along the northeastern coast of Papua
New Guinea (Chappell, 1974). The hot, buoyant lithosphere of the Woodlark
basin is pressing against the forearc of the South Solomon Island arc,
shoving the volcanic arc northward, reactivating a segment of the old
Oligocene North Solomon Island subduction zone (Cooper and Taylor, 1985),
and forcing the southwestern margin of the Ontong Java plateau to fold and
thrust over the southeastern Solomon Islands (Kroenke et al., in press,
1985). Farther east, the West Torres plateau is entering the North New
Hebrides trench, the d'Entrecasteaux ridge is uplifting the central New
Hebrides forearc (Collot et al., 1985), and the Loyalty ridge is impinging
on the South New Hebrides trench. In this setting of intense and extensive
tectonic activity can be seen evidence for the waning phase of one
subduction zone and the formative stage of another.

Observations

That stress is being transferred northward is evidenced by shallow
"intra-plate" seismicity (cover figure) at the western end of the Caroline
ridge (events located by the International Seismological Center [ISC] and
the National Earthquake Information Serivce [NEIS]), in the vicinity of
Ponape Island (an ISC- and NEIS-located earthquake; and D. Walker,

unpublished data), in the central Nauru Basin around 2.5° N, 170° E and near Kosrae (an ISC-located earthquake; and Walker and McCreery, 1985), in southern Kiribati southeast of Arorae Atoll (Lay and Okal, 1983), and in the vicinity of Western Samoa (ISC- and-NEIS located events). We believe that this seismicity indicates a shift in the Indo-Australia/Pacific convergent boundary and the development of a new subduction zone. The zone as defined by the seismicity (cover figure) stretches more than 5000 km across the Western Pacific.

At the western end of the zone, where the Caroline ridge is step-faulted down into the Mariana basin, the newly formed subduction zone itself may be discernible on the shaded relief free-air gravity map recovered from Seasat altimeter data by Haxby (1983). The seismicity forms a broad, diffuse zone in which some of the earthquakes are aligned north of the Caroline ridge and others occur south of the ridge (see cover figure)--all of which may indicate the tectonic complexity and instability of the trench-trench-trench triple junction. The epicenter nearest Ponape in the cover figure simply denotes the proximity of local earthquakes recorded by a temporary seismic station on Ponape in 1972 (D. Walker, unpublished data).

All of the earthquake epicenters in the Nauru basin (between Kosrae and Kiribati in the cover figure) were unreported by NEIS; one was reported by ISC (in 1967), and the remainder were detected only by the recently reactivated Wake Island hydrophone array (Walker and McCreery, 1985). The earthquake nearest Kosrae, moreover, was felt by the residents of the island. Although the Kosrae earthquakes may be related to the proposed Caroline Island hotspot (Keating et al., 1984), the occurrence of other earthquakes near Ponape and elsewhere in the Nauru Basin (see cover figure) leads us to believe that the Kosrae seismicity might also be related to the

formation of the new convergent boundary. Furthermore, the sea floor is deformed between the epicenters of the known earthquakes in the Nauru Basin. Broad, low swells are present along the southern side of the boundary (Fig. 2). The sea floor is upraised south of the boundary and depressed north of it, and structure suggestive of recent deformation and resembling trench-forearc morphology is revealed in a reflection profile across the boundary (Fig. 3). All of the foregoing suggest that sea floor northeast of the boundary is underthrusting that to the southwest of the boundary.

(Fig. 2)

(Fig. 3)

The earthquake epicenters shown southeast of Arorae (see box in cover figure) are the largest events of a major earthquake swarm (Fig. 4) reported by the ISC and NEIS. Focal mechanisms determined by body- and surface-wave analysis for these earthquakes have predominant thrust orientations, with consistent horizontal compression axes tending NNE-SSW (Lay and Okal, 1983). Thus, unlike many typical "oceanic" earthquakes (Mendiguren, 1971; Sykes and Sbar, 1974; Okal, 1980), the stress orientation of the Gilbert swarm is orthogonal to the presumed direction of plate motion. These "anomalous" orientations are, however, consistent with nearby subduction (i.e., the thrust axes are normal to the postulated Micronesian subduction zone). Furthermore, the swarm epicenters shown in Figure 4 form a cluster aligned parallel to the postulated boundary line shown in the cover figure.

(Fig. 4)

The earthquakes in the vicinity of Western Samoa (ISC- and NEIS-located events) near the junction with the Tonga trench also occur over a broad zone. The diffuse seismicity along the northern edge of the zone, closest to Western Samoa, might be related, in part, to the formation of the new convergent margin and, in part, to Tonga trench deformation (Natland, 1980). In contrast, the seismicity along the southwestern edge of the zone (north of Fiji) is aligned parallel to the strike of the old Vitiaz trench which,

in turn, suggests possible reactivation of subduction along that part of a former convergent margin that was active in Oligocene-early Miocene time (Kroenke, 1984).

Discussion

If the foregoing hypothesis is correct, new subduction zones might initially be characterized by low levels of seismicity generally occurring along pre-existing zones of weakness and near dying subduction zones that have accumulated numerous barriers to their continued existence. Since all of the earthquakes occurring along the Micronesian subduction zone are either known, or believed, to have shallow focal depths, the absence of intermediate- and deep- focus events adds credence to the belief that this is a new subduction zone involving only the uppermost layers of the oceanic lithosphere.

Also, if the hypothesis is correct, the new convergent margin may constitute the longest single continuous arc segment in the world. Seismicity would be expected to continue and even to increase along the new convergence zone. In addition, this new plate boundary may comprise a heretofore unrecognized tsunami-generating zone within the Pacific basin. Indeed, a small tsunami was reported to have occurred on 8 January just prior to the 10 January 1985 Kosrae earthquake (teletype message from Ponape to Pacific Tsunami Warning Center, 10 January 1985).

More comprehensive investigations are needed to test the hypothesis of a Micronesian subduction zone and to delineate the extent of seismicity in this region. Recent studies using an array of ocean bottom and SOFAR channel hydrophones located near Wake Island have established that the worldwide array of conventional seismic stations is incapable of detecting

some significant earthquakes within the interiors of oceanic plates (Walker and McCreery, 1985). Several earthquakes unreported by ISC and NEIS were recorded by the Wake hydrophones with large signal/noise (S/N) ratios at teleseismic distances. To date, the largest S/N ratio is about 40/1 for an earthquake at a distance of 2268 km (Fig. 5). This earthquake occurred in the Nauru Basin along the equator at about 170° E (Fig. 3). Comparisons with the Po/So phases of other earthquakes that were reported by NEIS from the Marianas subduction zone at comparable distances to Wake indicate that the unreported events located along the Micronesian subduction zone could have body wave magnitudes in excess of 5.0 (Fig. 5). Earthquakes unreported by ISC and NEIS were also recorded by a temporary seismic station on Ponape (Fig. 6). Possible explanations for the absence of these events in ISC and NEIS listings of earthquakes are the lack of high-frequency instruments in deep oceans where Po/So phases are best recorded (Walker, 1984) and relatively low energy levels of mantle-refracted, teleseismic P and S phases generated by some earthquakes in the interiors of oceanic plates. The previously mentioned significance of an unrecognized tsunami-generating zone is increased by the fact that substantial earthquakes from this region have gone undetected by the existing worldwide network of conventional seismic stations.

The foregoing considerations indicate that accurate assessment of seismicity along the proposed Micronesian subduction zone will require special instrumentation, possibly including ocean bottom seismometers and hydrophones, downhole (sub-bottom) seismometers, and temporary high-frequency stations on nearby islands, as well as the existing Wake Island hydrophone array. Marine geophysical surveys using high-resolution reflection profiling equipment and precision mapping techniques (such as

SeaMARC II; see Hussong and Fryer, 1983) also would provide useful information on the morphology and extent of deformation along the zone.

Acknowledgments

Loren W. Kroenke, Associate Geophysicist at the Hawaii Institute of Geophysics, received his BS degree in Geology from the University of Wisconsin in Madison and his MS degree in Solid Earth Geophysics and Ph.D. in Geology from the University of Hawaii. He has worked in reflection seismology and tectonics and is currently involved in tectonic studies of the western and southwestern Pacific. For the past twelve years he has been associated with the Committee for the Coordination of Joint Prospecting for Mineral Resources in South Pacific Offshore Areas (CCOP/SOPAC) helping to establish its Technical Secretariat and further its mineral exploration efforts.

Daniel A. Walker is an Associate Geophysicist engaged in earthquake research at the Hawaii Institute of Geophysics. A native of Cleveland, Ohio, he attended John Carroll University where he received a B.S. degree in Physics. Moving to the University of Hawaii in 1963, he received M.S. and Ph.D. degrees in Geophysics. For the past twenty-two years, he has studied seismic phases recorded on islands and in the deep-ocean basins of the Pacific.

References

Chappell, J., Geology of coral terraces, Huon Peninsula, New Guinea: A study of Quaternary tectonic movements and sea-level changes., Geol. Soc. Amer. Bull., 85, 553-570, 1974.

Coleman, P.J., and G.H. Packham, The Melanesian borderlands and India-Pacific plates' boundary, Earth Sci. Rev., 12, 197-233, 1976.

Collot, J.Y., J. Daniel, and R.V. Burne, Recent tectonics associated with the subduction/collision of the d'Entrecasteaux zone in the central New Hebrides, Tectonophysics, 112, 325-356, 1985.

Cooper, P.A., and B. Taylor, Polarity reversal in the Solomon Islands arc, Nature, 314, 428-430, 1985.

Falvey, D.A., and J.C. Mutter, Regional plate tectonics and the evolution of Australia's passive continental margins, BMR J. Austr. Geol. Geophys., 6, 1-29, 1981.

Glaessner, M.F., Geotectonic position of New Guinea. Bull. Am. Ass. Petrol. Geol., 34, 856-881, 1950.

Haxby, W.F., Gravity field of the world's oceans, recovered from Seasat altimeter data (map), Lamont Doherty Geological Observatory, March 1983.

Hess, H.H., and J.C. Maxwell, Major structural features of the South-West Pacific: A preliminary interpretation of H.O. 5485 bathymetric chart, New Guinea to New Zealand, Proc. 7th Pacif. Sci. Congr. New Zealand, 2, 14-17, 1953.

Hussong, D.M., and P. Fryer, Back-arc seamounts and the SeaMARC II seafloor mapping system, Eos, 64, 627-632, 1983.

Jaques, A.L., and G.P. Robinson, The continent/island-arc collision in
    northern Papua New Guinea, BMR J. Austr. Geol. Geophys., 2, 289-303,
    1977.

Karig, D.E., Ridges and basins of the Tonga-Kermadec island arc system, J.
    Geophys. Res., 75, 239-254, 1970.

Karig, D.E., Remnant arcs, Bull. Geol. Soc. Am., 83, 1057-1068, 1972.

Keating, B., D. Mattey, C. Helsley, J. Naughton, D. Epp, A. Lazarewicz, and
    D. Schwank, Evidence for a hotspot origin of the Caroline Islands,
    J. Geophys. Res., 89, 9937-9948, 1984.

Kroenke, L. W., Cenozoic tectonic development of the Southwest Pacific, U.N.
    ESCAP, CCOP/SOPAC Tech. Bull. No. 6, 126 pp, 1984.

Kroenke, L.W., J.M. Resig, and P.A. Cooper, Tectonics of the southeastern
    Solomon Islands: formation of the Malaita Anticlinorium, In Vedder,
    J.J., and D.L. Tiffin (eds), "Geology and Offshore Resources of Pacific
    Island Arcs-Solomon Islands Region". Earth Sciences Series, Circum-
    Pacific Energy and Mineral Resources Council, Houston, Texas, in press,
    1985.

Kroenke, L.W., R. Moberly, E.L. Winterer, and G.R. Heath, Lithologic
    interpretation of continuous reflection profiling, Deep Sea Drilling
    Project, Leg 7, Initial Rep. Deep Sea Drill. Proj., 7(2), 1161-1226,
    1971.

Lay, T., and E. Okal, The Gilbert Islands (Republic of Kiribati) earthquake
    swarm of 1981-1983, Physics of the Earth and Planetary Interiors, 33,
    284-303, 1983.

Mammerickx, J., and S.M. Smith, Bathymetry of the Northcentral Pacific, Map
    and Chart Series MC-52, Geol. Soc. Amer., 1985.

Mendiguren, J.A., Focal mechanism of a shock in the middle of the Nazca
    plate, J. Geophys. Res., 76, 3861-3879, 1971.

Moberly, R.M., Origin of lithosphere behind island arcs, with reference to the Western Pacific, Mem. Geol. Soc. Am., 132, 35-55, 1972.

Natland, J.H., The progression of volcanism in the Samoan linear volcanic chain, Amer. J. Sci., 280-A, 709-735, 1980.

Officer, C.B., Southwest Pacific crustal structure, Trans. Am. Geophys. Un., 36, 449-459, 1955.

Okal, E.A., The Bellingshausen Sea earthquake of February 5, 1977: evidence for ridge-generated compression in the Antarctic plate, Earth Planet. Sci. Lett., 46, 306-310, 1980.

Packham, G.H., A speculative Phanerozoic history of the South-west Pacific. In Coleman, P.J. (ed), The Western Pacific: Island Arcs, Marginal Seas, Geochemistry, Univ. W., Aust. Press, Perth, 369-388, 1973.

Packham, G.H., and J.E. Andrews, Results of Leg 30 and the geologic history of the Southwest Pacific and marginal sea complex. In: Andrews, J.E., G.H. Packham, et. al., Initial Rep. Deep Sea Drill. Proj., 30, 1975

Shaw, R.D., Seafloor spreading in the Tasman Sea: A Lord Howe Rise - Eastern Australian reconstruction, Bull. Aust. Soc. Explor. Geophys., 9(3), 75-81, 1978.

Sykes, L.R. and M.L. Sbar, Focal mechanism solutions of intraplate earthquakes and stresses in the lithosphere. In: Kristjansson, L. (ed), Geodynamics of Iceland and the North Atlantic Area, Reidel, Dordrecht, 207-224, 1974.

Walker, D.A., Deep ocean seismology, Eos, 65, 2-3, 1984.

Walker, D.A., and C.S. McCreery, Significant unreported earthquakes in "aseismic" regions of the Western Pacific, Geophys. Res. Lett., 12, 433-436, 1985.

Figure Captions

Cover. The map on the cover shows the region affected by a postulated

northward shift in convergence from the New Britain–San Cristobal–New

Hebrides trench system to the site of the new Micronesian trench. Deepening

shades of blue indicate increasing water depths in increments of 2000 m.

White pluses represent collision zones along the New Britain–San Cristobal–

New Hebrides trenches. Red dots indicate intraplate earthquake epicenters

not previously correlated with a convergent margin. The white box shows the

location of the Gilbert Island earthquake swarm (represented by the

epicenters for the three largest teleseisms). The ~~yellow~~ *crange* sawtooth line

shows the approximate location of the new subduction zone (Micronesian

trench); teeth point in the most likely direction of underthrusting.

Figure 1. Location of the present–day convergent boundary between the Indo-

Australia and Pacific plates (along the New Britain–San

Cristobal–New Hebrides trenches).

Figure 2. Bathymetry of the Nauru Basin (after Mammerickx and Smith, 1985).

The contour interval (solid lines) is 500 m. Intermediate

contours (dashed lines) indicate locations of elevated and

depressed areas north and south of the convergent boundaries,

respectively, believed to be structurally controlled by the

formation of the new Micronesian trench. Also shown are the

location of the DSDP Leg 1 reflection profile line, earthquake

epicenters (asterisks) from the cover figure, and the probable
location of the new Micronesian trench (shaded areas).

Figure 3.   DSDP Leg 7 reflection profile in the Nauru basin (Kroenke et al.,
1971), showing the surface expression of the postulated
Micronesian trench. The profile location is shown in Fig. 2.
Vertical exaggeration is approximately 12 to 1.

earthquake sworm

Figure 4.   Location of ~~seismicity~~ southeast of Arorae in the Gilbert Islands
~~swarm~~ (after Lay and Okal, 1983). The area is the same as shown
by the box in the cover figure. The curved line merely
represents the approximate location of the convergent boundary
as taken from the cover figure.

Figure 5.   Comparison of Po/So phases from a reported earthquake in the
Marianas to the Po/So phases of an unreported earthquake located
along the equator in the Nauru basin at 170° E by the Wake Island
hydrophone array. Both recordings are from the same hydrophone
and are at the same gain level. Data for the reported earthquake
are taken from National Earthquake Information Service (NEIS)
monthly listings, based on reported phases from 132 stations.

Figure 6.   Po/So phases recorded by a temporary seismic station on Ponape.
These earthquakes were unreported in ISC and NEIS listings. The

observed arrivals are similar in character to those of other
unreported earthquakes in the Western Pacific recorded eleven
years later by the Wake Island hydrophone array (see Fig. 5, and
Walker and McCreery, 1985). As these phases at Ponape were only
recorded by a single station, epicenter determinations are not
possible. Po/So intervals were used, however, to estimate the
origin times (in universal time) and epicentral distances shown
in the figure. For the eighteen months that the station was in
operation, the NEIS-reported earthquake closest to Ponape
occurred near New Ireland at a distance of 12.27°, or 1364 km.
The recordings shown are from a special high-frequency vertical
seismograph.

END

DATE
FILMED

12-86

DTIC
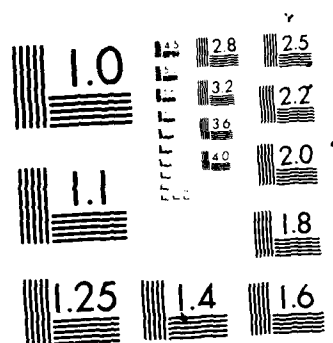
MICROCOPY RESOLUTION TEST CHART
NATIONAL BUREAU OF STANDARDS 1963 A

Kroenke and Walker

Figure 1

Kroenke and Walker

Figure 2

WSW ENE

New Trench

New Forearc
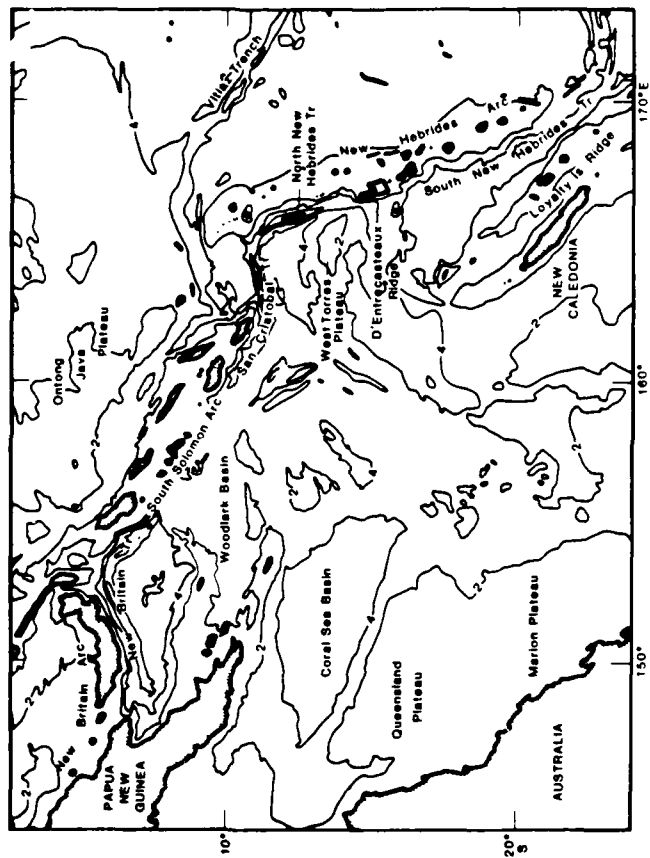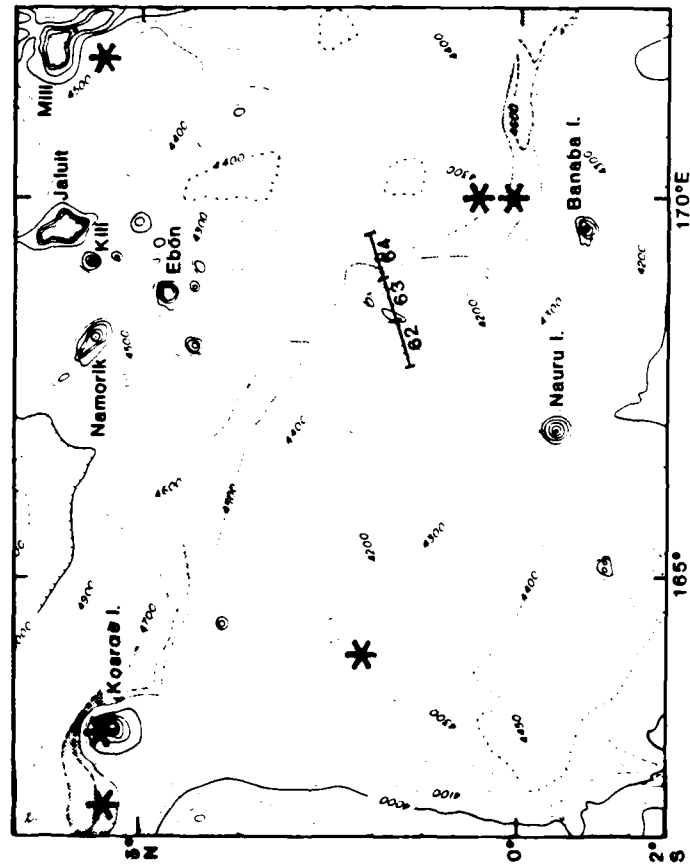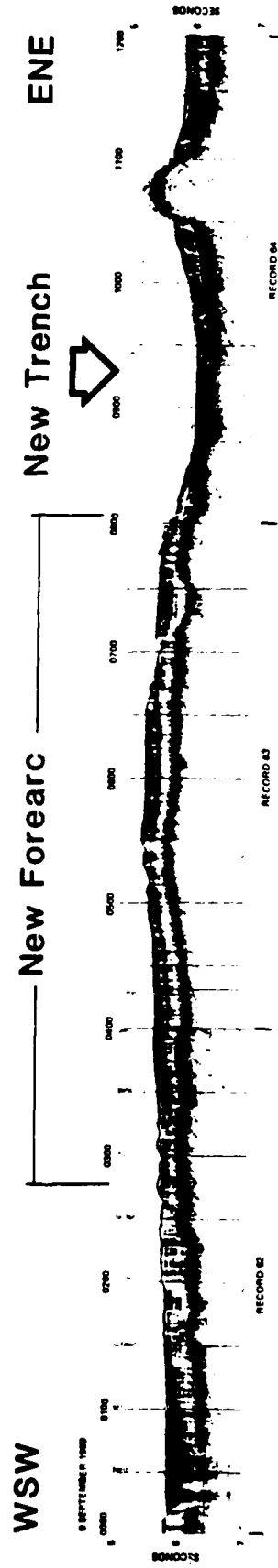
Kroenke and Walker

Figure 3

Kroenke and Walker

Figure 4
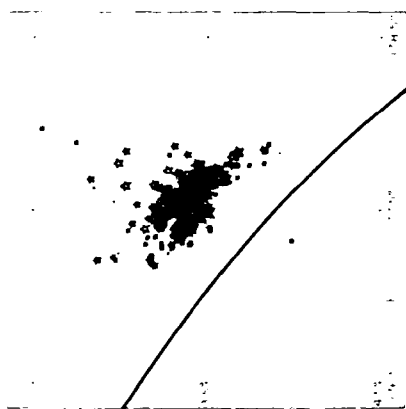
29 JUNE 1983 0.0°N,170.0°E –   UNREPORTED BY NEIS
2268 km
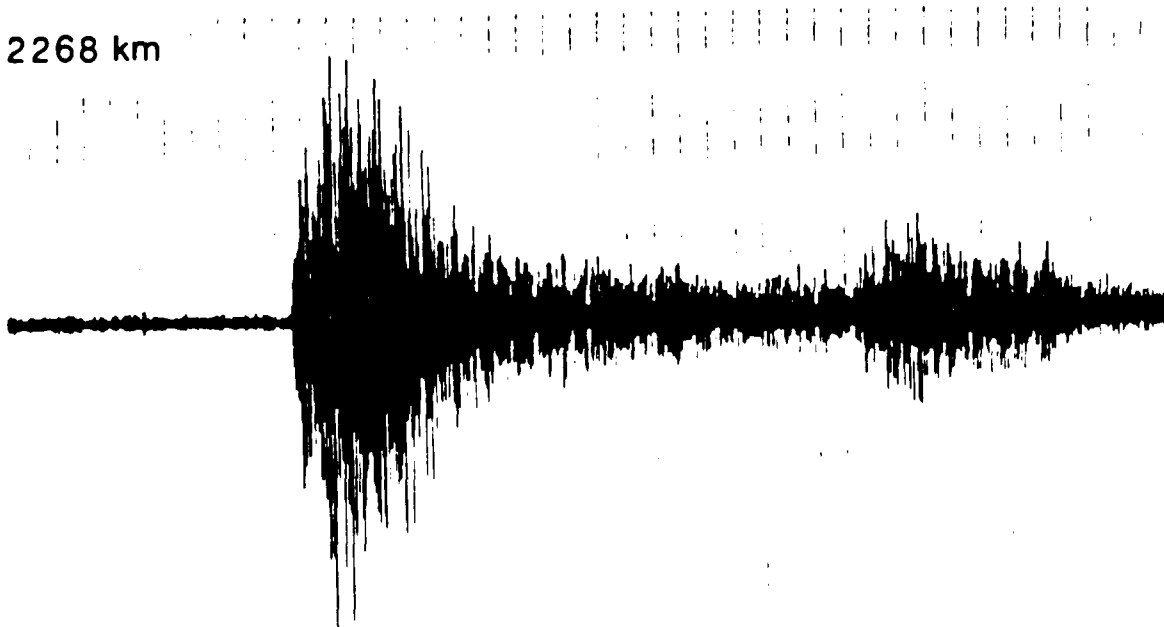
9 SEPT.1982 15.49° N,147.57° E 33km 5.4mb 132STATIONS
2069 km

|← 1 min.→|

Kroenke and Walker

Figure 5

14 July 1972   21:20:50   1.7°(190 km)
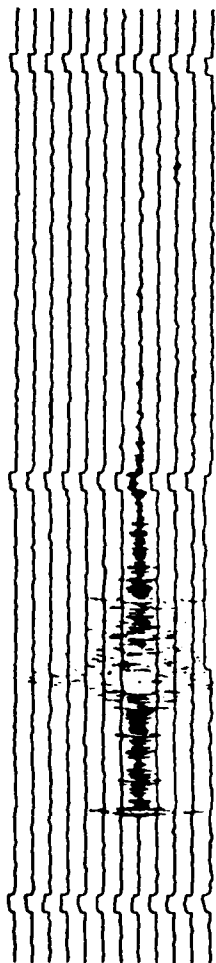
27 July 1972   07:35:38   6.8°(760 km)
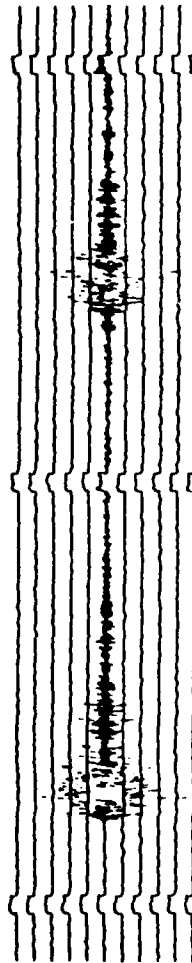
1 min

Kroenke and Walker

Figure 6

T-Phases from Test Explosions in the Tuamotu Islands

Recorded by the Wake Hydrophone Array

By Charles S. McCreery and Daniel A. Walker

ABSTRACT

T-phases from test explosions at the French nuclear test site in the Tuamotu Islands are well recorded by the Wake Island Hydrophone Array in the Northwestern Pacific at approximately 7500-km epicentral distance. An extrapolation of observed signal-to-noise ratios indicates that explosive events from this site with body-wave magnitudes as small as 3.3 should be detectable by the Wake Array. Differences observed between the spectra of these T-phases, and the spectra of T-phases generated by shallow-focus, similar magnitude earthquakes might be the basis for a discriminant. Additional data and investigation will be needed to evaluate whether these differences are due to source characteristics rather than effects along the prcpagation path.

INTRODUCTION

Earthquakes with epicenters near oceans are known to generate acoustic signals called T-phases which can propagate through the SOFAR (sound fixing and ranging) channel of the world's oceans with a high degree of efficiency over great ranges (e.g., Johnson and Northrop, 1966). Explosive sources may also generate T-phases [the strict definition of the T-phase applies only to earthquakes (Northrop, 1968); but, for simplicity, we include explosions]; and it is such signals from underground nuclear explosions at the French

test site in the Tuamotu Islands recorded by the Wake Island Hydrophone Array (Figure 1) which are the subject of this study.

The Wake array consists of eleven hydrophones. Six of the hydrophones are on the ocean bottom (about 5.5 km-depth) and make up the vertices and center of a 40-km pentagon, and five are located at three sites near the axis of the SOFAR channel (about 1-km depth). The combined array spans more than 300 km. Signals from eight of these hydrophones, five bottom and three SOFAR, have been recorded digitally by the Hawaii Institute of Geophysics on a continual basis since August, 1982.

In this study, we analyze T-phase signals from two explosions in the Tuamotus and from earthquakes in the Aleutian Islands, California, and Hawaii (Figure 1). Hypocenter information is given in Table 1. The emphasis of this analysis is: (1) estimation of the detection threshold at Wake of Tuamotu explosion generated T-phases in terms of magnitude; and (2) evaluation of T-phase spectra as the basis of a discriminant between explosions and earthquakes occuring near oceans.

DATA

Shown in Figure 2 is a playback of the T-phase from California (event 4, Table 1) as recorded by eight hydrophones in the Wake Array. In many respects, this record is typical. Signal levels on the bottom hydrophones are small in comparison to those on the SOFAR hydrophones. Signals on SOFAR hydrophones 20 and 40 have, in fact, exceeded the dynamic range of the recording system and are clipped. The T-phase signals also exhibit a gradual buildup and falloff of energy which extends over several minutes. Lumps of energy which appear after the main arrival are probably reflections off of nearby seamounts (e.g., Adams, 1979). In this study, we limited our
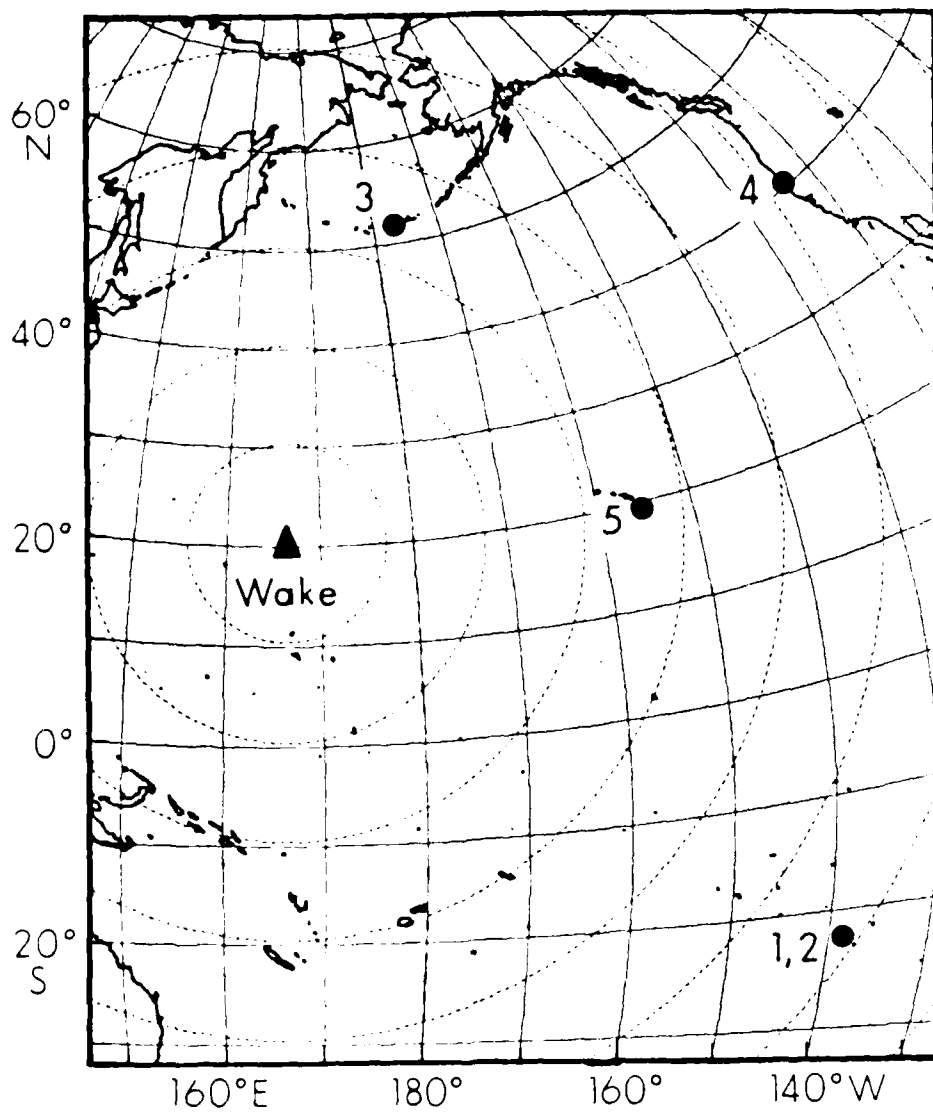
Fig. 1. Map showing the location of the Wake Island Hydrophone Array and the epicenters listed in Table 1. Circles radiating outward from Wake are at 10° intervals, and great circle paths from each epicenter to Wake may be drawn as a straight line.

Table 1. Hypocenters*

Event	Date	Origin Time (UT)	Latitude	Longitude	Depth (km)	Magnitude (mb)	Distance** (km)	Type	Region
1	06/06/84	17:43:57.7	21.932S	139.020W	0	5.4	7541.6	Explosion	Tuamotu Is.
2	05/12/84	17:30:58.2	21.808S	139.013W	0	5.7	7534.5	Explosion	Tuamotu Is.
3	10/04/82	07:46:53.2	51.771N	176.809W	62	5.4	3790.3	Earthquake	Aleutian Is.
4	08/24/83	13:36:30.9	40.305N	124.767W	30	5.5	6806.8	Earthquake	California
5	11/16/83	16:13:00.0	19.433N	155.450W	11	6.3	3981.4	Earthquake	Hawaii

*Data taken from the National Earthquake Information Service, Preliminary Determination of Epicenters listings.

**Distance was computed to bottom hydrophone 76
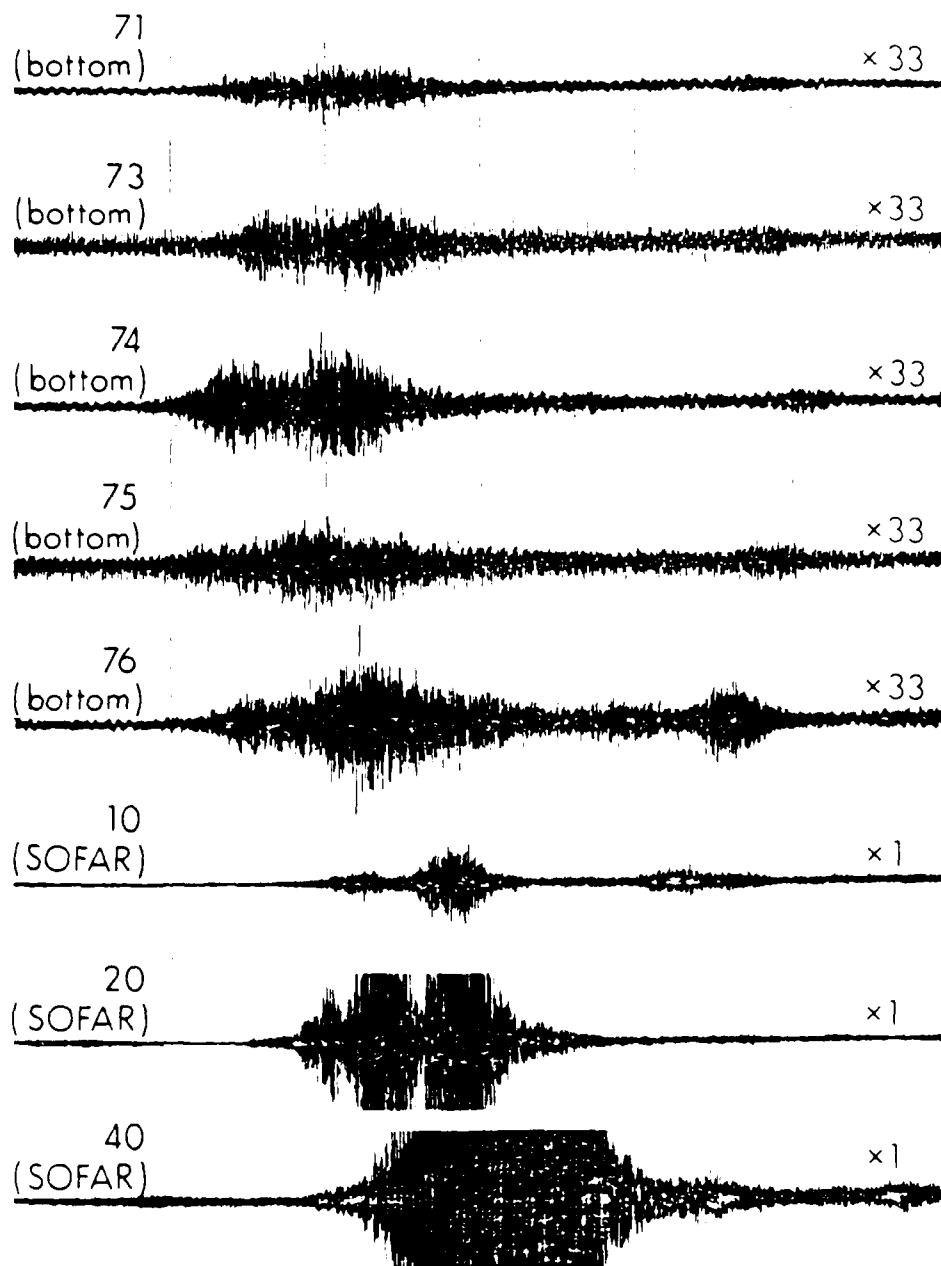
Fig. 2. T-phase signal from the California earthquake (event 4, Table 1) on eight hydrophones in the Wake Array. Hydrophone identification number and type are shown at the left of each trace, and the relative gain level is shown at the right. The time interval between vertical lines is one minute.

examination to the signals recorded by bottom hydrophone 76 and SOFAR
hydrophone 20. Reasons for this limitation were: (1) hydrophone 76 was
generally representative of all bottom hydrophones due to their proximity;
and (2) only hydrophone 20 of the SOFAR group was being recorded at the
times of the Tuamotu explosions due to hardware testing at Wake. Shown in
Figure 3 are compressed plots from these two hydrophones of the T-phases
from all of the events in Table 1. Note that the explosion T-phase onsets
are generally more impulsive than the earthquake T-phase onsets. Also note
that a large portion of the total energy in the explosion signals appears
concentrated near the beginning of the coda. These characteristics of the
time domain are similar to those previously reported by Milne (1959).

AVERAGE POWER SPECTRA

Computations of average power spectra referred to in this report were
made in the following manner. The section of time series of interest,
sampled at 80 samples per second, was divided into 512-point segments, each
with a 50% or 256-point overlap with adjacent segments (e.g., a 1024-point
section would be divided into three 512-point segments). The purpose of
this overlap was to ensure more complete coverage of the data after
windowing. Next, each segment was windowed and a 512-point FFT made,
producing 256 estimates of power spectral density. An average value for
each of the 256 estimates was then computed based on all the segments in the
section. These values were then smoothed in frequency using a 1-Hz window.
Average power spectra were also computed in identical fashion for a
corresponding section of ambient noise preceding each signal. This noise
power was then subtracted from the signal power (which was originally the
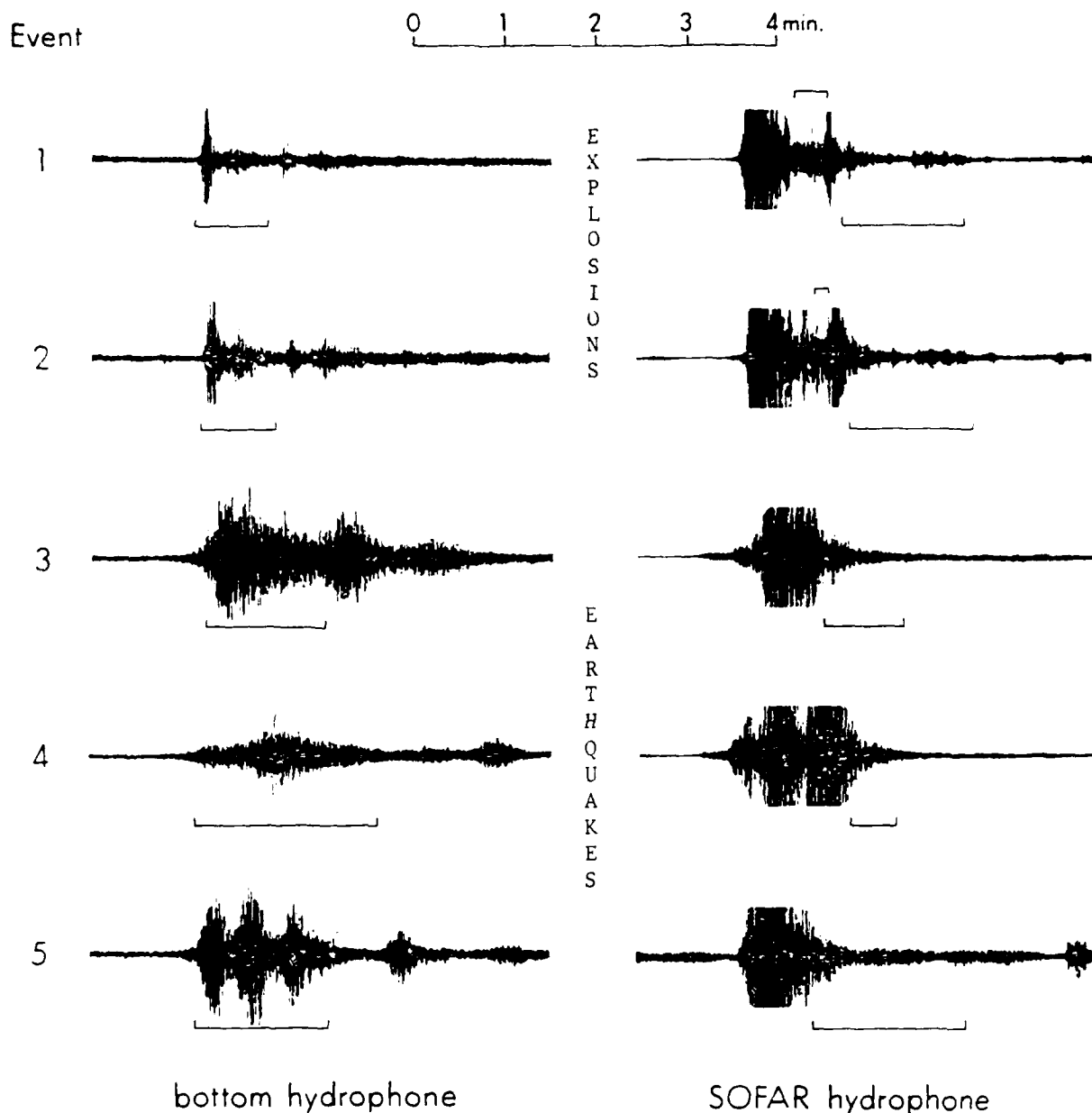
Fig. 3. Compressed plots of T-phases recorded by bottom hydrophone 76
and SOFAR hydrophone 20. Event numbers refer to events listed in Table 1.
Bottom hydrophone signals have been amplified by a factor of 20 relative to
SOFAR hydrophone signals. Truncated portions of SOFAR T-phases indicate
clipping by the digital recording system, and were not used in the spectral
analysis. Brackets indicate intervals over which average power spectra
shown in Figures 4 and 5 were computed.

signal plus noise). Only signal-to-noise levels greater than 4dB have been used in this report.

DETECTION THRESHOLD

It has long been known that the threshold for detection of earthquakes is much lower using T-phases than using any other seismic phase provided most of the travel path is oceanic. For example, Johnson and Northrop (op. cit.) estimated that T-phase surveillance extended the coverage of earthquakes in the Aleutian Islands to a magnitude about 0.7 lower than that provided by seismometer networks existing at that time. Figure 4 shows spectra from the Tuamotu explosion T-phases as recorded by the SOFAR hydrophone. Also shown are noise levels from a period several minutes prior to the T-phase arrivals. The maximum signal-to-noise ratios, which are at approximately 5 Hz, are about 35dB and 44dB from the magnitude 5.4 and 5.7 explosions, respectively. Applying a linear extrapolation to these data, using the ratio of 20dB per unit magnitude change, implies an average detectability threshold of approximately 3.6 in magnitude. Furthermore, Figure 3 shows that these spectra were not taken at the time of maximum amplitude, since at that time the signal was distorted by the recording system. Assuming, conservatively, that the maximum amplitude of these T-phases is a factor of two (6dB) larger, then the magnitude detection threshold of the Wake Array for explosions from the French Test Site is at least 3.3.

EXPLOSION/EARTHQUAKE DISCRIMINATION

Shown in Figure 5 is a comparison between the spectra of T-phases produced by explosion and earthquake sources. Since the explosions and
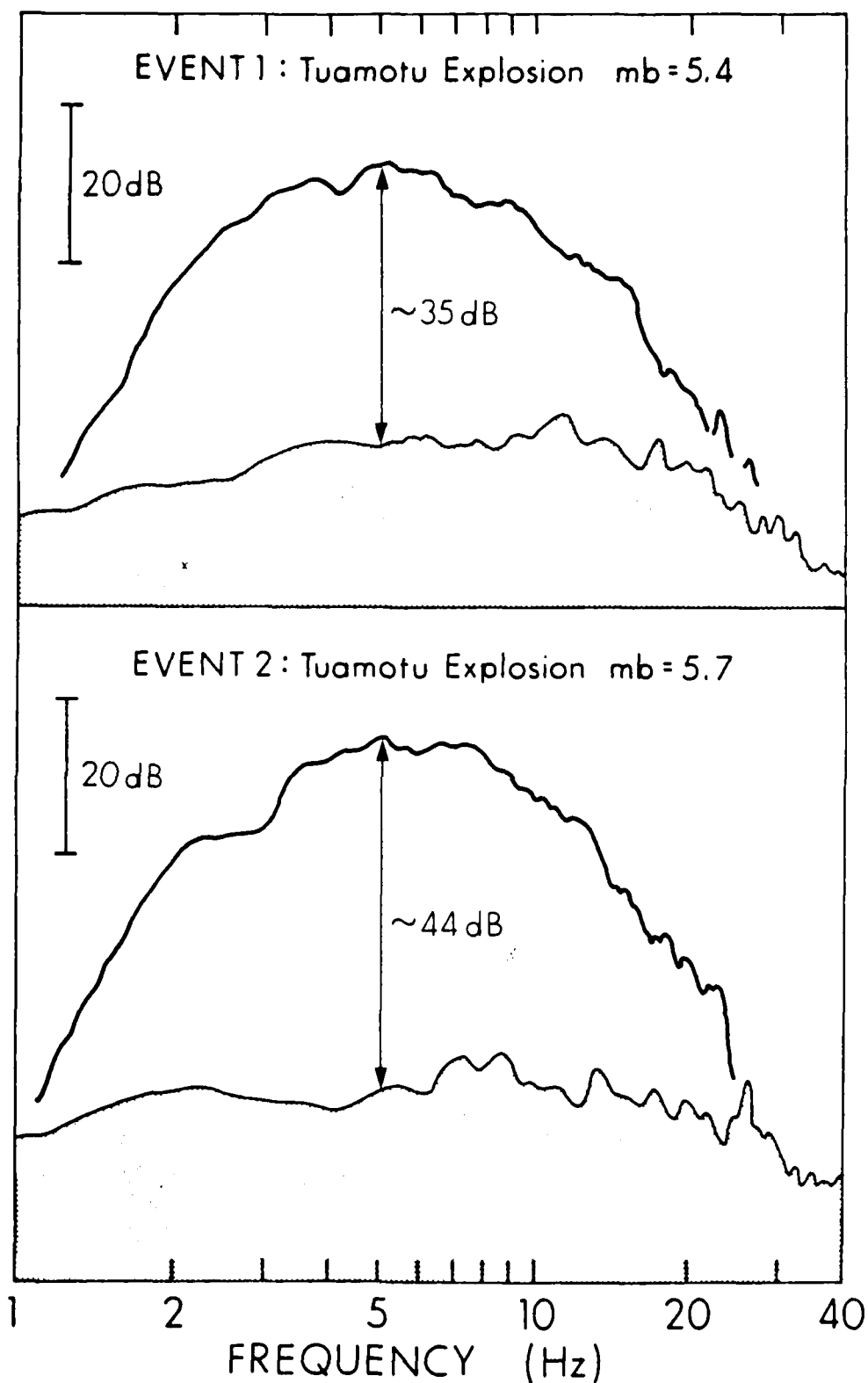
Fig. 4. Average power spectra for the T-phase arrivals from the
Tuamotu explosions as recorded by the SOFAR hydrophone. The time interval
over which these spectra were computed is indicated by the brackets above
the corresponding time series shown in Figure 3. Also shown are
corresponding noise levels (shaded region).
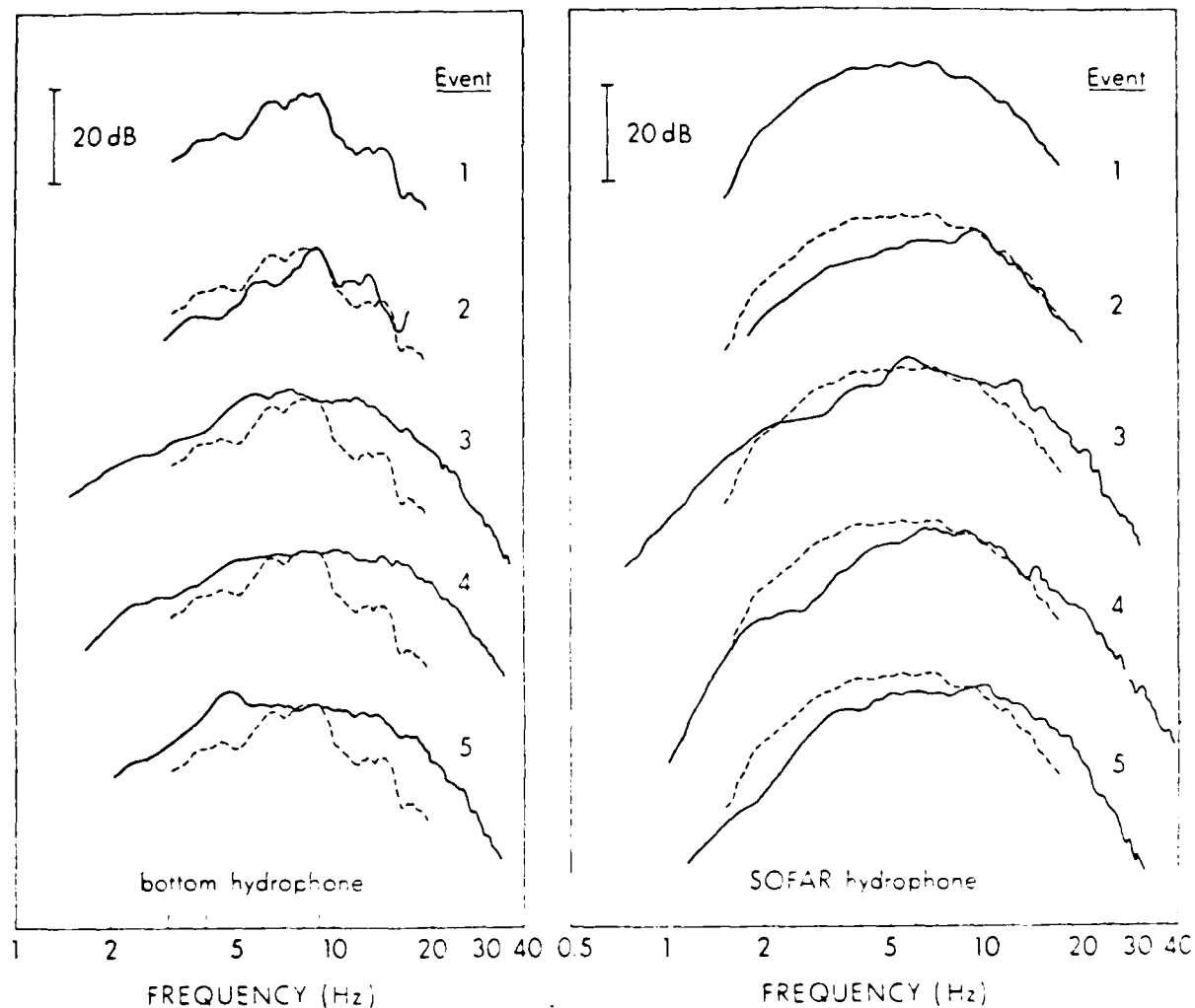
Fig. 5. Average power spectra of explosion (events 1 and 2) and earthquake (events 3, 4, and 5) generated T-phases as recorded by both a bottom and SOFAR hydrophone. The interval of time over which these spectra were computed is indicated by brackets below each corresponding time series as shown in Figure 3. The spectra of event 1 has been superimposed upon each of the other spectra for comparison by matching levels at 9 Hz.

earthquakes are of slightly different magnitude and are at different epicentral distances, emphasis for this comparison is not on absolute levels, but on characteristics of the spectral shape. Discriminants based on the spectral shape of P-wave coda have been shown to be effective (e.g., Evernden, 1977); and differences in the spectral shape of P have already been observed on the Wake Array between earthquakes and Soviet test explosions (McCreery et al., 1983). In order to facilitate this type of comparison, the spectra of the magnitude 5.4 Tuamotu explosion (event 1) shown in Figure 5 has been superimposed upon the spectra of each of the other events shown, by matching levels at 9 Hz. (The choice of this frequency was somewhat arbitrary, although it is the frequency of maximum energy for event 1 on the bottom hydrophone).

It would appear from the figure that there are some systematic differences between the subsets of explosion and earthquake generated T-phase spectra. On the bottom hydrophone the explosion T-spectra are relatively weaker at frequencies below 7 or 8 Hz, but this relationship does not hold on the SOFAR hydrophone. Above about 10 Hz, however, the explosion T-spectra are less energetic than the earthquake T-spectra for both the bottom and SOFAR hydrophones. This observation is quite similar to one made by Milne (op. cit.) who compared the spectra of T-phases generated by a nuclear explosion at Eniwetok and a California earthquake, and found relatively lower explosion energy levels between about 10 and 30 Hz. (This result was not explicitly stated but was taken from a figure showing the complete spectra).

These observations may not necessarily be the result of differences between the source spectra. Johnson et al. (1968) have shown that large differences in T-phase spectra exist between two types of arrivals, classic

and abyssal, which have different mechanisms for coupling into the water. It is certainly feasible that energy from a very shallow-focus explosion within an atoll might couple into the water differently than energy from an earthquake in a subduction zone under the Aleutians, or an earthquake under the continental shelf off of California, or an earthquake 11 km beneath Hawaii. Another factor which would affect the T-phase spectral shape is frequency-dependent scattering along the travel path. Although the three earthquakes studied have relatively unobstructed paths to Wake (see Figure 1), the path from the explosions to Wake is highly obstructed at its beginning by the numerous islands and seamounts that make up the Tuamotu chain. Additional study is necessary to resolve the uncertainties relating to the source of differences between the explosion and earthquake T-phase spectra.

CONCLUSIONS

Because of its highly efficient propagation characteristics within the SOFAR channel, and its wide range of observable frequencies, the T-phase is one of the most important types of seismic phases for the study of earthquakes and explosions occuring in proximity to the world's oceans. The Wake Array is an ideal tool with which to study these phases because it has sensors located on both the axis and edge of the SOFAR waveguide and because a large percentage of all earthquakes occur in the Pacific region. Analysis of T-phases from two nuclear test explosions in the Tuamotus and from earthquakes in the Aleutians, California, and Hawaii has produced the following results: (1) the threshold of detectability at Wake of T-phases from Tuamotu test explosions is probably at least as low as 3.3 in body-wave magnitude; and (2) the T-phase spectra from Tuamotu test explosions exhibit

relatively lower levels of energy at frequencies above about 10 Hz, than do earthquake T-phase spectra. This second result might be the basis for a T-phase discriminant between the two types of sources. However, it might also be caused by differences in the mechanism of energy coupling into the SOFAR channel or in the amount of scattering by islands and seamounts along the travel path. Additional data and research is necessary to clarify this question.

ACKNOWLEDGEMENTS

REFERNENCES

Adams, R. D. (1979). T-phase recordings at Rarotonga from underground nuclear explosions, Geophys. J. R. Astr. Soc., 58, 361-369.

Everndon, J. (1977). Spectral characteristics of the P codas of Eurasian earthquakes and explosions, Bull. Seismol. Soc. Amer., 69, 1153-1171.

Johnson, R. H. and J. Northrop (1966). A comparison of earthquake magnitude with T-phase strength, Bull. Seismol. Soc. Amer., 56, 119-124.

Johnson, R. H., R. A. Norris, and F. K. Duennebier (1968). Abyssally generated T-phases, Am. Geophys. Union Geophys. Mono. No. 12, 70-78.

McCreery, C. S., D. A. Walker, and G. H. Sutton (1983). Spectra of nuclear explosions, earthquakes, and noise from Wake Island bottom hydrophones, Geophys. Res. Lett., 10, 59-62.

Milne, A. R. (1959). Comparison of spectra of an earthquake T phase with similar signals from nuclear explosions, Bull. Seismol. Soc. Amer., 49, 317-327.

Northrop, J. (1968). Comments on a paper by J. B. Sheperd and G. R. Robson, The source of the T phase recorded in the eastern Caribbean on October 24, 1965, Bull. Seismol. Soc. Amer., 58, 743-744.

SCIENCE

Kaitoku Seamount and the Mystery Cloud of 9 April 1984

Daniel A. Walker, Charles S. McCreery, and Firmin J. Oliveira

Kaitoku Seamount and the Mystery Cloud of 9 April 1984

Daniel A. Walker, Charles S. McCreery, Firmin J. Oliveira

On 9 April 1984, crews of three separate commercial airliners en route from Tokyo to Anchorage, Alaska, observed a gigantic mushroom-like cloud 180 miles off the coast of Japan at approximately 38.5 N, 146.0 E (Fig. 1). It was described as moving rapidly up and away from a stratiform layer of clouds at about 4300 meters (14,000 feet) eventually reaching a maximum altitude of about 18,000 m and a diameter of 320 kilometers. Although the explosion of a nuclear submarine seemed possible, none of the passenger or cargo planes examined in Anchorage showed any signs of radioactivity. No fireball or flash was observed. Nor were there any unusual effects on flight instrumentation. Also, dust collected from the scene by an F-4 Phantom fighter-bomber deployed by the Air Self-Defense Force of Japan showed no abnormal levels of radioactivity (1–5).

Another means of testing an explosion hypothesis (conventional or nuclear) is provided by recordings from an array of hydrophones located near Wake Island (Fig. 1). This array consists of eleven hydrophones, six on the ocean floor in a 40-km pentagonal arrangement (one of the elements is at the center of the pentagon) and five in the SOFAR (sound fixing and ranging) channel at three sites spanning 300 km. Data from eight of these eleven hydrophones have been recorded on a computer-controlled digital tape system almost continuously since September 1982. Two of the hydrophones are simultaneously monitored on drum recorders so that the data may be easily evaluated on a daily basis. The sensitivity of the instruments, which are monitored on Wake Island, the great efficiency of sound transmission in the world's oceans, and the relative proximity of the array to the source of any presumed underwater explosion make it unlikely that such an event could escape detection.

Evidence from the Wake hydrophone array. The drum recordings were searched for significant events in the hours and days preceding the reported

sightings [approximately 14 to 15 hours universal time (UT)]. Continuously running spectrograms were also made for the 20 hours preceding the sightings. In neither the time nor frequency domain could a single prominent event be found that originated north and west of the array. Instead, the most conspicuous feature was a swarm of T-phases (Figs. 2 and 3) originating north and west of the array. We found that the swarm started

around 14 or 13 March (there are no data for 13 March) and terminated around 15 April. Figure 4 shows the estimated number of these T-phases from the drum recordings for 1 March through 30 April. [Had specially filtered playbacks of digital tapes rather than the drum recordings been used (their use was not justified because of costs), many more T-phases would have been observed.] These observations and considerations are consistent with those of the Réseau Sismique Polynésien stations in Tahiti. These stations reported more than 500 signals from 25 March through 30 April; 300 were observed between 2 and 9 April (6). The arrival times of the most prominent T-phases at all of the hydrophones in the array restricts the direction of the source of the T-phases to bearings within the 2-second contour of Fig. 1. Theoretical T-phase arrival times across the array, based on a propagation velocity of 1.48 km/sec (7), differ on the average by less than 2 seconds from the corresponding observed arrival times for any source located within that contour. Mean observed values used in comput-

ing the standard deviations were obtained from the arrival times of six T-phases with especially distinct onsets at all of the hydrophones.

We attempted to obtain independent confirmation of the source location from other seismic arrivals [that is, Po So phases (8)] but could find none at appropriate times preceding the strongest T-phases or those T's with large signal-to-noise ratios. Preliminary listings of earthquakes by the National Earthquake Information Service (NEIS) indicate no earthquakes within the 2-second contour during the swarm. (Most earthquakes reported by NEIS in the Mariana through Bonin portion of the circum-Pacific arc produce observable Po So phases at Wake. In fact, the Wake Island array often records Po So phases from earthquakes in this area that are not reported by NEIS.) Figure 3 shows a comparison of the character of these swarm-associated T-phases with the T-phases of earthquakes reported from the

Abstract. *On 9 April 1984, commercial airlines enroute from Tokyo, Japan, to Anchorage, Alaska, reported an unusual mushroom-shaped cloud at about 38.5 N, 146.0 E. On 8 and 9 April the intensity of volcanism from Kaitoku Seamount (26.0 N, 140.8 E), as indicated by T-phase recordings on an array of ocean bottom hydrophones, reached a maximum level and then declined rapidly. An examination was made of the possible relation of the cloud to eruptions of Kaitoku through an analysis of pilot depositions, satellite photos, wind charts, signal strengths and spectra of known man-made underwater explosions, as well as ascent rates of volcanic plumes and cumulonimbus clouds.*

same general area (Fig. 3). SOFAR recordings (Fig. 3, phone 20) of T-phases associated with the swarm are impulsive and decay rapidly, whereas similarly recorded T-phases associated with earthquakes are less impulsive and decay more slowly. We then showed that the swarm-type T-phases are related to a submarine volcanic eruption, an event that was confirmed by eyewitness accounts. We used the designation "submarine volcanic eruption" for the swarm-type T-phase in Fig. 3, 5, and 6 because of its importance, even though there is no certainty that an actual outpouring of material was associated with the particular T-phase chosen for these figures, nor, for that matter, with any of the several hundred other T-phases observed.

Spectrograms and spectra for the T-phases in Fig. 3 and for a T-phase from a man-made underwater explosion of unknown origin (9) are shown in Figs. 5 and 6, respectively. The swarm-type T-phase

resembles the T-phase from the underwater explosion more closely than it resembles the earthquake T-phase (Figs. 5 and 6). Swarms of strong, impulsive T-phases of short duration with weak or nonexistent seismic arrivals have been reported (10, 11). Such activity has been attributed to submarine volcanism and confirmed by eyewitness accounts of eruptions (12). Visually confirmed sequences originated at the Myojin volcano (31.9°N, 139.9°E) near Tori-shima at 30.7°N, 139.8°E, and near Farallon de Pajaros at 20.4°N, 144.8°E (Fig. 1). All of these volcanoes have long eruptive histories and are listed in *Volcanoes of the World* (13). Myojin is classified as a submarine volcano, and Tori-shima and Farallon de Pajaros are listed as stratovolcanoes with eruptive submarine flanks.

From the preceding considerations, it is reasonable to suggest that the source of the T-phase storm may be submarine volcanism, probably located in that portion of the circum-Pacific arc intersected by the 2-second contours. Known volcanoes in this region are at 27.2°N, 140.9°E (Nishino-shima); 26.1°N, 144.5°E (unnamed); and 26.0°N, 140.8°E (Kaitoku Seamount) (Fig. 1). Of these, the most certain candidate is Kaitoku. Evidence is provided by the following narrative (14).

On 7 March [1984] at 1230, the crew of a Japan Maritime Safety Agency (JMSA) transport plane flying about 130 km N of Iwo Jima observed a fan-shaped zone of discolored seawater that extended about 25 km WSW from a submarine vent. The maximum width of the discolored zone was about 9 km. A helicopter from the base at Iwo Jima flew over the area shortly thereafter, and its crew estimated that the extent of the reddish-brown water was roughly as large as Iwo Jima Island (about 5 by 8 km). The next morning, JMSA personnel observed continuous submarine eruptive activity. Gray or yellowish-brown water was ejected every 10 minutes, and waves spread outward from the vents. The sea colors included gray, white, yellowish-brown, and reddish-brown. The JMSA observers saw neither plumes nor floating ejecta, although small white plumes and rocks or reefs were seen during a flight by the Japan Maritime Self-Defense Force (JMSDF) at about noon the same day. On 12 March, personnel aboard a JMSDF patrol plane again saw floating material, and a plume about 100 m above sea level. Only discoloration was found during a JMSA flight 13 March. As of the 13th, no new island had been observed at the eruption site. The activity was located near the site of an eruption reported in 1543 at 26.00°N, 140.77°E.

40°N

○ Mystery cloud

Honshu

• Myojin
• Tori-shima

30°N

• Kaitoku
• Iwo Jima
△ Earthquake

20°N
• Farallon de Pajaros

Wake Island

140°E   150°E   160°E
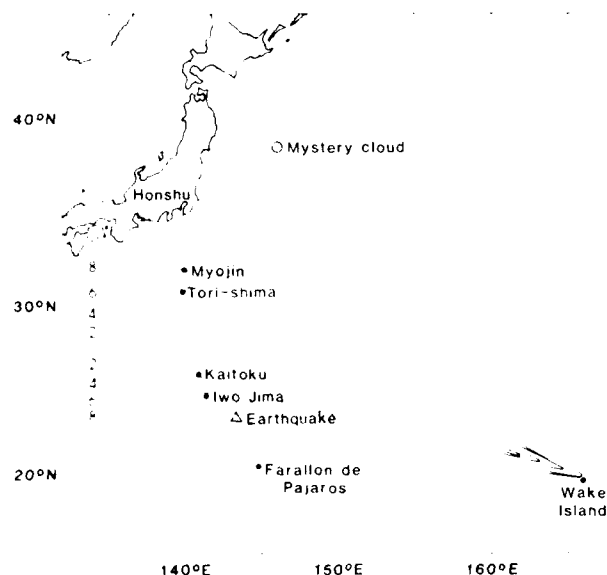
Fig. 1. Map showing the locations of the mystery cloud, Wake Island, some of the volcanoes south of Honshu in the Bonin, Volcano, and Mariana islands region, and an earthquake epicenter. Contours of standard deviations in seconds are shown for the location of the T-phase source for the swarm of March and April of 1984 (see text for further explanation).

March
2
8
14
19
22
28
30
31

April
3
6
8
9
11
16
21
27
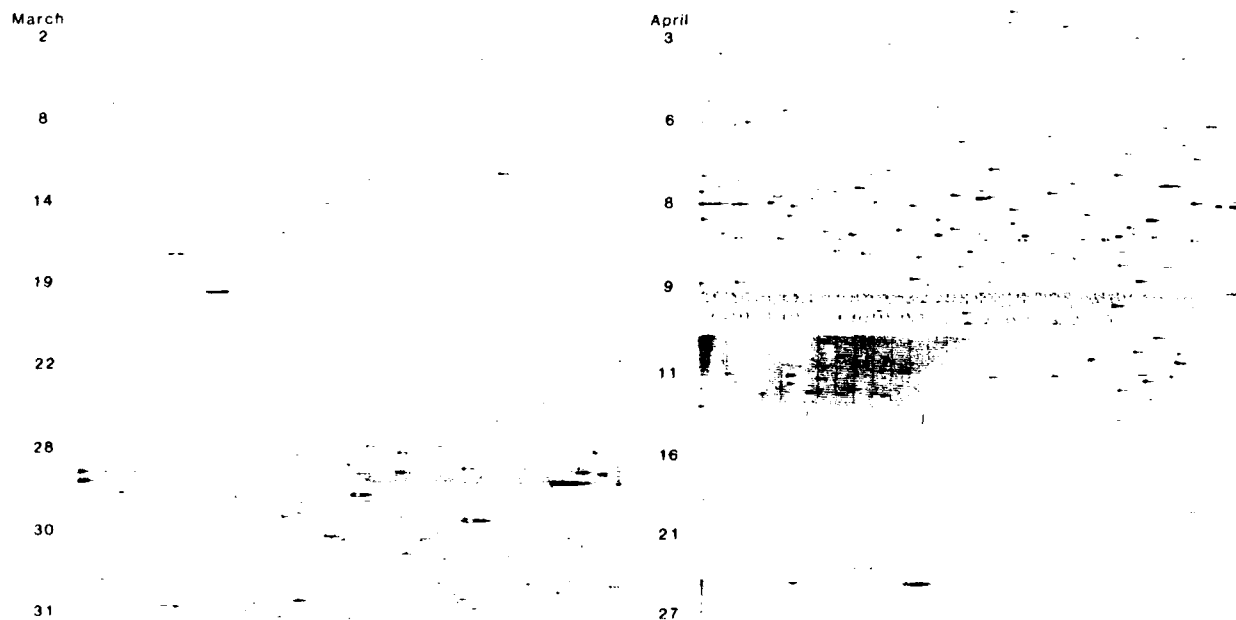
Fig. 2. Samples of hydrophone drum recordings from 1 March through 30 April 1984. Time increases from left to right and from top to bottom. Each recording is for a 24-hour period (48 horizontal traces) beginning around 0500 hours UT on the date indicated. Minute marks appear as vertical bands. A swarm of arrivals, T-phases from Kaitoku Seamount, reach their highest level around 8 April. Additional phenomena, more readily apparent on the full-sized originals of these and other recordings, include ground arrivals from distant earthquakes and underground explosions, ship noise, underwater explosions, biological noise, and wind- and storm-generated noise.

The histogram in Fig. 4 shows that some T-phase activity was observed at the time (7 through 12 March) of these visual observations. This level of activity is extremely low compared to that which followed, especially from 26 March through 14 April. The highest levels occurred on 31 March and 8 April, with the amplitudes of T-phases on 8 April being significantly larger than those observed on 31 March (Fig. 2). Was this high level of activity just 1 day before the sightings of the mystery cloud a coincidence?

Did Kaitoku produce the mystery cloud? A cloud that caused the concern of experienced flight crews can reasonably be considered to be very unusual. The captain of one of the airliners, a veteran of 41 years, immediately issued a Mayday alert to Anchorage International Flight Service and put his crew on oxygen as a precautionary measure (1). Later he stated that he had "never seen anything like it except in newsreels and films" (3). Similarly, the occurrence of large T-phase swarms over a 3- to 4-week period is very unusual. Since operation of the upgraded system at Wake began in September 1980, only one other suspected swarm was observed on the visible recordings. It occurred on 9 July 1983, lasted for only 26 hours, and had its origin along an azimuth north of Kaitoku.

Since Kaitoku generated a plume on 12 March, it seems possible that the greatly increased activity from 26 March through 14 April could have produced a substantially greater cloud. Such eruptive plumes frequently reach altitudes in excess of 5 km (15) and can form in a relatively short time. Examples include a 12-km cloud generated in about 2 minutes (16), a 20-km cloud in about 5 minutes, and a 30-km cloud in about 25 minutes (17).

Satellite photographs for 8 and 9 April were also examined for volcanic emissions (18). Because of extensive cloud cover south and east of Japan, no conclusions could be drawn from the photographs. If Kaitoku did, indeed, produce a plume around 9 April 1984, a crucial question is whether winds were favorable for transporting the plume to the observation site approximately 1470 km to the northeast. Since the mystery cloud was observed initially at an elevation of about 4300 m (2), wind analysis charts at the 700-millibar (~3000 m) and 500-mb (5500 m) levels were examined for 8 and 9 April (19). Wind directions were not favorable, generally heading southeast across the northern part of the Philippine Sea through the Bonin, Volcano, and Mariana islands area and on into the

western Pacific. Wind charts were available only at 12-hour intervals, but because of the consistency of wind patterns, any significant changes were unlikely during these 12-hour intervals.

Even if the negative evidence from the wind analysis is dismissed, other important questions have to be resolved. One is whether a volcanic plume transported to the site of the mystery cloud would have a spherical shape. Under the mechanism being considered, a powerful eruption over several hours would produce a cloud that is elongated horizontally. Therefore, if Kaitoku did produce the spherical mystery cloud, the eruption would have had to be of short duration, lasting 2 hours or less. The question then arises as to how such a cloud could have escaped detection at its source and throughout its path to the mystery cloud site. This, most likely, could have happened only if the eruption and transport occurred at night, since a cloud produced during daylight hours (assuming good visibility) could easily be observed from Iwo Jima, the nearest inhabited island (Iwo Jima, which has a maximum

elevation of 169 m, is about 130 km south of Kaitoku). Pilots on the Tokyo-Anchorage route made their observations at about 1400 UT. For a 10-hour travel time (implying average wind velocities of at least 147 km hour), this would suggest a time of origin for the cloud of about 0400 UT at Kaitoku. Sunset at Kaitoku would not have occurred until nearly 5 hours after the hypothetical eruption (20). Not only is Iwo Jima inhabited, but from 7 March through at least 10 May, the activity of this volcano was monitored by airplanes and helicopters of the Japan Maritime Safety Agency (JMSA), which has a base at Iwo Jima. They formally named this volcano Kaitoku Seamount and reported (2) that eruptive activity [...] mid to late March [...] vapor plumes [...] Beginning in April [...] Their only notation for 8 to 9 April [...] on 9 April the area [...] covered [...] km [...] previously reported [...] by 30 km [...] JMSA [...] ment of [...]

Submarine volcanic activity   Kaitoku Seam[...]

26.0°N, 140.8°E   11 April 1984   16 44 06   Δ=26[...]

Phone 73
x 20

Phone 20
x 3

16:49:03   T

Earthquake – Volcano Island region

23.4°N, 1343.3°E   13 January 1984   01:03.41.2   Δ=23 27°

Phone 73
x 40

Po   o

Phone 20
X 12

Po   So
01:05:00   1 minute   T
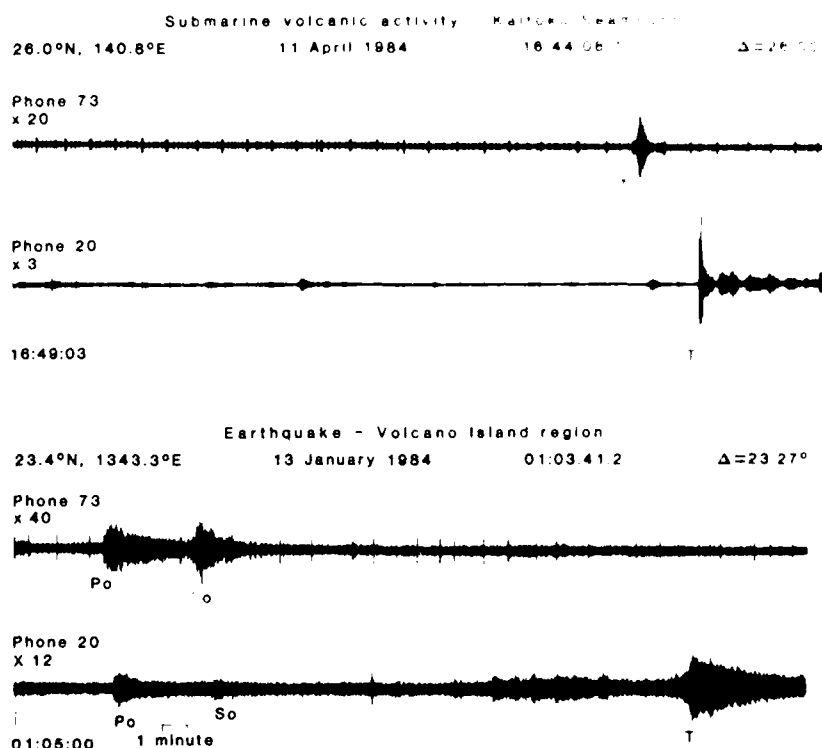
Fig. 3. One of the swarm-type Kaitoku T-phases from Fig. 2 shown in an expanded time scale. Also shown is an earthquake T-phase recorded on the same hydrophone. The earthquake-generated T-phase, unlike the swarm type T-phase, has associated ground arrivals [that is, Po, So phases (8)]. Phone 73 is one of the bottom phones (5.5-km depth) of the pentagonal array and phone 20 is a shallower phone suspended near the axis of the SOFAR channel (1-km depth). Relative gain levels are shown above the beginning of each trace. As indicated by these recordings, bottom phones are generally better receptors of ground phases, and SOFAR phones are generally better receptors of T-phases. Earthquake data were taken from the National Earthquake Information Service PDE listings. The depth and magnitude given for this earthquake are 33 km and 5.3 mb, respectively.
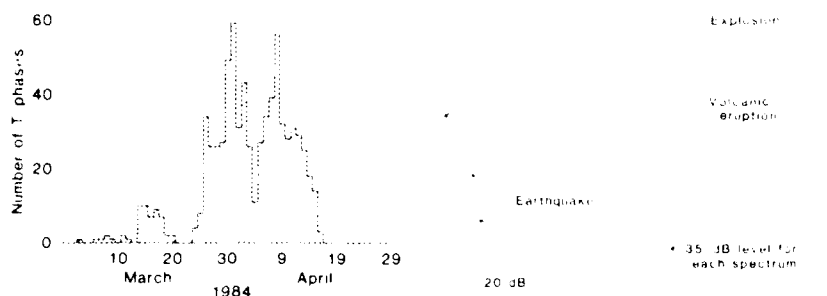
Fig 4 (left). Estimated daily number of T-phases on the drum recordings (see Fig 2) from 1 March through 30 April. Although numbers for 30 and 31 March are somewhat higher than the numbers for 7 and 8 April, it is apparent from Fig 2 that T-phases observed on the later dates have substantially greater amplitudes. No recordings are available for 13 March because of a power outage. Fig. 5 (right). Spectra for the T-phases shown in Fig 6. Only portions of each spectrum, where signal levels are at least 4 dB above the noise, are shown. System response has not been removed. A common level of 35 dB is indicated for each spectrum. Again, the similarities between the explosion and eruption spectra are evident.

32 seconds
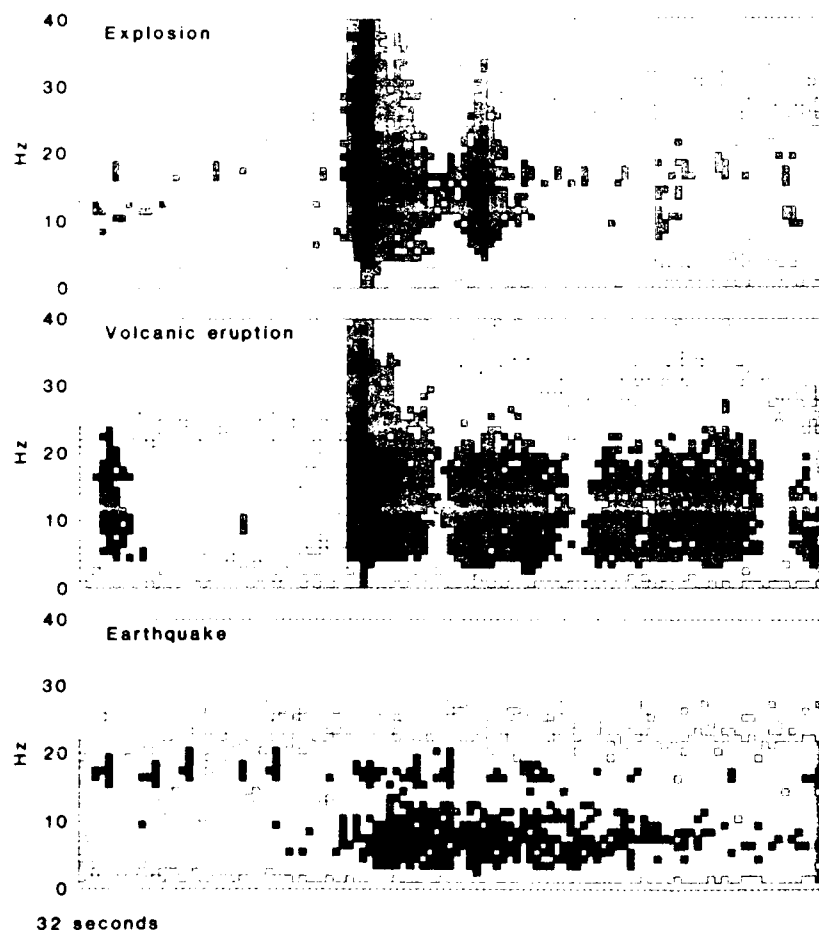
Fig 6 Spectrograms for a T-phase produced by a man-made underwater explosion and for the eruption and earthquake T-phases shown in Fig 3. All recordings are from phone 20. Time increases from left to right and frequency from bottom to top. Energy levels increase from light to dark with 12 decibels between shades. System response has not been removed. Brackets under each T-phase indicate the portion of the record from which the spectra shown in Fig 5 were made. A comparison of the impulsive character and high-frequency content of these spectrograms shows that the spectrograms of the explosion and eruption are most closely related.

in April must have been based entirely on visual inspection rather than seismic monitoring, since 253 T-phases from the volcano were counted on the drum recordings at Wake during the last 15 days of March as compared with 444 during the first 15 days of April.)

Another question concerns the rise time of the mystery cloud. It emerged from a stratiform layer at about 4300 m and rose in about 2 minutes (3) to a maximum altitude of 18,000 m where growth continued until the cloud dissipated about 40 minutes after the initial sightings (2). If a plume from Kaitoku was transported 1470 km to the mystery cloud site, what was the mechanism for a vertical ascent of the volcanic materials at a rate of about 7 km/min? The only known natural phenomenon capable of producing such rapid and extensive vertical motions are volcanic eruptions at their source. The highest recorded updraft velocities for cumulonimbus clouds are in the range of 90 miles per hour (2.4 km/min) (22). Furthermore, to produce an apparent ascent rate of 7 km/min for the cloud top (as was observed for the mystery cloud), the actual updraft velocity required would be approximately 14 km/min (23).

In view of the foregoing analysis, the submarine eruption of Kaitoku Seamount and the sighting of the mystery cloud must be coincidental.

Other Possible Explanations. Remaining hypotheses include other volcanic eruptions and man-made explosions. No known active submarine volcano exists at the site of the mystery cloud. As demonstrated by the Kaitoku investigations, any submarine volcanism at 38.5 N, 146.0 E, would have been detected by the Wake hydrophones. No such activity was found. The only other reported eruptions that might be remotely considered occurred at Klyucheveskaya Volcano (56.2 N, 160.8 E) in the Kamchatka Peninsula. Strombolian activity is reported only for 22 May, although the number of earthquakes increased from late March through May. No special mention is made of activity on 8 or 9 April (24). Klyucheveskaya Volcano is approximately 2250 km northeast of the mystery cloud site and winds were unfavorable (generally to the east-northeast) on 8 and 9 April at the 4300-m and 5500-m levels. No volcanism was reported for the Kurils; in Japan the long-term, well-monitored activity of Sakura-jima Volcano (31.6 N, 130.7 E; southwestern Japan, outside of the area shown in Fig. 1) continued throughout April with no reports of a large explosion

on 8 or 9 April (25). Twenty-five explosions were observed at Sakura-jima during April: one on 8 April and one on 9 April. The largest explosions occurred on 12, 19, and 29 April. For January, February, and March 1984, the number of explosions reported are 22, 26, and 34, respectively. It is reasonable to assume that if the moderate or small explosions on 8 and 9 April produced the mystery cloud, then many other similar clouds produced by even larger eruptions of Sakura-jima should have been sighted. The current eruptive phase of Sakura-jima began in 1955 (26). Suwanose-shima Volcano in the Ryukyu Islands (29.5 N, 129.7 E) (not shown in Fig. 1) has been active since November 1982, but nothing unusual was reported at this location for 8 and 9 April (27). As with Sakura-jima, if Suwanose-shima produced the 9 April mystery cloud, other similar clouds should have been sighted.

Conclusions. Wake Island hydrophone recordings were searched for possible explanations of the mystery cloud observed at 38.5 N, 146.0 E, by flight crews of commercial airlines. No evidence is found for a single large underwater explosion from this or other locations at the time of the sightings or in the hours preceding those sightings. Instead, the most conspicuous feature of the recordings is a swarm of impulsive T-phases that began in March 1984 and intensified to a maximum around 8 or 9 April, just before and during the sightings of the mystery cloud. The source of this activity was estimated to be in the Volcano Islands (south of Japan), and this estimate was confirmed by sightings of active submarine volcanism by the JMSA, which formally named the volcano Kaitoku Seamount. Because of Kaitoku's remoteness and the intensity of activity on 8 and 9 April, it seemed possible that during the nighttime hours favorable winds could have transported a volcanic plume northward approxi-

mately 1470 km over the Pacific to the mystery cloud site. Analyses of wind directions at 4300- and 5500-m levels, however, revealed that materials at these elevations over Kaitoku would be transported not to the north but to the east or southeast. Furthermore, even if favorable winds had been found, no natural mechanism could produce the observed rise time of the cloud at 38.5 N, 146.0 E (from about 4300 m to 18,000 m in approximately 2 minutes)—with the possible exception of another volcanic eruption at that site. Submarine volcanism at 38.5 N, 146.0 E, would have been recorded by the Wake hydrophones. No such activity was found. It is unlikely that any other volcanic eruptions could have produced the mystery cloud.

Therefore, on the basis of data available at this time, our analyses indicate that the mystery cloud was produced either by an as yet unknown natural phenomenon or by a man-made atmospheric explosion.

References and Notes

1. Transcription from Japan Airlines flight 036 to Anchorage International Flight Service on 9 April 1984, at 1406 Greenwich mean time. Federal Aviation Administration (FAA)—Alaska Region.
2. Report of interviews taken by Jim Derry, Special Agent, FAA-Alaska Region, with C. H. McDade, Captain, Japan Air Lines flight 036; Cornelis Vander Berg, Captain, KLM Royal Dutch Airlines flight 868, Reint Sol, First officer, KLM Royal Dutch Airlines flight 868, and Mike Howe, Captain, Flying Tiger Lines flight 078.
3. Anchorage Daily News, 10 April 1984, p. A-1.
4. Ibid., 12 April 1984, p. A-1.
5. Honolulu Advertiser, 10 April 1984, p. B-1. Newsweek, 30 April 1984, p. 25.
6. SEAN Bulletin 9-4, 8 (1984).
7. The value 1.48 km/sec was taken from R. Johnson and R. Norris [J. Geophys. Res. 73, 4695 (1968)].
8. For a recent discussion of Po So phases, see D. Walker [Eos 65, 2 (1984)].
9. This explosion T phase was one in a sequence of 11 observed between 0307 and 0518 hours on 9 April 1984. Four occurred at intervals of 5 minutes, three were observed later at 5-minute intervals, and the rest were recorded at random intervals. All of these phases were similar in their appearance and offset times on the differing hydrophones. Some variations in amplitude were observed. Estimated source locations are at an azimuth to the array approximately 50

north of west. Solutions within a 2-second contour begin along this azimuth at a range of about 300 km and extend to the antipode of the array. Included among the many source locations is the observed site of the mystery cloud. These explosions occurred 9 to 11 hours before the first sighting of the mystery cloud. Had a cloud been produced at those times (local midafternoon) at the mystery cloud site, it seems likely that it would have been observed before the sightings at 1400 U.T. Similar experiments in the northwestern Pacific are often recorded by the Wake hydrophone array.
10. R. Norris and R. Johnson, J. Geophys. Res. 74, 650 (1969).
11. R. Norris and D. Hart, ibid. 75, 2144 (1970); R. Johnson and R. Norris, ibid. 77, 4461 (1972).
12. For the Myojin volcano, see R. Morimoto [Bull. Volcanol. 2-23, 151 (1960)]; for Tori-shima, see (10); and for Farallon de Pajaros, see H. Kuno [Catalogue of the Active Volcanoes of the World Including Solfatara Fields, part 11, Japan, Taiwan, and Marianas (International Association of Volcanology, Rome, 1962)].
13. T. Simkin et al., Volcanoes of the World (Hutchinson Ross, Stroudsburg, Pa., 1981).
14. SEAN Bulletin 9-2, 3 (1984).
15. G. Macdonald, Volcanoes (Prentice-Hall, Englewood Cliffs, N.J., 1972).
16. ___, ibid., p. 328.
17. S. Thorarinsson, in The Eruption of Hekla 1947–1948, T. Einarsson, G. Kjartansson, S. Thorarinsson, Eds. (Visindafelag Islendinga, 1954), p. 2.
18. Infrared photographs taken at 3-hour intervals from Geostationary Meteorological Satellite 1. Space shuttle photography was also examined by C. A. Wood of the Lyndon B. Johnson Space Center, but no pictures were available for the northwestern Pacific.
19. The 500-mb and 700-mb wind charts for the northern hemisphere were provided by the National Climatic Data Center.
20. The Astronomical Almanac for the Year 1984 (Government Printing Office, Washington, D.C., 1983).
21. SEAN Bulletin 9-5, 6 (1984).
22. T. A. Schroeder, personal communication. He is assistant professor of Meteorology, University of Hawaii at Manoa, and former chairman of the American Meteorological Society's committee on severe local storms.
23. H. R. Byers and R. R. Braham, Jr., The Thunderstorm (Government Printing Office, Washington, D.C., 1948).
24. SEAN Bulletin 9-5, 4 (1984).
25. Ibid., p. 5.
26. Ibid. 9-3, 24 (1984).
27. Ibid., p. 25.
28. This research was sponsored by the Physical and Geophysical Sciences Directorate of the Air Force Office of Scientific Research under contract F49620-84-C-0003 and by the U.S. Arms Control and Disarmament Agency. We thank P. Steucke, Public Affairs Officer of the Federal Aviation Administration's Alaska Region, for providing transcripts and reports of interviews; T. Schroeder and J. Sadler for helpful comments and discussions on meteorological topics; G. P. L. Walker for discussions of volcanism; and A. Chang for bringing the mystery to our attention. We thank F. Berg and M. Garcia for reviewing this article and R. Punalei for editorial assistance. This is Hawaii Institute of Geophysics Contribution No. 1564.

23 October 1984; accepted 30 November 1984

University of Hawaii at Manoa

Hawaii Institute of Geophysics
2525 Correa Road • Honolulu, Hawaii 96822
Cable Address: UNIHAW

March 7, 1986

Christine Gilbert, Letters Editor
Science, AAAS
1333 H Street, NW
Washington, D. C. 20005

Dear Ms. Gilbert:

As suggested in your letter of 25 February 1986, we submit the following revised letter for publication in Science.

After the appearance of the article "Kaitoku Seamount and the Mystery Cloud of 9 April 1984" in Science (8 February 1985, pp. 607-611), the original data base was supplemented with additional testimony from Captain Van den Berg (KLM Royal Dutch Airlines flight #868) and another pilot (Captain Presley of Flying Tiger Airlines flight #022). Huub Eggen, editor of the Dutch publication Aarde & Kosmos, located Capatin Van den Berg and supplied us with a transcript of his interview along with six drawings depicting the event as viewed from the cockpit window. We submitted a number of additional questions which were subsequently answered by Van den Berg. [Eggen's article and the time-lapse drawings of the cloud appear in Aarde & Kosmos, v. 5, pp. 292-295, 1985.] To summarize the drawings we divide the event into four stages: (1) a towering cumulus-like cloud appearing to rise out of the stratiform layer; (2) fading of the cloud tower and replacement with a small semi-circular halo segment; (3) expansion of the halo to a full circle; and (4) further expansion and dissipation. The time elapsed from #1 to #3 was approximately 5 minutes. Stage #4 lasted for another 10 to 15 minutes, giving a total observation time of about 20 minutes from Van den Berg's vantage point. At the time Van den Berg was flying on air route A90 near the PAWES intersection at a speed of 500 knots. The change in Van den Berg's position from the begining to the end of his observations, along with Captain McDade's observations (Japan Airlines flight #036; 33 minutes behind Van den Berg on air route A90; approaching the PAWES intersection when he first sighted the cloud at 1349Z; 48 miles south of A90 and abeam of PAWES at 1406 when the sphere was dissipating), and Capatin Presley's observations (air route A90; behind McDade and approaching the SABES intersection) allows us to estimate the size and distance of the halo.

Our conclusion is that original estimated positions were in error. Additional data, primarily from Captain Van den Berg, places the event between the Kurils and Sakhalin. The altitude of the center of the halo at the maximum observed size is estimated in excess of 200 miles and the

AN EQUAL OPPORTUNITY EMPLOYER

diameter of the halo is estimated to be at least 380 miles. It seems
unlikely that a ground based explosion could produce this kind of an
effect. It is surprising to us that no official data has been provided by
government agencies and that such a significant observation from a region
of demonstrated military sensitivity was, and still remains, a mystery. In
retrospect, we believe that erroneous assumptions regarding the presumed
location of the mystery cloud may have contributed to the early dismissal
of a hypothesis which now deserves intense examination. The 10 April 1984
issue of the Anchorage Daily News reported that the Soviet Union had
informed Japanese officials that missile testing would begin on 9 April in
an area of the Pacific southeast of the northernmost Kuril islands. The 14
April 1984 issue of that paper reported that "a Japanese aviation official
confirmed Wednesday the Soviet Union had scheduled missile tests in the
northern Pacific, but not on the day or in the area where the mysterious
cloud burst was sighted".

Sincerely,

Daniel L. McKenna   Daniel A. Walker
Department of Meteorology   Hawaii Institute of Geophysics
University of Hawaii at Manoa   University of Hawaii at Manoa
Honolulu, Hawaii 96822   Honolulu, Hawaii 96822

DAW:en

Note regarding Appendix XI: Draft copies of "Stability of Yield Estimates Based on P and P Coda Recorded by Ocean Hydrophones" are not yet available for distribution at this time.

EARTHQUAKES IN THE "ASEISMIC" REGIONS OF THE WESTERN PACIFIC

Ken Muirhead[1] and R. D. Adams[2]

[1]Research School of Earth Sciences, Australian National University, Canberra.

[2]International Seismological Centre, Newbury, United Kingdom.

Abstract. Operators of a deep ocean hydrophone array near Wake Island in the northwest Pacific Basin have located several previously unreported earthquakes within 20° of Wake Island in the "aseismic" interior of the Pacific plate, and have suggested high attenuation in the source region to explain why these events have not been reported by seismological agencies. The largest such earthquake occurred on 1983 June 29, in the Kiribati region; readings were submitted to the International Seismological Centre, but the earthquake was excluded from the final analysis because of doubt about its location and interfering arrivals from other earthquakes. Closer examination now provides a well-determined seismological location and a magnitude of 4.7 (mb). Neither amplitudes nor frequency content of Australian records of the Kiribati earthquake support the existence of a region of abnormally high attenuation beneath the source. We suggest that the higher magnitudes reported from the hydrophone measurements result from the efficient coupling of energy from shallow intraplate earthquakes in the Pacific Basin into the P_o/S_o waveguide.

Introduction

Using recordings from an array of hydrophones near Wake Island in the northwest Pacific Basin, Walker and McCreery (1985) give details of several earthquakes originating from within the "aseismic" interior of the Pacific plate that were not reported by seismological agencies.

The largest of these occurred on 1983 June 29, near the equator in the basin between Nauru Island and Kiribati (Gilbert Islands) and will be referred to as the Kiribati earthquake. Although a direct estimate of the magnitude of these earthquakes could not be obtained from the hydrophones, the recorded amplitude of the Kiribati earthquake was several times larger than those of well reported earthquakes in the Mariana Islands, with magnitudes between 5.2 and 5.7 (mb), which were at similar distances from Wake Island. This comparison led Walker and McCreery to suggest that that either the large amplitudes were associated with the nature of the P_o/S_o waveguide (a high Q path close to the base of the crust c.f. Walker, 1977) in this area of the Pacific or that the body-wave magnitude of the Kiribati event could have been as large as 5.0 to 6.0.

Unlike the Mariana Islands earthquakes used for magnitude comparison, the Kiribati earthquake was not listed by the Preliminary Determination of Epicentres Service of the United States National Earthquake Information Service (NEIS). By assuming their second hypothesis, Walker and McCreery concluded that the tele-

---

[2]Also at Dept. of Geology, University of Reading.

seismic body-wave energy had been so attenuated that the signals were too small to be recorded by seismological stations around the Pacific; a conclusion which they sought to explain in terms of energy being trapped within the P_o/S_o waveguide, or alternatively, that energy on teleseismic ray paths had been highly attenuated by a region of low Q in the upper mantle beneath the epicentre. Walker and McCreery suggest that if either interpretation is correct, it is likely that other large events in the interiors of oceanic plates will have remained undetected.

We wish to show that earthquakes of the size of the Kiribati earthquake would normally be located by the present international network of seismological stations, and secondly that the magnitudes determined from hydrophone observations of the Pacific Ocean earthquakes have been overestimated.

Location

Although the Kiribati earthquake of June 1983 was not reported by the NEIS, it was found by the "search" procedure of the International Seismological Centre (ISC) which looks for associations among arrival times that have not been linked with earthquakes reported by other agencies [Adams et al., 1982]. Each month some 400 events are automatically located by this procedure. On inspection, about half are discarded as random misassociations or because they arise from too scant or implausible data. On the evidence then available, the event was discarded from the ISC files and was not included in the ISC bulletin. A closer examination, and the use of additional readings now gives a good seismological solution based on observations at 32 stations, well distributed in distance and azimuth (Table 1). The position found is 0.18°N, 169.97°E with standard errors in latitude and longitude of about 8 km. This position is close to that given by Walker and McCreery, but more accurately determined. The water depth in this region is about 4 km.

The lack of close stations (with the consequent focal depth - origin time tradeoff uncertainty) prevents the earthquake's depth being established geometrically, and the location has therefore been carried out assuming a surface focus. Later arrivals recorded at the Warramunga Seismic Array (WRA), shown in Figure 1, have been tentatively identified as phases associated with reflections from the sea bottom and surface. Similar phases are not well developed at the Yellowknife Array (YKA) and although these arrivals are consistent with a shallow event, uncertainty in sediment thickness prevents their use to give reliable estimates of focal depth.

The shallow depth is confirmed, however, by the origin time of the seismological solution, which is strongly dependent on the depth assumed. That derived from the Wake Island hydrophone pickings of Po, So and T phases, however, is largely independent of focal depth. After adjusting the Wake Island origin time for the revised epicentre, and the ISC origin time to take account of the 2 second offset in the Jeffreys-Bullen tables [Bullen, 1965], the ISC origin time for a surface

Table 1 The ISC solution for the 1983 June 29, Kiribati earthquake together with the relative station information.

```
ISC  Jun 29 16 15 02.2  0.18N   169.97E   0km 4.7mb
32 obs            ±0.4 ±0.06    ±0.07
      Kiribati (Gilbert Islands) region
```

Code	Station name	Delta deg	Az. deg	ISC ID	Ar time mn sec	ISC res
HNR	Honiara	13.81	226	P	18 22.0	0.1
PVC	Port Vila	17.89	185	P	19 17.2C	2.9
RAB	Rabaul	18.31	256	P	19 21	1.4
KVG	Kavieng	19.36	262	P	19 43	10.7
VUN	Vunikawai	19.91	156	P	19 41.8	3.3
SVA	Suva	20.01	156	P	19 41.5	1.9
KOU	Koumac	21.36	195	P	19 53.5D	0.0
NOU	Noumea	22.62	188	P	20 07.1C	0.9
MOM	Momote	22.67	264	P	20 11	4.2
CTA	Charters Towers	30.74	228	P	21 20.0	-1.6
BRS	Brisbane	32.01	210	P	21 31	-1.7
KRP	Karapiro	38.27	173	P	22 25.2	-0.9
GNZ	Gisborne	39.34	170	P	22 33	-2.1
YOU	Young	39.81	208	P	22 40.1	1.1
WB2	Warramunga Ar.	40.21	238	P	22 41.0	-1.4
CAN	Canberra	40.38	207	P	22 36.6	-7.1
MNG	Mangahao	40.92	174	P	22 46	-2.0
MSZ	Milford Sound	44.70	182	P	23 19	0.2
MAT	Matsushiro	46.64	324	P	23 39	4.7
BJI	Beijing	62.90	316	P	25 30	-2.7
COL	College Outpost	71.42	18	P	26 24.2	-1.9
SBB	Saddle Butte	75.31	54	P	26 50	0.6
PNT	Penticton	77.19	39	P	26 59.5	-0.2
INK	Inuvik	77.95	19	P	27 03.0	-0.5
SBA	Scott Base	77.97	181	P	27 05.1	1.6
SES	Suffield	82.84	39	P	27 29.6	-0.3
YKA	Yellow Knife Ar	83.13	27	P	27 30.9	-0.2
ALQ	Albuquerque	84.62	55	P	27 40	0.6
JCT	Junction City	90.11	60	P	28 06	0.0
SOB1	Sobradinho	147.99	107	PKP	34 51.0	3.3
ITR	Itaparica	150.47	108	PKP	34 57.0	5.4
BNG	Bangui	151.08	279	PKP	34 59.0	6.5

focus is later than the Wake Island time by only 0.9s, whereas this difference increases to 6.2s for an assumed depth of 33km.

Various factors can be invoked to explain why this event was not located earlier. One is simply the large number of earthquakes on a global scale. The ISC lists about 2,000 events a month, that is, several an hour. This can lead to confusion in the interfering of record traces at recording stations, and in wrong associations of readings with events. Both these factors were evident in this case.

On 1983 June 29, the ISC bulletin lists an earthquake in the Rat Islands only 2½ minutes after the Pacific event. Arrivals from the Pacific event would be in the coda of the Rat Islands earthquake at North American stations and some readings in Table 1 appear in the ISC bulletin as later phases (SBB, ALQ, JCT). The BJI reading was misassociated as an early arrival from the Rat Island earthquake. There is also evidence of a second interfering event in the Bismark Archipelago at stations RAB in New Britain and KVG in New Ireland.

The ISC search procedure finds more than 2,000 events a year unreported by NEIS or any other agency. In 1983 there were 38 of magnitude 5.0 (mb) or greater, mainly from the Fiji-Tonga-Kermadec region. Some such events may still go undetected, particularly in the

remoter ocean areas, but this may be explained by factors such as those mentioned above, without the necessity of invoking special geophysical conditions in these areas.

Magnitude

Walker and McCreery suggest that the teleseismic energy of the Kiribati earthquake was low compared with the magnitude they determined from hydrophone measurements. There are two methods whereby we can determine if the attenuation of teleseismic energy beneath the source region is abnormally high. The first is to examine the frequency content of short period teleseismic arrivals, because if this energy has passed through a region of abnormally low Q it is the high frequency energy which will be preferentially attenuated. Observations of this phenomena have been reported by many authors. Marshall et al. (1975) have shown that WRA P-wave recordings of shallow earthquakes from the Vanuatu and Tonga Islands regions, whose rays have passed through a low Q mantle at the source [Barazangi and Isacks, 1971], have significantly lower dominant frequencies (<1 Hz) than the recordings of deeper events from the same regions (≈2Hz). Similar conclusions have been reached by Der et al. (1985) who have shown that recordings from nuclear explosions detonated in tectonically active regions, where the mantle has a low velocity and low Q, are deficient in high frequency energy when compared with the recordings of nuclear explosions from tectonically stable regions.
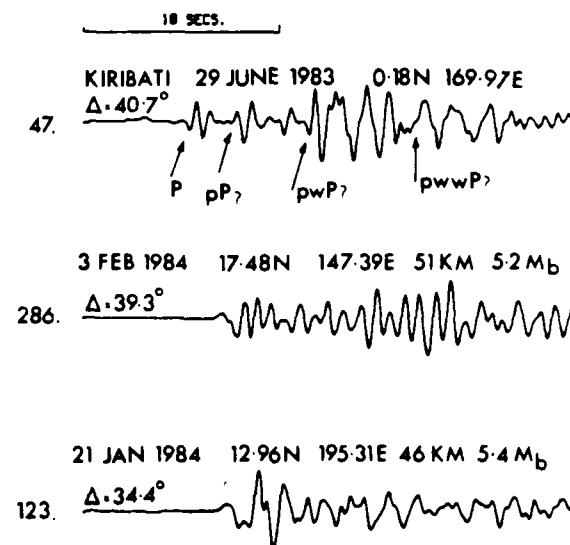
To determine whether the Kiribati earthquake is

Fig. 1. A comparison of the WRA seismic array beams of the Kiribati earthquake with those of two Mariana Islands earthquakes All traces have been normalised to the same peak to peak amplitude with the relative amplitudes being given by the numbers at the start of each trace. If the signals from the Kiribati event had been severely attenuated the higher frequencies would be lost and the dominant energy would be less than 1 Hz (c.f. Marshall et al., 1975). The frequency content of the first wavelets cf the Kiribati earthquake (1.5 Hz) is as high as the dominant frequencies of the other two events indicating that energy from this event has not passed through an abnormally low Q region.

KIRIBATI   29 JUNE 1983 0 18 N 169 97 E   Δ·42 8°

VERTICAL

RADIAL

TRANSVERSE

3 FEB 1984 17 48N 147 39E 51km 5 2mb   Δ·43 0°

VERTICAL

RADIAL

TRANSVERSE

21 JAN 1984 12 96N 145 31E 46km 5 4mb   Δ·38 1°
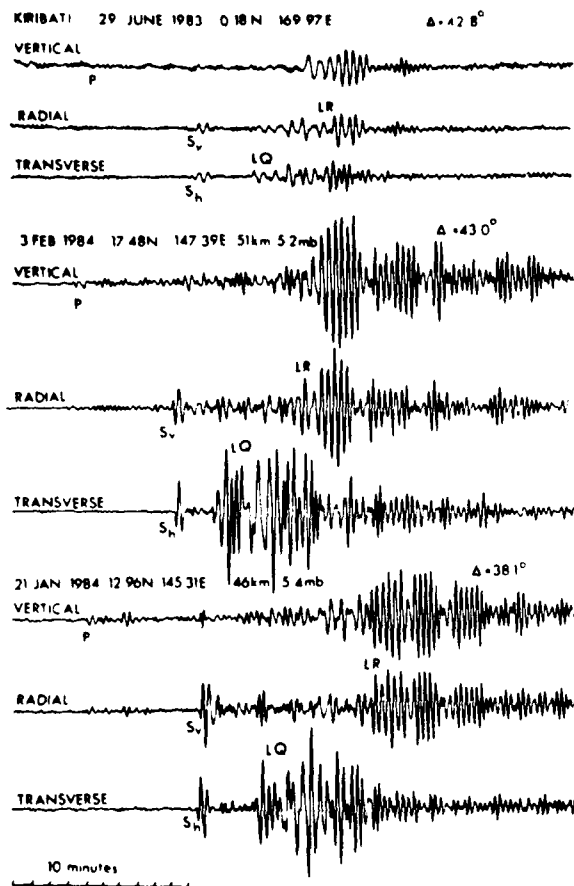
VERTICAL

RADIAL

TRANSVERSE

10 minutes

Fig. 2. A comparison of the Alice Springs long period wavetrains of the Kiribati event with those of the same two Mariana Islands earthquakes shown in Fig. 1. Each trace has been plotted with a uniform gain to illustrate that all long period wave groups (P, S_v, S_h, LQ and LR) of this event are smaller than those of the other events. This indicates that the magnitude of the Kiribati event was smaller than 5.0 (mb).

deficient in high frequency energy we compare WRA beams of its P-wave arrival with array beams of the two smallest Mariana Islands events used by Walker and McCreery in their amplitude comparisons. In our comparison, which is illustrated in Figure 1, each array beam has been normalised to the same peak to peak amplitude in order that the frequency content of each trace may be more readily interpreted. The relative amplitudes are given at the start of each trace. Figure 1 shows that although the signals from the Kiribati earthquake are considerably smaller than those of the other earthquakes, the first wavelets are remarkably simple which is indicative of a small uncomplicated focal mechanism. Furthermore, the dominant signal frequencies (≈1.5 Hz) of these wavelets are as high as those of the earthquake of magnitude 5.2 and higher than those of the earthquake of magnitude 5.4. This suggests that the attenuation in the mantle under the Kiribati earthquake cannot be significantly greater than that under the Mariana subduction zone. Later in the record the dominant frequency of the Kiribati signal is lower but this energy is likely to arise from reverberations in the water and sediments above the epicentre.

The second method we have used to determine whether there is a region of abnormally low Q under the Kiribati earthquake is to compare long period records from the same three earthquakes as have been used in Figure 1. In this analysis, the digital records from the long-period three component station at Alice Springs (in the centre of Australia) have been rotated to obtain radial and tangential components and the three orthogonal components for each event are shown plotted with the same normalisation factor in Figure 2. Because of the large wavelengths, the small amplitudes recorded from the Kiribati earthquake relative to the others cannot be explained in terms of a region of high attenuation beneath the source [c.f. Marshall et al., 1979]. In addition, because all the wavegroups (including P, S_v and S_h, as well as the Love and Rayleigh wavetrains) are smaller, it is difficult to appeal to source mechanisms, travel paths or the P_0/S_0 waveguide as a possible explanation. We are thus led to the conclusion that the central Pacific Ocean source regions are not anomolous as far as the propagation of teleseismic energy is concerned and that the magnitude of the Kiribati earthquake was smaller than has been proposed.

From two readings provided to the ISC (WRA-4.4, COL-5.1), the body wave magnitude of the Kiribati earthquake is estimated to be 4.75 (mb). Although subject to considerable uncertainties because of the small number of readings, this estimate is in good agreement with the surface wave magnitude of 4.7 which has been obtained from the Alice Springs long-period records.

Conclusion

The large amplitude with which the Kiribati earthquake of 1983 June 29, was recorded on the Wake Island hydrophones appears to arise, not because of the large magnitude of the event, but from exceptionally strong propagation of P_0 and S_0 phases, which are known to travel long distances with little attenuation, beneath the oceanic crust (Walker et al., 1978). It also shows that earthquakes away from subduction zones can couple energy into the P_0/S_0 waveguide very effectively. Walker (1977) has shown that these phases can suffer severe attenuation when they cross subducting margins, indicating that the waveguide is either not present, or is at least severely distorted in these regions. Under these circumstances it can be expected that the coupling of the Mariana Islands sources into the waveguide is relatively inefficient. On the other hand, the apparently shallow depth of the Kiribati earthquake indicates that it occurred within or close to the Po/So wavguide and this, in turn, would allow energy to be efficiently coupled into the waveguide.

A further contributing factor to the observed amplitudes at Wake Island could be the relative efficiency with which the Kiribati earthquake generated frequencies within the passband of the hydrophones. Intraplate earthquakes are normally associated with higher stress drops than interplate events [c.f. Kanamori and Anderson, 1975] and therefore, for a given size event, may be expected to have a higher corner frequency. Although the small relative amplitudes of the T phase compared with those of the P_0 and S_0 phases observed at Wake Island suggest that this is not the primary explanation, higher emitted frequencies may also provide a partial explanation for the large P and S amplitudes observed on the hydrophone array.

Of the other six events in the central Pacific Ocean that are listed by Walker and McCreery, only one (their event 5) was recorded by WRA and that was with low amplitude. This suggests that not only were their

magnitudes small (less than 4.0 mb), but also that the Wake Island hydrophone array is a particularly sensitive installation for detecting earthquakes in this area of the Pacific.

References

Adams, R. D., A. A. Hughes and D. M. McGregor, Analysis procedures at the International Seismological Centre, Phys. Earth planet Int., 30, 85-93, 1982.

Bullen, K. E., An introduction to the theory of seismology, Cambridge University Press, 292pp, 1965.

Baranzangi, M. and B. J. Isacks, Lateral variation of seismic-wave attenuation in the upper mantle above the inclined earthquake zone of the Tonga Island arc: deep anomaly in the mantle, J. Geophys. Res., 76, 8493-8516, 1971.

Der, Z., T. McElfresh, R. Wagner and J. Burnetti, Spectral characteristics of P waves from nuclear explosions and yield estimation, Bull. Seism. Soc. Am., 75, 379-390, 1985.

Kanamori, H. and D. L. Anderson, Theoretical basis for some empirical relations in seismology, Bull. Seism. Soc. Am., 65, 1073-1095, 1975.

Marshall, P. D., A. Douglas, B. J. Bartlett and J. A. Hudson, Short period teleseismic S waves, Nature, 253, 181-182, 1975.

Marshall, P. D., D. L. Springer and H. C. Rodean, Magnitude corrections for attenuation in the upper mantle, Geophys. J. R. astr. Soc., 57, 609-638, 1979.

Walker, D. A., High frequency P_n and S_n phases recorded in the Western Pacific, J. Geophys. Res. 82, 3350-3360, 1977.

Walker, D. A. and C. S. McCreery, Significant unreported earthquakes in "aseismic" regions of the Western Pacific, Geophys. Res. Lett., 12, 433-436, 1985.

Walker, D., C. McCreery, G. Sutton, and F. Duenebier, Spectral analysis of high frequency Pn and Sn phases observed in the Western Pacific, Science, 199, 1333-1335, 1978.

K. J. Muirhead, Research School of Earth Sciences, Australian National University, Box 4, Canberra, A.C.T., Australia.

R. D. Adams, International Seismological Centre, Newbury, RG131LX, Berkshire, United Kingdom.

DATE
FILMED
2-8